The recognition of infection in the brain: Toll-like receptor expression and innate immune responses to virus and prion infection

CLIVE STEWART MCKIMMIE

JANUARY 2005

Submitted for the degree of Doctor of Philosophy

The programme of research was carried out as part of a Wellcome Trust funded 4-year PhD entitled "The molecular and cellular basis of disease" at the Centre for Infectious Disease, Virology, Royal (Dick) Veterinary School, University of Edinburgh, Summerhall, Edinburgh, UK.

Contents

Declaration

I declare that the work presented in this thesis is my own except where otherwise stated. No part of this work has been or will be submitted for any other degree, or professional qualification.

Acknowledgements

I would like to thank my two supervisors **John Fazakerley** and **Mark Head.** It was Mark who first inspired my interest in the pathological processes of the brain during a mini-project in his laboratory at the National CJD surveillance unit and has consistently been helpful and interested in the project throughout. John has been an enormous help and an excellent supervisor. His door is always open and has taken his responsibilities as supervisor seriously. However, most of all his interest and fascination in the subject area is highly infectious and has been an important motivator in the completion of the project.

There are numerous others who have been helpful throughout the project and which without would not have been possible. I would especially like to thank **Claire Cotterilll** for constant help and advice on the intricacies of successful tissue culture. **Alan Brown**, **Lucy Breakwell** and **Rennos Fragkoudis** have also helped with various aspects of quantitative PCR methodology. I would also like to thank **Amanda Boyd** who has been invaluable in undertaking almost all the animal handling involved with this project. In addition, **Audrey Graham** and **Cat Dixon** have both individually been a willing source of advice and support.

I would like to thank the Scottish Centre for Genomic Technology and Informatics (ScGTI) for the collaboration that enabled the generation of the custom microarray. Several people have helped ensure the success of this project, including; **Douglas Roy** for help and advice; **Klemens Vierlinger** and **Marie Craigon** for printing and fabrication of microarrays; and finally **Thorsten Forster** who has provided invaluable advice on the complexities of statistics.

In addition, I thank **Nick Johnson** for his help and collaboration with the work relating to the Rabies virus infections.

Finally, I would also like to thank **Kave Shams** who, not only helped with the design and typography of numerous presentations, has been an indispensable source of support and comfort over the past few years.

Figures, tables and appendices

Chapter 4

Chapter 5

Chapter 6

Appendices

Abbreviations

ACAMP	Apoptotic cell associated molecular patterns
AD	Alzheimer's disease
Ag	Antigen
AIDS	Acquired immunodeficiency syndrome
BBB	Blood brain barrier
BDNF	Brain-derived neurotrophic factor
Bp	Base pair
BSA	Bovine serum albumin
cDNA	copy DNA
CFA	Complete Freund's adjuvant
CJD	Creutzfeldt-Jakob disease
Clecsf	C-type lectin superfamily
CMV	Cytomegalovirus
CNS	Central nervous system
COX	Cylco-oxygenase
CSF1	Colony stimulating factor 1
dbcAMP	dibutyryl cyclic adenosine monphophate
DC	Dendritic cell
DD	Death domain
dpi	Days post infection
dsRNA	Double stranded RNA
EAE	Experimental allergic encephalitis
EEE	Eastern equine encephalitis
EF	Elongation factor
eGFP	Enhanced green fluorescent protein
ELISA	Enzyme-linked immunosorbent assay
ER	Endoplasmic reticulum
EST	Express sequence tag
GAPDH	Glyceraldehyde-3-phosphate dehydrogenase
GARG	glucocorticoid-attenuated response gene
GFAP	Glial fibrillary acidic protein
GFP	Green fluorescent protein
GM-CSF	Granulocyte-macrophage-colony stimulating factor
GNAS	Guanine nucleotide-binding factor
GSK	Glycogen synthase kinase
HAD	human immunodeficiency virus (HIV) associated dementia
HEK293	Human embryonic kidney 293
HIV	Human immunodeficiency virus
Hsp	Heat shock protein
HSV	Herpes Simplex virus
ICAM	Intercellular adhesion molecule
IFN	Interferon
IFN-α/β-R	IFN-α/β-receptor
Ig	Immunoglobulin
IKK	IκB kinase
IL	Interleukin
IMD	Immune deficiency
IP-10	γ-IFN-inducible-protein 10
IRAK	IL-1R-assocaited kinase
IRF3	IFN-regulatory factor 3

IRG	Immunoresponsive gene
LCMV	Lymphocytic choriomeningitis virus
LLME	L-leucine methyl ester
LPS	Lipopolysaccharide
LRR	Leucine rich repeat
MAL	MyD88-adaptor-like protein
MARCO	Macrophage receptor with collagenous structure
MDC	Monocyte-derived dendritic cells
MHC	Major histocompatibility complex
MIF	Macrophage migration factor
MIP	Macrophage inflammatory protein
MOI	Multiplicity of infection
Mrc	Mannose receptor
MyD88	Myeloid differentiation factor 88
NADPH	Nicotinamide adenine dinucelotide phosphate
NCF1	Neutrophil cytosolic factor 1 (also known as p47phox)
NMP	N-methyl-2-pyrrolidinone
NO	Nitric oxide
Nos2/iNOS	Inducible nitric oxide synthase
nsP	Non-structural protein
OAS	2'-5' oligoadenylate synthetases
PAMP	Pathogen associated molecule
PBS	Phosphate buffered saline
PBSA	PBS albumin
PCR	Polymerase chain reaction
PDC	Plasmacytoid dendritic cell
PGRP	Petidoglycan recognition protein
PID	Post infection day
PKR	Protein kinase R
PMT	Photomultiplier tube
PrP^{C}	Prion protein (cellular)
PrP^{Sc}	Prion protein (scrapie)
PRR	Pattern Recognition Receptor
Ptgs	Prostaglandin synthase (also known as COX)
RIP1	Receptor-interacting protein 1
RPE	Retinal pigment epithelial cell
RT-PCR	Reverse transcriptase PCR
QPCR	Quantitative PCR
ScGTI	Scottish Center for Genomic Technology and Informatics
SEM	Standard error of the mean
SFV	Semliki Forest virus
SOD	Superoxide dismutase
SR	Scavenger receptor
SRCL	Scavenger receptor with C-type lectin
SsRNA	Single-stranded RNA
Scya	Small inducible cytokine A (chemokine family)
TAB	TAK- binding protein
TAK	Transforming growth factor-activated kinase
TANK	TRAF family member-associated NF-κB activator
TBK1	TANK-binding kianse 1
TGF	Transforming growth factor
Th	T helper

TIFF	Tagged Image File Format
TIR	Toll/IL-1 receptor
TIRAP	TIR domain-containing adaptor protein
TLR	Toll-like receptor
TMEV	Theiler's murine encephalomyelitis virus
TNF	Tumour necrosis factor
TRAF	Tumour necrosis factor receptor associated factor
TRAM	TRIF-related adaptor molecule
TREM	Triggering receptor expressed on myeloid cells
TRIF	TIR domain-containing adaptor protein inducing factor
tRNA	transfer RNA
TSE	Transmissible spongiform encephalopathy
VCAM1	Vascular cell adhesion molecule 1
VEE	Venezuelan equine encephalitis
VLP	Virus-like particle
VSV	Vesicular stomatitis virus
WEE	Western equine encephalitis
WNV	West Nile virus

Abstract

The mechanisms that mediate innate recognition of infections in the immunospecialised environment of the central nervous system (CNS) have not been characterised. This thesis explores the capability of the CNS to detect infections and activate immune responses. The majority of CNS neurones are post-mitotic and cannot be replaced if lost or damaged. Consequently, the resting CNS is devoid of most immune processes, although substantial inflammatory responses can be initiated by specialised glial cells. The innate immune system recognises conserved molecular patterns on microorganisms by a set of pattern recognition receptors which include the Toll-like Receptors (TLR). A growing consensus suggests they are key to the initiation of innate immune responses. Cellular expression of TLR imparts the ability to detect infection and determine pathogen type. A multitude of TLRs have now been cloned, although their function and expression patterns have not been described in the CNS. This thesis aims to explore whether cells of the CNS express TLRs and whether they are capable of responding to different stimuli. To explore gene expression a novel custom microarray was designed, developed and validated to assay the expression of selected gene transcripts involved in innate immune responses. These included a multitude of pattern precognition receptors, in addition to transcripts associated with stress responses and a variety of cytokine, chemokine and interferon (IFN) transcripts. In addition, a highly sensitive quantitative PCR technique was developed. Utilising both techniques this thesis reports the first systematic analysis of TLR gene expression in the CNS.

Gene transcript levels were first studied in glial cells at rest. Cells were stimulated with bacterial lipopolysaccharide, or by infection with the neuroinvasive Semliki Forest virus (SFV). Both microglia and astrocytes in culture expressed a multitude of TLRs that were differentially modulated in a specific manner depending on the nature of the stimulus. The expression of TLR suggests glial cells are capable of recognising a vast array of microbial-associated molecules. Such a strategy may be an essential requirement for an organ mostly devoid of recognisable immune processes.

In vivo, the resting CNS exhibited extensive TLR expression with TLR 3 expressed at exceptionally high levels, comparable to that of lymphoid tissue, but varying with mouse strain. The data reported here show for the first time that TLRs in the brain are upregulated during viral encephalitis. Furthermore, this response was appropriate to the pathogen, with selective up-regulation of TLRs that sense viral infection. Intracerebral inoculation with either SFV or rabies virus initiated substantial upregulation of TLR 2, 3 and 9. Type-I IFN independent mechanisms mediated the up-regulation of TLR 2 following SFV infection, whilst for the two TLRs that mediate recognition of viral nucleic acids, TLR 3 and TLR 9, upregulation of gene expression was dependent upon and proportional to the type-I IFN response. It is likely that by up-regulating TLR 3 and 9, type-I IFN acts to increase the sensitivity of cells in the vicinity of virally infected cells. In this hypothesis, basal levels of TLR detect viral RNA and induce type-I IFN synthesis. This IFN acts in both an autocrine and paracrine way to up-regulate a number of genes including TLR itself. In this way cells in the vicinity of virally infected cells have their virus sensing mechanisms upregulated. This parallels events with protein kinase R, another interferon inducible activator of innate cellular defences.

Transmissible spongiform encephalopathies are a group of diseases characterised by chronic neurodegeneration and glial cell activation. This thesis demonstrates that the CNS significantly upregulated several TLRs, and in the case of TLR 2, by 10-fold towards terminal disease. This response further describes the apparent non-productive innate immune activation of these cells during these diseases. In summary, the finding that the brain has the ability via TLR expression to detect infection and discern its type provides an important contribution to understanding pathological processes in this organ.

Chapter 1 Introduction

Contents

1 Introduction

This thesis studies innate immune responses of the CNS during viral encephalitis and during transmissible spongiform encephalopathy. This introduction will provide a background on the innate immune system and its ability to recognise conserved molecular patterns on microrganisms that are conferred by Toll-like receptors (TLR). TLR give the innate immune system an ability to recognize both the presence of infection and the type of infection. This introduction reviews the current state of knowledge of TLR, their ability to recognise infection and to control the course of immune responses. Particular emphasis is given to the mechanisms that control TLR expression. The ability of TLR to trigger the potent anti-viral interferon system is also reviewed here. In addition, this introduction will describe immune responses of the CNS. The resting CNS lacks almost all forms of recognisable immune process, and yet infections can be detected and immune responses initiated. Specialised glial cells reside in the CNS and are capable of producing inflammatory mediators and inducing brain inflammation. Particular emphasis is given to innate immune responses to viruses and viral encephalitis. The mechanisms that mediate and control inflammatory responses in the CNS remain only partially characterised and are discussed at length. Semliki Forest Virus (SFV) is a well-studied virus that is used as an experimental model of viral encephalitis and is reviewed here. Finally, the transmissible spongiform encephalopathies represent a group of uniquely transmissible neurodegenerative disorders that results in substantial neuropathogenesis including the activation of glial cells and are reviewed here.

1.1 Toll-like receptors

1.1.1 Innate and adaptive immune systems

The mechanisms by which a metazoan organism detect the presence of infectious agents and eliminates them without massive damage to self-tissues is a problem that has troubled scientists for the past century. Pathogens are almost infinite in their molecular diversity and possess the ability to rapidly evolve with high replication and mutation rates. To combat this threat, metazoan organisms have evolved a vast range of defences, which in vertebrates can be broadly divided into two categories: the innate and adaptive immune systems.

Adaptive immunity relies on the production of millions of antigen receptors that differ in their specificity. The system relies on one or more of these receptors being specific for any pathogen that may infect a host, enabling the clonal expansion of specific antigen-recognizing lymphocytes and the immunity that it brings. Whilst this adaptive response provides so-called immunological memory, it has in isolation two fundamental flaws. Firstly, randomly generated receptors cannot determine the biological context of the antigen, a process that is necessary for stimulating the right type of effecter response. Secondly, the clonal expansion takes 4 to 5 days before an effective defence is generated; this is too late to repel many fast-replicating pathogens. Thus, successful adaptive immune responses rest on an evolutionary ancient and more universal innate immune system. Innate immunity is not only responsible for the almost instantaneous detection of infection and in determining its form, but also has a role to play in controlling the initiation and the type of the adaptive immune response. Indeed, the ability to detect pathogens is arguably the most important task undertaken by the immune system, since appropriate recognition of microbes is critical for mounting a response that can effectively combat invading pathogens.

Despite Elie Metchnikoff's seminal description of phagocytosis by starfish larvae cells in 1884, comparatively little has been published concerning the mechanisms that mediate innate recognition of microbes - being overshadowed by developments in adaptive immune research. It is now clear that innate recognition is mediated by a finite set of structurally and functionally diverse receptors that can trigger defences such as complement activation, phagocytosis, and the expression of pro-inflammatory genes, interferons and defensins. The recent discovery of Toll-like receptors (TLR) has created a new wave of interest in the field of innate immunity. TLR are thought to play a crucial role in the recognition of molecular signatures of microbial infection, and engage differential signalling cascades that once activated are pro-active in the control of T helper cell differentiation. This represents a marked shifting in immunologist's thinking and has changed ideas about the pathogenesis

and treatment of infectious, cancer, immune and allergic diseases. Accordingly, our knowledge of TLR and their signalling pathways has increased greatly over the past few years (Medzhitov and Janeway, Jr., 2000; Akira and Takeda, 2004).

1.1.2 Pathogen associated molecular patterns (PAMPs)

That the innate immune system detects constitutive and conserved molecules that result from microbial metabolism was first suggested by Charles Janeway in what is now widely regarded as a landmark paper (Janeway, Jr., 1989). There are a multitude of molecular pathways unique to microrganisms, such as housekeeping functions or structural molecules conserved within a given class of pathogen e.g. lipopolysaccharide, lipoproteins and lipopteichoic acids are only made by bacteria, and as such can be regarded as molecular signatures of bacterial invaders (Medzhitov, 2001; Janeway, Jr., 1989). These microbial signatures may even be somewhat different in different species within a given microbial class; however, these fine differences exist in the context of a common molecular pattern. An example of this is the lipid-A portion of lipopolysaccharide (LPS), which is an invariant molecular pattern found in all gram-negative bacteria and now known to be the vital trigger of LPS-mediated inflammation. Conversely, the non-immunogenic O-antigen portion of LPS is highly variable in LPS from differing strains and hence is not a molecule recognized by the innate immune system. Janeway named these conserved microbial structures Pathogen Associated Molecular Patterns (PAMPs). An individual PAMP was proposed to bind and be recognized by receptors of the innate immune system - termed Pattern Recognition Receptors (PRR) (Janeway, Jr., 1989).

1.1.3 The Pattern Recognition Receptors

Until 1999, well-defined PRR were few and far between. CD14, a GPI-linked lectin was known to be vital for the recognition of LPS (Wright et al., 1990), whilst Scavenger Receptors were suggested to have a role in recognizing bacterial proteins (Pearson, 1996), the macrophage mannose receptor was shown to recognize bacterial sugars (Fraser et al., 1998) and a small family of receptors were implicated in the recognition of highly immunogenic N-formyl peptides (Le et al., 2001). Since then there has been a large increase in the number of PRR with the discovery that the mammalian Toll-like Receptors (TLR) are pattern recognition receptors.

1.1.4 Toll in Drosophila

The involvement of Toll in innate immunity was first described in *Drosophila*. Toll is a transmembrane protein that was first identified as a critical component of the pathway that controls dorsal/ventral patterning in the developing embryo (Anderson et al., 1985) (Hashimoto et al., 1988). Toll is activated upon ligation to a secreted factor Spätzle, which in turn activates the serine/threonine kinase Pelle via the adapter protein Tube. Pelle acts by promoting the degradation of the ankyrin-repeat protein Cactus, which associates with the Rel-type transcription factor Dorsal in the cytoplasm. Once Cactus is degraded, Dorsal is free to translocate to the nucleus where it regulates transcription of specific genes (Belvin and Anderson, 1996).

This pathway is strikingly similar to the mammalian IL-1 receptor pathway: activation of the IL-1R leads to NF-κB activation by degradation of IκB in the cytoplasm, allowing translocation of the transcription factor to the nucleus, where it initiates transcription of a multitude of genes involved in inflammation and immune responses. Not only are the pathways qualitatively similar but the composition of the key players possess striking homology. Indeed, the cytoplasmic domains of *Drosophila* Toll and mammalian IL-1R are highly conserved and have become known as the Toll/IL-1 receptor (TIR) domain. Upon observation of these intriguing similarities it was suggested Toll may regulate immune responses in *Drosophila* (Belvin and Anderson, 1996). Within a remarkably short time this suggestion was proved correct by several studies including an excellent report that demonstrated several key players of the Toll pathway including Toll itself, Spätzle, Tube and Pelle were involved in immune responses to fungal infection in adult flies (Lemaitre et al., 1996). In this study the authors mutated all four genes and found the resultant mutants were highly susceptible to fungal infection. This defect was due to their inability to mount effective immune responses, including the expression of Drosomycin, an essential element of the *Drosophila* immune response to pathogenic fungi. Further studies identified several Dorsal-like transcription factors (similar to NF-. B in mammals) and found that Dorsal-type immune factor was critical for anti-fungal responses, whilst Dorsal itself was primarily involved in the Toll pathway that controls dorsal/ventral patterning (Meng et al., 1999; Rutschmann et al., 2000). The Toll pathway also initiates immune responses to gram-positive bacteria. In this pathway Relish, a Dorsal/NF-κB like transcription factor, was shown to be critical for the induction of anti-bacterial peptides that play a role in resistance to gram-positive bacteria (Rutschmann et al., 2002).

Spätzle is a secreted protein that is inactive until cleaved by a serine protease during infection and only the cleaved form can bind to Toll. The serine protease inhibitor Spn43Ac,

which prevents cleavage of Spätzle, further regulates this process (Levashina et al., 1999). Thus it seems that Toll does not directly bind to microbes or their associated molecules, but rather is activated upon infection by an elaborate upstream signalling system. The mechanism by which fungal responses activate the Toll pathway is yet to be described. However, recent work has suggested a mechanism for Toll activation following infection with gram-positive bacteria: PGRP-SA is a peptidoglycan recognition protein that recognises peptidoglycans within gram-positive bacteria walls. Flies mutated to lack PGRP-SA have an impaired immune response to gram-positive bacteria but not to fungi. Thus PGRP-SA appears to specifically recognise gram-positive bacterial infections and in turn activates the Toll pathway (Michel et al., 2001; Werner et al., 2000).

Immune responses to gram-negative bacteria are mediated by a distinct pathway first identified by a mutation in the *immune deficiency* (*imd*) gene (Lemaitre et al., 1995) that ends with Relish translocating to the nucleus to induce anti-bacterial genes such as Diptericin. The *imd* mutants are highly susceptible to infection by gram-negative bacteria but possess normal anti-fungal responses (whereas the opposite is true for Toll mutants). A receptor that specifically recognises gram-negative bacterial infection has not been identified in the IMD pathway. Initially, 18-wheeler (a member of the Toll family) was proposed to constitute the IMD receptor, but expression of Diptericin was later shown to be normal in flies lacking 18-wheeler (Williams et al., 1997b; Khush et al., 2001). Further work has now demonstrated that a member of the PGRP family, PGRP-LC, may well be the IMD receptor. Critically, flies lacking PGRP-LC are unable to express Diptericin in response to infection (Choe et al., 2002; Gottar et al., 2002). Thus a non-Toll related receptor appears to initiate signalling in the IMD pathway and has contributed to a growing excitement concerning the role PGRPs play in sensing infection within flies. There are over 15 different PGRP members identified to date and these could be involved in sensing a variety of different microbes in *Drosophila*.

1.1.5 Toll like receptors in mammals

It was a matter of months following the discovery that Toll mediates host immunity to fungal infections, that a mammalian homologue of Toll, Toll-Like receptor 4 (TLR 4) was identified and shown upon over-expression to trigger the release of inflammatory mediators (Medzhitov et al., 1997). There are now 13 TLR known to exist and they are predominantly expressed on cell types that are likely to first encounter antigen such as phagocytic cells. TLR 1 to 9 are expressed in both mice and humans although TLR 10 is present in mice only as a degenerate pseudogene. TLR 11, 12 and 13 are expressed in mice but lack human

orthologs (Medzhitov et al., 1997; Rock et al., 1998; Takeuchi et al., 1999b; Chuang and Ulevitch, 2001; Chuang and Ulevitch, 2000; Du et al., 2000; Tabeta et al., 2004). They all share a similar structure possessing leucine rich repeat (LRR) motifs in their extra-cellular portions and an intracellular TIR domain (Slack et al., 2000). The extracellular regions of TLR are composed of 19 to 25 tandem repeats of the LRR motif. Each repeat is 24 to 29 amino acids long and together forms a horseshoe-like structure. These concave structures are thought to constitute the portion of the protein that directly binds to and so recognises microbial components and other endogenous host ligands (Bell et al., 2003). Sequence analysis of the TLR family demonstrates they can be divided into five subfamilies by comparison of their amino acid sequences: TLR 2, 1, 6 and 10 form one family, TLR 9, 7, 8, 11 and 12 form another family, whilst TLR 3, 4 and 5 each lie in individual groupings – see figure 1 (Du et al., 2000). A recent study has suggested TLR 13 is most similar to TLR 3 (Tabeta et al., 2004). TLR 1 and 6 are highly similar: they exhibit 69% identity in overall amino acid sequence, their TIR domains are particularly conserved being 90% identical and are located in tandem on the same chromosome – suggesting they are the product of a gene duplication event (Takeuchi et al., 1999b). TLR 2 has two exons although the coding region lies solely within exon 2. The TLR 9 subfamily are all encoded by two exons, with TLR 7 and 8 possessing 42.3% identity overall and 73% identity within their TIR domains and are both located in close proximity on the X- chromosome (Chuang and Ulevitch, 2000; Du et al., 2000). TLR 4 and 5 have 4 and 5 exons respectively, whilst TLR 3 possess five exons with the coding sequence uniquely lying in a multitude of exons: exons 2, 3, 4 and 5. Figure 1 highlights the phylogenetic relationship of human TLR.

1.1.6 TLR play a fundamental role in the recognition and sensing of microbes

The vast majority of work studying TLR function has concentrated on the detection of differing bacterial pathogens, with the gram-negative bacterial component lipopolysaccharide (LPS) given particular attention. However, it is becoming increasing clear that viruses are also subject to innate sensing by TLR. TLR responses *in vivo* pose a realistic threat to viruses, as demonstrated by the presence in *Vaccinia* virus of three genes that act as direct negative regulators of the TLR signalling pathway, one of which strongly affects virulence *in vivo* (Bowie et al., 2000; Harte et al., 2003; DiPerna et al., 2004). Since studies pertaining to bacterial components have been instrumental in describing TLR function this introduction will begin by exploring the role of TLR in immune responses in general. Figure 2 summarises the known function of TLR, their sub-cellular location and

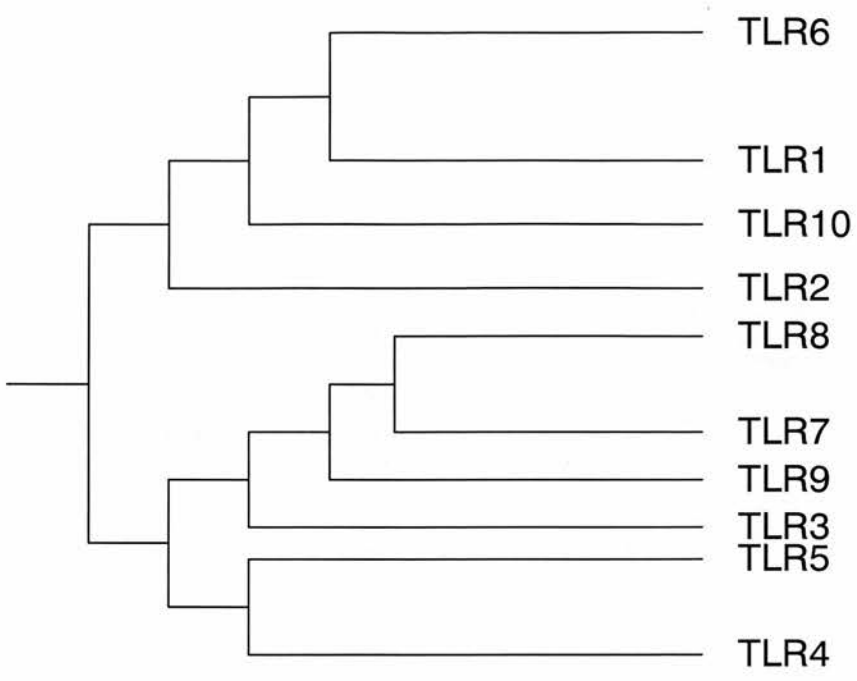

Figure 1, phylogenetic tree of known human TLRs. Based upon this analysis there exists several groupings of TLR: i) TLR 1, 2, 6 and 10 belong to the TLR 2 grouping; ii) TLR 7, 8 and 9 belong to the TLR 9 grouping; iii) TLR 3, 4, and 5 each exist as separate members. The sequence homology of mouse TLRs is similar albeit with three additional TLRs: TLR11 and 12 being most closely related to the TLR9 subfamily and TLR13 most closely related to TLR3. This figure has been adapted from Chuang, T. & R.J. Ulevitch (2001).

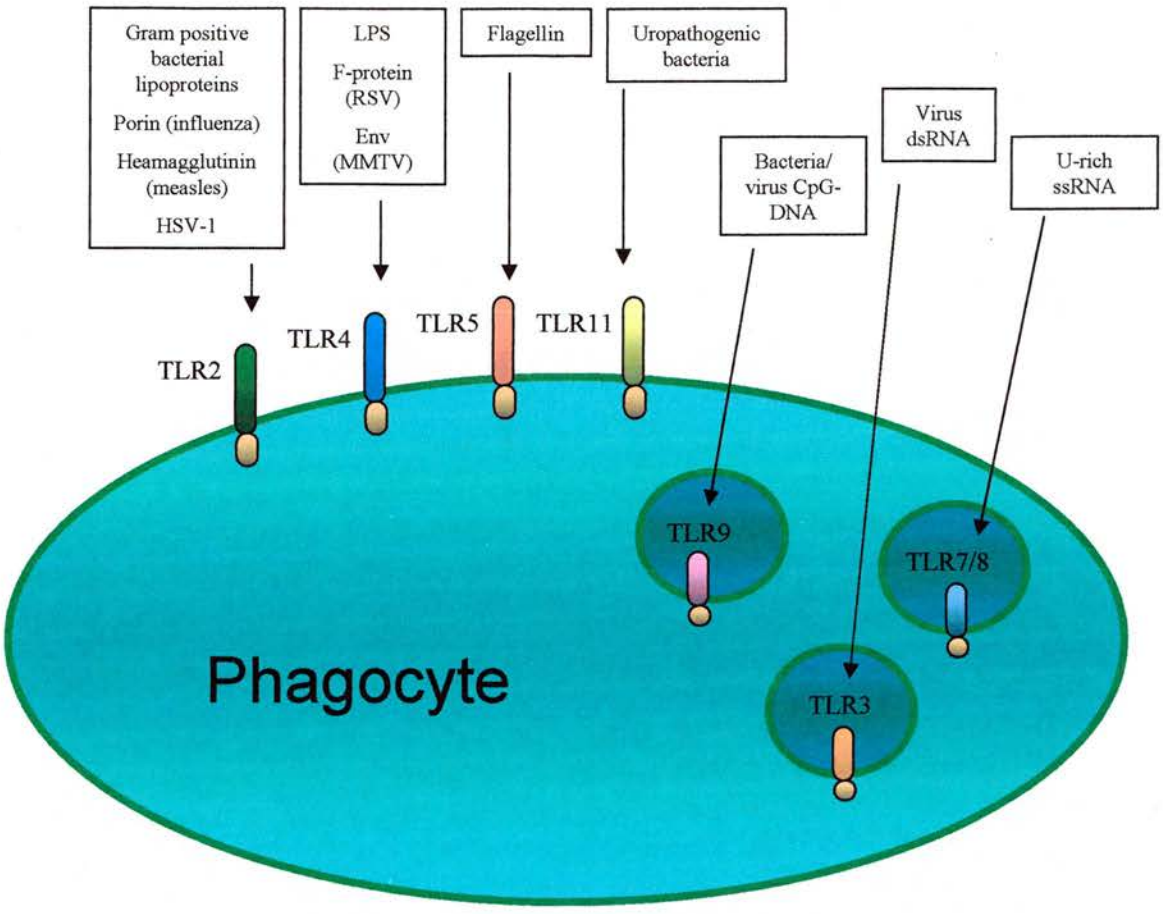

Figure 2 TLR recognise a wide variety of structurally diverse molecules. TLR 1, 2, 4, 5, 6 and 11 are expressed on the cell surface and can be recruited to phagosomes to mediate recognition. TLR 3, 7, 8 and 9 are expressed within endosomes to which molecules such as CpG-DNA are transported. TLR 2 works in collaboration with TLR 1 and TLR6 to mediate recognition of bacterial lipoproteins (adapted from O'Neill, 2004).

their respective ligands, whilst Table 1 summarises in more detail the differing microbial components that TLR have been documented to recognise to date.

1.1.7 TLR 4 recognises a variety of microbial components including lipopolysaccharide

TLR 4 was the first mammalian member of the Toll family identified. Study of this molecule has elucidated a significant portion of TLR biology. TLR 4 was first described in a seminal paper that over-expressed a dominant positive *TLR 4* mutant in the macrophage THP-1 cell line resulting in the expression of several key inflammatory genes that activate the adaptive immune system (Medzhitov et al., 1997). As such, it was the first indication that TLR were involved in mammalian immune responses. In the following year two groups independently demonstrated it was TLR 4 that was responsible for recognising a potent stimulator of the immune system, LPS (Poltorak et al., 1998; Qureshi et al., 1999). Since these seminal papers, several other members of the TLR family have been shown to be essential for the recognition of a wide variety of microbial components. Historically, there have been two mouse strains that were much studied due to their inability to respond to LPS, possessing a so-called LPS hypo-responsive phenotype: the C3H/HeJ and C57BL10/ScCr strains. It was discovered that the C3H/HeJ strain possessed a point mutation in the *TLR 4* gene, with a highly conserved proline residue being replaced by histidine. Whilst the C57BL10/ScCr stain had a null mutation in the TLR 4 gene. Further proof of the role that TLR 4 plays in mediating LPS-induced inflammation was demonstrated in a later study that purposefully disrupted the *TLR 4* gene in wild-type mice, resulting in the generation of the LPS hypo-responsive phenotype (Hoshino et al., 1999).

Unlike *Drosophila* Toll, TLR 4 is thought by many to directly bind LPS in a complex with CD14 (which is thought to tether LPS molecules), and MD-2 which enhances LPS responsiveness in cell lines and the absence of which in mice generates an LPS hypo-responsive phenotype (Jiang et al., 2000; Da Silva et al., 2001; Nagai et al., 2002; Shimazu et al., 1999). Like *Drosophila* Toll, TLR 4 recognises several endogenous ligands such as heat shock proteins. These are secreted factors made during stress induced by a wide variety of conditions such as heat, UV radiation and infection. They are known to induce activation of macrophages and as such have been labelled as endogenous "danger signals" (Takeda et al., 2003; Gallucci and Matzinger, 2001). Macrophage activation by heat shock protein 60 occurs via signalling through TLR 4, although studies have suggested that it doesn't directly bind to the TLR (Ohashi et al., 2000; Habich et al., 2002). Indeed, the whole premise that TLR 4 binds directly to any of its ligands, including LPS, is still a matter of debate. Several

studies have provided convincing evidence that it is TLR 4 that provides specificity and hence binds to LPS (Lien et al., 2000; Poltorak et al., 2000; Hajjar et al., 2002). Conversely, others have suggested that it is MD-2 that in actuality confers the ability to recognise LPS (Viriyakosol et al., 2001; Akashi et al., 2001). Further research is required to clarify this important distinction.

LPS can also be delivered directly to the cytoplasm by membrane internalisation and is recognised by Nod1 an intracellular protein that like TLR 4 possesses LRR domains (Inohara et al., 2001). This intracellular recognition protein may also be responsible for recognising the cell-invasive pathogen *Shigella flexneri* (Girardin et al., 2001).

TLR 4 may also recognise a number of viral envelope glycoproteins. Viral glycoproteins mediate virus binding and entry to host cells and as such can be sensed without the need for viral repication or gene expression. The respiratory syncytial virus was the first virus demonstrated to activate a member of the TLR family eliciting NK-κB activation in a TLR 4 dependent manner (Kurt-Jones et al., 2000). Further more, mice lacking TLR 4 were less able to resist infection by this virus (Haynes et al., 2001). The mouse mammary tumour virus has also been shown to activate immune repsones in part through TLR 4 in B cells (Rassa et al., 2002) and cannot be effectivly cleared by TLR 4 deficient mice (Jude et al., 2003). Importantly, in both cases each virus appears to trigger TLR 4 activation through recognition of their envelope glycoproteins. Intriguingly, a further study has shown that the mammary tumour virus may utilise TLR 4 along with TLR 2 on dendritic cells to aid entry by upregulating its entry receptor CD71. As such, this finding highlights a novel viral stratergy that utilises the host mechanisms that are designed to detect them (Burzyn et al., 2004).

1.1.8 TLR 2, 1 and 6 subfamily recognises a multitude of microbial components

TLR 2 appears to recognise a variety of organisms and their associated components such as lipoproteins from gram-negative bacteria, mycoplasma and spirochetes (Aliprantis et al., 1999; Brightbill et al., 1999; Lien et al., 1999; Hirschfeld et al., 1999). Peptidoglycans and lipopteichoic acid from gram-positive bacteria also activate TLR 2 (Schwandner et al., 1999; Yoshimura et al., 1999; Underhill et al., 1999b; Lehner et al., 2001) as does zymosan from yeast amongst others (Underhill et al., 1999a). Mice engineered to lack functional TLR 2 have demonstrated the necessity of this protein for protection against a variety of pathogens including *Staphylococcus aureus* (Takeuchi et al., 2000) and for normal responses to peptidoglycan (Takeuchi et al., 1999a) and lipoproteins (Takeuchi et al., 2000). TLR 2 can also recognise atypical LPS from bacteria such as *Leptospira interrogans*, which is

structurally distinct from LPS found on enterobacteria such as *Escherichia coli* (Werts et al., 2001).

TLR 2 may also recognise envelope glycoproteins of viruses. The measles virus appears to activate TLR 2 through recognition of its haemagglutinin protein, activating NF-κB and inducing cytokine release (Bieback et al., 2002). In addition to the measles virus, some reports have suggested components of the cytomegalovirus (CMV) may be recognised by TLR 2. CMV is a complex *Herpes* virus and soluble forms of its glycoproteins activate NF-κB and IRF3, inducing an anti-viral state in cells (Boehme et al., 2004). In a highly artificial *in vitro* setting, TLR 2 (but not TLR 4) was shown to be required for HEK293 pro-inflammatory responses to CMV, suggesting some component of the immune response to this virus involves recognition by TLR 2 (Compton et al., 2003). In support of TLR 2's role in sensing *Herpes* infection comes a report that demonstrates Herpes Simplex virus type 1 is recognised *in vivo* by TLR 2, since TLR 2 deficient mice exhibited lower serum IL-6 levels and less pronounced immunopathology in the CNS (further discussed in section 1.2.4) (Kurt-Jones et al., 2004).

The role that TLR 6 plays within innate immunity was analysed by introducing a dominant negative form into the RAW264.7 macrophage cell line. This study highlighted that the mutated TLR 6 prevented the cell line from responding to a variety of microbial components previously identified as signalling through TLR 2. In addition, TLR 6 and 2 were shown to co-immunoprecipitate, implying they can become spatially connected (Hajjar et al., 2001). A further study utilised mice lacking either functional TLR 2 or 6: mice that lacked TLR 6 demonstrate a deficient response to mycoplasma lipoproteins (otherwise known as a TLR 2 ligand) although they possess a normal responses to bacterial lipoproteins (another distinct TLR 2 ligand). Macrophages isolated from mice deficient in TLR 2 could respond to neither molecule (Takeuchi et al., 2001). Taken together, this data suggests that TLR 6 associates with TLR 2 and confers specific recognition between two different types of lipoprotein. TLR 1 has also been shown to associate with TLR 2 to confer specific recognition (Wyllie et al., 2000). It is speculated that other TLR may similarly heterodimerise and so greatly expand the possible number of microbial structures recognised by this rather finite set of recognition receptors.

1.1.9 TLR 5 recognises bacterial flagellin

Chinese hamster ovary cells expressing TLR 5 were used in a study to demonstrate that this receptor was responsible for recognising the potent immunogen flagellin (Hayashi et al., 2001). Flagellin has highly conserved regions that are common to flagellins from a broad

spectrum of gram-negative bacteria. It is this conserved region that possesses both the immunostimulatory motif and is the region that signals through TLR 5 (Eaves-Pyles et al., 2001). Thus the innate immune system has defined one of the few structurally related molecules of flagellated bacteria as a pathogen-associated molecule and in doing so can signal infection by recognising this class of pathogen through one specific receptor, TLR 5.

Interestingly, plants possess a gene called *Fls2* which encodes a transmembrane receptor-like kinase that possesses LRR motifs and has structural similarities to mammalian TLR. Incredibly, a deficiency in FLS2 appears to confer flagellin-sensitivity to Arabidopsis (Gomez-Gomez and Boller, 2002). In addition to FLS2, several other plant proteins possessing a TIR domain have been identified and appear to be involved in host responses to pathogens (Asai et al., 2002). Hence, the TIR domain represents a truly ancient mechanism for microbial recognition that not only spans across the animal kingdom from vertebrates to arthropods, but also to the plant kingdom.

Receptor	Ligand	Origin of Ligand	References
TLR 1	Triacyl lipopeptides	Bacteria and mycobacteria	(Takeuchi et al., 2002)
TLR 2	Lipoproteins/lipopeptides	Various bacterial pathogens	(Aliprantis et al., 1999)
	Peptidoglycan	Gram-positive bacteria	(Takeuchi et al., 1999a)
	Lipopteichoic acid	Gram-positive bacteria	(Schwandner et al., 1999)
	Lipoarabinomannan	Mycobacteria	(Means et al., 1999)
	Phenol-soluble modulin	*Staphylococcus epidermis*	(Hajjar et al., 2001)
	Glycoinositolphospholipids	*Trypanosoma cruzi*	(Coelho et al., 2002)
	Porins	*Neisseria*	(Massari et al., 2002)
	Atypical LPS	*Porphyromonas ginivalis*	(Hirschfeld et al., 2001)
	Zymosan	Yeast	(Underhill et al., 1999b)
	Haemagglutinin	**Measles virus**	(Bieback et al., 2002)
	Unknown – glycoprotein?	**Herpes simplex virus 1**	(Kurt-Jones et al., 2004)
TLR 3	Double stranded RNA	**Viruses**	(Alexopoulou et al., 2001)
TLR 4	LPS	Gram-negative bacteria	(Poltorak et al., 1998)
	Fusion protein	**Respiratory syncytial virus**	(Kurt-Jones et al., 2000)
	Envelope protein	**Mouse mammary-tumour virus**	(Rassa et al., 2002)
	Heat-shock protein 60	Host	(Ohashi et al., 2000)
	Heat-shock protein 70	Host	(Vabulas et al., 2002)
	Fibrinogen	Host	(Smiley et al., 2001)
TLR 5	Flagellin	Bacteria	(Hayashi et al., 2001)
TLR 6	Diacyl lipopeptides	*Mycoplasma*	(Takeuchi et al., 2001)
	Lipoteichoic acid	Gram-positive bacteria	(Schwandner et al., 1999)
	Zymosan	Yeast	(Ozinsky et al., 2000)
TLR 7/8	Imidazquinoline	Synthetic compounds	(Hemmi et al., 2002)
	Single-stranded RNA	**Viruses**	(Heil et al., 2004; Diebold et al., 2004)
TLR 9	CpG-containing DNA	Bacteria and **DNA viruses**	(Hemmi et al., 2000; Tabeta et al., 2004)
TLR 11	Unknown	Uropathogenic bacteria	(Zhang et al., 2004)

Table 1. TLR recognise a multitude of microbial compounds, some of which are listed here. Viral interactions with TLR are highlighted

1.1.10 TLR 3 recognises viral double stranded RNA

Double stranded RNA (dsRNA) is a strong activator of type I interferons (IFN-α and -β) that mediate potent anti-viral effects and stimulates the immune system. The production of type I interferons is absolutely critical for defence against virus infections and is discussed later in section 1.1.17. Many viruses produce dsRNA during the replication cycle either as an essential intermediate in RNA synthesis or as a by-product generated by symmetrical transcription of DNA virus genomes. Some of these anti-viral mechanisms are elicited by activation of a dsRNA protein kinase R (PKR). Fibroblasts cultured from mice deficient in PKR have impaired responses to poly(I:C), a synthetic dsRNA that possesses similar immunogenic properties to viral dsRNA (Yang et al., 1995; Chu et al., 1999). Despite these *in vitro* findings the IFN response is often intact upon virus infection in PKR deficient mice (Balachandran et al., 2000a; Levy, 2002; Abraham et al., 1999). This suggests that additional recognition receptors are involved in the recognition of viral dsRNA.

TLR 3 was shown to be a key dsRNA sensing molecule during host anti-viral responses in a paper by Alexopoulou *et al.* (Alexopoulou et al., 2001). HEK293 cells that are ordinarily non-responsive to dsRNA were made responsive by transfection with TLR 3, initiating activation of NF-κB upon dsRNA exposure, suggesting TLR 3 alone was *sufficient* for dsRNA sensing. Furthermore, macrophages derived from TLR 3 deficient mice are non-responsive to poly(I:C) and purified Lang reovirus genomic dsRNA and are unable to elicit IFN production – suggesting TLR 3 expression is also *necessary* for dsRNA sensing. TLR 3 deficient mice were also resistant to shock induced by poly(I:C) treatment, suggesting TLR 3 contributes to the *in vivo* recognition of and responses to extracellular dsRNA (Alexopoulou et al., 2001). Furthermore, the effecter responses initiated by TLR 3-poly(I:C) interaction can inhibit murine γ herpes virus 68 replication in bone marrow derived cultures (Doyle et al., 2002). A more recent study has investigated the role TLR 3 plays during Cytomegalovirus (CMV) infection (Tabeta et al., 2004). Mice deficient in TLR 3 possessed elevated virus loads, and could not upregulate key inflammatory cytokines, IFN-β or activate natural killer cell to the levels observed in wild-type mice infected with CMV. In addition, the activation of Natural Killer cells was found to be significantly decreased in mice lacking TLR 3 during CMV infection (Tabeta et al., 2004). In this study, mice deficient in TLR 9 were also shown to have a dramatically reduced anti-viral response (further discussed in section 1.1.11). Mice deficient in TLR 3 exhibit markedly different immune responses to West Nile virus (WNV). Spleen infection is more substantial and inflammatory cytokine expression is reduced in mice lacking TLR 3 expression (Wang et al., 2004).

Taken together it seems highly probably that TLR 3 recognises the unique molecular pattern of dsRNA. However, some doubts remain over the functional significance of TLR 3 during natural infections, since the principle cell type in human and mouse blood that produces type-1 IFNs are plasmacytoid dendritic cells (Asselin-Paturel et al., 2001; Siegal et al., 1999), and several publications suggest TLR 3 is either absent or expressed at low levels in these cells (Kadowaki et al., 2001a). One can speculate that PKR and TLR 3 act together or indeed with other members of the TLR family, or that signalling through either may be sufficient to initiate the IFN system. Unfortunately, there is little in the literature that informs us of how PKR and TLR 3 collaborate.

The *in vivo* significance of TLR 3 function has been questioned in a recent report that infected TLR 3 deficient mice with four different viruses: lymphocytic choriomeningitis virus (LCMV), vesicular stomatitis virus (VSV), CMV and reovirus. Virus titres were similar in TLR 3 deficient and wild type mice for all four viruses, as were T cell responses. The ability of TLR 3 deficient mice to promote immunological memory also appeared to be similar to wild-type mice. In addition, reovirus-associated immunopathology in the brain was found to be similar, as were the mortality levels. Importantly, this study did not examine whether activation of innate immunity, in particular type I IFN production, was abrogated in TLR 3 deficient mice. Nevertheless, TLR 3 signalling does not appear to influence the generation of effective antiviral responses for these four viruses given at these particular doses (Edelmann et al., 2004). A separate report has shown IRF3 (a signalling molecule downstream of TLR 3 described in section 1.1.15) deficient mice were more susceptible to CMV infection when given at higher doses (Hoebe et al., 2003) as were TLR 3 deficient mice in the study by Tabeta *et al.* (Tabeta et al., 2004), which also described changes in innate immune responses. In addition, several studies have shown robust type-I IFN responses are mediated by TLR 3 signalling *in vitro* (Alexopoulou et al., 2001; Kulka et al., 2004; Jiang et al., 2003) Thus, there are conditions where TLR 3 does signal in a functionally meaningful manner. One can speculate that the *in vivo* functional significance of TLR 3 signalling may be restricted to the early control of an overwhelming infection requiring fast and strong interferon type-I responses to prevent host death (Edelmann et al., 2004). Consequently, it has been suggested that the concentrations of dsRNA made during "natural" infection are often not sufficient to bind to and significantly influence TLR 3 signalling when compared to the high concentrations of dsRNA used for *in vitro* studies (Edelmann et al., 2004).

The subcellular location of TLR 3 differs between cell types. Fibroblast cells express TLR 3 on the cell surface whilst both immature and activated dendritic cells demonstrate TLR 3

expression that is restricted to sub-cellular compartments (Matsumoto et al., 2003). Studies using immature monocyte derived dendritic cells have shown TLR 3 is expressed within intracellular vesicles and that the retention within this compartment is reliant on the specific sequence that links the extracellular LRR domain and the cytoplasmic TIR domain (Funami et al., 2004). Analysis has revealed that when TLR 3 is ectopically expressed within a murine B cell line, it is found only within multivesicular bodies – a subcellular compartment situated in the endocytic trafficking pathways (Matsumoto et al., 2003).

To summarise, several studies have suggested the activation of TLR 3 and the subsequent secretion of IFN-α/β helps to establish a localised antiviral state that limits viral replication at the site of infection. Conversely, one *in vivo* study has cast some doubt on whether the concentration of viral dsRNA during "natural" infection is high enough to trigger significant TLR 3 signalling. TLR 3 is unique from all other TLR in several ways. Firstly, the protein lacks a critical proline residue that is conserved in all other TLR (indeed this is the mutation that was responsible for generating the TLR 4 associated LPS hyporesponsive phenotype in C3H/HeJ mice). Secondly, its gene is uniquely encoded by 4 exons and the complete gene sequence is spread over 5. Thirdly, the expression of TLR 3 is maintained in certain mature DC subsets that ordinarily down-regulate all other TLR upon maturation - see later for more details (Muzio et al., 2000).

1.1.11 TLR 7, 8 and 9 recognise microbial nucleic acids

Bacterial and viral DNA are potent immunogens due to the presence of unmethylated CpG motifs that are infrequent in vertebrate genomes, and represent a prototypic molecular pattern that distinguishes a certain class of pathogen. Mice deficient in TLR 9 fail to respond to CpG inoculates demonstrating that TLR 9 is necessary for sensing CpG motifs (Hemmi et al., 2000). TLR 9 alone is also sufficient to confer CpG recognition in HEK293 cells (Bauer et al., 2001). Recognition occurs in the endosome where it is expressed (Wagner, 2001; Ahmad-Nejad et al., 2002) and not at the cell surface like ligands for TLR 1, 2 and 4 that are actively recruited from the cell surface to phagosomes upon stimulation (Takeuchi et al., 1999a; Ozinsky et al., 2000).

In addition to the role TLR 9 plays in sensing bacterial CpGs, this important receptor is also critical for sensing the DNA of herpes simplex virus type 1, herpes simplex virus type 2 and murine CMV, all of which contain genomes rich in CpG DNA motifs (Krug et al., 2004; Tabeta et al., 2004; Lund et al., 2003). Mice with non-functional TLR 9 are highly susceptible to CMV infection, produce low levels of IFN-α and IFN-β, and cannot activate natural killer cells in response to infection, unlike their wild-type counterparts. Specifically,

CMV titres are elevated by four orders of magnitude in TLR 9 deficient mice and exhibit a 90% decrement in the amount of type I IFN produced. TLR 3 knockout mice were also shown to exhibit deficiencies in their response to CMV infection, although not to such a degree as observed in TLR 9 mutants. TLR 3 deficient mice exhibited a 60% decrement in the amount of type I IFN and suffer an elevated CMV titre of three orders of magnitude. These findings are rather surprising since the TLR 3/Trif signalling axis is independent of the TLR 9/MyD88 signalling axis (see section 1.1.15). Nevertheless, the two pathways do elicit the production of type I IFN in a co-dependent manner.

TLR 9 is expressed within the endoplasmic reticulum (ER) of macrophages and monocyte derived dendritic cells and not on the cell surface. Studies using fluorescent CpG DNA show that within minutes of exposure, CpG DNA enters monocyte derived dendritic cells via the endosome pathway and are rapidly transported to a tubular lysosomal compartment. Concurrent with CpG transport, TLR 9 is actively redistributed from the ER to the CpG DNA-containing structures, which also accumulate MyD88. As such, this represent a novel mechanism of cellular activation involving the recruitment of an immune receptor from the ER to CpG-containing structures where signal transduction is initiated (Latz et al., 2004; Leifer et al., 2004).

Until two landmark papers were published simultaneously in *Science*, 2004, little was known concerning the *in vivo* function of TLR 7 and its close relative TLR 8 - apart from their well established roles as receptors for a family of anti-viral compounds that includes imiquimod (Hemmi et al., 2002). Imiquimod possesses potent anti-viral properties, owing to its ability to induce inflammatory cytokines, especially IFN-α, and has been approved for the treatment of genital warts caused by infection with human papillomavirus. Imiquimod and its related compounds all have structures similar to nucleic acids and the finding that TLR 7 deficient mice cannot respond to these compounds suggested that TLR 7 might sense viral infection by recognising viral nucleic acids that resemble the anti-viral compounds (Hemmi et al., 2002). This suggestion has since been verified independently by two groups showing that in murine dendritic cells, TLR 7 recognises single stranded RNA (ssRNA) rich in uracil – such as influenza RNA and synthetic polyU RNA. TLR 8 appears to have an analogous function in humans (Heil et al., 2004; Diebold et al., 2004). The authors further suggest that viral and cellular ssRNA can be distinguished from each other, since ssRNA released by cells to the extracellular environment is rapidly degraded. Thus, RNA taken up by phagocytic cells within the confines of a virus particle can be presented to TLR 7/8 with the confidence that it is not of cellular origin - since self RNAs will rarely reach the endocytic compartment where TLR 7/8 reside.

To summarise, it appears likely that the TLR 9 subfamily including TLR 7, 8 and 9 may all participate in the discrimination of microbial nucleic acid-like structures. This parallels the situation in the TLR 2 subfamily, which discriminates between differences in bacterial lipoproteins (Takeda et al., 2003).

1.1.12 TLR 11 recognises uropathogenic bacteria

TLR 11 is a newly described TLR that has recently been shown to play role in sensing bacteria that cause infections of the bladder and kidney (Zhang et al., 2004). TLR 11 was discovered by searching the EST databases for sequences with similarity to TLR 4 and was discovered in a mouse liver EST database. Further analysis revealed that TLR 11 was particularly abundant in the kidney and bladder of mice. Mice generated to lack TLR 11 harboured 10,000 times as many bacteria in their kidneys compared to wild-type mice, and could not mount pro-inflammatory responses. Interestingly, humans possess a truncated version of TLR 11 that is almost certainly inactive. This might explain why humans are particularly susceptible to urinary tract infections (Zhang et al., 2004; O'Neill, 2004).

1.1.13 TLR are expressed in a variety of cells that are likely to first encounter antigen

Several studies have reported the expression patterns of TLR in several key cells of the immune system and are summarised in table 2 and 3. Suitable antibodies that label TLR have not been readily available, particularly for murine TLR. Thus, work that has studied TLR expression has mostly relied on assaying RNA levels. Macrophages express most TLR mRNAs except TLR 3 according to one report (Muzio et al., 2000), which stated that TLR 3 was only found on mature dendritic cells. Another study found human phagocytes, including monocytes expressed all TLR mRNAs including TLR 3, albeit at low levels. B cells express TLR 9 and 10 at very high levels and TLR 1, 3, 6, 7, 10 and RP105 at intermediate levels, whilst T cells expressed predominantly TLR 3 and 9, although all TLR were detectable at lower levels (Zarember and Godowski, 2002; Bourke et al., 2003). A third study determined monocytes express high levels of TLR 2, intermediate levels of TLR 4, 5, 6 and 8, weak levels of TLR 9 and no TLR 3, 7 and 10 (Hornung et al., 2002). Most human tissues were shown to express at least one TLR with the spleen expressing all TLR 1-10. Regrettably, only one sample was assayed for each respective tissue, casting some doubt over its reliability (Zarember and Godowski, 2002). The fact that TLR 3 was readily detected in other cell populations appears to contradict the report by Muzio *et al.* However, it may be explained by the differing assays employed in each case, with the report by Zarember and

Godowski utilising the more sensitive Taqman assay. Comparatively little work has been undertaken on murine cells and tissues to systematically describe TLR expression.

Expression appears to be highly varied among different dendritic cell subsets and is species specific. Human monocyte-derived dendritic cells (MDCs) express at high levels TLR 3 and at immediate levels TLR 1, 2, 3, 4, 5, and 8. Conversely, plasmacytoid dendritic cells (PDCs) predominantly express TLR 7 and 9 (Kadowaki et al., 2001b; Krug et al., 2001). Another study demonstrated both PDCs and B cells predominantly express TLR 7 and 9. Indeed, only these cells were shown to be directly responsive to CpG motifs whilst monocytes, natural killer cells and T cells, which expressed no TLR 7 and little TLR 9, could not respond directly to CpG motifs. Although, co-culture of these cell types individually with PDCs rendered them responsive to CpGs (Hornung et al., 2002). MDCs mature upon exposure to microbial components and as they mature the expression of TLR 1, 2, 4, and 5 are lost whilst the expression of TLR 3 increases (Visintin et al., 2001). The exact cellular expression pattern of TLR mRNAs is confused and more work is required to clarify the matter in both human and murine systems.

Several studies have investigated the expression of TLR on other cell types that contribute to inflammatory responses. Mast cells are important mediators of acute inflammation and appear to express TLR 2, 4, 6 and 8 but not TLR 5 (Supajatura et al., 2001; McCurdy et al., 2001). The expression of TLR has also been studied in epithelial cells. Epithelial cells cover mucosal surfaces such as the respiratory tract and form a protective and continual barrier to bacterial exposure, and yet do not generally induce an inflammatory response. However, epithelial cells do respond if pathogenic bacteria invade into the basolateral compartment where TLR 5 is specifically expressed (Gewirtz et al., 2001). There is little TLR 4 in the intestine mucosa unless the host suffers from inflammatory bowel disease in which TLR 4 is upregulated (Cario and Podolsky, 2000). Consistent with this data is the idea that inflammatory bowel disease may result from exaggerated inflammatory responses to commensal bacteria. Nevertheless, all the data indicate that TLR are finely regulated within epithelial cells and generally absent unless stimulated.

1.1.14 TLR expression can be modulated by microbes and cytokines

The mechanisms behind TLR expression are not well understood. TLR expression is finely tuned and can be altered by either exposure to microbial components, microbial invasion, and/or cytokines. These complex interactions are summarised in tables 2 and 3.

Several studies have demonstrated that murine cells such as phagocytes can alter their TLR expression patterns in response to innate immune stimuli. LPS enhances the expression of

	Technique	TLRs assayed	Monocytes	MDCs	Mature MDCs	PDCs
Muzio *et al.* 2000	Northern blot	1 to 5	1,2,4,5	1,2,3,4,5	-	-
Zarember and Godowski, 2002	Taqman QPCR	1 to 10	1,2,3,4,5,6,7,8,9,10	-	-	-
Hornung *et al.* 2002	SYBR QPCR	1 to 10	1,2,4,5,6,8,9	-	-	1,6,7,9,10
Kadowaki *et al.* 2001	QPCR	1 to 10	1,2,4,5,8	1,2,3,4,5,6,10	-	7,9
Visinitn *et al.* 2001	Northen blot	1/6, 2,3,4,5	1/6,2,4,5	1/6,2,3,4	3	-
Bosisio *et al.* 2003	Northen blot	1 to 10	-	-	-	-

	Technique	TLRs assayed	T cells	B cells	NK cells
Muzio *et al.* 2000	Northern blot	1 to 5	1	1	-
Zarember and Godowski, 2002	Taqman QPCR	1 to 10	3, 9	1, 3, 6, 7, 9	-
Hornung *et al.* 2002	SYBR QPCR	1 to 10	1,2,3,5,6,8,9	1,2,6,7,9,10	1,2,3,5,6,9
Kadowaki *et al.* 2001	QPCR	1 to 10	-	-	-
Visinitn *et al.* 2001	Northen blot	1/6, 2,3,4,5	-	-	-
Bosisio *et al.* 2003	Northen blot	1 to 10	-	1,6,7,8,9,10	-

Table 2. TLRs expressed by human cells of the immune system. Those TLRs highlighted in red represent those TLRs that are expressed most highly.

	Technique	TLRs assayed	LPS		LPS		IFN-gamma	
			Monocytes/Macrophages		THP-1 macrophage		Monocytes/Macrophages	
			Up regulated	Down regulated	Up regulated	Down regulated	Up regulated	Down regulated
Zarember and Godowski, 2002	Taqman QPCR	1 to 10	2,3,4,7,8	1,5,6,9	1,2,3,4,7,8	none	-	-
Visinitn *et al.* 2001	Northen blot	1/6, 2,3,4,5	2,4	1/6, 5	-	-	-	-
Bosisio *et al.* 2002	Northern, Western, FACS	4	-	-	-	-	4	-

Modulation of TLRs in human monocyte/macophages. Those TLRs highlighted represent the the TLR that is most dramatically altered

	Technique	**TLRs assayed**	**LPS**		**poly(I:C)**		**IFN-alpha/beta**	
			Monocytes/Macrophages		**Monocytes/Macrophages**		**Monocytes/Macrophages**	
			Up regulated	**Down regulated**	**Up regulated**	**Down regulated**	**Up regulated**	**Down regulated**
Matsuguchi *et al*.2000	QPCR and Western blot	2,4	2	4	-	-	-	-
Wang *et al*. 2000	RPA	2,4	2	4	-	-	-	-
Nomura *et al*.2000	Northen blot and FACS	4	-	4	-	-	-	-
Sweet *et al*.2002	QPCR	4,9	-	-	-	-	-	-
Roger *et al*.	Northerns, FACS, promoter	4	-	-	-	-	-	-
	assays				-	-	-	-
Doyle *et al. 2003*	QPCR	3,4	3	4	3	-	3	-
Miettinen *et al*. 2001	Northern	1 to 9			-	-	1,2,3,7	-

Modulation of TLRs in murine monocyte/macrophages.

Table 3. A summary of TLR expression patterns following infection or stimulation

TLR 2 in macrophages whilst TLR 4 was down-regulated, both at the RNA and protein level (Matsuguchi et al., 2000). As such, it has been suggested that this may be one mechanism by which the phenomena of LPS tolerance is mediated (Nomura et al., 2000). Following exposure to live *Salmonella* murine macrophages rapidly down regulate TLR 4 protein levels so that by 6 hours the receptor is undetectable. Conversely, *Salmonella* exposure does not alter TLR 2 expression within 6 hours, but by 24 hours is significantly elevated (Weiss et al., 2004), suggesting TLR expression is differentially regulated over time. In addition, mice infected with *Mycobacterium avium* upregulate their levels of TLR 2 in macrophages by increasing TLR 2 promoter activity with chromatin remodelling. Concurrently, levels of TLR 4 were found to be down-regulated (Wang et al., 2000; Wang et al., 2001; Wang et al., 2002). Another study looked at the levels of TLR 2 in γδ T cells. γδ T cells are considered to be primordial innate sensors of infection that lack the antigen receptor diversity of other T cells. These cells upregulate TLR 2 upon infection with *E.coli* (Mokuno et al., 2000).

The level of TLR expression exerts an effect on the function of immune cells. Indeed, the level of TLR expression affects macrophage responses to microbial stimuli. Macrophage responses have been correlated with levels TLR expression by analysing macrophages deficient in either TLR 2 or TLR 4 or both. TLR 4 ligands appear to induce an early TNF-α response, whilst TLR 2 ligands generate a later TNF-α response. These responses correlate with the timing of TLR expression, such that TLR 4 ligands induce a response only whilst TLR 4 is expressed, whilst TLR 2 ligands can only induce cytokine release once TLR 2 has been upregulated (Weiss et al., 2004). Furthermore, monocyte-derived dendritic cells induced to upregulate TLR 7 expression have increased sensitivity to the TLR 7 ligand imiquimod (Mohty et al., 2003). Together these data suggest that TLR expression change can have dramatic effect on the responsiveness of macrophages to microbial stimuli.

A limited number of studies have looked at TLR expression during virus infections. One study used Northern analysis to demonstrate an apparent upregulation of TLR 1, 2, 3 and 7 in bone-marrow derived macrophages infected with Influenza A and Sendai virus. This upregulation was suppressed by treatment with blocking antibodies to IFN-α/β, suggesting that IFN mediates virus induced activation of innate immunity via modulation of TLR expression *in vitro* (Miettinen et al., 2001). Human monocytes isolated from HIV-infected patients display enhanced expression of TLR 2, although TLR 4 levels were unaffected. Furthermore, *in vitro* stimulation of human monocytes with the HIV envelope proteins triggers an increase in TLR 2 expression, supporting a possible link between HIV infection and TLR 2 expression. Interestingly, stimulation of the TLR 2 pathway with a TLR 2-specific agonist significantly increased viral replication along with enhanced cytokine

production (Heggelund et al., 2004). In addition, infection of mice with *mycobateria* upregulates HIV-1 expression, a phenomenon that is not observed in TLR 2 deficient mice, suggesting innate activation of the TLR 2 pathway enhances HIV replication *in vivo* (Bafica et al., 2003; Bafica et al., 2004).

Several cytokines regulate TLR expression. Colony stimulating factor 1 (CSF1) down-regulates TLR 9 in macrophages and strongly suppresses CpG-induced production of inflammatory cytokines (Sweet et al., 2002). Macrophage inhibitory factor (MIF) is a cytokine that mediates inflammation and sepsis and (Bozza et al., 1999) upregulates and/or maintains TLR 4 expression (Roger et al., 2001; Roger et al., 2003). IFN-γ can prime macrophages and phagocytes to respond to LPS and evidence suggests it is the upregulation of TLR 4 by this cytokine that mediates this priming (Bosisio et al., 2002). The expression of TLR 2 but not TLR 4 in macrophages can be upregulated by a series of cytokines including IL-1β, IL -2, IL -15, IFN-β and TNF-α (Matsuguchi et al., 2000). Further work has shown the expression of TLR 2 and 4 in renal epithelial cells can be induced by exposure to IFN-γ and TNF-α and so contributes to the detection of bacterial invasion in the lumen of tubules and the induction of an inflammatory response (Wolfs et al., 2002).

A study by Doyle *et al.* demonstrated that IFNα/β signalling could induce upregulation of TLR 3. This study utilised bone marrow-derived macrophages from mice lacking a functional IFNα/β receptor and found TLR 3 expression did alter upon exposure to poly(I:C) or LPS, which ordinarily upregulates TLR 3 expression in this cell type. The addition of recombinant IFN-β caused a dose-dependent increase in TLR 3 in macrophages from wild-type mice. This data demonstrates bone marrow derived macrophages that are cultured and matured *in vitro* are capable of responding to type I IFNs by upregulating TLR 3 expression (Doyle et al., 2003).

1.1.15 TLR signalling is complex and multi-faceted

TLR recognise a variety of differing microbial components and respond appropriately: LPS stimulates pro-inflammatory cytokines such as TNF-α whilst viruses induce anti-viral type-I IFNs. The intracellular signalling mechanisms that underlie this specificity are being characterised at an increasingly rapid rate. Two main pathways have been characterised that respond to TLR activation; one involves activation of the TLR adaptor protein MyD88 followed by NF-κB activation and consequent induction of a pro-inflammatory state; the second involves a MyD88-independent pathway that utilises the TLR adaptor TRIF and leads to induction of IFN-β. Indeed, it now appears that the ability of immune cells to utilise

different combinations of TLR adaptors allows several different signalling pathways to be initiated. Figure 3 summarises our current understanding of TLR signalling.

1.1.15.1 The MyD88-dependent pathway leads to pro-inflammatory gene expression

Upon binding to their respective ligands. TLR undergo activation by dimerisation and undergo conformation changes that enable the recruitment of cytosolic downstream adaptors including myeloid differentiation factor 88 (MyD88), IL-1R-assocaited kinases (IRAKs), transforming growth factor-activated kinase 1 (TAK1), TAK-1 binding protein (TAB1), TAB2 and tumour necrosis factor receptor associated factor 6 (TRAF6) (Akira and Takeda, 2004).

MyD88 is a key TLR signalling molecule originally isolated as a gene induced by IL-6 differentiated macrophages (Lord et al., 1990). It possesses a death domain (DD) as its N-terminal domain followed by a TIR domain. Myd88 can form dimers with other proteins via both its TIR domain (for example TLR) and its DD (Myd88 homodimers). Studies have shown that MyD88 is recruited to activated TLR as a homodimer and functions as an adaptor linking TLR/IL-1R with downstream signalling molecules that possess DDs (Dunne et al., 2003).

IRAKs are a family of proteins that all contain N-terminal death domains (DDs) and a central kinase domain that phosphorylates down stream targets. IRAK4 interacts with MyD88 and IRAK1 to mediate TLR signalling. Mice with deficiencies in IRAK4 demonstrated a total lack of LPS responsiveness whilst mice deficient in IRAK1 exhibited mildly deficient LPS responses (Swantek et al., 2000). Interestingly, humans who possess deficiencies in IRAK4 have been identified. These patients could not respond to IL-1, IL-18 or stimulation with a multitude of TLR ligands (TLR 2, 4, 5 and 9) (Picard et al., 2003).

TRAF6 functions as a signalling mediator for both the TNF receptor and TIR superfamily. Upon TLR activation TRAF6 activates the NF-κB transcription factor with the use of TAK1 and two adaptor proteins TAB1 and TAB2. (Bradley and Pober, 2001; Yamaguchi et al., 1995; Takaesu et al., 2003). TAB1 functions to enhance TAK1 kinase activity whilst TAB2 acts to link TAK1 to TRAF6 (Takaesu et al., 2000).

NF-κB is a member of a family of transcription factors, each of which function as homo- and hetero-dimers. They are ordinarily sequestered in an inactive state in the cytoplasm by molecules of the inhibitor IκB family. The activation of NF-κB is mediated by the IκB kinase (IKK) complex, which phosphorylates the inhibitory IκB component and as such labels it for proteasome-mediated degradation. The removal of IκB enables the now fully

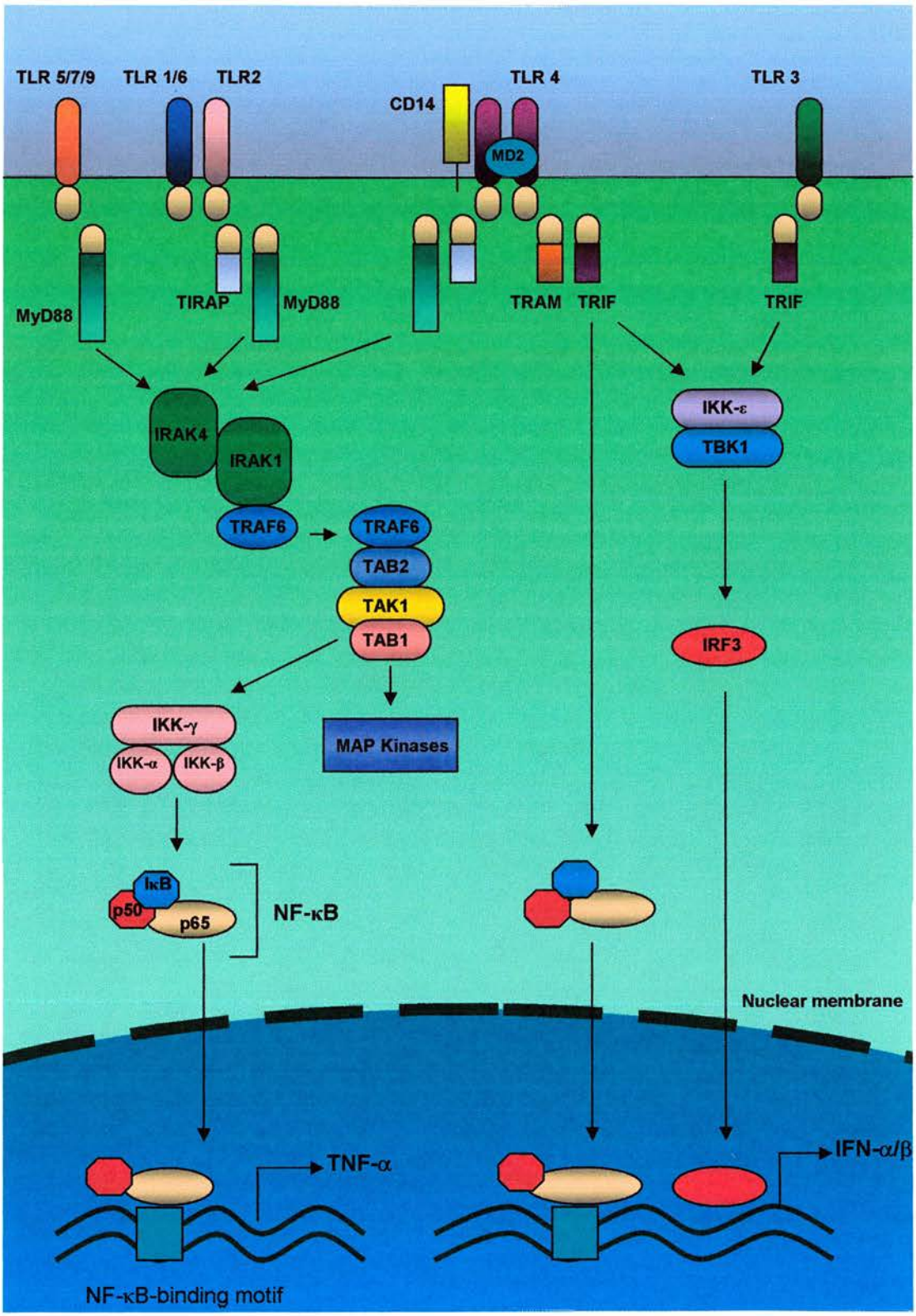

Figure 3 TLR signalling pathways. TLR can signal through at least two pathways to initiate either pro-inflammatory cytokine or type-I IFN expression. Some data suggests TLR 9 may activate type-I IFN expression, although the mechanism remains to be elucidated

active NF-κB to translocate to the nucleus where it can mediate transcription of a multitude of pro-inflammatory genes (Karin and Ben Neriah, 2000; Adachi et al., 1998; Akira and Takeda, 2004). These interactions are illustrated in figure 3.

1.1.15.2 MyD88-independent pathways

MyD88 is an essential component of the TLR pathway that mediates responses to a wide range of microbial components. Indeed, mice deficient in MyD88 cannot produce TNF-α or IL-6 in response to IL-1 or microbial components recognised by TLR 2, 4, 5, 7 or 9 (Takeda et al., 2003; Adachi et al., 1998). However, closer study of these mice revealed the existence of a MyD88-independent pathway that also mediates signalling in response to LPS and dsRNA (Kawai et al., 1999). Whilst most TLR utilise the MyD88-dependent pathway, a subset of TLR responses remains intact in MyD88-deficient mice. MyD88 deficient cells exposed to LPS induce a variety of genes, many of which are IFN-inducible, such as glucocorticoid-attenuated response gene 16 (GARG16) and immunoresponsive gene 1 (IRG1) (Kawai et al., 2001). Conversely, cells that are deficient in TLR 4 alone cannot induce either pro-inflammatory genes or IFN-inducible genes in response to LPS. Together this suggests the induction of IFN-inducible genes (such as GARG16 and IRG1) in response to LPS was possible despite the lack of MyD88 (Kawai et al., 2001). Studies have shown that ligands for TLR 2, 5, 6, and 7 do not engage this alternative MyD88-independent pathway (Toshchakov et al., 2002; Akira and Takeda, 2004).

The MyD88 pathway was studied in respect to DC maturation and found that maturation induced by LPS could occur through either MyD88-dependent or -independent pathways. However, maturation via the MyD88-independent pathway only occurs secondary to the production of IFN-β, suggesting this pathway leads to the production of type I interferons (Hoshino et al., 2002). Importantly, TLR 3 appears to signal through the MyD88-independent pathway to induce IFN-β production, since MyD88 deficient cells respond normally to poly(I:C). Thus, TLR 2, 5, and 7 signal exclusively through the MyD88-dependent pathway, whilst TLR 3 signals exclusively through the MyD88-independent pathway, and TLR 4 can signal through both pathways. The MyD88-independent pathway is illustrated in both figure 3 and figure 4 and is further discussed below in section 1.1.15.4.

1.1.15.3 TLR provide specificity to innate immune responses through the differential use of TIR-containing adaptors

The activation of different TLR results in the induction of differing patterns of gene expression. The molecular mechanisms that underlie these differences are now, in part,

explained by the existence of several adaptors that are used by different TLR. These adaptors include MyD88, TIRAP (TIR domain-containing adaptor protein, also known as MyD88-adaptor-like protein, MAL), TRIF (TIR domain-containing adaptor protein inducing factor, also known as TICAM1) and TRAM (TRIF-related adaptor molecule, also known as TICAM2).

TIRAP was the second TIR-containing adaptor identified after MyD88 and functions in the MyD88-dependent pathway following activation of TLR 1, 2, 4 and 6 alone (Horng et al., 2001; Fitzgerald et al., 2001; Yamamoto et al., 2002a).

A third TIR-containing adaptor, TRIF (also identified concurrently as a TLR 3-binding molecule, and called TICAM1) functions in the MyD88-indpendent pathway. TRIF-deficient mice possess impaired activation of IFN-regulatory factor 3 (IRF3), along with decreased expression of IFN-inducible genes (Yamamoto et al., 2002b; Oshiumi et al., 2003). Independently, a group studying the LPS-hyporesponsive phenotype *Lps2* discovered *Trif* was the gene responsible for both TLR 3- and TLR 4-activation of the MyD88-independent pathway and was abrogated in the *Lps2* strain (Hoebe et al., 2003). Together, these studies demonstrated that TRIF is essential for TLR 3- and TLR 4-activation of the My88-independent pathway, which subsequently leads to the expression of IFN-β and in turn the IFN-inducible genes.

Interestingly, TRIF deficient mice have normal responses to TLR 2, 7, 5 and 9 ligands but exhibit deficient responses to LPS signalling through TLR 4, despite normal MyD88-pathway signalling. This suggests the induction of pro-inflammatory cytokines through TLR 4, requires signalling through the MyD88-dependent and -independent/TRIF dependent pathways (Hoebe et al., 2003; Yamamoto et al., 2002a). By contrast, the activation of the MyD88-dependent pathway alone is sufficient to induce cytokine expression in response to activation of TLR 2, 5, 7 or 9 – none of which activate the MyD88-independent/TRIF dependent pathway. It is not known why TLR 4-mediated responses requires both MyD88-dependent and -independent pathways to induce cytokine expression. Perhaps this represents an extra mechanism by which the host protects itself against lethal cytokine excess that occurs during septic shock.

Finally, further database searches revealed the existence of another TIR containing adaptor, TRAM. TRAM appears to function in conjunction with TRIF and TLR 4, but does not associate with TLR 3, to mediate expression of IFN-inducible genes through the MyD88-independent pathway (Yamamoto et al., 2003). Figure 3 and 4 illustrates the differential use of the TIR-containing adaptors by TLR.

1.1.15.4 The antiviral MyD88-independent/TRIF dependent pathway involves IRF3 and NF-κB

Expression of IFN-β and hence all the IFN-inducible genes requires activation of IRF3 and NF-κB, as described in figure 4 (Yoneyama et al., 1998). IRF3 is expressed constitutively and is phosphorylated upon virus infection at its C-terminal regulatory domain by two IKK-related proteins: IKK-ε and TBK1 (Sharma et al., 2003; Fitzgerald et al., 2003). Phosphorylation enables dimerisation and consequent translocation to the nucleus where it activates transcription of type I IFNs. Once secreted, type I IFNs can signal in an autocrine fashion to activate the expression of IFN-inducible genes (including IFN itself) via Janus Kinase/STAT pathways and further enhance IFN expression (Taniguchi and Takaoka, 2002). Stimulation with LPS can also induce IFN-β production via TLR 4-mediated IRF3 activation in a Myd88-independent manner. However, the activation of IRF3 through TLR 3 is more rapid and potent than that triggered through TLR 4 signalling. Indeed, TLR 3 signalling initiates a more pronounced phosphorylation of IRF3 than TLR 4 signalling. These findings may explain why TLR 3 ligands trigger a more sustained release of IFN-β (Doyle et al., 2003; Servant et al., 2003; Akira and Takeda, 2004).

Transcriptional activation of the *IFN-β* gene appears to require activation of both IRF3 and NF-. B (figure 4). TRIF can mediate activation of NF-κB through its C- or N-terminal domains, whilst TRIF can only activate IRF3 through its N-terminal domain (Yamamoto et al., 2002b). TRAF6 interacts with TRIF, thus allowing TRIF to activate NF-κB independently of MyD88 (Sato et al., 2003). As stated above IRF3 is activated by TBK1, which associates with the N-terminal of TRIF. Thus, the N-terminal region of TRIF directly associates with TRAF6 and TBK1, leading to activation of NF-κB and the IRF3 gene respectively. The C-terminal of TRIF can also activate NF-κB via an interaction with the receptor-interacting protein 1 (RIP1) (Meylan et al., 2004).

To summarise, TLR 3-mediated IFN-β expression occurs as a consequence of two pathways that diverge from its TIR domain: one that triggers NF-κB via a TRIF/TRAF6 interaction; and one pathway that activates IRF3 through the kinase activity of TBK1 and IKK-ε. Figure 4 illustrates these findings diagrammatically.

The response of dendritic cells (DC) to CpG motifs is less well understood. TLR 9 activation also leads to the induction of type-I IFN synthesis. CpG motifs activate IFN-α expression in human PDCs, which predominantly express TLR 7 and 9 (Krug et al., 2001; Krug et al., 2003) and in other murine DC subsets (Hemmi et al., 2003). Type-I IFN expression is not inducible in MyD88 deficient cells, suggesting that the TLR 9/MyD88-dependent pathway

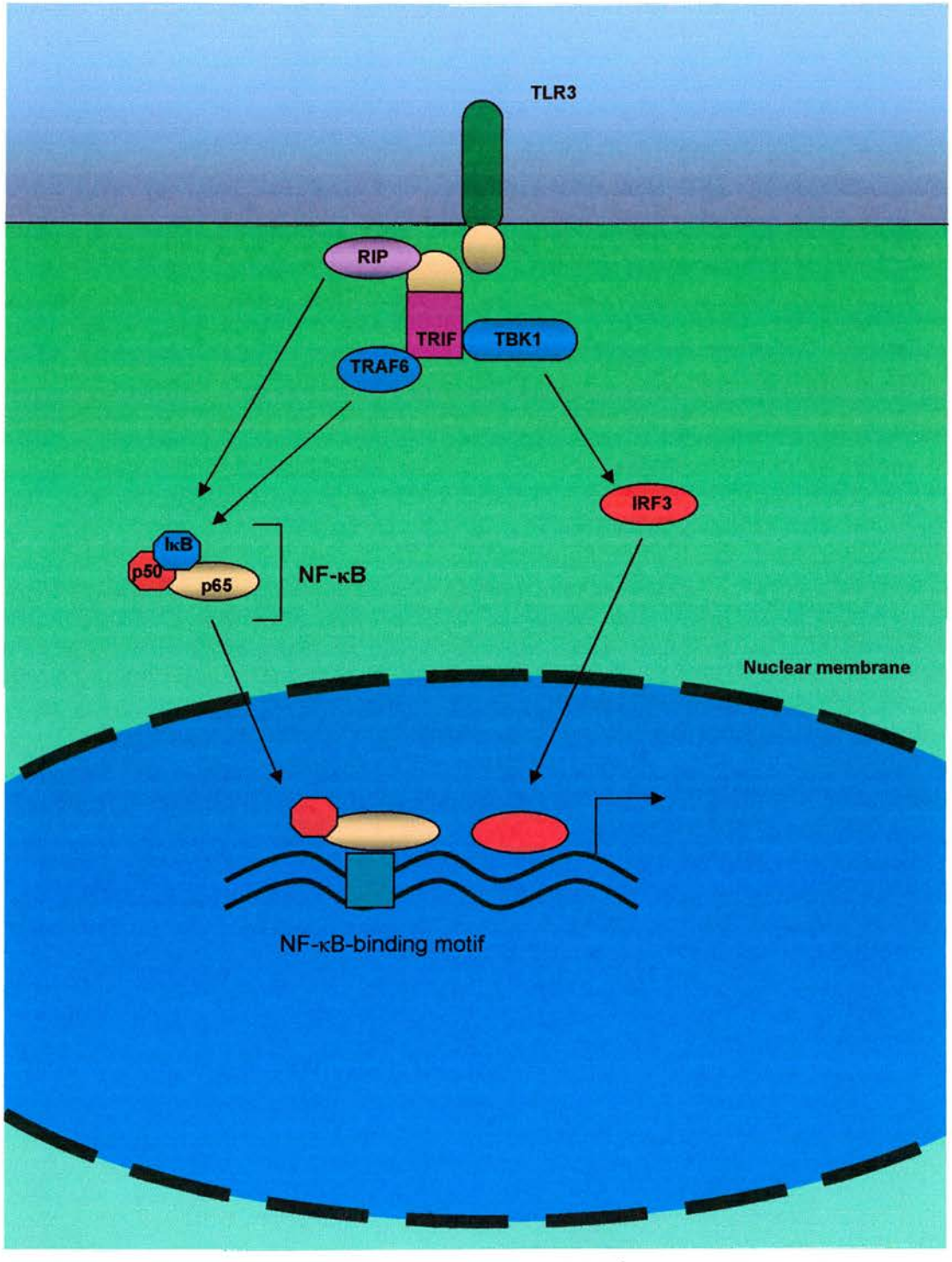

Figure 4, TLR 3 signalling activates both IRF3 and NF-κB through a MyD88-independent manner. Activated TLR 3 can associate with TRIF through the binding of their common TIR domains. The localisation of TRIF to the plasma membrane allows RIP, TRAF6 and TBK1 to associate. RIP and TRAF6 act to free NF-κB of its inhibitory component, whilst TBK1 activates IRF3. Activation of these transcription factors induces their translocation to the nucleus where upon they induce production of IFN-β. IFN-β acts in a paracrine and autocrine fashion to further upregulate type-I IFN and initiates a potent anti-viral response.

is essential for cellular responses to CpG motifs found in viruses and bacteria (Hemmi et al., 2003).

1.1.15.5 Negative regulation of TLR signalling

It is perhaps not surprising that animals have developed mechanisms for modulating TLR-responses following activation – since excessive production of cytokines can lead to lethal systemic disorders such as septic shock (Akira and Takeda, 2004). In macrophages following LPS-mediated activation, levels of IRAK-M increase in the cytoplasm. This IRAK family member prevents the dissociation of the IRAK1-IRAK4 complex from MyD88, thus inhibiting the TLR signalling pathway (Kobayashi et al., 2002). In addition, the expression of SOCS1 is induced following LPS and CpG exposure in macrophages (Dalpke et al., 2001). Ectopic expression of this gene in macrophages prevents LPS induced NF-. B activation, implying it directly down regulates TLR-signalling pathways, perhaps via its ability to bind to IRAK1 (Nakagawa et al., 2002). Mice deficient in either IRAK-M or SOCS1 are both hypersensitive to LPS and produce excessive quantities of cytokines. MyD88s is an alternatively spliced variant of MyD88 that lacks a domain critical for the recruitment of IRAK4. Expression of MyD88s is induced in macrophages following LPS exposure and is thought to down-regulate TLR signalling by directly competing with MyD88 (Burns et al., 2003). More recently, membrane-bound orphan receptors that contain cytoplasmic TIR domains (called SIGRR and ST2) have been identified. Mice deficient in these molecules are hyper sensitive to LPS (Wald et al., 2003).

Given the central role TLR play in sensing infection and activating immune responses it is not surprising that infectious agents have evolved mechanisms to inhibit TLR signalling. The *Vaccinia* is a complex poxvirus that expresses homologues of proteins encoded by the host immune system such as secreted decoys for cytokines. This virus also encodes proteins that inhibit TLR signalling including A46R and A52R, which act as dominant negative inhibitors in the TLR pathway and decrease NF-κB activation and cytokine release (Bowie et al., 2000; Harte et al., 2003). Furthermore, the poxvirus protein N1L is amongst the strongest determents of *vaccinia* virulence and functions to inhibit IRF3 and NF-κB so that IFN-β production is curtailed (Bartlett et al., 2002; DiPerna et al., 2004)

Both host- and microbe-derived inhibitory proteins are examples of molecules that negatively regulate the TLR pathway by their association with downstream adaptors of the TLR pathway. These studies suggest there are multiple mechanisms that exist for dampening down the responses that are activated by TLR signalling.

To summarise, the mechanisms that mediate TLR signalling are being rapidly elucidated. TIR-containing adaptors such as MyD88, TIRAP, TRIF and TRAM have crucial roles to play in the TLR pathway, providing specificity to the response generated by individual TLR. There is still much to discover; for example how differing viruses generate differing immune responses is still to be determined, with much of the current literature focussed on the mechanisms that mediate TLR responses to bacterial products.

1.1.16 Modulation of immune responses by TLR

1.1.16.1 TLR signalling primes dendritic cells to modulate T cell activation

Although long considered as non-specific, innate immune responses may be crucial in the transmission of appropriate information to the immune cells that are involved in acquired immunity. Indeed, recognition of infection by TLR triggers activation of not only innate immunity but also adaptive immunity. Most signals that initiate adaptive immune responses are provided by dendritic cells (DCs), a cell type that resides in the periphery, has a high capacity to endocytose and functions to detect the first signs of infection. DCs are readily activated by various TLR ligands such as; LPS, CpG DNA, peptidoglycan, lipoproteins and cell walls of *Mycobacteria*, which initiates their maturation (Hemmi et al., 2000; Tsuji et al., 2000; Hertz et al., 2001; Kaisho et al., 2001). As DCs mature their cell surface receptors are rapidly internalised and new receptors expressed so that they can migrate to and enter the lymph nodes. DCs also respond to TLR ligands by expressing a variety of cytokines that modulate T cell responses, losing their ability to endocytose and expressing key co-stimulatory molecules. Upon entry to lymph nodes the matured DCs can activate resident T cells by presenting antigen in the context of their MHC-II receptors to naïve T cells and so initiate an antigen specific immune response (Banchereau and Steinman, 1998; Reis e Sousa, 2001; Reis e Sousa, 2004).

The ability of DCs to steer the adaptive immune response down either a Th1-dominant response verses a Th2-dominant one has been suggested by a number of studies. This work suggests the type of TLR ligand recognised by DCs could drive distinct DC responses that in turn drive distinct adaptive immune response. Myd88 deficient mice immunised with an antigen (Ag) along with complete Freund's adjuvant (CFA) exhibit deficiencies in; the production of the Th1 cytokine IFN-γ, the activation of CD4 T cells and the production of Ag-specific IgG2a, all of which suggest the Th1 response is compromised in these mice. (Schnare et al., 2001; Kaisho et al., 2002). Furthermore, Th1 immune responses otherwise provoked by a protozoan parasite in wild-type mice, are abolished in mice lacking Myd88

(Jankovic et al., 2002). Taken together, it would seem that the Myd88-dependent signalling pathway primarily initiates Th1 immune responses.

Further evidence for the role TLR play in specifying the type of adaptive response comes from work that suggests activation of TLR 4 or TLR 9 initiates production of IL-12. This cytokine along with IFN-γ primes T cells to initiate a Th1 dominated response whilst IL-4 and IL-10 are characteristically produced during a Th2 response (Rissoan et al., 1999; Liu et al., 2001; Liu, 2001). Using LPS as a TLR 4 ligand and PGN as TLR 2 ligand, Re and Strominger showed that monocyte- derived DCs preferentially expressed IL-12 (Th1 response) or IL-10 (Th2 response) when stimulated through TLR 4 or TLR 2 respectively (Re and Strominger, 2001). A further more comprehensive study confirmed this finding using murine cells; LPS, peptidoglycan and zymosan trigger distinct programs of innate cytokine production in mice (Qi et al., 2003). The three microbial TLR activators were shown to be inherently different in their abilities to induce IL-10 and IL-12 production. Overall the results show LPS was a much stronger IL-12 inducer but weaker IL-10 stimulator than the TLR 2 ligands peptidoglycan and zymosan, which primarily stimulated T cells to express IL-10 and IL-4. The authors conclude that their results reveal that LPS, peptidoglycan, and zymosan differentially condition DCs to prime Th effecter phenotypes, suggesting that distinct microbial TLR agonists can be a cue that DCs sense in order to differentially direct Th effecter development (Qi et al., 2003). Together this data suggests TLR signalling in DCs are involved in determining the balance of Th1 / Th2 responses - an important finding considering the massive impact these responses have on the course of immune responses.

1.1.16.2 TLR signalling can directly result in microbial killing

TLR appear to be directly involved in the induction of antimicrobial activity. In *Drosophila*, the Toll pathway leads to the synthesis of antimicrobial peptides. The power of these antimicrobials have been demonstrated by a study that found a single anti-microbial peptide is sufficient to rescue the susceptibility of Spätzle/IMD double mutant flies to microbial infection (Tzou et al., 2002). These peptides have been well-characterised and as such represents a conserved and evolutionary ancient mechanism to kill microbes (Zasloff, 2002). In mammals, the best-described analogues of these antimicrobial peptides are the β-defensins. These peptides are made at the very front line of defence between pathogen and host in several kinds of epithelial cell; in the gastro-intestinal and respiratory tracts, and the skin (Zasloff, 2002). In addition, the paneth cells at the base of the crypts of the GI tracts secrete α-defensins in response to LPS or bacterial challenge (Lehrer and Ganz, 2002).

Stimulation of a lung epithelial cells with lipoproteins led to TLR-2 mediated induction of β-defensin-2 (Birchler et al., 2001). Together, these findings indicate that TLR are likely to mediate the secretion of antimicrobial peptides, hence regulating the direct killing of microrganisms at the epithelial interface between host and the environment.

In addition, TLR 2 signalling in macrophages can directly lead to microbial killing by inducing nitric oxide (NO)-dependent and independent killing of intracellular *Mycobacteria* (Thoma-Uszynski et al., 2001), whilst TLR 2 and TLR 4 deficient macrophages cannot kill phagocytosed *Salmonella* to the same extent as wild type cells (Weiss et al., 2004).

Another mechanism by which TLR may directly result in the killing of microbes is via the induction of apoptosis. Macrophages infected with invasive bacteria or viruses undergo apoptosis and in doing so may limit the spread of the pathogen (Zychlinsky et al., 1992; Allsopp and Fazakerley, 2000). Exposure of several differing kinds of microbial components to macrophages and epithelial cells can induce apoptosis such as LPS and lipoproteins. Macrophages lacking TLR 2 have a reduced capacity to enter into apoptosis upon exposure to lipoproteins, suggesting TLR may have a role to play in this phenomenon (Aliprantis et al., 1999).

1.1.17 Interferons mediate a potent anti-viral response

The interferon (IFN) response is a potent anti-viral tool that is used effectively by the host to rapidly suppress virus replication upon infection. Indeed, the effectiveness of the IFN response has led to many viruses developing mechanisms that work against either the production or actions of IFNs. It has even been suggested that all viruses must inhibit the IFN response in some shape or form if virus replication is to occur at all *in vivo*. Moreover the degree of virulence that a particular strain possesses may well be party based on its ability to circumvent the IFN response (Goodbourn et al., 2000).

The IFNs are a family of multifunctional secreted proteins that are categorised into two groups: type I IFNs are produced in direct response to virus infection and consist of the products of the IFN-α multigene family, which are predominantly expressed by leukocytes and the product of the IFN-β gene that is expressed by most cell types. In contrast, type II IFN consists of only IFN-γ that is expressed by activated T cells and natural killer (NK) cells during adaptive immune responses to viral infection (Goodbourn et al., 2000). As such the type I IFNs can be considered an innate immune response and will be discussed here.

The importance of type I IFNs has been exemplified by studies that utilise mice engineered to lack a functional receptor for type I IFNs, termed the IFN-αβ-Receptor. These mice cannot respond to IFN and hence cannot mediate any of its potent effects. As such, these

mice cannot mount effective immune responses to a wide variety of viruses and die soon after infection (Muller et al., 1994; Fiette et al., 1995; Hwang et al., 1995; Rousseau et al., 1995; van den Broek et al., 1995; Mrkic et al., 1998; Grieder and Vogel, 1999). Type I IFNs initiate a wide variety of mechanisms that can be grouped into three main strategies to resist viral infection: 1.) IFNs stimulate an anti-viral state in target cells whereby the replication of virus is blocked or impaired due to the synthesis of a number of enzymes that interfere with both cellular and viral processes; 2.) IFNs can slow the growth of target cells and/or make them susceptible to apoptosis; 3.) IFNs can have profound immuno-modulatatory effects and stimulate adaptive immune responses (reviewed in:(Goodbourn et al., 2000)).

IFN-β is the first IFN induced directly by viral infection and is followed by IFN-α4 expression. Once these two IFNs are expressed, autocrine and paracrine mechanisms result in the synthesis of interferon regulatory factor 7 (IRF7) that in turn initiates the production of more type-I IFN family members (Erlandsson et al., 1998; Au et al., 1998; Marie et al., 1998; Sato et al., 1998). The initial activator of IFN-β expression is intracellular dsRNA (Jacobs and Langland, 1996), which signals through TLR 3 and PKR depending on the cell type (Alexopoulou et al., 2001; Boehme and Compton, 2004), and is rapidly released to the extracellular environment. Binding of IFN-α/β to its receptor on the surface of cells initiates its biological activities by bringing together the two major sub-units IFNAR1 and IFNAR2 to form an active dimer that signals through a Jak/STAT pathway (Mogensen et al., 1999). Activated STAT hetrodimers translocate to the nucleus where they bind to a consensus sequence upstream of all IFN-inducible genes called the ISRE and initiate gene expression (Shuai et al., 1994; Veals et al., 1992).

A considerable amount of research has focused on the pivotal roles that the dsRNA-dependent protein kinase R (PKR) and the 2'-5' oligoadenylate synthetases (OAS) play in the anti-viral response, both of which are upregulated by IFN-α/β signalling (Figure 5). Activated PKR has a multitude of actions involved in the control of transcription and translation, although it is ordinarily inactive in the cytoplasm (Meurs et al., 1990). Binding of dsRNA unmasks a catalytic domain enabling a variety of functions including: phosphorylation of the translation initiation factor eIF2 which in turn inhibits recycling of initiating factors and hence translation (Meurs et al., 1992); participation in signalling cascades such as NF-κB activation and STAT1 activation (Wong et al., 1997); and finally in the initiation of apoptosis (Tanaka et al., 1998).

The OAS system constitutes a group of enzymes whose expression is induced by IFNs and whose activity is triggered by dsRNA. OAS enzymes catalyse the synthesis of ATP oligomers in the unusual 2'5'conformation (Kerr and Brown, 1978). These 2'5'ATP

oligomers bind to and activate the endonuclease RNase L, which mediates the cleavage of single-stranded mRNA (both cellular and viral) thereby inhibiting protein synthesis. RNase L tends to be activated in the immediate "vicinity" of the activator (dsRNA), ensuring viral transcripts are preferentially destroyed over cellular mRNA (Nilsen and Baglioni, 1979).

In addition to PKR and OAS, the IFN-inducible Mx proteins interfere with RNA virus replication, particularly that of the negative stranded RNA viruses such as those in the *Bunyaviridae* (Frese et al., 1996), Mx proteins have GTPase activity and probably inhibit the trafficking or activity of viral polymerases (Stranden et al., 1993). Importantly, additional uncharacterised anti-viral effects of IFN must exist, since mice triply deficient in PKR, RNase L and Mx1 can still successfully resist some virus infections (Zhou et al., 1999).

IFNs can also inhibit cell growth and change a cell's propensity to initiate apoptosis by a variety of mechanisms. For example, IFNs upregulate the level of the cyclin-dependent kinase inhibitor p21, which plays a crucial role in the progression of the cell cycle from G1 into the S phase (Subramaniam et al., 1998; Sangfelt et al., 1999). IFN goes further than cell arrest and triggers apoptosis by various routes, including PKR and OAS associated activity, but also more directly by inducing the expression of the inactive precursors for caspase1, caspase 3 and caspase 8 (Figure 5) (Chin et al., 1997; Subramaniam et al., 1998; Balachandran et al., 2000b).

Finally, IFN-α/β production also has potent immunomodulatory effects. IFN-α/β is produced constitutively at low levels by plasmacytoid dendritic cells which represent the main producers of IFN following virus infection. Upon infection these cells can produce large amounts of IFN that have systemic effects (Siegal et al., 1999). Once secreted, IFN-α/β has the ability to upregulate a cell's ability to present internal antigens to leukocytes in the context of MHC-I molecules and thereby promote $CD8^+$ T cell responses (Goodbourn et al., 2000). In addition, IFN-α/β enhances the cytotoxicity of NK cells by upregulating levels of perforins and inducing IL-15 production by macrophages that promotes NK proliferation (Kaser et al., 1999; Fawaz et al., 1999). IFN-α is an important cytokine for the generation of protective T-cell mediated immune responses to viruses, either directly or by maintaining the survival of T cells once activated (Sun et al., 1998; Marrack et al., 1999).

Type I IFNs provide the host with a powerful tool for restricting viral replication and spread at sites of viral infection in a rapid and potent manner. Thus, it is not surprising that viruses have evolved mechanisms to counteract the IFN-α/β response. Indeed, there is a plethora of examples in the literature of viruses that either inhibit IFN production or interfere with IFN signalling. Many viruses attempt to minimise IFN-α/β production by sequestering the main

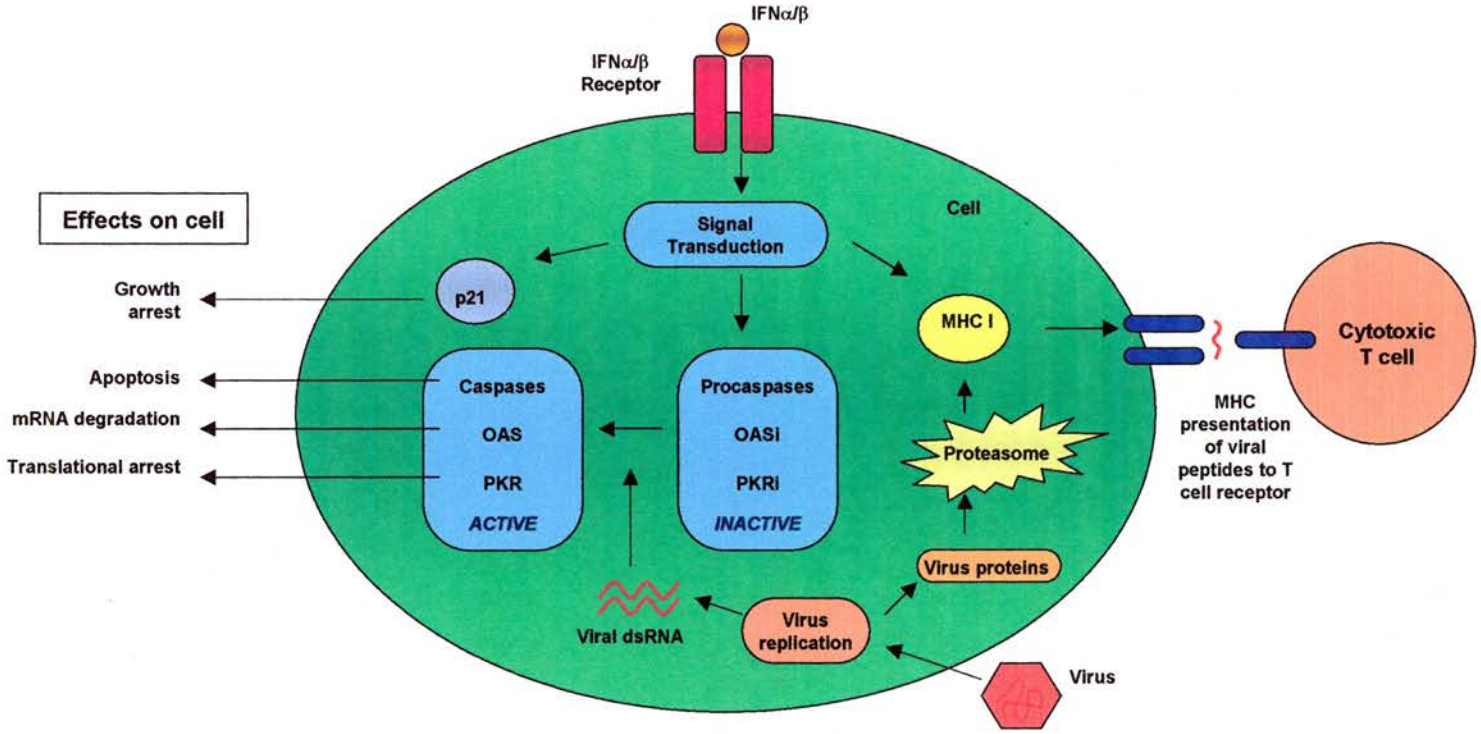

Figure 5, type I interferons have numerous biological properties. There are numerous IFN-α/β sub-types produced upon viral infection, however they all bind to and function through one receptor: IFN-αβ-R. Binding of IFN to this receptor triggers dimerisation and initiates a signalling cascade that results in expression of IFN-inducible genes. These gene products are characteristically inactive unless they become activated by the presence of intracellular viral dsRNA, ensuring their potent activities are only induced under conditions of infection. IFN signalling promotes a pro-apoptotic state by up-regulating pro-caspases, which upon conversion to its mature form promotes cell apoptosis and so removes infected cells along with its viral progeny. IFN also increases expression of OAS and PKR as inactive precursors, which upon viral infection shut down the cells ability to transcribe new mRNA and translate new proteins – a vital step that inhibits viral replication. IFNs also induce the synthesis of gene products that arrest the cell cycle, such as p21 that inhibits G_1/S phase-specific cyclin-dependent kinases. IFN also act to increase the expression proteins involved in the processing and presentation of viral proteins to cytotoxic T cells (such as MHC-I, proteasome components and peptide transporter molecules). In addition, IFNs have further anti-viral functions in addition to those shown here and are discussed in the text. Adapted from: (Goodbourn *et al.* 2000).

activator of the IFN system, dsRNA. For example, the reovirus major capsid protein σ3 binds dsRNA (Lloyd and Shatkin, 1992), as does the σA protein of the avian reovirus (Martinez-Costas et al., 2000). Importantly, differences in reovirus virulence have been linked to differences in the ability of σ3 protein to sequester dsRNA – suggesting IFN suppression by this route is instrumental in the determination of virulence (Bergeron et al., 1998). In addition to reoviruses, several other viruses attempt to hide their dsRNA by expressing dsRNA-binding protein such as the NS1 protein of influenza virus (Lu et al., 1995), the E3L protein vaccinia virus (Chang et al., 1992) and products of the nsP3 gene of porcine rotaviruses (Langland et al., 1994). Further examples of IFN-α/β suppression come from; the African swine fever virus which encodes a homologue of IκB that inhibits NF-κB mediated induction of IFN-β (Powell et al., 1996); the human papillomavirus type 16 which expresses an inhibitor of IRF-3 that ordinarily mediates IFN-α/β production (Ronco et al., 1998); several poxviruses that encode soluble IFN-α/β receptor homologues that bind and sequester IFNs, thereby blocking their biological activity (Symons et al., 1995); whilst human cytomegalovirus disrupts IFN signalling by decreasing levels of key members of the signalling cascade downstream of the IFN-α/β-R (Miller et al., 1998). In addition to these few examples are a multitude of examples whereby viruses interrupt IFN-α/β detection, signalling, and its functions directly; these are beyond the scope of this introduction but are well reviewed by Goodbourn *et al.* (Goodbourn et al., 2000).

1.2 The CNS is a highly complex tissue possessing a specialised immune environment

The CNS is the most complex organ in the mammalian body. It possesses a vast number of neurones that interconnect to form the most intricate cellular network known to science. This organ is also one of the most vital; many neuronal nuclei and circuits cannot be replaced if damaged or lost. Neurones are sensitive to various forms of assault, be it physical, chemical, inflammatory or infective and are protected by a variety of mechanisms. The blood-brain-barrier (BBB) acts to separate the organ from the blood, whilst glial cells act to support neuronal function, aid recovery from insult and guide CNS immune responses. Due to the consequences of CNS damage there exists a variety of mechanisms that prevent unnecessary or inadvertent immune activation.

1.2.1 The blood-brain-barrier (BBB) protects the brain

The BBB constitutes an important barrier that prevents the passage of cells and many proteins into the CNS from the systemic circulation. This cellular barrier is composed of endothelial cells that adhere tightly to each other and are surrounded on the tissue side by a circle of astrocytic processes, whilst vascular cells express few adhesion molecules for circulating leukocytes to bind. Epithelial cells found in other organs are not joined tightly in this way and ordinarily allow a whole host of proteins, aqueous compounds and mobile cells to pass around them. In comparison, the tight barrier in the brain prevents proteins, most non-lipid soluble compounds and mobile cells such as lymphocytes, dendritic cells and monocytes from entering. This barrier is essential for the exclusion of most pathogens, non-endogenous substances, and hormones, and acts to maintain a steady environment for neurones whose non-renewable nature requires special protection. The CNS has long been considered to be immunoprivileged due the absence of key components of the immune system and a lymphatic system. Unlike other tissues, patrolling lymphocytes and dendritic cells, which are the typical cellular sensors of microbes, cannot be found in the resting CNS. Indeed, the tissue architecture is unique in that it lacks lymphatics (Hickey et al., 1991; Pachter et al., 2003). In addition, levels of complement are undetectable as are antibodies and MHC expression. (Kakinuma et al., 1998; Paul et al., 2003; Halevy et al., 1994; Lustig et al., 1992).

Immune responses in the CNS are tightly controlled. Microglia are kept in a quiescent state by CD200-CD200R neuronal interactions (Hoek et al., 2000), whilst astrocytes contribute to immune suppression by expressing the immunosuppressant cytokine TGF-β along with neurotrophins such as brain-derived neurotrophic factor (BDNF) and nerve growth factor (NGF), all of which encourage microglial quiescence, suppress T cells and deactivate any infiltrating antigen-presenting cells that manage to pass the BBB (Gordon et al., 1998; Hailer et al., 1998). The few T cells that enter the resting brain become anergic and undergo apoptosis or leave through an as yet uncharacterised mechanism (Hickey et al., 1991; Piccio et al., 2002). In addition, plasmacytoid DCs the main producers of type–I IFN following virus infection are also not observed in the CNS, suggesting alternative mechanism must exist to regulate immune responses in the CNS.

Importantly, the BBB can be compromised during times of trauma, ischaemia, pressure, inflammation and infection, allowing an infiltrate of leukocytes and serum proteins (Cotran, 2004). During viral encephalitis a flood of mononuclear cells enters the brain along with antibodies that can neutralise virus and label virus and infected cells for clearance (Pachter et

al., 2003; Amor et al., 1996; Morris et al., 1997). Whilst virally infected cells in the periphery are eliminated by the immune system there is relatively little cytolytic clearance in the CNS, suggesting there are alternative mechanisms for CNS viral clearance (Griffin, 2003; Levine et al., 1991). Fundamentally, it has remained puzzling how infection is sensed and how immune responses are co-ordinated within a tissue that lacks such critical components of the immune system.

1.2.2 Microglia are resident facultative phagocytes of the CNS

The long-standing tenet that the CNS is an immunologically privileged site has undergone considerable revision with the notion that microglia have immune functions. Microglia express several key immunologically related receptors including complement receptors (Moller et al., 1997), Fc receptors (Peress et al., 1993), scavenger receptors (Husemann et al., 2002), cytokine receptors for IL-1, IL-2, IL-3, IL-4, IL-6, IL-10, IL-12, IL-13, IL-15, IL-18, IFN-γ, IFN-α/β and many chemokines (Hanisch, 2002). *Ex vivo* microglia isolated from the uninfected brain express the co-stimulatory molecules B7-2, ICAM-1 and CD40 and can be induced to express high levels of MHC-II molecules, suggesting they have a capacity to interact with and stimulate T-cells (Carson et al., 1998). Accordingly, microglia are thought to play a pivotal role during CNS immune responses and have been described as the resident antigen-presenting cell of the CNS, although in the resting CNS remain in a quiescent state until activated by injury or infection (Streit, 2002).

The function, integrity and survival of neurones are dependent on the presence of large numbers of glial cells under normal and pathological conditions. Indeed, microglia can be considered a hybrid between leukocytes and glial cells; they function to both provide protection and support to neurones, and as sentinels for infection. Microglial activation has been consistently associated with neuropathology in a variety of neurological diseases, from trauma and infection to chronic disease such as prion disease and Alzheimer's disease (AD) (Streit, 2002; Rezaie and Lantos, 2001; Eikelenboom et al., 2002). Microglia are exquisitely sensitive to their environment and can become activated even without obvious neuronal pathology (Raivich et al., 1999). Indeed, they are activated early in the response to infection or injury and are major players in both innate and adaptive immune CNS responses (Raivich et al., 1999; Benveniste et al., 2001).

There has been much debate over the ontogeny and function of microglial cells, since they are often confused with circulating monocyte-derived macrophages that occasionally migrate into the CNS (Streit et al., 1999). It is now generally accepted that microglia originate during embryogenesis from mesodermal cells, probably of the haematopoietic lineage (Cuadros and

Navascues, 1998; Cuadros and Navascues, 2001), which after invasion into the CNS rapidly proliferate to form a vast pool of self-propagating, professional phagocytes based on their characteristic expression of F4/80 antigen, FcR and Mac-1 (Streit, 2002). Bone marrow chimera studies in adult mice show that only a small proportion of microglia enclosed by the BBB are derived from circulating bone marrow precursors. Conversely, cells with a morphology similar to that of microglia that populate the perivascular tissue alongside the blood brain barrier are derived from circulating monocytes and are unlikely to be functionally analogous to the resident CNS microglia (Hickey and Kimura, 1988).

In adults, resident microglia are a stable population of cells with low levels of cell division, whose numbers can also receive occasional addition from perivascular macrophages. Infiltrating perivascular macrophages can be distinguished by their relatively high expression of CD45. The perivascular $CD45^{high}$ macrophages are effective antigen presenting cells and stimulate T cell proliferation. Conversely $CD45^{low}$ microglia isolated from the resting brain fail to present antigen effectively and cause T cell anergy *in vitro* unless activated with IFN-γ, or microbial components such as LPS (Aloisi et al., 2000; Ford et al., 1995). However, microglia isolated from brains infected with Theiler's murine encephalomyelitis virus (TMEV) express all the necessary markers for antigen presentation and can effectively activate T cells to produce IFN-γ *ex vivo*. TMEV initiates a chronic demyelinating disease characterised by inflammatory lesions of demyelination. Microglia isolated from infected mice express a multitude of pro-inflammatory cytokines and iNOS at levels equivalent to those produced by invading macrophages (Mack et al., 2003). Cultured microglia infected with TMEV express high levels of IFN-α/β, pro-inflammatory cytokines and several chemokines such as MIP-1α and readily activate T cells. Microglia stimulated with LPS, peptidoglycan and CpG motifs also express inflammatory mediators (Olson and Miller, 2004). Microglia isolated from the brains of mice exhibiting demyelination initiated by experimental allergic encephalitis (EAE) are also able to effectively present both exogenous and endogenous antigens to T cells (Juedes and Ruddle, 2001). Together these studies inform that microglia promote T cell anergy in the resting brain, whilst in the infected and inflamed brain are effective T cell activators and mediators of inflammation. The mechanism that switches microglia between these two states is uncharacterised; although one can hypothesise that microglia possess an innate ability to sense infection or damage without prior priming by IFN-γ or other inflammatory mediators.

The activation of microglia in the virus-infected brain can be associated with a concurrent increase in neurological damage. This finding has been well characterised in human immunodeficiency virus (HIV) associated dementia (HAD), in which microglia have been

linked to neurodegeneration. The brains of HAD patients exhibit wide spread glial activation and loss of neurones that manifests clinically as a progressive chronic dementia with cognitive and motor dysfunction (Perry and Marotta, 1987). The predominant mechanism of HAD neuropathogenesis appears to involve the response of infiltrating macrophages and resident microglia. Microglia can be stimulated by infection with HIV itself, by interaction with viral proteins or by immune stimulation in response to factors secreted from adjacent infected cells (Garden et al., 2002). Microglia constitute the major infected cell type in the CNS and compelling evidence suggests that microglial infection occurs before the onset of AIDS and is sufficient to promote CNS pathology even when therapeutic intervention controls HIV infection in the periphery (Major et al., 2000). The topographical distribution of apoptotic neurones is closely associated with markers of microglial activation (Adle-Biassette et al., 1999). Furthermore, in HAD patients elevated levels of pro-inflammatory cytokines such as TNF-α (Sippy et al., 1995), iNOS activity (Zhao et al., 2001) and excitatory amino acids, all of which are neurotoxic, are evident (Giulian et al., 1996). In primate models neurobehavioral abnormalities associated with infection progress more rapidly in animals exhibiting greater microglial activation, suggesting that the release of inflammatory mediators from infected microglia may be the cause the of neurologic dysfunction (Berman et al., 1999; Garden et al., 2002).

Studies that have investigated other CNS virus infections have also suggested microglia promote inflammation. Infection of microglia with coronavirus increased NO production (Edwards et al., 2000), whilst infection of a glial cell line with the measles virus led to increased expression of MHC-I (Aloisi et al., 2000). Microglia persistently infected with TMEV directly upregulate cytokines involved in innate immunity (such as IL-6 and IFN-α) along with MHC-II, IL-12 and co-stimulatory molecules B7-1, B7-2 and ICAM-1, enabling effective presentation of antigen to T-cells (Olson et al., 2001).

Whilst resident microglia have the potential to become highly phagocytic, resting microglia in the uninfected CNS are unlikely to be involved in phagocytic activity. When rats were injected with a marker of phagocytic activity (fluoro-gold), only the perivascular microglia, but not the resident microglia, were labelled (Pennell and Streit, 1998). However, separate *in vivo* studies using the fluoro-gold marker have shown resident microglia to be engaged in high levels of phagocytosis during neurodegeneration of the optic nerves (Thanos et al., 1994) and within cortical lesions (Sorensen et al., 1996). Hence, perivascular microglia are the only constitutive macrophages present within the brain. Resident microglia can be considered facultative phagocytes – ordinarily quiescent but, when called upon, are capable of ingesting vast quantities of material. When activated in the adult CNS, microglia

transform from a process bearing (ramified) morphology to a rounded macrophage-like morphology and ingest dying cells. Conversely, mild neuronal injuries cause microglia to adopt a reactive so-called hyper-ramified state which ensheaths regenerating neurons and appear to help in the process of recovery (Barron et al., 1990; Streit et al., 1999). Microglia are widely cultured for research purposes as primary cell cultures and as immortalized amoeboid cell lines. Purification and culturing techniques tend to activate microglia and these cells possess a rounded morphology and an almost constitutive capacity to phagocytose particles *in vitro* (Hayes et al., 1988).

Whilst microglia are capable of sensing microbial components, they can also be activated indirectly through neuronal/glial dialogue. Damaged neurones can communicate to both microglia and astrocytes by expressing the CNS-specific chemokine fractalkine, which is a neuronal membrane bound factor that is rapidly cleaved following neuronal damage (Neumann et al., 1997; Harrison et al., 1998; Rappert et al., 2002; Chapman et al., 2000).

Collectively, these studies have demonstrated that activated microglia can be major producers of cytokines, chemokines, and other neurotoxic compounds, are active phagocytes and can stimulate T-cells. However, the extent of their participation in the initiation and progression of CNS inflammation and microbial sensing remains to be determined. Indeed, the relative contribution microglia make to CNS inflammation compared to astrocytes and infiltrating macrophages is an active topic of debate (Streit, 2002; Liberto et al., 2004).

1.2.3 Astrocytes are a major glial cell type with a multitude of roles

Astrocytes are dynamic cells that maintain the homeostasis of the normal CNS and can play a pro-activate role during immune responses. Astrocytes express numerous receptors that enable them to respond to virtually all known neuroactive compounds, including; neurotransmitters, neuropeptides, cytokines, growth factors and toxins. Astrocytes not only play a role in neuronal support and signal processing, but also function as sentinels for CNS damage and infection. Astrocytes are also critical for the establishment and maintenance of the BBB through interactions with endothelial cells. Upon perturbation of the CNS homeostatic environment, astrocytes become activated; increasing their metabolic activity, increasing in size (hypertrophy) and number (hyperplasia) and help promote angiogenesis, remyelination, neuronal survival and restoration of the BBB. Activation is associated with an increased production of the intermediate filaments such as glial fibrillary acidic protein (GFAP) (Krum and Rosenstein, 1998; Albrecht et al., 2003; Dreyfus, 1998; Janzer and Raff, 1987; Liberto et al., 2004). During immune responses "reactive" astrocytes exacerbate tissue damage via the release of pro-inflammatory cytokines, reactive oxygen species and NO that

inhibits neurite outgrowth and kills oligodendrocytes (Liberto et al., 2004). However, microglia produce far higher levels of these cell damaging intermediates and cytokines than astrocytes – and it is therefore questionable to what extent astrocytes contribute to the initiation and perpetuation of immune responses and the pathogenic mechanism that mediate CNS damage during infection and injury (Liberto et al., 2004).

1.2.4 TLR expression and function in the CNS remains largely uncharacterised

Our knowledge of TLR has rapidly expanded over a relatively short period of time and little attention has been given to their expression and function in neuronal tissue. Since monocytes possess a broad repertoire of TLR expression and microglia have some functional similarities to these cells, it may speculated that microglia will express TLR, although since microglia are not derived from circulating monocytes this assumption is far from certain. Microglia in culture are capable of responding to a variety of pathogens and their components such as LPS and CpG-DNA (Olson and Miller, 2004; Dalpke et al., 2002), suggesting they possess a mechanism for microbial sensing. Similarly, astrocytes are also activated by LPS and CpG-DNA and express cytokines (Lee et al., 2004). Despite the participation of glial cells in CNS immune responses there exists little in the literature to inform us of TLR expression and function in these important cells. Whether innate recognition is conferred by glial expression of TLR or by inter-glial, inter-leukocyte and/or neuronal-glial dialogue is uncertain. Some recent work has begun to address these questions. The CNS exhibits a well-organised innate immune reaction to systemic bacterial infection and cerebral injury. Intravenous injection of LPS initiates severe endotoxaemia that alters the BBB and causes severe neurological damage. Studies have shown the circumventricular organs, which lie within the brain but lack a BBB constitutively express CD14 and TLR 4, as determined by *in situ* hybridisation. Circulating LPS rapidly upregulates CD14 and TLR 4 within the circumventricular organs, followed by a massive upregulation of TNF-α and a subsequent upregulation of TLR 2, TLR 4 and CD14 in microglia across the parenchyma (Lacroix et al., 1998; Laflamme and Rivest, 2001; Laflamme et al., 2001). The activation of parenchymal microglia during endotoxaemia is associated with a robust induction of genes that encode cytokines, chemokines and proteins of the complement system and leads to severe neurological dysfunction (Brochu et al., 1999; Nadeau and Rivest, 2000; Thibeault et al., 2001). TLR 4 deficient mice do not exhibit inflammatory CNS responses to LPS, whilst TLR 2 deficient mice do respond to LPS stimulation but fail to elicit such a profound cytokine response – suggesting TLR 2 cooperates with TLR 4 in the CNS to mediate maximal cytokine release (Laflamme et al., 2003). Work in rats has shown that LPS

exposure sensitises the brain to ischaemic injury and alters TLR 4 expression (Eklind et al., 2001), whilst work investigating LPS-induced injury of oligodendrocytes in mice has documented a pro-active role for TLR 4 expressing microglia (Lehnardt et al., 2002; Lehnardt et al., 2003). Interestingly, work studying a mouse model of multiple sclerosis (EAE) observed an increase in CNS TLR 2 mRNA in association with CNS pathology and the induction of inflammatory molecules (Zekki et al., 2002). In addition, an increase in human TLR 3 and 4 expression is observed around inflamed blood vessels in multiple sclerosis (Bsibsi et al., 2002).

In addition, work studying a mouse model of motor neurone disease suggests activation of innate immunity in the brain exacerbates neurodegeneration. Transgenic mice that possess a mutant form of super oxide dismutase 1 (which is responsible for 20% of all human familial forms of the disease), exhibit motor axon degeneration. These mice exhibit elevated levels of TLR 2 as the CNS degenerates and is an example of innate immune activation that occurs without microbial stimulus, suggesting innate immunity is activated by endogenously-derived mediators in addition to microbial components. Motor neurone disease progression is also enhanced upon chronic LPS stimulation and TLR 2 upregulation closely associates with disease severity. In this model, despite a robust inflammatory response, there is no evidence of lymphocyte activation or other acquired immune responses (Nguyen et al., 2004). In addition to LPS, CpG-DNA is a potent inducer of neuronal injury. CpG-DNA is not directly toxic to neurones in culture but does initiate neuronal damage in mixed neurone/glial cultures and in hippocampal slice cultures, suggesting CpG-DNA signals through glial TLR 9 to initiate production of various neurotoxic molecules such as NO and TNF-α (Iliev et al., 2004). Together this work suggests the CNS expresses functional TLR and further highlights the detrimental effects of innate immune responses to CNS cells and tissue architecture.

Microglia cultured from post-mortem human brain samples express all TLR 1 -9 as measured by RT-PCR (end product, semi-quantitative PCR). TLR 2 and 3 is also detected in astrocytes and oligodendrocyte cultures, although since these represent primary cultures, microglial contamination cannot be excluded. The level of TLR from human to human varies considerably, however a perceived increase in TLR expression is observed in cultures derived from donors with neurodegeneration. In addition, TLR 3 and 4 protein expression is highly variable from cell to cell within a culture and is predominantly intracellular for microglia and extracellular for astrocytes (Bsibsi et al., 2002).

A recent report has ascertained TLR levels in murine microglia cultures by quantitative RT-PCR. This work showed microglia express mRNA for TLR 1-9 and that microglia recognise

a variety of bacterial and virus–associated molecules. Upon stimulation with LPS, peptidoglycan, poly(I:C) or TMEV infection; cytokine and chemokines are upregulated and TLR expression levels altered. In addition, stimulation with TLR ligands upregulates microglial expression of MHC-II and co-stimulatory molecules, enabling microglia to efficiently present antigens to T cells (Olson and Miller, 2004). Microglial innate immune responses to *Staphylococcus aureus* have also been characterised. Cultured N9 microglia respond to *S.aureus* by expressing a variety of pro-inflammatory cytokines (Kielian et al., 2002). The expression of TLR 1, 2 and 6 along with CD14 is enhanced upon *in vitro* culture with *S aureus* as determined by semi-quantitative PCR and FACS analysis, which may serve to augment microglial activation *in situ* during CNS infection. In addition, astrocyte cultures from TLR 2 deficient mice exhibit reduced cytokine responses to *S. aureus* and particularly to peptidoglycan. This suggests that *S.aureus* is indeed sensed by glial cells and that this recognition is conferred by TLR 2, as is the case for macrophages in the periphery (Esen et al., 2004; Yoshimura et al., 1999).

Primary cultures of murine astrocytes express constitutive levels of TLR 2, 4, 5 and 9 as determined by RT-PCR and are upregulated following stimulation with various PAMPs (end-product analysis, semi-quantitative; TLR 1, 3, 6, 7 and 8 were not assayed). Following PAMP stimulation astroglial NF-κB translocates to the nucleus and IL-6 is expressed, suggesting that TLR signalling occurs in astrocytes (Bowman et al., 2003). In this report protein expression didn't accurately replicate the authors finding for TLR 2 upregulation in response to flagellin. Furthermore, the semi-quantitative PCR technique was not well described and no data was given to demonstrate the quantitative nature of the assay – such as a standard curve or diluting assay (Bowman et al., 2003). Questions must remain over the validity of the RT-PCR data from the Bowman *et al.* papers since the quantitative nature was not clearly substantiated. There is a clear need for these issues to be further explored using the more robust quantitative approach of quantitative PCR.

For certain virus infections, mice deficient in specific TLR appear to be protected from immune-mediated pathology but are more susceptible to higher CNS virus titres. HSV-1 infected TLR 2 deficient mice suffer higher virus titres but importantly exhibit decreased levels of CNS mononuclear infiltrates, chemokines and serum IL-6, and are resistant to lethal HSV-1 challenge. This would suggest decreased mortality and inflammation is achieved at the expense of a concurrent decrease in an ability to clear the virus. A deficiency in TLR 4 does not alter the kinetics of HSV-1 infection. These results suggest that TLR 2-mediated cytokine responses to HSV-1 are responsible for a portion of the morbidity and pathology associated with HSV-1 infection (Kurt-Jones et al., 2004). In addition, TLR 3 deficient mice

exhibit significantly reduced levels of CNS inflammation and pathology upon infection with WNV (Wang et al., 2004).

In summary, these reports suggest cultured CNS cells express functional TLR, although TLR expression in the resting and virally infected CNS remains to be characterised. Preliminary studies suggest murine glia express TLR *in vitro*, although this is yet to be confirmed *in vivo*. TLR expression is complex and is little understood, especially in the immunospecialised context of the CNS, and yet deficiencies in TLR result in dramatically altered susceptibility to CNS infection in the case of TLR 2 and 3. There is clear requirement for a more detailed and systematic analysis of TLR expression in the CNS.

1.3 Viral encephalitis and neurotropic viruses

The clearance of virus from the CNS requires a finely balanced response that successfully eliminates the virus without damaging essential non-renewable cells such as neurones. Fortunately, viral infections of the CNS are relatively uncommon but once initiated are potentially devastating to the individual. The CNS is particularly susceptible to persistent viral infections; a combination of the relative inaccessibility of this tissue to leukocytes/serum proteins and the longevity /non-renewable nature of neurones.

1.3.1 Viral encephalitis is disease of high morbidity and mortality

Viral encephalitis is an inflammatory disease in which viral infection of the CNS often leads to death or severe neurological defects. The most characteristic histological features include, perivascular and parenchymal mononuclear cell infiltrates, glial cell activation, and neuronophagia. A multitude of viruses can cause encephalitis from complex DNA viruses such as the HSV-1, to simple RNA viruses such as Semliki-Forest virus (SFV). In particular, there are several positive-stranded RNA viruses that cause encephalitis from the *Togaviridae* and *Flaviviridae* that share several phenotypic and life-cycle characteristics. Representatives of these two genera have a worldwide distribution, are almost exclusively transmitted to their vertebrate hosts via an arthropod vector and exhibit a broad range of pathogenicity in humans and animals (Strauss and Strauss, 1994; Solomon, 2004). Ordinarily, human infection is incidental to the natural transmission cycle, which is propagated by wild or domesticated animal populations. However, auxiliary mosquito-borne human-to-human transmission can be apparent during epidemics of infection. Little can be done for patients suffering from viral encephalitis apart from basic supportive treatments. Mortality is high and most survivors are left with severe neurological sequelae (Cotran, 2004). A better

understanding of the pathogenic mechanisms at play in viral encephalitis would undoubtedly better inform our understanding of these devastating conditions and enable the development of therapeutic strategies to combat these diseases.

1.3.2 Alphaviruses are neuroinvasive and infect a wide range of animals

Alphaviruses are positive stranded RNA viruses of the *Togaviridae* family. There are 23 alphaviruses that are known to cause human illness, which present principally as CNS infections or as a syndrome of febrile illness and rash (Tsai, 2002). Phylogenetic analysis suggests these viruses arose in the New World with subsequent introductions into the Old World (Strauss and Strauss, 1994). They can only be transmitted naturally by arthropods, primarily mosquitoes, the specificity of which is determined by the vector's ability to support viral replication in midgut cells, enable dissemination within the arthropod and exhibit infection of the salivary glands (Tsai, 2002). Natural infections can be observed in a broad range of animals including birds, mammals, reptiles and amphibians, although only those hosts that develop elevated blood viremia ($>10^{3.5}$/ml) for several days, contribute to further viral transmission. Uniquely, horses appear to be particularly susceptible to infection with alphaviruses and can contribute to amplification of viral levels and facilitate transmission to other hosts in the immediate area such as humans. The range of animals that can be infected with alphaviruses is broad; laboratory infection of mice, hamsters, guinea pigs, rats, rabbits, and non-human primates with encephalitogenic alphaviruses can all result in the host developing encephalitis (Strauss and Strauss, 1994; Tsai, 2002).

1.3.3 Alphavirus pathogenesis

Following natural infection virus-infected saliva is deposited in extravascular tissue whilst the mosquito feeds. Similarly, experimental infection with a needle results in local viral replication that results in Langerhan cell activation, drainage to the local lymph nodes and consequent activation of the adaptive immune system. Viral replication in the tissues results in a brief blood viremia, which is severely curtailed by the host's potent interferon response and then neutralised by antibodies. Alphaviruses can be efficiently neuroinvasive since viremia is rapidly followed by a CNS infection that passes across the blood-brain-barrier via infection of the cerebral vascular endothelial cells. In rare cases alphaviruses can enter the CNS by tracking along peripheral nerves to the olfactory bulb following intra-nasal infection. CNS pathology reflects both viral and immunopathogenic mechanisms that result from the expression of cytokines, interferons and other immune mediators such as NO,

which are important in balancing viral clearance with immune-mediated damage (Fazakerley, 2002; Tsai, 2002).

In both humans and mice, an age-dependent susceptibility of infants to alphavirus encephalitis is observed epidemiologically, a phenomenon that may be due to either the changing susceptibility of neurones to undergo virus-induced apoptosis as they mature or the changing nature of neuronal circuitry and metabolism as the CNS develops and ages (Griffin et al., 1994; Allsopp and Fazakerley, 2000). The production of immunoglobulins appears to be protective and mediates viral clearance from peripheral tissues, the blood and brain (Griffin and Hardwick, 1997). Whilst it is not understood exactly how antibody mediates protection functions, studies using Sindbis virus have shown antibodies reactive to the viral E2 glycoprotein are critical for viral clearance and prevent the release of budding virus (Griffin et al., 2001).

1.3.4 Several alphaviruses impact upon human health and economically important animals

Eastern equine encephalitis (EEE) virus was first isolated in 1933 in North America and results in a severe, often lethal CNS infection in humans. EEE also infects bird populations and has resulted in several devastating outbreaks in commercial pheasant, turkey, partridge and emu flocks. The virus is distributed across wide areas of North and South America although human infection is concentrated in costal areas on the Atlantic seaboard and directly correlates with the geographic distribution of its mosquito vector *Culiseta melanura*, primarily in freshwater swampland. Fortunately, infection of humans are rare averaging 5 to 10 cases each year in the USA (Tsai, 2002). Western equine encephalitis (WEE) virus infects humans, horses and bird populations in the western USA, parts of Canada and South America. Whilst infection rates were relatively high in the 1960's, the disease is now very rare with only 4 cases reported between the years 1987 and 1998 in the USA (Tsai, 2002). In contrast Venezuelan equine encephalitis (VEE) virus is a disease of exceptionally high mortality (up to 40% in some cases) and occurs sporadically as epidemics of infection in conjunction with epizootic transmission among horses. These epidemics have been recorded to affect tens of thousands of humans and hundreds of thousands of equine cases; primarily in Venezuela, Colombia and Central America (Rivas et al., 1997; Tsai, 2002). Horses appear to be excellent amplifying hosts exhibiting particularly high viremia that facilitate rapid animal-to-animal transmission by a variety of mosquito vectors (Rivas et al., 1997). In addition to the alphaviruses that cause encephalitis, there are several genus members that do not cause encephalitis such as the Chikungunya virus and O'nyong-nyong viruses, which

cause repeated epidemics of infection throughout the tropics and produce haemorrhagic symptoms followed by severe joint pains that can last many years post infection in humans (Deller, Jr. and Russell, 1968; Tsai, 2002).

1.3.5 Flavivirus infections are a major public health concern

Several viruses of the *Flaviviridae* cause encephalitis in humans across the world. Like alphaviruses, they can be transmitted by arthropod vectors and result in high viremia followed by CNS invasion. Japanese Encephalitis virus causes up to 50,000 cases each year in south-east Asia, one third of which are fatal and of those that survive, half have serious neurological sequelae. Children and the elderly appear to be particularly susceptible to CNS infection. The West Nile virus has received much publicity in the past few years due to its rapid spread across the USA, decimating certain wild bird populations and resulting in over 6,000 cases of human encephalitis in 2003/2004 alone. In continental Europe, tick-borne encephalitis continues to be a public health concern (Solomon, 2004). Clearly there is an urgent need to elucidate pathogenic mechanisms and develop therapies for these diseases.

1.3.6 Semliki Forest virus (SFV) is an experimental model of viral encephalitis

1.3.6.1 SFV is a member of the alphavirus genus of *Togaviridae*

Like all members of the *Togaviridae* family, SFV is a small icosahedral virus that possesses a positive stranded RNA genome of approximately 11Kb that possesses a 5' cap and is polyadenylated. SFV possesses an icosahedral capsid and is enveloped by a lipid bilayer (hence the name *Togaviridae* coming from the Latin "Toga" meaning "cloaked"). SFV occurs naturally in Africa where it infects horses, humans and its mosquito vector (*Aedes aegypti*) from whence it was originally isolated in the Semliki forest of Uganda (Mathiot et al., 1990; Smithburn and Haddow, 1944). Since its identification 60 years ago it has been extensively used in the laboratory. There are a variety of strains with differing levels of virulence and include the prototype L10 strain and SFV4 strain that invariably result in fatal fulminant panencephalitis upon introduction to the mouse host. As such, they have been classified as being virulent strains (Pusztai et al., 1971; Glasgow et al., 1991; Santagati et al., 1995). Several avirulent strains have also been used extensively in the laboratory, such as the A7(74) strain that results in a mild, transient encephalitis that upon viral clearance results in a chronic demyelinating disease that mimics several characteristics of human demyelinating diseases such as Multiple Sclerosis (Fazakerley and Walker, 2003; Fazakerley, 2004).

The RNA genome of SFV is infectious upon transfection into cultured cells as is the RNA from *in vitro* transcribed cDNA plasmids that encode the genome. These properties have been exploited to rapidly generate mutants and are the basis for the SFV vector system that is used extensively for recombinant expression in eukaryotic cells, and which has much promise for use as transient gene therapy and in vaccine technologies (Berglund et al., 1996; Fleeton et al., 2001; Morris-Downes et al., 2001; Atkins et al., 1999).

1.3.6.2 SFV replication

Upon entry to the cytoplasm, the RNA genome of SFV can act directly as a message RNA. Replication of the genome is via a negative strand intermediate that gives rise to a full-length genomic RNA copy and a subgenomic message that represents the 3' third of the genomic RNA. The subgenomic RNA species encodes the structural genes of SFV; the capsid protein C, followed by the envelope glycoproteins E2, E3 and E1. The full-length genomic RNA species encodes from 5' to 3' four non-structural proteins termed nsP1, nsP2, nsP3 and nsP4 that are involved in viral RNA replication, followed by the structural genes listed above. The presence of a particularly potent sub-genomic promoter, located immediately upstream of the structural genes, leads to the synthesis of many sub-genomic RNA copies, such that during the course of infection the sub-genomic species out-numbers the full length RNA species. This leads to many copies of structural proteins per copy of RNA genome during the assembly of mature virus (Strauss and Strauss, 1994; Lemm et al., 1994).

The cellular receptor by which SFV binds to is yet to be elucidated, although limited data has suggested MHC-I molecules (Helenius et al., 1978). It is known that the virus enters the cell via the endosomal route (Marsh et al., 1984). Fusion of endosome with lysosomal creates a highly acidic environment that alters the conformation of the E1 glycoprotein, triggering the fusion of viral and endosomal membranes (Kielian and Helenius, 1985; Omar and Koblet, 1988; Wahlberg and Garoff, 1992). Upon fusion, the capsid is liberated into the cytoplasm and RNA synthesis begins in association with smooth membrane structures termed cytopathic vacuoles (Grimley et al., 1968; Grimley and Friedman, 1970). Complexes of capsid and viral RNA migrate to underlie the plasma membrane and viral budding occurs (Pathak and Webb, 1978).

1.3.6.3 Entry of SFV into the host

The natural transmission of the virus is via its mosquito vector, which directly transfers virus into venous blood and extravascular tissue. Experimentally, several routes of inoculation have been used to study SFV pathogenesis (Bradish et al., 1971; Bradish et al., 1975).

Following intraperitoneal inoculation the virus replicates in peripheral muscles – including the skeletal, cardiac and smooth muscle (Amor et al., 1996; Pusztai et al., 1971). Viral replication is exceptionally rapid producing a high titre viremia within 24 hours that peaks at 48 hours and is rapidly cleared by innate immune mechanisms that are yet to be characterised along with neutralising IgM antibodies (Fazakerley et al., 1993; Pusztai et al., 1971). All strains of SFV are neuroinvasive and readily cross the BBB by infecting the cerebral endothelial cells to initiate foci of perivascular CNS infection (Fazakerley et al., 1993; Soilu-Hanninen et al., 1994).

SFV can also be directly inoculated into the brain that results in a more extensive CNS infection; the white matter tracts are particularly susceptible to infection via this route. Alternatively, SFV can be introduced to the CNS via intra-nasal inoculation in which the virus directly infects the olfactory neurones that terminate in the nasal passage. Virus then spreads along the olfactory nerves to infect the olfactory bulbs in the brain (Kaluza et al., 1987; Oliver and Fazakerley, 1998). SFV can readily infect certain neuronal populations and oligodendrocytes, although astrocytes tend to be refractory to infection as determined by immunostaining of infected brain (Balluz et al., 1993; Amor and Webb, 1988; Atkins et al., 1999).

1.3.6.4 Productive and restricted replication

Virulent strains such as SFV4 and L10 can spread rapidly across the brain from the initial perivascular sites of infection. Accordingly, mice infected with virulent strains develop fulminant panencephalitis, and die three to four days post infection (Fazakerley et al., 1993). Conversely, the dynamics of infection with avirulent strains such as A7(74) varies dramatically with the age of the host. Neonates cannot contain viral spread within the CNS and develop panencephalitis that leads to death within 48 hours. Fascinatingly, once mice have matured to 14 days of age they can successfully restrict the spread of the SFV A7(74) to the initial sites of perivascular CNS infection. This finding was dramatically illustrated in a study that showed 100% of infected mice aged 12 days died upon infection with A7(74), whilst 100% of infected mice aged 14 days survived infection with the same batch of virus (Fleming, 1977; Oliver and Fazakerley, 1998). Age-related mortality appears to be a fundamental characteristic of many viral encephalitides in both animals and humans. For example, Japanese Encephalitis exhibits a mortality that is far higher in young children (Solomon, 2004).

Several key studies have suggested the maturity of the adaptive immune system has little to do with these dramatic age-related differences, since adult mice completely lacking T cells

or mice lacking both B or T cells, and hence not capable of mounting adaptive immune responses, do not succumb to fatal panencephalitis upon infection with avirulent strains (Amor et al., 1996; Fazakerley and Webb, 1987c; Fazakerley et al., 1993). Rather it appears to be the maturity of the neurones and the state of neuronal connectivity in the developing mouse brain that determines whether avirulent SFV strains can spread across the brain. Indeed, it appears that the propensity for neurones to facilitate viral replication and release new virus alters as they mature and their connections with their surrounding neurones changes. Interestingly, these studies also highlight that the propensity for neurones to undergo viral-induced apoptosis changes as neurones mature, such that adult neurones are refractory to apoptosis upon infection. Many cells of the periphery upon infection undergo "altruistic" cell suicide– a phenomenon widely believed to be an evolutionary ancient strategy of multi-cellular organisms to limit viral infection. Neurones appear to be an exception to this rule exhibiting a rather "selfish" failure to undergo apoptosis, presumably due to their irreplaceable nature (Allsopp et al., 1998; Allsopp and Fazakerley, 2000; Oliver and Fazakerley, 1998; Oliver et al., 1997). The role that the adaptive immune response plays in limiting viral spread in the CNS of neonates is of little consequence since the mice die before any meaningful response can be initiated. There have been no studies that have addressed the role that the innate immune system may play or whether its maturity changes upon development.

The ability of virulent SFV strains to spread across brain is little understood. SFV4 infection spreads across the brain within two to three days, occurring before a naïve adaptive immune system can respond. Putatively, the ability of SFV4 to spread across the brain may be due to either or both circumvention of the host innate immune response, along with an ability to replicate in mature neurones that the A7(74) strain lacks.

The genetic loci that determine the virulence of differing SFV strains remains only partly characterised. In common with several other alphaviruses, mutations introduced into viral glycoproteins alter virulence. Viral glycoproteins are a fundamental constituent of the mature virus and mediate binding to host cells and fusion with host membranes. Chimeric SFV4 engineered to express the E2 glycoprotein from the avirulent A7(74) strain is apathogenic upon infection into mice, suggesting the avirulent nature of A7(74) is partially conferred by RNA sequence of the E2 gene. Single amino acid changes in the structural proteins can also attenuate the virus *in vivo* (Santagati et al., 1995). However, further work has cast some doubt on these studies, suggesting that the attenuation of viral pathogenicity in these studies is due to the incompatibility of differing spike proteins that when recombined from differing strains affects functionality. Indeed, when all the structural genes of SFV4 were completely

replaced with those from A7(74), the recombined virus was still lethal and highly virulent (Tuittila et al., 2000). Thus, it is unclear what contribution the structural genes of SFV make towards virulence. Conversely, work has demonstrated that the non-structural genes have a curial role in determining virulence (Tuittila et al., 2000). Successive mutations in the nsP3 gene of SFV cumulatively affect neurovirulence (Tuittila and Hinkkanen, 2003). In addition, work has suggested that variations in nsP2 sequence may alter virulence. nsP2 is involved at a number of critical stages of viral replication. Uniquely, nsP2 possesses a nuclear localisation signal that mediates translocation to the nucleus; suggesting nsP2 may possess additional roles besides its roles in RNA replication (which occurs solely in the cytoplasm). When this gene is mutated at a single codon in the translocation signal, nsP2 is confined to the cytoplasm and does not enter the nucleus (Fazakerley et al., 2002; Rikkonen, 1996). Critically, this mutant is less virulent *in vivo*, exhibiting lower viral titres and limited spread throughout the brain compared to the wild-type SFV4 strain. Thus, minor alterations to the primary amino acid sequence of the replicase genes can have a considerable effect on *in vivo* virulence (Fazakerley et al., 2002). Studies that have utilised Sindbis virus (a close relative of SFV in the alphavirus family), have also shown non-structural proteins can contribute to differing levels virulence (Heise et al., 2000). The mechanism of this virulence is yet to be characterised, although virus with nsP2 mutations differentially modulate the host's interferon response. This work demonstrated that mutated nsP2 induces far more type I IFN upon infection, along with more pronounced activation of 170 IFN-inducible genes suggesting wild-type nsP2 most likely acts by decreasing IFN production and thus minimising virus visibility to the host (Frolova et al., 2002).

1.3.6.5 Immune responses to SFV

Immunocompetent Balb/c mice clear avirulent strains of SFV from the blood within 3 days and from the brain within 8 days after intraperitoneal infection (as measured by plaque assay that measures infectious virus only) (Fazakerley et al., 1993; Suckling et al., 1978). Limited work using RT-PCR has demonstrated viral genes can be detected several weeks post infection in the brain, although this remains to be confirmed (Donnelly et al., 1997). Levels of neutralising IgM antibodies are detected in the blood within the first few days post infection, followed by the production of IgG2a antibodies and finally a slow IgG1 antibody production that persists for several weeks (Fazakerley et al., 1993). The blood brain barrier becomes leaky between day 4 and 10 post infection, permitting the passage of

immunoglobulins and leukocytes into the brain, with inflammation peaking at day 7 post infection (Parsons and Webb, 1982; Soilu-Hanninen et al., 1994).

Adult mice that lack T cells (*nu/nu*) can also survive an infection with the avirulent A7(74) strain without developing panencephalitis. As in fully immunocompetent animals, levels of neutralising IgM antibody rise within the first few days, however IgG antibodies can not be detected since the lack of T-cells prevents class switching in B cells. These mice clear blood viremia as normal and the systemic infection is controlled - presumably due to the potent anti-viral effects of interferon and the production of IgM antibodies that bind to and neutralise blood-borne virus. However, these mice cannot clear infectious virus from the brain and exhibit a life-long persistent CNS infection that appears to be otherwise sub-clinical (Amor et al., 1996; Fazakerley and Webb, 1987c). Adult mice that lack both T cells and B cells (*Scid*) can also survive infection with A7(74) for several weeks and like *nu/nu* mice, do not develop panencephalitis. These mice can produce neither cell-mediated immune responses nor neutralising IgM antibodies. *Scid* mice cannot clear infectious virus from either the blood or brain and eventually die, most probably from systemic infection rather than a neurological cause. Adoptive transfer studies with infected *Scid* mice have demonstrated that introduction of serum from infected *nu/nu* can mediate clearance of blood viremia, demonstrating that IgM is sufficient to clear blood viremia (Amor et al., 1996; Suckling et al., 1982). Transfer of serum from immunocompetent Balb/c mice, which produce both IgG and IgM antibodies, to infected *Scid* mice clears the majority of infection from both the periphery and the CNS, however some infectious virus remains, suggesting that cell-mediated responses are necessary for complete CNS clearance (Amor et al., 1996). Primarily, these studies inform us of the differential roles that antibodies have in clearing virus in immunocompetent mice. Secondarily, they reaffirm the potency of the innate IFN response, which protects the mouse for so long from succumbing to viral overload in the absence of an adaptive immune response.

Interestingly, immunocompetent mice develop lesions of inflammatory demyelination throughout the oligodendrocyte-rich white matter tracts of the brain (Kelly et al., 1982; Suckling et al., 1978). Neither *nu/nu* nor *Scid* mice develop demyelination despite the persistence of virus, suggesting that an adaptive immune system is critical for both clearance of CNS virus and for the development of SFV-induced demyelination (Amor et al., 1996). Further studies have highlighted the critical role that T cells play during SFV-induced demyelination. Experiments in which mice are immunosuppressed by either total body irradiation, cyclosporin, cyclophosphamide or cycloleucine all demonstrate T cell responses are pathogenic and are required to generate lesion of demyelination (Amor and Webb, 1987;

Fazakerley and Webb, 1987c; Fazakerley and Webb, 1987b; Fazakerley and Webb, 1987a; Fazakerley et al., 1993). In addition, experiments in which CD8+ cells were depleted with the use of monoclonal antibodies demonstrated that cytotoxic T cells were responsible for mediating demyelination, whilst depletion of CD4+ T cells greatly reduced CNS inflammation but not demyelination (Subak-Sharpe et al., 1993).

Several cytokines characteristic of a pro-inflammatory response can be readily detected within the CNS 7 days post infection, including; IL-1α, IL-1β, IL-3, -6, -10 and TNF-α (Morris et al., 1997). The cytokine profile along with the initial production of IgG2a followed by a slow IgG1 response both suggest that a Th1 T cell response is initiated upon SFV infection and is followed by a Th2 immune response (Fazakerley, 2004).

Cellular immune responses during SFV infection have also been characterised; 4 days post infection onwards one can observe infiltrating mononuclear and perivascular cells, with the influx peaking at day 7 post infection (Parsons and Webb, 1982; Morris et al., 1997). The areas of SFV infection and cellular infiltrate coincide as does the activation of microglia and astrocytes. These glial cells can be found to upregulate their MHC-II expression so that it becomes detectable by immunocytochemistry. Otherwise little is known concerning the role microglia and astrocytes play during SFV pathogenesis. In response to infection, endothelial cells upregulate adhesion molecules, such as VCAM1 so that blood-borne leukocytes can enter the CNS (Morris et al., 1997; Soilu-Hanninen et al., 1997). The majority of infiltrating cells appear to be MHC-II negative and primarily constitute CD8+ T cells, although some B cells can also be found (Amor et al., 1996; Morris et al., 1997).

Remarkably, there are few studies that have studied the innate immune responses of viral encephalitis and SFV is no exception. Levels of type-I IFNs parallel viremia following intraperitoneal infection of SFV and mice engineered to lack a functional IFNα/β receptor all die within 48 hours post infection (Bradish et al., 1975; Muller et al., 1994; Fazakerley et al., 2002). The course of death in these animals appears to be extraneural with wide-spread infection of peripheral organs, most notably the exocrine pancreas (Fazakerley, 2004). Intracerebral inoculation of virus results in a widespread infection of oligodendrocytes, meningeal and ependymal cells (infection of the latter two cell-types rarely is observed in wild-type mice). Interestingly, the limited infection of neurones remains a feature of SFV infection in IFNR deficient mice, indicating the restricted replication of avirulent SFV in mature neurones is independent of type-I interferon responses (Fazakerley, 2004). The extent to which each differing sub type of IFN is induced and the roles they play resisting viral replication remains to be determined. There are no publications relating to how CNS cells sense SFV infection and whether Toll-like Receptors are involved in SFV recognition. In

fact, it is not clear whether TLR are expressed in the resting mouse brain. Fundamentally, it is not clear how the CNS senses virus or others infections, or how immune responses are initiated and implemented.

1.3.7.5 Summary: SFV as a model for viral encephalitis

SFV is closely related to several viruses that impact upon human and animal health, such as eastern, western and Venezuelan equine encephalitis viruses. The pattern of disease and mechanisms of pathology are analogous to diseases caused by several flaviviruses that greatly impact on human health, such as Japanese Encephalitis virus. Thus, studying the pathogenesis of SFV better informs our understanding of not only SFV but also of several clinically relevant viruses that cause encephalitis in humans. Studies on SFV pathogenesis also help us to better understand the more fundamental interactions between neurotropic viruses, the CNS and the immune system - interactions that are likely to be fundamental to a multitude of encephalitides. Laboratory infection of mice with SFV provides one model system to address the many unexplained puzzles of viral encephalitis.

1.4 Amyloid-related diseases

Amyloid is a term used widely to describe an aggregation of insoluble matter that can be visualized under standard histopathological examination. It commonly manifests as an amorphous extracellular substance that, with progressive accumulation is associated with atrophy in adjacent cells. The phrase, coined by pathologists in the early half of the 20th century is now, in the molecular era, known to describe a whole variety of protein aggregates whose subunits can differ widely in their composition. Common features of amyloid are its high content of cross β-pleated sheet folded proteins, its non-branching fibrils of indefinite length as seen under electron microscopy and its almost absolute association with pathology. The role of amyloid has been implicated in a whole variety of diseases from type II diabetes to conditions of neurodegeneration such as Creutzfeldt-Jakob disease (CJD) and Alzheimer's disease, although the exact cellular and molecular mechanisms that underlie this involvement are not well characterized (Cotran, 2004).

1.4.1 The Prion diseases

The deposition of abnormally folded protein in a pathological setting has been much studied in the context of neurodegeneration, especially in respect to the prion diseases and in Alzheimer Disease. Prion diseases (also referred to as transmissible spongiform

encephalopathies) are rare, invariably fatal neurodegenerative diseases of animals and humans. They present as a highly heterogeneous group of disease that can be divided into three groups: familial, acquired and sporadic (Brown et al., 1994). Familial prion diseases are all associated with inheritance of an abnormal form of the Prion Protein (PrP) gene. Prion diseases can also be acquired via contact with infectious tissue that has originated from a diseased animal. However, the majority of cases in humans are still classified as sporadic with the cause of these devastating diseases still a mystery. In the past few years the awareness of prion disease has been heightened with the appearance of bovine spongiform encephalopathy and its highly probable ability to spread to humans as variant CJD via the consumption of BSE –infected meat (Bruce et al., 1997). Current modelling suggests that the total number of new variant CJD cases could be anything between 600 and 136,000 depending on the incubation period of the disease agent (Ghani et al., 2000).

Prion diseases have several distinguishing characteristics: primarily they represent a group of uniquely transmissible amyloid-related diseases; additionally they all share a pathology that presents as a spongiform degeneration of the brain under histopathological examination. Accompanying this is the appearance of activated glial cells and the concurrent formation of abnormal aggregates that primarily consist of an aberrant, protease-resistant form of PrP known as PrP^{Sc}. High levels of neuronal apoptosis are a salient feature of prion diseases and often lead to gross atrophy of the brain, with extreme pathology centred around PrP^{Sc} deposition (Masters and Richardson, Jr., 1978). The clear association of PrP^{Sc} deposition with pathology has lead to the hypothesis that the presence of PrP^{Sc} is responsible for the pathogenic effects of prion diseases (Prusiner, 1998).

The cellular form of PrP (PrP^{C}) is protease sensitive and is found expressed as a GPI-linked cell surface protein of unknown function. PrP^{Sc} is generated in a post-translational process as PrP^{C} transforms into PrP^{Sc}. Both PrP^{C} and PrP^{Sc} possess identical primary structures, the critical difference between them being the three-dimensional folding of their amino acid chains. PrP^{C} is mostly alpha helical in structure whilst PrP^{Sc} appears to have a high composition of β-pleated sheets, giving PrP^{Sc} an ability to form large polymeric aggregates (Riek et al., 1996). To explain these puzzling infectious diseases, Pruisner proposed a protein-only prion hypothesis whereby an infecting PrP^{Sc} molecule binds to it's cellular counterpart PrP^{C} and converts it into a conformation identical to that of the infecting PrP^{Sc} molecule – a process that does not require the presence of a genome on the part of the pathogen (Prusiner, 1998).

The physiological function of PrP^{C} is not known although PrP is not essential for viability, as knockout mice appear to be fertile and healthy. However, cultured neurons from these mice

do appear to be far more susceptible to oxidative damage (Milhavet et al., 2000). The expression of PrP is an absolute requirement for susceptibility to prion diseases, which has led to speculation that either PrP is the critical component of the etiological agent, since no PrP^C is available for conversion, or that PrP^C acts as a receptor for the agent (Weissmann, 1999). Interestingly, it appears that transgenic mice that express low levels of PrP^C appear to be more tolerant to PrP^{Sc} infection (Fischer et al., 1996). Conversely mice over expressing PrP^C require very little PrP^{Sc} before clinical symptoms appear (Bueler et al., 1994). However, it should be noted that the expression of PrP^C is clearly not the only factor that determines the susceptibility of cells to undergo PrP^{Sc}-induced cell death. The Purkinje neurons of the cerebellum strongly express PrP^C and yet are comparatively resistant to cell death, whilst other neuronal populations with similar PrP^C expression levels are severely affected (Kretzschmar et al., 1986). Additionally, non-CNS PrP^C expressing cells such as follicular dendritic cells or peripheral neurons exposed to PrP^{Sc} during the course of an infection, do not suffer from obvious degeneration (Mabbott and Bruce, 2001). Nevertheless, Prion diseases represent an amyloid-related disease whose CNS-centred pathology seems to rest on the presence of abnormal polymeric PrP^{Sc} molecules.

Prion diseases characteristically exhibit an absence of immune responses. Indeed, conceivably it may be that the inability of the host to respond and clear PrP^{Sc} infection is directly attributable to the absence of an immune response (Mabbott and Bruce, 2001). Disease progression is unaffected in mice lacking T cells or B cells, whilst mice engineered to express antibodies specific to PrP fail to propagate infection, suggesting the initiation of an adaptive immune response can halt and even prevent disease (Heppner et al., 2001) Despite the lack of an adaptive immune response, glial cells become highly activated - particularly towards terminal disease (see section 1.4.3). The absence of an immune response to prions suggests they lack the immunogenicity to activate adaptive immune responses. When mice are exposed to CpG-DNA as a prophylaxis post scrapie infection, the incubation time is extended by 40%, and even longer following repeated CpG-DNA inoculation. This rather surprising finding is most likely due to activation of TLR 9 signalling in cells of the innate immune system such as macrophages that conceivably upregulate antigen presentation and initiate a limited adaptive immune response that delays disease progression (Sethi et al., 2002). This interesting possibility is not unlikely since the ability of CpG-DNA to induce resistance against other diseases has been demonstrated in mice (Zimmermann et al., 1998).

1.4.2 Alzheimer's disease (AD) and the amyloid cascade hypothesis

AD is a progressive dementing neurological illness that affects hundreds of thousands of predominately elderly people in the developed world and hence is one of the largest areas of pharmaceutical research. Similar to prion diseases the deposition of amyloid fibrils appears to be central to pathology, although AD appears to be non-transmissible upon inoculation in animal models. The major hallmark of AD pathology is the presence of senile plaques – a tangled focus of inflammatory cells that centres on an aggregation of abnormal β-amyloid. The amyloid cascade hypothesis states that the inappropriate cleavage of the Amyloid Precursor Protein results in the production of pathogenic amyloid fibrils (as reviewed by: (Selkoe, 1999)). These fibrils are proposed to be intrinsically neurotoxic, causing a cascade of changes within a neuron that leads to its eventual destruction (Hardy and Higgins, 1992). In addition, the identification of activated microglia within AD plaques, coupled with the presence of numerous inflammatory proteins suggests that inflammation is an integral part of the neurodegeneration. It has been proposed that the continued presence of β-amyloid plaques persistently activates microglia; a process that results in chronic "inflammation" (Meda et al., 1995; Benveniste et al., 2001). Consequently, it has been suggested that the activation of microglia may play a key role in the pathogenesis of this amyloid related disease.

1.4.3 The role of microglia during neurodegeneration

Central to research within the field of prion diseases is the question of whether the toxicity of the PrP^{Sc} is due to the gain or loss of function of PrP^{Sc}. The primary mechanism by which PrP^{Sc} asserts its pathogenic effects is yet to be fully elucidated, however it is probably a combination of two mechanisms. The gain of function hypothesis states that as P rP converts to the PrP^{Sc} form, it gains the ability to be directly or indirectly toxic to cells. Alternatively, the conversion of the physiological PrP^{C} to its non-functional counterpart will impart an induced knockout phenotype to an infected cell that could feasibly affect its survival (Giese and Kretzschmar, 2001). The microglial cell appears to be a central component of these pathogenic mechanisms by contributing to neuronal death following PrP^{Sc} infection, whilst the action of microglia in AD has also been tightly coupled to that of neurodegeneration (Minagar et al., 2002). Microglia are activated in all known cases of prion disease and in numerous other neurodegenerative conditions. Critically, it now appears that microglial activation is not only strictly associated with neurodegeneration (and hence PrP^{Sc} deposition) (Williams et al., 1994), but precedes neuronal death, as originally demonstrated in the hippocampus of mice infected with the 301V strain of BSE (Williams et al., 1997a).

Additionally, a large time course study using *three* different strains of scrapie demonstrated microglial activation occurred early during the incubation period, with activation clearly occurring before significant neuronal apoptosis and prior to the onset of clinical symptoms in all the models studied (Giese et al., 1998).

Convincing *in vitro* evidence suggests that for the toxicity of prion fragments to be fully realized, microglia must be present in CNS cultures. Brown *et al.* showed that pre-treatment of primary neuronal/glial cultures with L-leucine methyl ester (LLME) effectively removes all microglia from cultures and attenuates PrP^{Sc} toxicity. Further addition of untreated microglia restores the toxicity of PrP^{Sc} and high levels of neuronal apoptosis occurr. More recently another group has further elucidated the killing of prion-damaged neurones by microglia and shown that microglia-mediated killing is cell-mediated and requires cell-to-cell contact (Brown et al., 1996; Bate et al., 2001; Bate et al., 2002).

Taken together the above observations support the idea that microglial activation and its association with amyloid-induced pathology appears to be similar in several diseases of neurodegeneration, irrespective of differences in aetiology, or composition of amyloid.

1.4.4. The role of PRR in the recognition of altered self

A growing consensus is emerging that PRR not only recognize the unique molecular patterns associated with microrganisms, but also unique molecular patterns that are generated in a variety of homeostatic and disease processes. Scavenger receptors and CD14 are well characterised as receptors for both bacterial components and apoptotic cells (Savill et al., 2002). The process of apoptosis involves the expression of several novel markers, such as phosphatidylserine, that label cells as dying. Thus, receptors that recognise both non-self also recognise the altered self of apoptotic cells.

PRR may also have a role to play in the pathogenesis of atherosclerosis. This disease process involves the accumulation of oxidised low-density lipoprotein in blood vessels that attracts and activates immune cells, primarily macrophages. Atherosclerotic lesion progression has been shown to depend on persistent, chronic inflammation in the artery wall and this inflammatory reaction leads to increased thickening of vasculature that can eventually precipitate blockage of the vessel. MyD88 and TLR 4 deficient mice demonstrate a reduction in atherosclerosis through a decrease in macrophage recruitment to the artery wall and associated reduced chemokine, cytokine and prostaglandin levels (Bjorkbacka et al., 2004; Michelsen et al., 2004), whilst TLR expression was significantly upregulated in atherosclerotic plaques in humans (Edfeldt et al., 2002). Thus, the presence of an altered

form of a host protein, oxidised low-density lipoprotein, engages a pro-inflammatory signaling cascade that is also engaged by microbial pathogens.

The initial stimulus that activates microglia in TSE is likely to be the abnormal form of the prion protein, PrP^{Sc}. In the prion infected brain, PrP^{Sc} can be found as polymers of repeating units in the form of amyloid fibrils (Wille et al., 2002). Potentially these abnormal repeating patterns may be recognised by PRR such as TLR and trigger a response more appropriate for defence against pathogens than endogenously derived protein, be they infections in the case of TSE, or non-infections as in the case of AD. Surprisingly antibodies that have been raised against DNA also recognise PrP^{Sc} (but not PrP^{c}), suggesting DNA and PrP^{Sc} share a repeat motif that may be recognised by TLR in addition to antibodies (Zou et al., 2004). Several studies have suggested PRR are involved in the recognition of amyloid and the pathogenesis of neurodegeneration; CD14 binds β-amyloid and is upregulated in mouse models of AD (Fassbender et al., 2004), whilst microglia deficient in CD14 cannot kill neurones through β-amyloid induced inflammation (Bate et al., 2004); and mice deficient in CD36 have marked reductions in the recruitment of microglia following β-amyloid injections and secrete lower levels of neurotoxic, inflammatory mediators (El Khoury et al., 2003). Together this suggests that PRR may recognise amyloid and trigger an innate immune response that is damaging to CNS tissue.

1.5 Hypotheses

Toll-like receptors are a family of pattern recognition receptors that recognise a broad spectrum of microbial components. Expression of these receptors confers the ability to innately sense infection and initiate differential signalling cascades that are specific to the pathogen type. The resting brain is separated from the systemic circulation by the blood brain barrier and has no obvious immune process. Lymphocytes, dendritic cells and other leukocytes are absent, whilst the expression of MHC, complement and other immunological molecules are almost non-existent. Despite the apparent immunoprivileged environment, immune responses can be generated. Glial cells have been proposed to fulfil some immune function in the CNS. They are activated in numerous disease states *in vivo* and by microbial components *in vitro*. The mechanisms by which glia are activated continue to be characterised. There has been a substantial amount of interest and research in TLR function in the past few years, although there has been comparably little in respect to TLR in the brain. TLR expression continues to be characterised in cultured neural cells although TLR expression in the CNS is yet to be studied. It is highly likely that glia express TLR along with other PRR. Microglia are the principal phagocyte of the CNS, can express high levels of cytokines and activate adaptive immune responses, although they are not analogous to tissue macrophages found in other organs. Astrocytes may contribute to CNS immune responses through the production of pro-inflammatory mediators and interferon in addition to their roles as support cells to neurones. It is highly likely that the expression of TLR on both cell types provides one mechanism by which these intriguing cells are activated. TLR signalling in the infected CNS would trigger inflammatory processes and synergise adaptive immune responses. SFV is efficiently neuroinvasive and initiates encephalitis. Viral encephalitis results in substantial morbidity and mortality in humans and animals, and underlines the sensitivity of the CNS to immune processes and inflammatory reactions. The role that microglia play in the initiation and perturbation of inflammation is yet to be fully defined, although the expression of TLR and associated inflammatory responses to virus by glia would further emphasise the pro-active role glia has in this process. In addition, it is likely that any TLR expression change during viral infection will reflect the nature of the infections agent and those TLR involved in recognition of virus are likely to be upregulated.

The level of TLR expression imparts differing sensitivity to microbial components. It is highly likely that glia dynamically regulate TLR in an appropriate and specific manner. Macrophages down regulate TLR 4 upon exposure to LPS and become refractory to further stimulation by endotoxin. Similarly, glial cells are likely to respond to microbial challenge by altering TLR expression. The mechanisms that regulate TLR expression are little

understood. Conceivably, direct binding of microbial components to cell surface receptors may signal to alter TLR expression. In addition, cytokines and interferon may by themselves further augment TLR expression in an autocrine and paracrine manner. It is likely that during the specific case of virus infection, interferon signalling will alter TLR expression.

The expression of TLR in the brain has implications for both infectious disease and diseases of chronic neurodegeneration. Glia become activated in the degenerating brain and are closely associated with neuronal damage. It is possible that glia are activated by TLR in numerous disease states including prion disease. Glia upregulate several makers of innate immune activation in the prion infected CNS and it is likely that some TLR are also upregulated. In addition to their substantiated role in recognising non-self, PRRs (including TLR) may also function to recognise altered-self, such as oxidised LDL in atherosclerosis and the abnormal repeating patterns of amyloid in disorders of neurodegeneration. The exact nature of the infectious agent in prion disease is still a matter of debate; nevertheless it is likely that infection of mice with scrapie will result in changes in TLR as a consequence of CNS infection and homeostatic perturbation. In addition, there is a distinct possibility that microglia and other phagocytes utilise PPR to recognize the repeating patterns of amyloid fibrils. It is conceivable that microglia aberrantly recognize amyloid fibrils as a pathogen associated molecular pattern and respond accordingly. The binding properties of PRR are fairly plastic so that they can bind common "molecular signatures" which vary among different species within a given class of microrganism and endogenous ligands. Thus a particular PRR may be able to bind and become activated to both an exogenous pathogen and an endogenous, aberrantly folded protein. Indeed, TLR2 is capable of recognising a vast range of different patterns (see table 1), whilst TLR4 can recognise both LPS - an exogenous molecular pattern, and the endogenous Heat Shock Protein 60 protein, whilst another PRR, CD14, can bind both LPS and the unique molecular patterns exposed on the surface of apoptotic cells. The molecular patterns of amyloid fibrils are unlikely to have been a major selective pressure during evolution of the immune system and there would have been little chance for the development of tolerance, since the unique repeating pattern of PrP^{Sc} or of β-amyloid is one that is generally only present once reproductive age has passed.

Microarrays and quantitative real time PCR (QPCR) are sophisticated methodologies that permit analysis of gene expression. It is likely that these expression technologies will provide useful in characterising glial and CNS responses to infection and stimulation, with particular emphasis on TLR expression.

1.6 Aims and objectives

This thesis aims to characterise the innate capability of glia and CNS tissue to recognise infection. This will be undertaken by studying the expression profile of PRR, particularly TLR, using microarray and QPCR technology.

To achieve this aim a series of objectives have been identified:

1.) To design, validate and utilise a novel custom microarray to assay levels of gene transcripts on microglia involved in innate immune responses, and will involve;
   - assaying all known PRR, a panel of cytokines, chemokine and stress-associated gene transcripts
   - designing suitable probes for microarray analysis and array layout
   - determining experimental procedures for generating optimal microarray signal
   - optimising the ability of the microarray platform to generate reproducible signals and minimise variation
   - validating the ability of the microarray to discern changes in gene expression
   - determining gene transcript changes in microglia stimulated with a classical innate immune stimulus, LPS and upon infection with SFV

2.) To design a reliable and sensitive QPCR protocol for assaying gene expression;
   - to determine the expression of all known murine TLR
   - to determine expression of several key pro-inflammatory cytokines and IFN

3.) To grow cultures of neural cells and determine TLR expression:
   - at rest
   - following stimulation with LPS
   - following infection with SFV

4.) To determine the extent of TLR expression *in vivo* and specifically:
   - whether TLR are expressed in the resting/uninfected brain
   - whether TLR are expressed in the virus infected brain
   - whether TLR expression alters during the course of infection, whether this requires T-cell infiltration and whether this is specific and appropriate to the pathogen
   - whether a functional IFN system is required for TLR expression changes
   - whether CNS TLR expression is modulated during the course of prion infection

2 Materials and methods

Contents

2.1 Cell culture and viruses

2.1.1 Cell culture

N9 microglia and N2a neurobalstoma cells were a kind gift from Alun Williams (Institute of Comparative Medicine, Department of Veterinary Pathology, Glasgow University Veterinary School, Bearsden Road, Glasgow). N9 cells express typical markers of resting mouse microglia and have been extensively used as representatives of primary mouse microglial cells (Ferrari et al., 1996; Meda et al., 1995; Righi et al., 1989). N9 cells were grown in RPMI supplemented with 5% heat-inactivated foetal calf serum, 2 mM glutamine, 100 units/ml penicillin and 100 μg/ml streptomycin at 37°C/5%CO_2. The N2a cell line was established by R.J. Klebe and F.H. Ruddle from a spontaneous tumour of a strain A albino mouse (Olmsted et al., 1970) and was grown in DMEM supplemented with 5% heat-inactivated foetal calf serum, 2 mM glutamine, 100 units/ml penicillin and 100 μg/ml streptomycin at 37°C/5%CO_2.

J774.1 macrophages are an immortalised cell line and were grown in RPMI supplemented with 10% heat-inactivated foetal calf serum, 2 mM glutamine, 100 units/ml penicillin and 100 μg/ml streptomycin at 37°C/5%CO_2.

Primary astrocyte cultures were grown from neonatal mouse brain by a modification of an established protocol to generate mature cells that were analogous to their *in vivo* counterparts in the adult brain (Juurlink and Hertz, 1985). These cultures were generated in collaboration with Claire Cotterill, Centre for Infectious Disease, University of Edinburgh, UK. Briefly, P2 mouse brains (CBA crossed with C57Bl/6) were harvested and meninges removed. The cortex and cerebellum were cut finely, cells dissociated with enzymatic digestion in papain and DNAse I for 1 hour at 37°C, and triturated through a 19 and 21 gauge needle. Resulting brain homogenates were grown for 11 days in DMEM with 10% horse serum, 2mM glutamine and 25 μg/ml gentamycin. Following shaking to remove microglia (200 rpm for 1 hour) and oligodendrocyte precursors (350 rpm for 18 hours), the primarily astrocyte culture was further purified by growing for 7 days in DMEM with 20% foetal calf serum to differentiate remaining oligodendrocyte precursors to type 2 astrocytes, and out grow non-dividing contaminating cells. Astrocyte cultures were finally grown for a further 6 days in DMEM 10% FCS with 0.2 mM dibutyryl cyclic adenosine monophophate (dbcAMP) to differentiate astrocytes and kill any remaining contaminating microglia. Purity of the cultures was determined by immuncytochemical staining for glial fibrillary acidic protein (GFAP) – a well-defined marker of astrocytes (Eng, 1985) and CD11b a marker of the most

likely contaminating cell, microglia. QPCR was undertaken on cultures to confirm the presence GFAP at the mRNA level.

2.1.2 Virus stocks

The SFV 4 and A7(74) strains used in this study were grown by Lucy Breakwell (a PhD student in the laboratory). Both stains were grown in confluent BHK-21 cells maintained in Glasgow's modified Eagles medium (GMEM), supplemented with 10% foetal calf serum, 200 mM L-glutamine, penicillin and streptomycin at 37°C, 4% CO_2. BHK-21 cells were infected with a MOI of 0.01 and incubated for 22 hours. Infectious supernatant from these cells were harvested, clarified at 1000 g for 20 minutes and stored at –80°C.

2.2 Immunocytochemistry

Primary astrocyte cultures were transferred to 8-well chamber slides (Nunc) and grown for 6 days with 0.2 mM dbcAMP added to medium. 5 x 10^4 cells were seeded per well.

Slides were taken from then incubator and the cells were immediately washed twice for five minutes each in PBS and then fixed using 4% paraformaldehyde in PBS for 15 minutes. Following two additional 5 minute washes, cells were permeabilised using 0.1% TritonX-100 in PBS for 15 minutes and washed four times in PBS to remove detergent. Prior to application of antibodies, the cells were blocked using 10% normal goat serum (NGS) in PBS for one hour at room temperature. Anti-GFAP (goat polyclonal, Chemicom) at 1:100 in 10% NGS/PBS, or anti CDllb:FITC at 1:10 in 10% NGS (Serotec, UK), or control antibodies were added to cells for one hour at room temperature. Cells were subjected to 3 five-minute washes with PBS. CD11b stained cells were fixed again in paraformaldehyde, washed once more, covered with aqueous Dako fluorescent mounting medium (Dako), cover slipped and sealed. GFAP labelled and control labelled cells were incubated with 1:100 rabbit polyclonal anti-goat IgG conjugated to FITC in 10% NGS/PBS, for one hour at room temperature. Cells were subjected to two further 5-minute washes, fixed again in paraformaldehyde, mounted and sealed for microscopy.

2.3 Stimulation of N9 cells with Lipopolysaccharide (LPS) and phorbol 12-myristate 13-acetate (PMA)

Cells were seeded into T25 flasks and allowed to grow for 24 hours at which point cells were 90% confluent (4x10^6 cells per flask). Cells were stimulated with the addition of either LPS (*E.coli* O55:B5, Sigma) 100 ng/ml or PMA (Sigma) to 10 ng/ml. Following incubations of various lengths (see results section), media supernatants were collected for IL-6 ELISA

assay, whilst attached cells were washed in Versene EDTA solution and detached from the plastic using 0.25% trypsin. Following quenching of trypsin with addition of 10 ml RPMI with 5% FCS, cells were pelleted at 600 g for 5 minutes to pellet cells and then washed in PBS, re-pelleted and either suspended in RNAlater (Sigma) or immediately lysed in RLT buffer (Qiagen) for RNA extraction (see section 2.10.2 for more details).
RNA was used for microarray hybridisations (section 2.11) and QPCR analysis (section 2.12).

2.4 IL-6 ELISA assay

Supernatants from LPS and PMA stimulated cells were assayed for their IL-6 content using an in house ELISA developed and undertaken by Clive Bate (Institute of Comparative Medicine, Department of Veterinary Pathology, Glasgow University Veterinary School, Bearsden Road, Glasgow).

2.5 Infection of N9 cells with SFV4

Cells were seeded into T-80 flasks at $2x10^6$ cells per flask and left to grow for 14 hours until 50% confluent. Cells were infected with SFV4 at a Multiplicity of Infection (MOI) of 0.5 in 5 ml media – to obtain infection of only a small fraction of the total cells. Flasks were well shaken every 10 minutes for one hour to ensure even distribution of virus and then left to incubate at 37°C/5% CO_2. Four uninfected flasks were immediately harvested for RNA, whilst two uninfected flasks were assayed for Caspase 3 activity (section 2.8 for more details). Six flasks of infected cells (four for RNA and two for caspase assay) were then harvested at each of the following time-points: 3, 12 and 24 hours post infection. Cell pellets included both attached cells and cells that had detached during the time of incubation with virus. Cell pellets destined for RNA extraction were immediately lysed and RNA extracted, whilst pellets destined for caspase assay were lysed and frozen for later analysis.

2.6 Infection with SFV4 and LPS stimulation of N2a cells

Cells were seeded at $1x10^6$ cells per T-80 flask and left to grow for 18 hours. Cells were either infected with SFV4 at a MOI of 0.5 in 5 ml media, so that only a small fraction of the total cells were infected. Flasks were well shaken every 10 minutes for one hour to ensure even distribution of virus and then left to incubate at 37°C/5% CO_2. Other flasks of N2a cells were stimulated concurrently with LPS at 100 ng/ml and harvested as above (section 2.3) at 0, 3 and 12 hours post infection/stimulation.

2.7 Infection with SFV4 and LPS stimulation of astrocyte primary cultures

Astrocytes were seeded to T-25 flasks and incubated for 6 days in dbcAMP (see above for exact culturing conditions) and either infected with SFV4 at an MOI of 5 in 5 ml media. Flasks were well shaken every 10 minutes for one hour to ensure even distribution of virus and then left to incubate at 37°C/5% CO_2. Other flasks of astrocytes were stimulated concurrently with LPS at 100 ng/ml. Cells were harvested as above (see section 2.3) at 12 hours post stimulation with LPS and 20 hours post infection with SFV4. Three flasks of uninfected and three flasks of infected cells were also assayed for caspase 3 activity.

2.8 Caspase 3 assay of cell pellets

Cell pellets were assayed for caspase 3 activity using the caspase 3 assay kit (Sigma) that utilises the unique activity of caspase 3 to cleave the substrate Acetyl-Asp-Glu-Val-Asp p-nitroanilide (Ac-DEVD-pNA), to release the colourimetric compound p-Nitroaniline (pNA). Cell pellets of $2x10^6$ cells were lysed for 20 minutes on ice in 40 µl lysis buffer (50 mM HEPES, pH7.4, 5 mM CHAPS, 5 mM DTT) and the resulting homogenate spun for 20 minutes at 17 000 g/4°C. Supernatants were immediately assayed or frozen at -80°C for storage. Caspase activity of supernatants were assayed in 96-well clear plastic plates: 5 µl supernatant was added to 85 µl Assay buffer (20 mM HEPES, pH7.4, 0.1% CHAPS, 5 mM DTT, 2 mM EDTA) and 10 µl substrate (2 mM). Additionally, the specificity of each assay was confirmed by incubating 5 µl supernatant, 75 µl Assay Buffer and 10 µl caspase specific inhibitor Acetyl-Asp-Glu-Val-Asp-aldehyde (Ac-DEVD-CHO). Assay mixtures were incubated in the dark for at least 90 minutes, along with p-NA standards of known concentration diluted in assay buffer, and the absorbance of each well was measured at 405 nm. Concentrations were calculated using the molar absoptivity of $\varepsilon^{mM} = 10.5$. Each supernatant was assayed in duplicate, along with two assays per sample containing inhibitor. To determine the level of specific caspase 3 activity, the amount of non-specific conversion undertaken in the presence of the caspase 3 inhibitor was subtracted from the those wells lacking inhibitor to reveal the level specific caspase 3 activity. To act as a positive control, each cell line was induced into apoptosis using Staurosporin (Sigma) at 1 µg/ml for four hours and the resulting cell pellet assayed concurrent with other samples.

2.9 Infection of mice with SFV, sampling and tissue processing

All animal experiments were approved by the University of Edinburgh ethical review committee and were carried out under the authority of a UK Home Office Animal Licence using defined clinical end-points representative of lethal virulent infection. Mice were housed in environmentally enriched boxes and were kept under specific pathogen free conditions.

2.9.1 Intra-peritoneal inoculation

Mice were inoculated via the intra-peritoneal route so that inoculation could occur without direct damage to the brain. Mice were inoculated with either SFV A7(74), 0.1 ml containing 5 x 10^3 PFU (stock 50,000 PFU / ml) in PBSA or were inoculated PBSA alone to act as controls.

2.9.2 Intra-cerebral inoculation

Mice were inoculated via the intra-cerebral route so that a large amount of virus would enter the brain directly (compared to inoculation via the intra-peritoneal route).

Mice were temporally anaesthetised with halothane and a 0.02 ml inoculum of either 1x10^3 pfu of SFV A7(74), 1x10^3 pfu of SFV 4, or PBSA alone was given intra-cerebrally.

N.B. all animal work was undertaken with assistance of Amanda Boyd who undertook all steps that required a Home Office personal animal licence.

2.9.3 Sampling of brain tissue from mice following infection

Mice were terminally anaesthetised with a halothane:oxygen mix and intracardially perfused with sterile PBS. Once anaesthetised, the thoracic cavity was opened and the right atrium of the heart was cut. The left ventricle was cannulated using a needle and >8ml of PBS was carefully and slowly administered until the liver and lungs gained a pale colour indicative of blood clearance. The extent of perfusion of the brain was scored using an arbitrary scale of 1 (no perfusion) to 10 (perfect perfusion). The brain was removed and bisected laterally down the midline. One half of the brain was immediately placed in RNAlater (Sigma) for gene expression analysis. The other half of the brain were either fixed in PLP for 4hours at 4°C and passed through graded sucrose solutions of 12%, 16% and finally 18% in PBS (two, twenty minute incubations in each solution) for future use in immunocytochemistry on frozen (cryostat cut) sections or fixed in 4% phosphate buffered formal saline and sent to the histology service for paraffin embedding and sectioning.

2.10 RNA extraction

Total RNA was extracted from samples using the RNeasy Mini kit (Qiagen, Crawley, UK). This process is based on the ability of silica-gel-based membranes to selectively bind RNA

above 200 bases in length. This process partially enriches for mRNA since the majority of 5S rRNA and tRNAs are selectively excluded. Proteins, lipids and DNA do not bind to these columns (see www.qiagen.co.uk for more details).

2.10.1 RNA purification from brain and spleen

RNA was extracted from tissue samples using the RNeasy Mini kit as per manufacture's instructions with the alterations indicated below. Briefly, tissues were removed from RNA Later and 80 mg tissue homogenised in a cooled glass homogeniser (2 ml), mixed with 1.6 ml RLT buffer (containing β-Mercaptoethanol at 10 µl per ml RLT and guanidine thiocyanate) and passed through a 19 gauge needle twenty times. The resulting homogenate was either frozen or mixed with an equal volume of 70% ethanol (molecular grade) to alter binding properties of RNA and loaded on to two RNeasy columns per 80 mg sample (40 mg of tissue per column). Columns were washed once with RW1 buffer (containing ethanol) and contaminating DNA digested using on-column digestion with DNAse1 (Qiagen) for 15 minutes. Following two more washes with RW1 buffer and RPE buffer (constitutes 95% ethanol), RNA was eluted in 30 µl RNase free water and the integrity and concentrations of the RNA was determined using an Agilent 2100 Bioanalyser (Agilent Technologies, Edinburgh, UK) as per manufacture's instructions. Briefly, 1.5 µl of RNA was heated to 70^0C for 2 minutes and cooled on ice for at least 5 minutes. Meanwhile, the RNA Agilent chip was prepared by loading gel and markers as per manufacture's instructions. Each chip was loaded with up to twelve 1µl samples of total RNA. Concentrations were determined by comparison to RNA ladder (150 ng) and integrity determined with visualisation of the 18S and 28S ribosomal bands/peaks and lack of small, degraded RNA fragments (see figure 6).

2.10.2 RNA purification from cell cultures

Total RNA was extracted from cultured cells using the RNeasy Protect Mini kit (Qiagen) as per manufacture's instructions. Briefly, cell pellets of not more than $1x10^7$ were either lysed immediately after harvesting or following preservation in RNA later, were pelleted by centrifugation at 4000 g for 10 minutes, re-suspended in RLT lysis buffer, loaded onto RNeasy columns and contaminating DNA digested using on-column digestion (Qiagen). RNA was eluted in RNase free water and the integrity and concentration determined by the Agilent 2100 Bioanalyser (Agilent Technologies, Edinburgh, UK) as per manufacture's instructions.

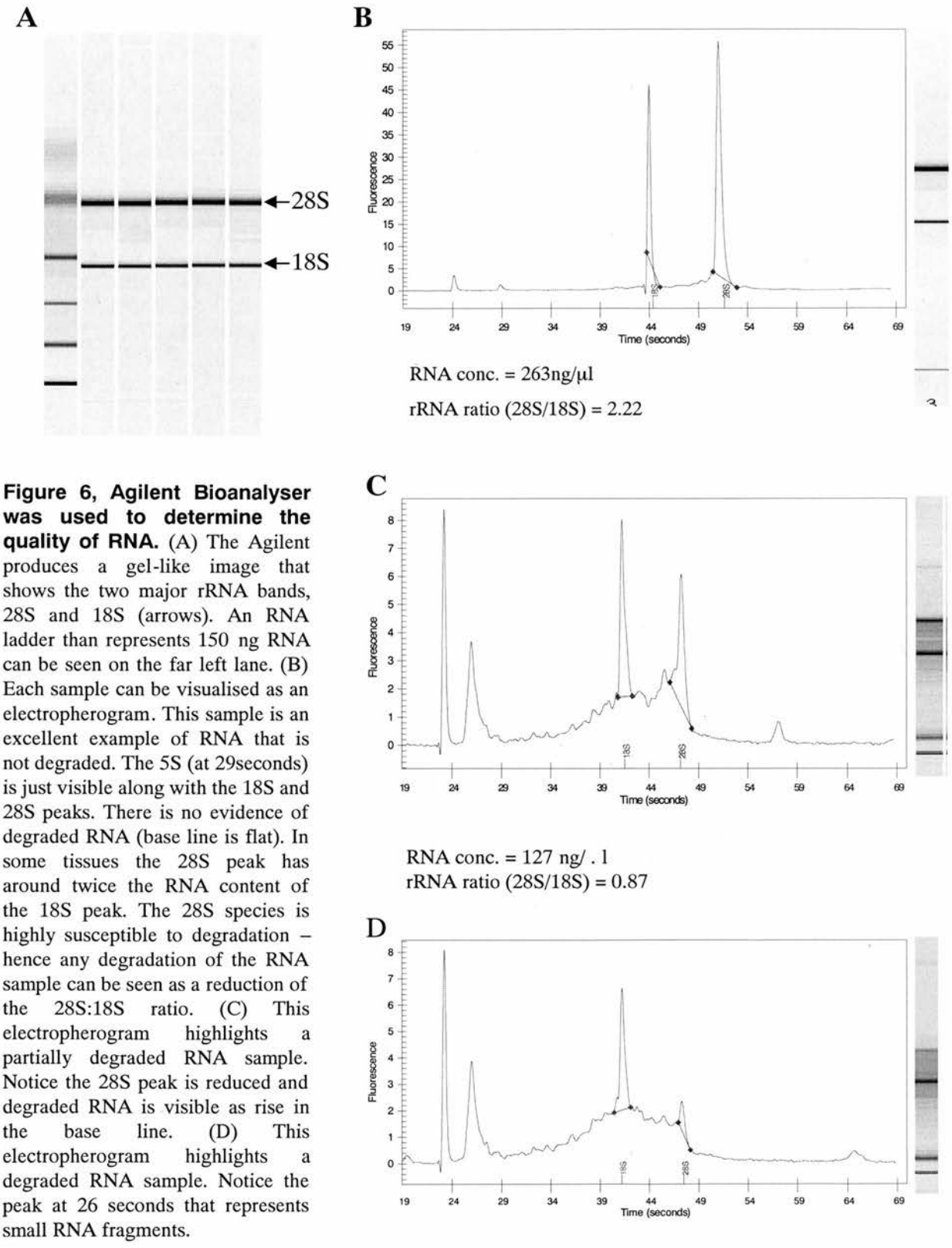

Figure 6, Agilent Bioanalyser was used to determine the quality of RNA. (A) The Agilent produces a gel-like image that shows the two major rRNA bands, 28S and 18S (arrows). An RNA ladder than represents 150 ng RNA can be seen on the far left lane. (B) Each sample can be visualised as an electropherogram. This sample is an excellent example of RNA that is not degraded. The 5S (at 29seconds) is just visible along with the 18S and 28S peaks. There is no evidence of degraded RNA (base line is flat). In some tissues the 28S peak has around twice the RNA content of the 18S peak. The 28S species is highly susceptible to degradation – hence any degradation of the RNA sample can be seen as a reduction of the 28S:18S ratio. (C) This electropherogram highlights a partially degraded RNA sample. Notice the 28S peak is reduced and degraded RNA is visible as rise in the base line. (D) This electropherogram highlights a degraded RNA sample. Notice the peak at 26 seconds that represents small RNA fragments.

2.11 Microarray fabrication, preparation, cDNA labelling and hybridisation

2.11.1 Probe design and array fabrication

Customised DNA arrays were fabricated by The Scottish Centre for Genomic Technology and Informatics (ScGTI), Edinburgh, UK. Each array contained 282 50-mer long probes complementary to 161 genes printed in triplicate and 10 SpotReport probes (Stratagene, SpotReport™) printed ten times each. Probes were dissolved in 3 X SSC buffer and arrayed onto either poly-L-lysine-coated glass slides or Corning-Gap ™ glass slides, using a Microgrid II arrayer (Genomic Solutions).

Prior to printing glass slides were coated in poly-L-lysine using the following method. Slides were first washed in 0.5 M NaOH dissolved in a 60% ethanol:water mixture for 2 hours on a rotating platform. Slides were thoroughly washed in distilled water to remove all traces of NaOH and ethanol before a 1 hour incubation with 0.1 M poly-L-lysine in 10% PBS. Slides were then submerged in distilled water five time, spun dry for 5 minutes at 500 rpm and heated in an oven at 45°C for 15 minutes. Slides were stored in desiccators at room temperature until used. Alternatively slides from Coring Gap were purchased ready for printing and did not require poly-L-lysine coating.

To determine the success of each print-run a representative microarray was hybridised to SpotCheck, a Cy-3 labelled random 9-mer solution (Genetix). 20 . 1 of Spot Check was denatured at 95°C for 5 minutes, followed by cooling on ice for 5 minutes then applied to the array surface (arrays had been prepared and blocked as described in section 2.11.4). The SpotCheck solution was allowed to hybridise for 20 minutes in the dark at room temperature and then subjected to the following stringency washes in 250 ml glass baths with vigorous stirring; 1X SSC/0.2% SDS for 5 minutes, 0.1X SSC/0.2% SDS for 5 minutes and 0.1X SSC for 5 minutes. Slides were then spun dry at 1000 rpm for 1 minute and read using an Affymetrix 418 scanner.

Quality controlled microarrays were stored in desiccators at room temperature prior to use. For more detailed description of array design see results section 3.1. All probe sequences are listed in appendix 2.

2.11.2 Spiking of total RNA with SpotReport™

25 μg of purified RNA was spiked with 0.2 ng mRNA (Stratagene SpotReport™), carried in 10 ng/μl of yeast transcription RNA buffer. RNA was precipitated by the addition of 0.5 volumes ammonium acetate (7.5 M) and 2.5 volumes 100% ethanol and incubated at -80°C

overnight. Samples were centrifuged at 12,000 g for 25 minutes at 4°C. The resulting pellet was washed twice in 80% ethanol at 12,000 g for 5 minutes at 4°C. The pellet was then re-suspended in 9 µl of DEPC-treated water and stored at -80°C. For more detailed description see results section 3.1.

2.11.3 cDNA Synthesis from total RNA for microarray analysis

cDNA was synthesis by reverse transcription (RT) was undertaken using one of two methods. The first method involved a custom based approach using individual reagents and did not rely on any commercially available kits designed specifically for microarray labelling reactions. Briefly, 25 µg of RNA was incubated with 2 µg Oligo-dT at 70°C for 10 minutes to denature RNA, followed by 5 minutes incubation on ice. An RT master mix was made containing per reaction; 6 µl 5X Buffer (SuperScript II), 3 µl DTT (0.1 M), 0.6 µl dNTP mix (25 mM each, except dCTP which was 15 mM), 3 µl Cy3-dCTP (1 mM) and 2 µl SuperScript II reverse transcriptase (Invitrogen). 14.6 µl of master mix was added to each RNA sample and incubated for 2 hours at 42°C. Resulting cDNA samples were incubated with 15 µl 0.1 M NaOH at 70°C for 10 minutes, followed by the addition of 15 µl of 0.1 M HCl to neutralise and 0.5 µl Tris-HCl (pH 7.5) for buffering. Labelled cDNA was mixed with 20 µg COT-1 human DNA (Invitrogen, Life Technologies) to buffer labelled cDNA for subsequent purification steps and reduce non-specific binding of DNA to the microarray surface. YM-30 microfiltration columns (Amicon) were used wash once in 500 µl and then to reduce the final volume of labelled cDNA to < 8 µl. YM-30 columns enable all molecules below 30,000 MW to pass through along with water during centrifugation at 4000 g. Samples were immediately processed for hybridisation to the microarray (see section 2.11.5).

Alternatively, cDNA was synthesised from total RNA using the FluoroScript™ cDNA Labelling System (Invitrogen, Life Technologies). Briefly 25 µg of total RNA was incubated with 0.5 µg of Oligo-dT at 70°C for 5 minutes to denature RNA, followed by 5 minutes incubation on ice. RT master-mixture was made containing per reaction; 4 µl 5X Fluoroscript™ buffer, 2 µl DTT (0.1 M), 1 µl dNTP mix (0.5 mM each, except dCTP which was 0.3 mM), 2 µl Cy3-dCTP (1 mM) and 1 µl Fluoroscript™ (15 U/µl). 11 µl of the resulting master mixture was added to the denatured RNA to give a total volume of 20 µl. The resulting RT mixture was incubated at 50°C for 1 hour. The reaction was stopped by the addition of 2 µl of 200 mM EDTA. Resulting cDNA samples were incubated with 15 µl 0.1 M NaOH at 70°C for 10 minutes, followed by the addition of 15 µl of 0.1 M HCl to

neutralise and 0.5 µl Tris-HCl (pH 7.5) for buffering. Labelled cDNA was mixed with 20 µg COT-1 human DNA (Invitrogen, Life Technologies) to buffer labelled cDNA for subsequent purification steps and reduce non-specific binding of DNA to the microarray surface. Excess Cy3-dCTP label was removed from cDNA by elution through S.N.A.P™ columns as per manufacturer's instructions (Invitrogen, Life Technologies). YM-30 microfiltration columns (Amicon) were used to reduce the final volume of labelled cDNA to < 15 µl. Thus, a YM-30 column further purifies the labelled cDNA and concentrates it. Samples were immediately processed for hybridisation to the microarray (see section 2.11.5).

2.11.4 Microarray slide preparation

Microarray slides were prepared for hybridisation to labelled cDNA with a methodology similar to that previously described (Ebrahimi et al., 2003). Oligonucleotide probes were firstly cross-linked to Corning-Gap ™, poly-lysine coated slides under UV light (3000 units). The array of probes can be visualised whilst the surface is dry, however following re-hydration the probes can no longer be seen without the naked eye. Hence, prior to rehydration the array area was demarcated using a diamond pen to scratch the surface surrounding the array. Arrays were re-hydrated in a humidity chamber containing 3X SSC for 5 minutes at room–temperature and then placed on a hotplate at 70°C for 10 minutes. Following incubation, slides were repeatedly submerged in a 170 mM succinic anhydride/N-methyl-2-pyrrolidinone solution buffered by a borate at a final concentration of 40 mM vigorously for seven submersions. Following a further 15 minutes with vigorous stirring, slides were submerged in ≅ 95°C milliQ water for 2 minutes followed by submersion in absolute alcohol and spun dry at 1000 rpm for 1 min.

2.11.5 Hybridisation protocol

Labelled target cDNA samples from section 2.12.3 were immediately mixed with 3.46 µl 20X SSC, 0.58 µl 10% SDS and appropriate volume of nuclease-free water to give a final volume of 20 µl. The resulting hybridisation mixture was incubated at 100°C for 2 minutes followed by incubation at 37°C for 30 minutes. Samples were spun for two minutes to remove any precipitates, volume adjusted to 20 µl if necessary and added to the array surface by application to the underside of a 22 mm x 25 mm LifterSlip (Merck) cover slip that distributes an equal volume of cDNA across the array. Arrays were placed in a humidified chamber, sealed and incubated at 57°C overnight in the dark. The next day microarrays received the following stringency washes in 250 ml glass baths with vigorous stirring; 1X SSC/0.2% SDS for 5 minutes, 0.1X SSC/0.2% SDS for 5 minutes and 0.1X SSC for 5

minutes. Slides were then spun dry at 1000 rpm for 1 minute and read using an Affymetrix 418 scanner.

2.11.6 Microarray Analysis

Image quantification was carried out in a similar way as described previously (Forster et al., 2003). Probe signal and background signal was determined using Quantarray^{Tm} (PerkinElmer, Boston, USA). To normalise signal intensity across the array slide, arrays were intra-normalised using SpotReport™ Oligo Array Validation System (Statagene, La Jolla, CA, USA). For a particular array the average median of negative control probes + 2 times standard deviations were used to calculate background signal. Probes producing a signal at or lower than background levels were considered below the threshold of detection. Arrays were then inter-normalised by comparing the 75th percentile of 30 housekeeping probe signals of each array. The median value of each probe spot (printed in triplicate) was selected to represent each probe for a particular array. Selecting the median in this way prevents probes that produce erroneous exceptionally high signals from contributing to the data (Forster et al., 2003). The signal of each probe was converted to a log base$_2$ value for comparison between arrays. More detail on the analysis of array data can be found in results chapter 3.1.

2.12 Quantitative polymerase chain reaction (QPCR)

2.12.1 Reverse transcription of RNA for Quantitative Polymerase Chain Reaction

cDNA was synthesised from total RNA by reverse transcription (RT) using Superscript II. 5 μg of RNA was mixed with 0.5 μg oligo-dT primer, dNTPs (0.5 mM each final), denatured at 65°C for 5 minutes and placed on ice for 5 minutes. An RT master mix was made up to contain per reaction; 5 μl 5X buffer, 2 μl 0.1 M DTT, 0.5 μl RNAsin (RNase inhibitor). 6.5 μl of master mix was added to each denatured RNA sample and incubated for 2 minutes at 42°C. 50 units of Superscript II was added and incubated for 60 minutes at 42 °C followed by a 15-minute inactivation step at 70°C.

Samples were diluted either 1 in 5 or 1in 10 in nuclease free water and used as template for QPCR. Samples that were to be directly compared within a quantitative PCR were reverse transcribed using the same master mix to avoid inter-day and inter mixture variability in reverse transcriptase activity (all reagents from Invitrogen).

2.12.2 Primer Design

A set of "inner" primers were designed for use in the quantitative PCR machine (Rotorgene 3000, Corbett Research, Australia) and an "outer" set of primers were designed for creating PCR products to act as standard templates. All primers were designed using Primer3 software (available online @: http://www.broad.mit.edu/cgi-bin/primer/primer3_www.cgi/) and verified for low spontaneity to form duplexes and hairpin loops using Oligo6 software (Molecular Biology Insights, CO, USA).

Primer specification:

- between 18 and 20 base-pair (bp) in length
- between 45 and 55% GC content (50% optimal)
- Max self complementarity: 2
- Max 3'self complementarity: 1
- Outer primers were allowed to possess higher self complementarity levels if the software could not suggest suitable primers using the above criteria
- BLAST analysis (http://www.ncbi.nlm.nih.gov/BLAST/) was used to ensure primer sequences were specific to gene of interest alone

Both sets of primers were tested for specificity by undertaking a standard PCR using cDNA substrate sourced from either resting or infected brain RNA. PCR products were separated using electrophoresis through an agarose gel (2%) and visualised using ethidium bromide. PCR primers were deemed suitable for QPCR if single, clear and distinct bands of the correct predicted size were found on the gel, indicating PCR specificity. The presence of multiple bands or smears on the gel implied primers would not be suitable for QPCR. PCR products were also visualised using the Agilent Bioanalyser as per manufacturer's instructions. All primer sequences can be found in table 4.

2.12.3 Generation of DNA standards for QPCR

The generation of a standard curve is essential for quantifying the levels of the gene of interest in the test samples. A standard DNA template for each gene assayed was generated by taking the PCR product generated using the outer primers, purifying the PCR product on a PCR purification column as per manufacturer's instructions (Qiagen) and diluting this product to generate serial dilutions. Each dilution was a factor of 10 more dilute than the previous. Each of these dilutions was used as a template for a QPCR using the inner primers for amplification. The ability of the QPCR platform to discern that the template is present at

Gene	Genbank	Inner1	Inner2	PCR product size
		5 'TO 3'	5 'TO 3'	(bp)
TLR1	NM_030682	TACAGTTCCTGGGGTTGAGC	TAGTGCTGACGGACACATCC	216
TLR2	NM_011905	CGTTGTTCCCTGTGTTGCT	AAAGTGGTTGTCGCCTGCT	119
TLR3	NM_126166	TTGCGTTGCGAAGTGAAG	TAAAAAGAGCGAGGGGACAG	406
TLR4	NM_021297	TTCACCTCTGCCTTCACTACA	GGGACTTCTCAACCTTCTCAA	225
TLR5	NM_016928	CAGGATGTTGGCTGGTTTCT	CGGATAAAGCGTGGAGAGTT	169
TLR6	NM_011604	ATGGCACAGCGGACTTACTT	ATGAGAGCCCAGGTTGACAG	170
TLR7	NM_133211	GCTGTGTGGTTTGTCTGGTG	CCCCTTTATCTTTGCTTTCC	270
TLR8	NM_133212	GACTTCATCCACATCCCAAA	TCCCAATCCCTCTCCTCTAA	156
TLR9	NM_031178	GAAAGCATCAACCACACCAA	ACAAGTCCACAAAGCGAAGG	304
TLR13	NM_205820	CTGTCTTCACCAACGGGATT	CAAGTCGGCACCATTCACT	131
CathepsinD*	NM_009983	GCTGTTCTGTTCTGTGGTTC	TTCTGTCCTCTTCTTGCTCCTTC	326
GAPDH*	NM_001001303	AACTCCCACTCTTCCACCTT	GCCCCTCCTGTTATTATGG	269
GFAP*	NM_010277	GAAAACCGCATCACCATTCC	CGCATCTCCACAGTCTTTACC	128
IL-6	NM_031168	TTCCATCCAGTTGCCTTCTT	ATTTCCACGATTTCCCAGAG	171
IL-1alpha*	NM_010554	GATGTCCAACTTCACCTTCA	ACAAACTTCTGCCTGACGA	228
IL-1beta*	NM_008361	GTGTAATGAAAGACGGCACA	AGAAACAGTCCAGCCCATAC	269
INF-alpha4	NM_010504	AGGACAGGAAGGATTTTGGA	GCTGCTGATGGAGGTCATT	186
IFN-beta**	NM_010510	CACAGCCCTCTCCATCAACT	GCATCTTCTCCGTCATCTCC	152
TNF-alpha*	NM_013693	CCCTTTACTCTGACCCCTTT	AACCTGACCACTCTCCCTTT	260
SFV E1***	X74491	CGCATCACCTTCTTTGTG	CCAGACCACCCGAGATTTT	173
Beta-actin	NM_007393	CGTTGACATCCGTAAAGACC	CTGGAAGGTGGACAGTGAG	202

Table 4A, sequences for primers used in QPCR reactions. Primers are referred to as the "inner" primers.

Gene	Genbank	Outer1	Outer2	PCR product size
		5' TO 3'	5' TO 3'	(bp)
TLR1	NM_030682	CCTTTGATGCCCTGCCTAT	ATGCCAAACTATCTGGAGGA	436
TLR2	NM_011905	GCTGAAAACACTCCCAGATG	GCCAGTCAACCAGGATTTG	211
TLR3	NM_126166	CCAACTCAGAAGATTACCACCT	GGGATGTGAAGCAAGTGAAA	849
TLR4	NM_021297	ACAGCAGAGGAGAAAGCATC	TCCCATTCCAGGTAGGTGTT	393
TLR5	NM_016928	GCCTGTAACTTCTCCCAAGG	ATTCTCATCGTGGTGGTGGT	535
TLR6	NM_011604	TCATCTTGCTGGAACCCATT	CAGGTAGGAACTGAAAACCACA	262
TLR7	NM_133211	CTGAGGTTTTTGAGGGTATGC	CTGTATGCTCTGGGAAAGGTT	844
TLR8	NM_133212	CTGTTTTACTGGGATGTTTGG	TTTCTTGCTCTGGTTTATGCTC	269
TLR9	NM_031178	GGTTCCAAGGTCTGGTCAAC	GCATCATCTGCCTCTTCAGG	423
TLR13	NM_205820	AATGGCACAAAACGGAGAAAG	AGAAAAGTGGCTGCTGGTGA	432
CathepsinD*	NM_009983	TAGTGTTGCTGGACCCTTG	CCCCCAGGTTCATAGTTTT	392
GAPDH*	NM_001001303	TGTCTCCTGCGACTTCAA	TGCAGCGAACTTTATTGATG	341
GFAP*	NM_010277	CCAGTTACCAGGAGGCACTT	TCACATCACCACGTCCTTG	338
IL-6	NM_031168	TCCAGAAACCGCTATGAAGT	CTCCAGAAGACCAGAGGAAA	370
IL-1alpha*	NM_010554	TCCTGACTTGTTTGAAGACC	TAGTTTGGTTGAGGGAATCA	425
IL-1beta*	NM_008361	GCAACGACAAAATACCTGTG	GCCGAGGACTAAGGAGTGT	412
INF-alpha4	NM_010504	TGGCTAGGCTCTGTGCTTTC	GGAGGTTCCTGCATCACAC	385
TNF-alpha*	NM_013693	GTGAAGGGAATGGGTGTTC	TGGAAAGGTCTGAAGGTAGG	370
Beta-actin	NM_007393	GTACTCCTGTTGCTGATCC	GTACTCCTGCTTGCTGATCC	272

Table 4B, sequences for primers used to generate DNA templates standards. Primers are referred to as the "outer" primers as the PCR product encompasses the sequence to which the "inner" primers bind. NB There are no outer primers for SFV E1 of IFN-. as a plasmid containing the gene sequences was used as a DNA standard for these QPCRs.

* primers designed by Alan Brown
** primers designed by Lucy Breakwell
*** primers designed by Rennos Fragkoudis

differing levels in the serial dilutions indicates the range and sensitivity of the quantification process. The use of standards also permits relative and absolute quantification of unknown transcript levels in samples.

The absolute amount of each standard was determined by analysing the mass of each PCR product using the Agilent Bioanalyser (Agilent Technologies). Copies of each transcript were then calculated using the following formulas with β-actin given as an example:

β-actin PCR product was 278 bp in size and had a concentration of 7.035×10^{-8} g per µl.

Copies of molecule per mole = 6.023×10^{23} (Avagadro's constant)

Average molecular weight for double stranded nucleotide = 660 Daltons

Molecular weight of double stranded DNA = 660 Daltons * PCR product length

= 660 * 278 bp

= 183,480 Daltons

Copies DNA per µl = $(6.023 \times 10^{23}$ * mass per µl) / Molecular weight DNA

= $(6.023 \times 10^{23} * 7.035 \times 10^{-8}) / 183{,}480$ Daltons

= 2.309×10^{11} copies per µl

2.12.4 Quantitative PCR assay

The PCR mixture (total volume 20 µl) contained; 2 µl 10X PCR buffer, 2.8 µl $MgCl_2$ (25 mM). 0.4 µl dNTP mix (10 mM each), 2 µl cDNA, 0.4 µl of each primer (50 pmol/µl), 0.15 µl FastStart Taq polymerase (Roche Applied Science, Germany), 0.7 µl SYBR (BioGene Ltd.) and 11.15 µl nuclease free water. Following a hot start at 95°C for 10 minutes to activate the hot-start Taq polymerase, an amplification cycle was carried out for 40 cycles at the following temperatures; 95°C for 30 seconds, 62°C for 20 seconds, 72°C for 20 seconds on a RotorGene 3000 (Corbet Research, Australia). Fluorescence was measure at the end of each 72°C step. At the end of the PCR a melt curve analysis was performed as per manufacturers instruction: measuring fluorescence during a incremental increase in temperature from 65°C to 94°C. A serial dilution of PCR fragments containing template of interest was also assayed concurrently to convert cycle number of exponential amplification to copies of template of interest (Brown et al., 2003).

Alternatively, QPCR was undertaken with a Roche LightCyler™, utilising the LightCyler-FastStart DNA Master SYBR Green I mix (Roche Applied Science, Germany). Briefly, the fast start Taq master mix was prepared as per manufacturers instructions and $MgCl_2$ added to a final concentration of 4 mM. 2 µl of cDNA (diluted 1 in 10) was added to 18 µl master-mix and placed in the LightCycler and heated as follows: 95°C denaturation for 10 minutes

followed by 40 cycles of: 94°C for 10 seconds, 62°C for 5 seconds and 72°C for 10 seconds. Melt curve analysis was undertaken by measuring fluorescence from 65°C to 95°C.

2.12.5 Normalisation of cDNA samples

To allow effective comparison of gene levels between samples, normalisation of cDNA levels was undertaken. The amount of cDNA between samples can inadvertently be varied by multiple factors including: variation introduced during RNA extraction, differential RNA degradation, the amount of RNA used in the reverse transcription reaction and the reaction efficiency of the reverse transcription. This variation was reduced by; 1.) Using exactly 5 μg of non-degraded total RNA (as determined by Agilent Bioanalyser) – hence in effect normalising to levels of 18S rRNA; 2.) All samples that were directly compared within a quantitative PCR were reverse transcribed using the same master mix to avoid inter-day and inter mixture variability in reverse transcriptase activity; and 3.) Housekeeping genes were used to normalise samples as described previously (Brown et al., 2003; Vandesompele et al., 2002; Suzuki et al., 2000). Housekeeping genes are those genes that are required for cell metabolism, are expressed in all cells and have no role to play in cell differentiation (Suzuki et al., 2000). One can assume that the levels of all housekeeping cDNA will be varied in proportion to one another and genes transcripts of interest.

Levels of two housekeeping genes (β-actin and/or GAPDH) were assayed via QPCR to determine the level of cDNA present within a specific sample (an example of the normalisation process is given in Table 5). β-actin is a major cytoplasmic structural protein whilst GAPDH is an important glycolytic enzyme that catalyses the oxidative phosphorylation of glyceraldehyde-3-phosphate to 1,3-diphosphoglycerate. β-actin was primarily used as a control, since a review of the literature has reported the expression of this gene to be more reliable than other commonly used controls– particularly for *in vivo* work (Suzuki et al., 2000). Each sample was allocated a ratio of its β-actin /GAPDH content in relation to the 75th percentile of β-actin /GAPDH levels of all samples assayed. This ratio was subsequently used to normalise the levels of genes of interest (see table 5 for an example).

In actuality, any sample whose housekeeping genes varied by more than a factor of 2 from the 75th percentile, were disqualified and excluded from the analysis due to error that can be introduced by such large scale alteration of the raw data.

A	B	C	D	E
Sample Name	**Assayed level of gene X**	**Level of house keeping gene**	**Ratio to 75th Percentile**	**Normalised level of gene X**
	(copies/µl)	(copies/µl)	**(column C/71.25)**	**(column B/D)**
LPS1	10	40	0.561	18
LPS2	50	200	2.807	18
LPS3	12	45	0.632	19
LPS4	10	10	0.14	71
LPS5	8	40	0.561	14
	75^{th} percentile	**71.25**		

Table 5 An example of normalisation using a housekeeping gene to determine levels of "gene X". Notice that pre-normalised levels indicate that sample LPS2 has a high value of 50 copies of gene X and that sample LPS4 has a low value of just 10 copies (column B). Once the cDNA levels have been normalised the results demonstrate the level of gene X in sample LPS2 was in fact quite low compared to the majority of the samples. This was because the amount of cDNA present in this sample was high. Conversely, the level of gene X in sample 4 appears low in pre-normalised levels although in actuality the level is much higher - since there was only a small amount of cDNA in this sample. The 75^{th} percentile of housekeeping gene copy number is determined and used as a reference since this value unlike other measures, such as the mean average, are affected little by outliers that may skew the result in a particular direction. A ratio is then determined for each sample and in doing so measures the difference of each sample from the 75^{th} percentile. Levels of gene X can then be altered on the assumption that the ratio of housekeeping gene to gene X is uniform.

Chapter 3. The development of a custom microarray that assays the expression of genes involved in innate immune responses.

Contents

3.1.1 Introduction

Microarrays enable the collection of gene expression data for a large number of genes in a single experiment. Each microarray contains features (spots) representing hundreds to thousands of genes that are surveyed in an assay in which a sample representing the mRNA expressed in the cell of interest are labelled with a distinguishable marker and allowed to hybridise to features on the array. The microarray platform assumes that the relative amount of hybridisation for each of the labelled extracts for each feature represents the relative population of the corresponding mRNA species in the experimental sample. Microarrays have successfully been used to identify novel gene expression pattern in many scientific fields of interest. They have been particularly useful in identify putative mechanisms of disease processes where little was previously known. Microarrays can discern new trends and identify patterns of gene expression that can lead to new hypothesis of cellular function and pathogenesis; both *in vitro* such as the actions of glucocorticoids on immune cells (Galon et al., 2002); and *in vivo* such as the complex interactions that occur during scrapie neuropathogenesis (Brown et al., 2004). However, the cost of commercial microarrays is prohibitively expensive and makes their use inappropriate for extensive research work.

Here, a custom glass slide DNA oligonucleotide microarray platform has been developed that is relatively inexpensive. Probes complementary to a variety of genes of interest were designed and arrayed onto a glass slide. RNA from the cells of interest was used to generate first-strand cDNA labelled with the spectrally distinguishable fluorescent dye Cy3 and hybridised to the microarray. The arrays were scanned following hybridisation and independent grey-scale images were generated for control and test samples as 16-bit Tagged Image File Format (TIFF) files. These images were analysed to identify spots and measure the relative fluorescent intensities of each spot. Once each spot was identified and measured, signal intensities were normalised to effectively compare within, and between arrays. The whole process of designing and developing a reliable microarray platform required considerable time and resources and is described here.

3.1.2 Objectives

To design and develop a microarray platform:

1. That possesses probes that function under the same conditions of hybridisation:
    a. probes must be, as a population, thermodynamically homogenous
    b. probes must be refractory to secondary structure formation
2. With optimised hybridisation conditions

3. That produces a strong, specific, detectable signal that is consistent across the array surface
4. That demonstartes little inter-array variation i.e. replicate arrays produce a consistent signal

To undertake these objectives a custom microarray was designed and validated with the help and guidance of several members of the Scottish Centre for Genomic Technology and Informatics (ScGTI), including Douglas Roy, Klemens Vierlinger, Marie Craigon, Thorsten Forster and Peter Ghazal.

3.2 Design of microarray

3.2.1 Choice of target genes

The microarray platform was designed with the aim to primarily characterise pattern recognition receptor (PRR) expression and the first task was to define a list of specific genes to be assayed. The exact definition of a PRR is somewhat vague and so a variety of genes were included. All TLR and TLR-like proteins (such as Rp105 and Nod1) were included along with several lectins that bind microbial associated sugars (such as CD14), secreted PRRs (such as Mannose Binding Lectin 1), scavenger receptors that bind both exogenous and endogenous proteins (such as SR-AI), the peptidoglycan recognition protein (PGRP) family, the N-formyl peptide receptors and other putative PRRs including the triggering receptor expressed on myeloid cells (TREM) family. Several other genes that have putative functions such as the PrP^{Sc} receptor were included in the list (such as complement receptor 1 and PrP itself) (Mabbott and Bruce, 2001). Genes that function to recognise the unique molecular patterns of apoptotic cells, such as the phosphatidylserine receptor and the integrins were also included in the list since these apoptotic cell associated molecular patterns (ACAMPs) may be recognised in a fashion analogous to pathogen associated molecular patterns (PAMPs) (Gregory, 2000). It is advantageous to characterise the inflammatory state of immune cells along with PRR expression, since one can discern trends in PRR expression in the context of other markers of innate immune activation. Thus, in addition to PRRs the microarray was also designed to assay a multitude of key genes involved in the process of inflammation and stress-associated responses including; several key pro-inflammatory cytokines (such as TNF-α), anti-viral mediators (such as IFN-β) several chemokines (such as MIP-1α) and a variety of genes that either mediate stress responses or are induced as a reaction to conditions of cellular stress (such as nitric oxide

synthase (Nos), superoxide dismutase (SOD), cylco-oxygenases (COX) and heat shock protein 25 (Hsp25)). In addition to these genes, termed "genes of interest", a variety of positive and negative controls were chosen. The number of control probes included on the microarray was sufficiently high to allow effective statistical analysis. The positive controls represent genes that are constitutively expressed within all murine cells and whose presence is mandatory for cell survival - genes that are often referred to as housekeeping genes. A total of 15 housekeeping genes were chosen, some which are highly expressed (such as β-actin) and housekeeping genes that are generally expressed at lower levels (such as glycogen synthase kinase-3β) (Warrington et al., 2000). The reasons for including probes that recognise housekeeping genes are two fold – demonstration that the microarray platform adequately detects gene expression in each sample and demonstration of the sensitivity of the platform to detect transcripts present at differing levels. Finally, several genes with no homology to known mammalian genes were identified so that probes could be generated on the assumption that they recognise no known murine gene products. These probes were referred to as the "negative controls" and included genes such as *celA* from *Ruminous flavefaciens* and *Chlorophyll A-B binding protein 7* from *Arabidopsis thaliana*.

3.2.2 Design of oligonucleotide probes

Microarrays can differ in the type of DNA arrayed across the surface. There are cDNA arrays where PCR products are typically used as probes for array spots, and oligo arrays where the spots are made of oligonucleotides. PCR products offer the advantage of amplification so that limited template DNA and clone banks can be spotted multiple times after amplification from a single source plate. However, reliance on amplification means that there are a number of precautions needed to prevent contamination and the sequence is typically 400 to 1000 bp long. Conversely oligonucleotides are purchased at high expense and can only be used for a limited number of print runs before more oligonucleotides have to be purchased.

Oligonucleotides are typically used in the range of 25 to 80 bp, and are generated synthetically in a form ready for spotting. They are less prone to the problems of contamination and can be produced quickly, without resources and time being spent on extensive cDNA library work and sequencing. Importantly, unlike PCR spots oligonucleotides can be *designed* to; minimise cross hybridisation with other genes; have lower secondary structures; and have similar hybridisation efficiencies at a given temperature. Therefore, with careful design oligonucleotide spots are more likely to hybridise at a similar efficiency. In comparison, PCR spotted arrays demonstrate higher

variation in the efficiency of hybridisation between individual spots. Also, oligonucleotides are better able to distinguish between highly related genes such as the TLR, unlike PCR spots that due to their size are likely to bind all members of a closely related gene family. (Lockhart et al., 1996; Kane et al., 2000).

Oligonucleotide probes were designed using Oligo6 software to suggest possible hybridisation probes complementary to cDNA from mRNA transcripts. From the list of probes suggested by the software for an individual gene, two were selected as probe sequences based on a variety of criteria. These criteria were based on the predicted thermodynamics of the probe, its probability of forming unwanted secondary structures, its hybridisation target on the cDNA sequence and its specificity. Probes that possess stable secondary structures may not bind to their target sequence with sufficient strength at hybridisation temperatures. The Oligo6 software can predict the spontaneity of probes to form duplexes and hairpin loops and this was used to exclude certain probes. A well-functioning microarray possesses probes that exhibit similar thermodynamic properties, since each probe has to hybridise to its target sequence under the same hybridisation conditions such as temperature and salt concentration. Indeed, populations of probes with homogenous thermodynamic characteristics are more likely to generate a measurable signal within the dynamic range of a given microarray platform (Kane et al., 2000).

Consequently, the probes were chosen to have the following characteristics:

- Tm between 87°C and 94°C (90^{0}C optimal)
- ΔG between -84 and -96 kcal/mol (the more negative the ΔG value the stronger the binding between probe and complementary cDNA strand)
- ΔG of predicted hairpin structures above -1.5 kcal/mol (the more negative the ΔG value the more stable the hairpin loop)
- Tm of predicted hairpin structures must not exceed 45°C (20°C to 30°C optimal)
- ΔG of predicted probe duplexes must be above -10 kcal/mol
- probes must bind as close to the 5' polyT tail of the cDNA as possible without compromising above criteria. Each gene must have one probe that binds within 600 bp of the 5' polyT tail
- all probes must not possess a stretch of 16 or more contiguous bases that are complementary to any known mouse mRNA sequence (other than target sequence)

The location on the cDNA sequence to which the probe binds was highly restricted. This was due to several factors including the limitations of the cDNA synthesis reaction. The process

of converting mRNA to cDNA that incorporates Cy-dye labeled nucleotides was highly inefficient, which means longer cDNA strands were synthesized in low amounts. This means the cDNA representing the 3'end of the mRNA were greatly enriched and very few cDNA representing the entire mRNA transcript were produced. For this reason probes were designed to bind close to the 5' polyT tail. Another advantage of designing probes that bind to the 5' polyT tail is that this region represents the 3' untranslated region of the mRNA. These sequences tend to be more gene-specific and decrease the probability of cross-hybridisation to other gene transcripts.

Any probe sequence is likely to be complementary to non-target sequences for a stretch of nucleotides. Studies have shown that 50-mer probes that possess 16 or more contiguous bases that are complementary to a given labeled cDNA will bind and contribute to the spot signal (Kane et al., 2000). This characteristic is a particular problem for microarrays, which by their nature are 1-dimensional (unlike Northern gels that are 2 dimensional). Hence, all probes were BLAST searched to determine the extent of their specificity. Any probes that possessed 16 or more contiguous bases to other murine sequences were excluded, an event that happened frequently. On average for every final probe selected, four were excluded on the basis of their cross-complementarity to other murine transcripts.

Due to the strict criteria for probe design, not all specifications could be met for some probes. In these cases a hierarchy of criteria was chosen for probe specification. It was decided that the thermodynamic homogeneity of the probe population was more important than an individual probes theoretical ability to form secondary structures. Thus, the Tm and ΔG value of each probe was most critical, whilst the ability of the probe to form duplexes, its ability to bind to 16 or more contiguous bases of other murine transcripts and the probes site of complementarity to within 600bp of mRNA 3' end, was considered dispensable if no probes could be designed with all specifications met. For example, if no "perfect" probe could be designed then a probe with duplex formation would be preferable over a probe that exhibited divergent Tm/ΔG values. The ability of the probe to form a duplex was considered a low priority, since duplex formation is unlikely on glass microarrays due to the low probability of substrate-bound probes to form duplexes. The characteristics of the probes are shown in figure 7 and are described in detail in appendices 2 to 6.

Originally 75 mer probes were designed - however, these 75 mer probes were frequently found to contain stretches of contiguous oligonucleotides complementary to more than one gene and appeared to represent common nucleotide motifs. To avoid this, 50 mer probes were used. Smaller probes result in a lower signal upon hybridisation. However, because of their reduced length are less likely to possess a stretch of nucleotides that represents a

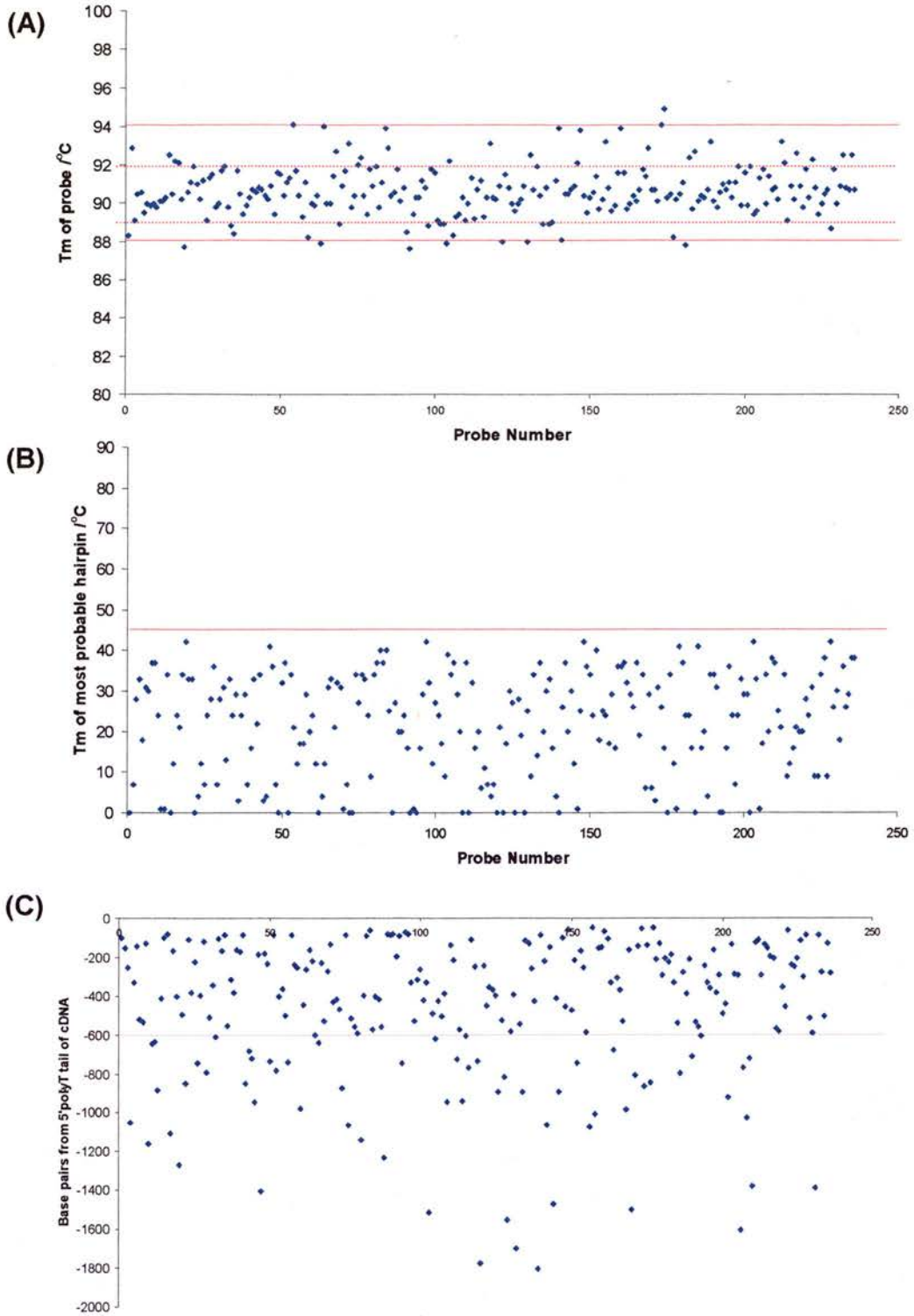

Figure 7, characteristics of oligonucleotide probes. (A) The predicted Tm of each probe, almost all of which are between 88 and 94°C, and the majority of which are between 89 and 92°C. Those probes that lie outside this narrow range represent a gene sequence that generates few probe sequences that match the strict criteria outlined in section 3.2.2. Each gene has at least one probe that possess a Tm between 89 and 92°C. (B) The predicted Tm of the most likely hairpin secondary structure, all of which are below 45°C and are unlikely to occur at hybridisation temperatures. (C) Distance of probe binding site from the 5' polyT tail of the cDNA. Each gene has at least one probe that binds within 600 bp of the cDNA 5' end and most genes have both probes binding within this region

common motif. Additionally, 50 mer probes were cheaper to synthesise (a significant point) and underwent more sophisticated quality control by the manufacturer (MALDI-TOF mass spectrometry), which was not possible for 75mer probes.

3.2.3 50-mer probes were arrayed randomly across the glass surface

As discussed above, two probes for each gene of interest were designed. These probes along with probes complementary to housekeeping genes (positive controls) and genes of non-animal origin (negative controls) were given an arbitrary number generated at random by Excel ™ (Microsoft Office 2000) and this was used to rank all probes such that there was no user-influenced order to their ranking. The probes were then arrayed onto the glass substrate according to this order by Klemens Vierlinger at the Scottish Center for Genomic Technology and Informatics (ScGTI) using a MicroGrid II arrayer (Genomic solutions). It was important to randomly distribute the probes across the array since this reduces the possibility of hybridisation error skewing the results. For example, if there was a defect in a particular hybridisation for a certain area of the array surface and two probes complementary for the same gene were arrayed side-by-side in this area, then both probes would give erroneous signals. Conversely, if the two probes are arrayed in different areas of the array surface then this is unlikely to happen. Likewise if one area of the array possessed all probes complementary for housekeeping genes and this area hybridised less well, then this would give an erroneous signal for all the positive controls. Randomly distributed positive controls are less likely to be influenced as a population in this way.

The randomly ordered probes were arrayed as four sub-arrays. Each sub-array contained a particular probe printed in triplicate. Figure 8 demonstrates the layout of the array. The rationale for printing each probe in triplicate was two-fold. Firstly, printing in triplicate allowed more reliable data to be produced from the array. Following hybridisation to a labeled cDNA substrate the signal from each "spot" or "element" was measured. The value of each triplicate repeat was compared and from these three values the median was used for further analysis and the others discarded (more details on data analysis are discussed below). By undertaking this screening, almost all outliers (those elements that give erroneous signals due to hybridisation defects) were excluded and a fair representative of the probe's signal was obtained. Figure 22 demonstrates how this decreased variation in the probe signal (Forster et al., 2003). Secondly, printing probes in triplicate enables the user to undertake more sophisticated quality control of each hybridisation. Theoretically, an ideally printed microarray that undergoes an ideal hybridisation should give the same signal for a particular probe that is printed multiple times across the array i.e. a perfect hybridisation is one in

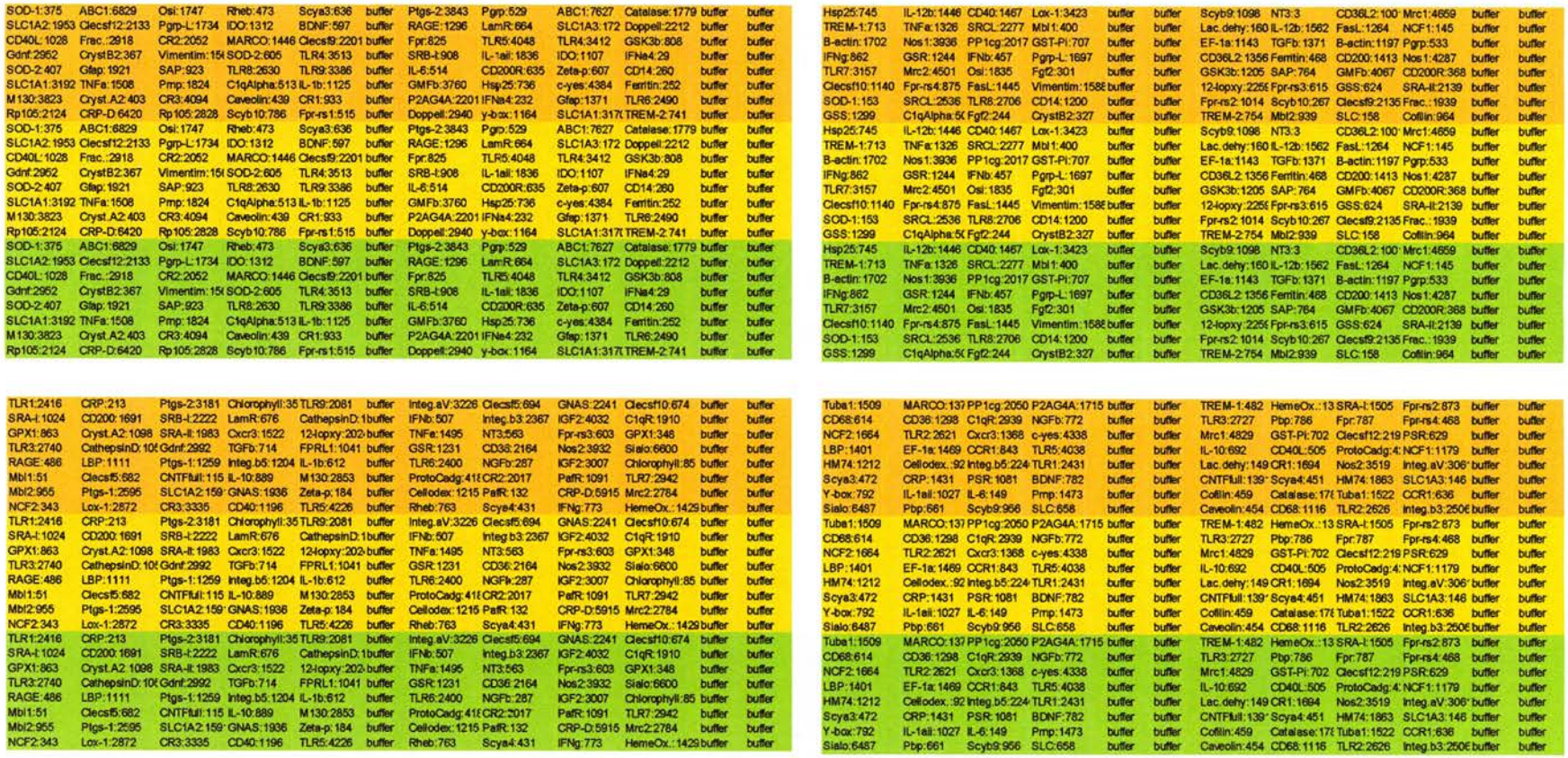

Figure 8, layout of probes on the first generation microarray. The array is ordered into four sub-arrays. Each sub-array possesses a group of unique probes that are printed in triplicate. Each probe is named after the labelled gene transcript it binds to (e.g. SOD-1) and where it binds to the transcript from the 5' end. For example, SOD-1:375 is printed in triplicate at the far top left of the array. It binds to the SOD-1 transcript at a site that on the mRNA that is 375bp from the 5'end of the published mRNA sequence (all the Genbank accession numbers that relate to these sequences can be found in appendix 2).

which a specific probe will give exactly the same signal wherever it is placed on the array. However, in practice the strength of a signal for a particular probe *can* alter across the array surface due to a variety of reasons brought about by in perfect probe printing, array blocking and hybridisation. To determine whether the signal for a specific probe changes, the user has to simply compare the values of the triplicates and any deviation in signal will be detected and if warranted the data for that hybridisation can be discarded.

Along with probes the array was spotted with buffer alone. The rationale for the inclusion of buffer spots was two-fold. Firstly they were used as a measure of background signal. Secondly, the buffer spots were used to evaluate the quality of the microarray printing process. During the printing process, the printing pins pick up DNA from a source plate and print the DNA onto the microarray slides at pre-defined coordinates. The printing pins then move to a wash solution where the DNA is removed from the pins before the next DNA probe is collected. This process is repeated until the microarray printing is complete. If the DNA is not completely removed from the printing pins at the wash station, any DNA remaining on the pins will be combined with and printed with the next probe, producing spots printed with combined DNA (a process referred to as DNA carryover). Evidence of carryover can be found by detecting hybridisation signal from one or more of the buffer spots. Figure 9B shows a close up of one sub-array and demonstrates that buffer spots did not generate any signal suggesting that DNA carryover did not occur.

3.2.4 cDNA transcripts were labeled using a single dye

Labelling all samples with a single dye has multiple advantages when compared to dual labelling with both Cy-3 and Cy-5. Dual labelling involves labelling a reference/control sample with Cy-3 and the test sample with Cy-5 and hybridising both cDNA populations onto the same array. Conversely, a labelling technique that relies on using just one Cy dye requires undertaking separate hybridisations for each sample. Dual labelling is advantageous if one wants to undertake a simple comparison between two samples e.g. control and test sample - mainly because one doesn't have to undertake inter-array comparison. However, single dye labelling is an almost pre-requisite for credible comparisons between multiple samples e.g. control, test 1, test 2, test 3, test 4 etc.

Undertaking multiple inter-array comparisons when using the dual-labelling method requires sophisticated data analysis, because all the data exists as ratios whilst single-dye hybridisations rely on absolute normalised data sets. The generation of ratios means the value of specific data points is lost, and this increases the complexity of data analysis. For example, if a dual labelled experiment suggested that a gene expression level was up by two-

fold, it would not be possible to tell whether this resulted from the gene expression changing from an arbitrary value of 2 to 4, or from 2000 to 4000. The latter change of 2000 to 4000 might be a significant result whilst the former might mean little. To undertake even simple inter-array analysis using the dual dye labelling method requires two steps of normalisation: one, to normalise between the two dyes on each chip (Lowess normalisation) and two, to normalise between the chips themselves. To undertake inter-array comparison using the single dye labelling method requires only one more simple process of normalisation - between the arrays themselves. This has the added advantage that the comparisons can be more complex and thorough (Forster et al., 2003).

There are also some other minor problems with dual labeling that make it an unfavorable choice. The two Cy dyes have differing levels of fluorescence intensities, stabilities and levels of "quenching" - all of which complicate the data analysis. The scanning process involves subjecting the microarray to bursts of intense light. Consequently, the relative fluorescent signal from the Cy-5 dye decreases substantially in comparison to the more stable Cy-3 signal following repeated scanning. Normal daylight exposure can also dramatically reduce the fluorescence of Cy-5. The process of image capture involves multiple scans and because of the differing dye stabilities the primary scan can have a different ratio to that of the last scan. In addition, scans of the same hybridisation at a later date after exposure to daylight are likely to produce erroneous ratios. This factor is an important one since it is the ratio of Cy3 to Cy5 that is measured in these hybridisations (rather than absolute levels that are measured in single-labeled hybridisations). The commercial Affymetrix ™ chip system used widely for assaying genome wide expression profiles also uses a single-dye labeling system, suggesting this is the best method (Forster et al., 2003).

Inter-array comparison has been considered difficult because reproducibility between arrays can be prone to error. This partly explains why dual labeling has been the more popular option to date. The production quality of microarray chips now enables effective inter-array comparison. The fact that most microarray experiments have utilised dual labeled microarrays should not be seen as a vindication of that method but rather as a sign that array technology has limited researchers approach until now.

3.3 Development and optimisation of microarray

3.3.1 Optimisation of hybridisation temperature

The first step in optimising hybridisation conditions was the optimisation of hybridisation temperature. The thermodynamics of DNA-to-DNA binding state that longer probes remain bound at higher temperatures than shorter probes. Secondly, as the temperature of hybridisation increases for a given probe of a given length, the percentage of probe bound to its labelled complementary cDNA sequences decreases, which results in a lower signal on the microarray (i.e. the amount of bound cDNA is inversely proportional to the temperature). Non-specific binding of a given probe to a random labelled cDNA also occurs, albeit at lower temperatures than specific sequences. Thus, the ideal hybridisation temperature is low enough to allow sufficient binding of probe to its specific cDNA sequence but high enough to prevent non-specific binding. Previous work at the ScGTI using 75-mer probes has shown 65°C to be an ideal temperature whilst Affymetrix gene chips, which use 25-mer probes, are hybridised at 45°C. Since the array designed here utilised 50-mer probes it is highly likely a suitable temperature would exist somewhere between 45°C and 65°C. An experiment was undertaken in which labelled cDNA was hybridised to the array at a variety of temperatures from 50°C to 67°C. The ideal temperature is one in which positive control probes generate the highest possible signal without causing negative control probes to generate significant signal from non-specific binding. The J774.1 macrophage cell line was grown until semi-confluent, RNA extracted and its quality assayed using the Agilent bioanalyser. The J774.1 macrophage line was used since this cell line is known to express a multitude of PRR, such as CD14 and all housekeeping genes. The RNA was used to make labelled cDNA using SuperScript II, mixed into one pool and hybridised to the arrays. Any variations in signal were thus due to hybridisation efficiency and not the quality of the cDNA. The temperature of each hybridisation oven was checked using an alcohol-based thermometer and a thermocouple-based thermometer. Following overnight hybridisation and washes, the arrays were scanned (figure 9A and 9B). Upon simple visual inspection of these scans it is evident that cDNA has bound to the array at both 50°C and 57.5°C, suggesting these temperatures are not too high to prevent specific binding. To accurately determine which temperature was optimal, the signal intensities of all probes were plotted as a whisker diagram (figure 10). Thorsten Forster (ScGTI) kindly assisted in the creation of these diagrams. They show the distribution of all probes as grouped in four categories: those signals produced by spots of buffer alone, signals from probes that bind to genes of interest, signals from negative control probes, and lastly signals form probes that bind to housekeeping genes. The signals from

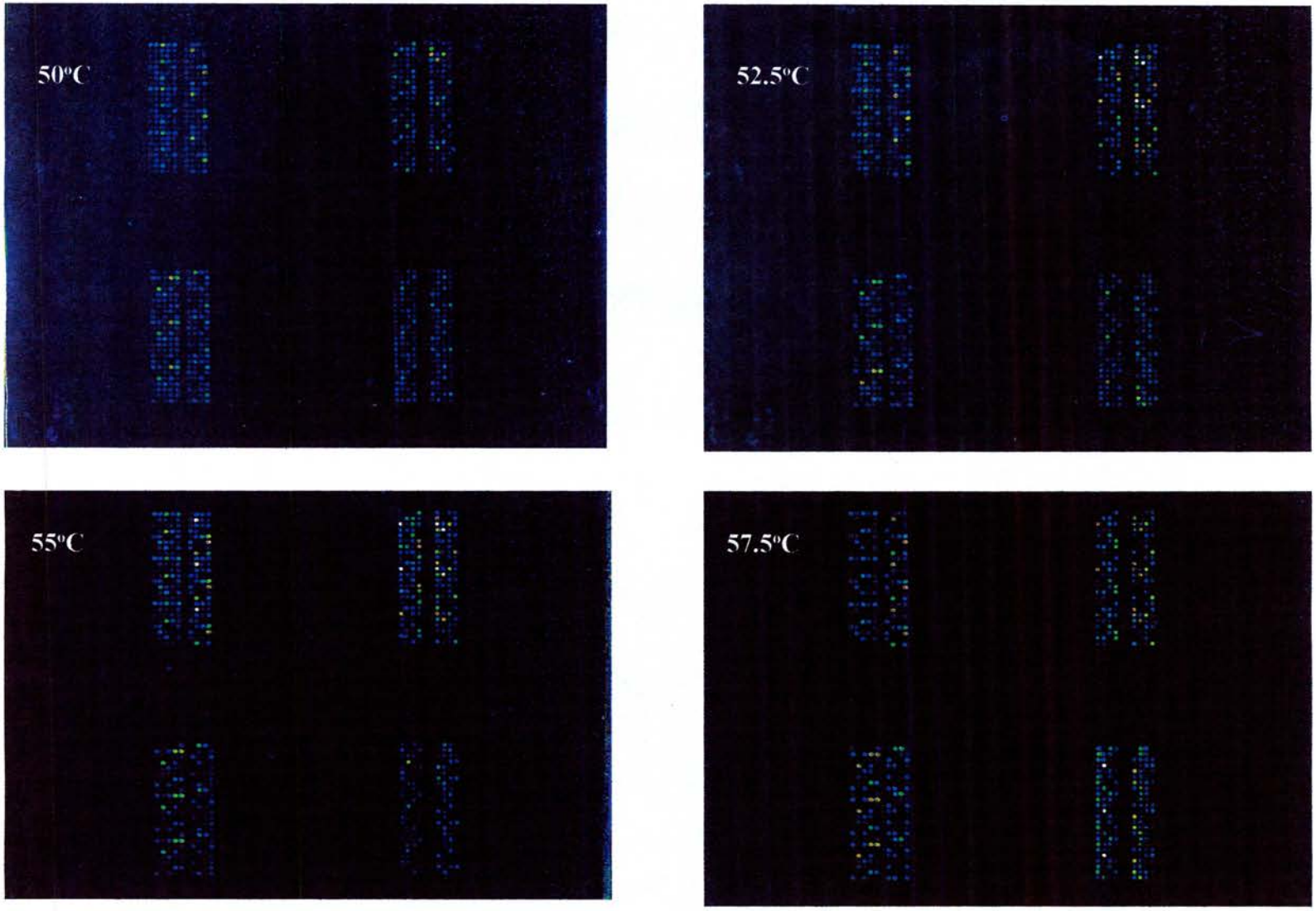

Figure 9A, scans of the hybridisations undertaken at the temperatures labelled. The background signal declined as the hybridisation temperature increased. Signal intensity was visualised here as a colour scale with increasing intensity denoted from black to, blue, green, yellow, red and white (maximal signal intensity).

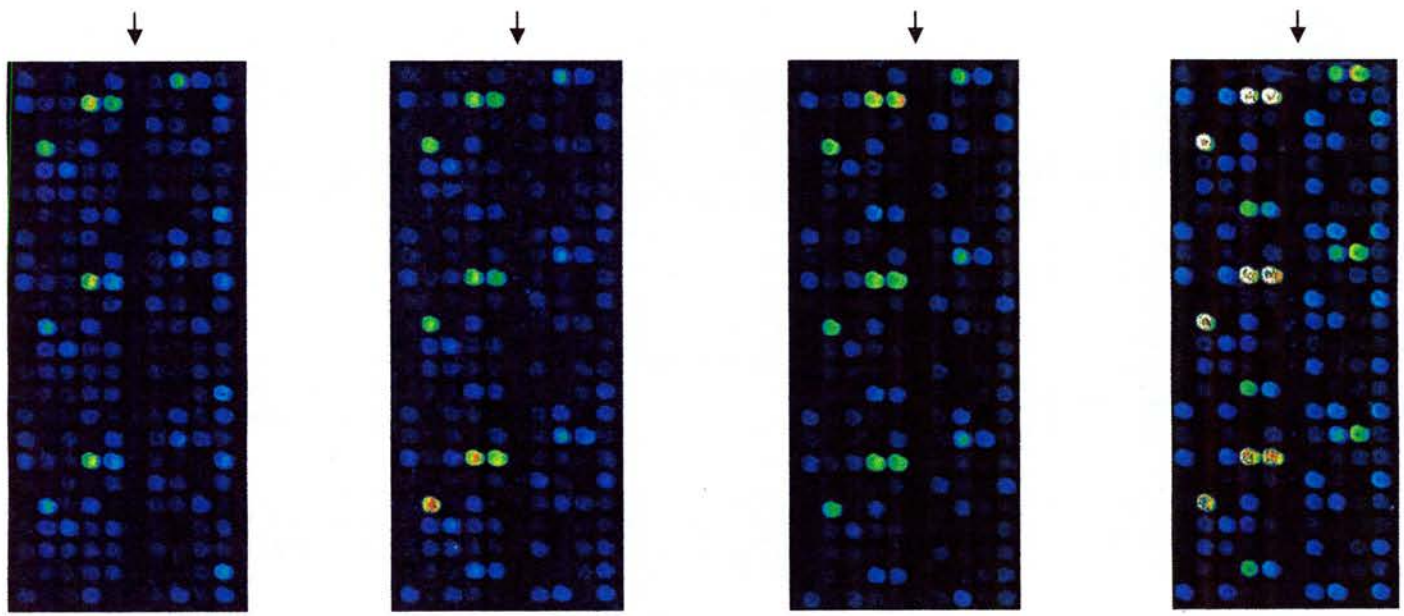

Figure 9B, close-up of the lower left hand sub-array. The signal : background ratio increased as hybridisation temperature increased. The lower level of background at the higher temperatures allowed more sensitive scanning of the array to generate stronger probe signal. In addition, the buffer spots did not exhibit any signal, suggesting that DNA carryover was minimal and did not contribute to the signal intensity (columns of buffer spots are labelled with arrow). Signal intensity was visualised here as a colour scale with increasing intensity denoted from black to, blue, green, yellow, red and white (maximal signal intensity).

buffer spots were all minimal as expected and represent the background level binding of cDNA to the array surface. For all four temperatures the probes that bind to genes of interest were highly variable in their signal intensities. This was to be expected since not all genes were expressed in this resting macrophage cell line - indeed the low mean signal intensity suggests most genes were either not expressed or were expressed at a level too low for the array platform to detect. The signal intensity of the negative probes is critical since they inform on the level of non-specific binding by labelled cDNA to non-complementary probes. It was evident that the ratio between the mean signal of the negative probes and the mean of the positive control changed dramatically as the temperature increased. At 50°C the negative and positive probes produced a signal that was not too dissimilar, whilst at 57°C the signal intensity of the positive control probes was substantially higher than that of the negative control probes. Not only were these two signal means very different but there was very little overlap of the signals generated by positive controls and negative controls at 57°C, suggesting the ideal hybridisation temperature was 57°C or higher.

To determine whether a temperature higher than 57°C would give a higher positive control: negative control probe signal ratio, another experiment was undertaken at 52, 57, 62 and 67°C. Figure 11 shows the whisker plots of these hybridisations and clearly demonstrates that 57°C was the optimal temperature, possessing the highest positive: negative probe signal ratio. The hybridisations at other temperatures exhibited populations of positive control probes that produced signals that were not substantially different from the negatives.

3.3.2 Optimisation of blocking strategy and cDNA production

Prior to hybridisation the array surface was processed to block sites that would otherwise non-specifically bind labelled cDNA. Different blocking strategies had differing results. The data presented so far relied on a simple blocking procedure that was effective but inconsistent. This method relied on using in-house manufactured poly-L-lysine coated slides that immediately prior to hybridisation were blocked using succinic anhydride dissolved in anhydride N-methyl-2-pyrrolidinone (similar to method described in 2.11.4). This blocking protocol occasionally resulted in artefacts that obscured meaningful data. Considering the high cost of microarray labelling and of the arrays themselves, it was essential to spend time developing the best blocking strategy. An experiment was undertaken to compare the relative blocking efficiency of the succinic anhydride/NMP method alone with succinic anhydride/NMP plus an addition blocking in bovine serum albumin (BSA). The BSA mixture was created by dissolving 2.2 g of BSA (fraction V) in 100 ml nuclease free water, adding 55 ml 20X SSC and 2.2 ml 10% SDS and heating to 42°C. Following blocking in

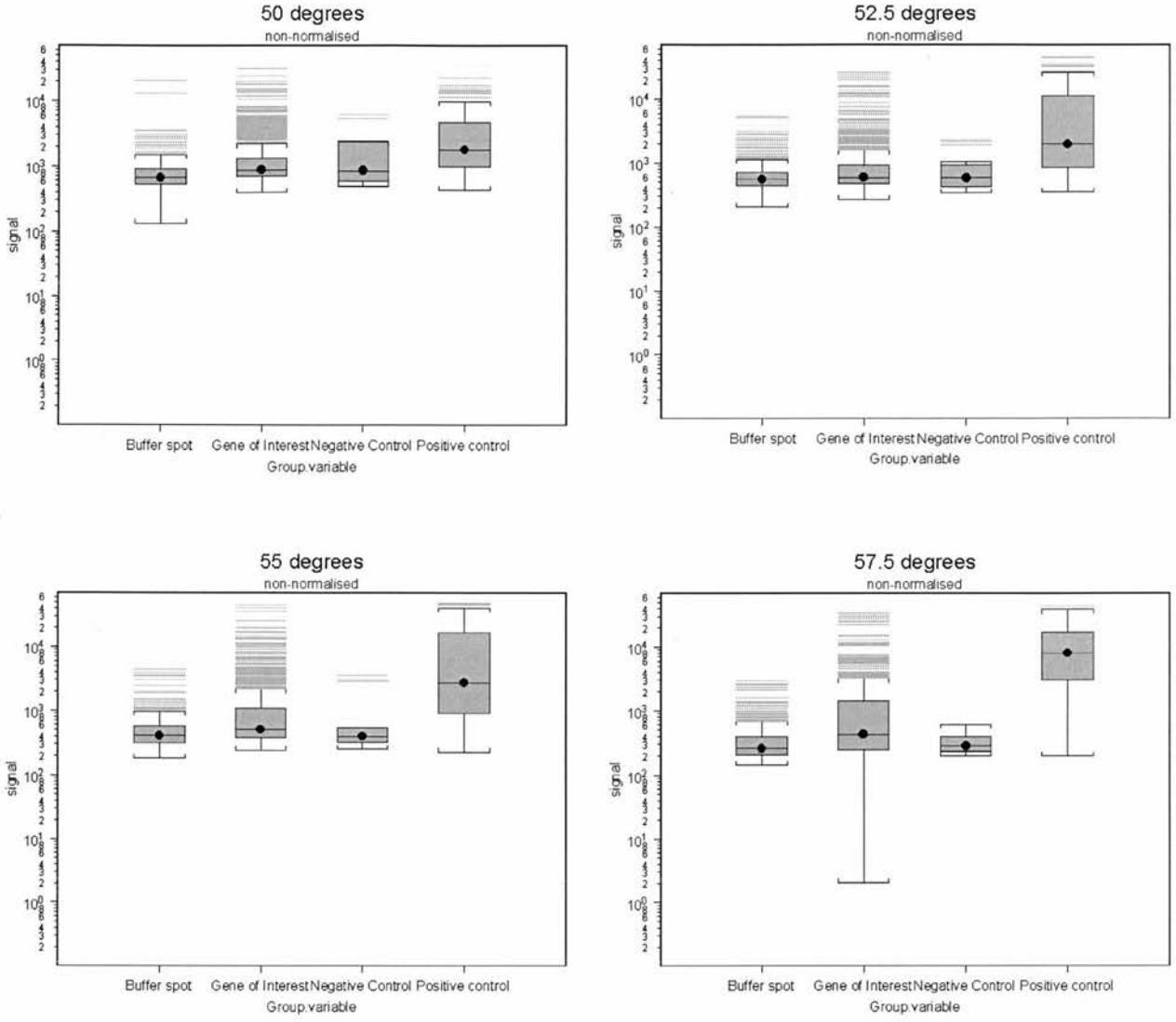

Figure 10, whisker plots showing the spread of probe signal intensities for buffer spots, gene of interest probes, negative control probes and positive control probes. Samples sourced from the same cDNA substrate were used for each hybridisation and were undertaken at: 50°C, 52.5°C, 55°C and 57.5°C as labelled. Each whisker plot shows the spread of probe signals: the grey block signifies all the data points between the 25th and 75th percentile (constituting 50% of all values). The line that intersects a black dot signifies the mean average of all data points. The area that is covered by the two horizontal brackets, which is connected by a vertical straight line, constitutes 90% of all the data points. The remaining values that fall outside of these (referred to as outliers) are signified with grey lines. Notice that the maximal difference between negative control signal and positive control signals was at 57°C. The expression of genes of interest are expected to be highly variable and mostly lowly expressed in this resting macrophage cell line. The probe signal values are plotted on a log scale

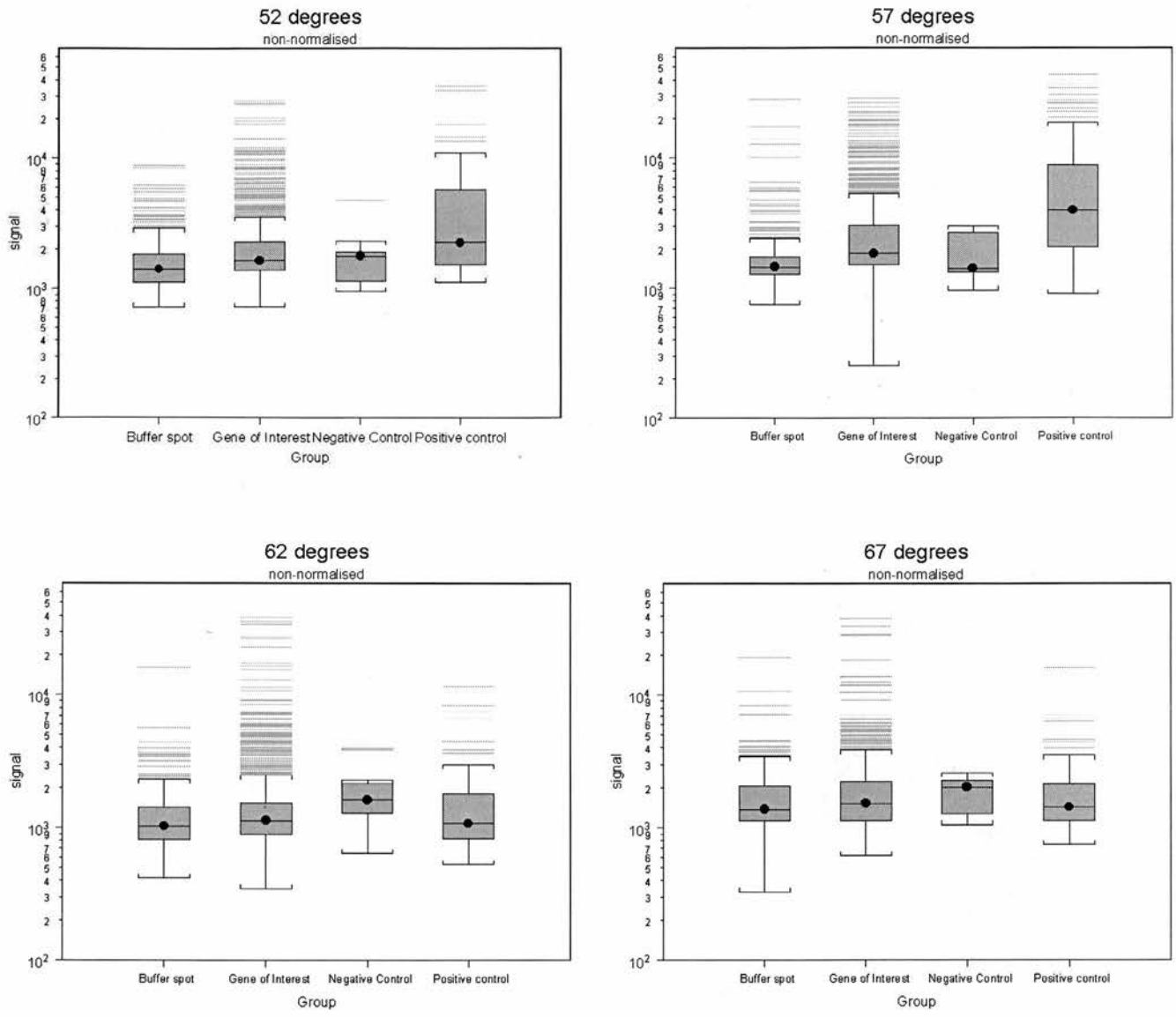

Figure 11, whisker plots demonstrating the spread of probe signals at differing hybridisation temperatures. The positive control probes at 52, 62 and 67°C are not substantially different from the negative control probes. However, the mean of the positive probe s hybridised at 57°C is substantially higher as is the spread of the data points. Notice that the mean of the ge nes of interest are also higher than the negative controls only at this temperature. The probe signal values are p lotted on a log scale.

NMP, two arrays were washed and dried as before and then immersed in the BSA mix for 45 minutes. Following this the arrays were washed by submerging the slides in 500 ml milliQ purified water twice, then in 250 ml isopropanol five times and spun dry. Two other arrays were also blocked using the same NMP mixture but were not further blocked with BSA. J774.1 macrophage labelled cDNA was then hybridised to the two groups of arrays and their background fluorescence measured (figure 12). There was a clear difference between the two methods of blocking, not only did the additional step of BSA blocking reduce general background signal, but the presence of fluorescent artefacts was reduced. Indeed, analysis of the data from these arrays showed that the ratio of positive control signal to negative control signal was higher following BSA blocking (figure 13). It should be noted that despite the improvement there was still considerable background signal present.

To determine whether background and fluorescent artefacts were partly due to inconsistencies in the manufacture of in-house poly-lysine coated slides, an experiment was undertaken to determine whether commercially available Corning Gap™ slides produced a lower background signal. Corning Gap slides have the advantage of being subjected to more thorough quality control by the manufacturer although they increase the cost of the experiment. In addition, these slides require slightly different processing compared to the in-house manufactured slides (as detailed in 2.11.4): an exposure to UV that cross-links the 50-mer oligonucleotide probes followed by a blocking step in the NMP/succinic anhydride solution alone (figure 14). The results demonstrated that Corning Gap slides consistently produced a lower background than in-house manufactured slides blocked with either NMP or NMP/BSA.

The level of cDNA production is critical for the generation of a sensitive microarray platform. Not only does the total amount of cDNA have to be optimised but also the length of each cDNA strand must be long enough to encode the site complementary to its probe. An experiment was undertaken to compare the relative abilities of two different enzymes to produce labelled cDNA: Superscript II verses the Fluoroscript™ microarray labelling system (Invitrogen). The Fluoroscript enzyme has been specifically altered so that incorporation of Cy-dyes occurs more readily and has been optimised by the suppliers for microarray labelling (see section 2.11.3). In addition, the Fluoroscript enzyme has the advantage of using less reagents including Cy3-dCTP, making it more affordable and takes half the time to make cDNA, an important consideration due to the time consuming nature of the microarray protocol. An experiment was undertaken to analyse differences in cDNA labelling by comparing the signal intensities of the housekeeping probes. In this experiment the same RNA substrate was labelled using the separate enzymes and hybridised to the array

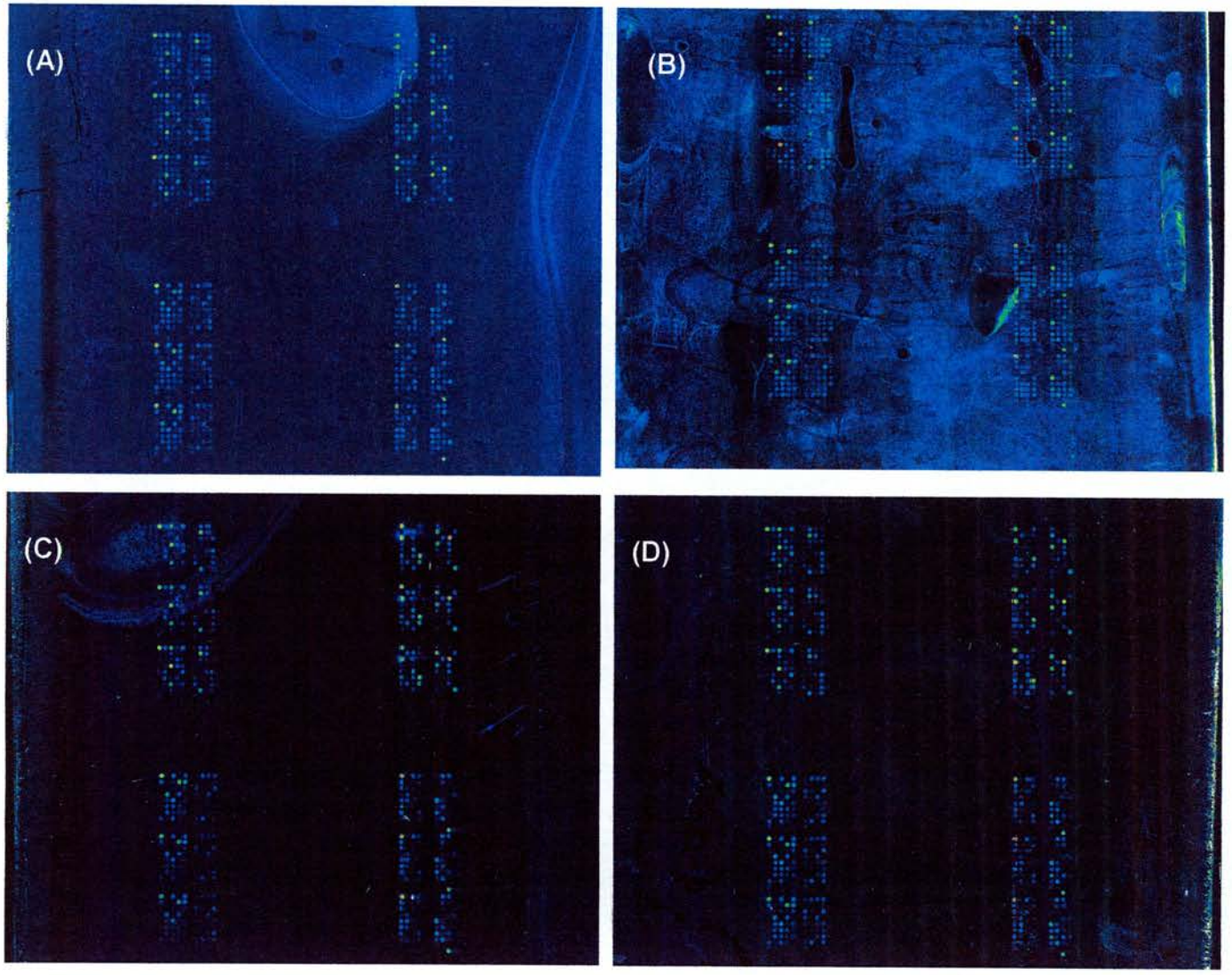

Figure 12. Arrays blocked with NMP solution and BSA provided a platform with a lower background that was less prone to fluorescent artefacts. (A and B) Arrays blocked with NMP solution alone. Notice the presence of fluorescent artefacts. (C and D) Arrays blocked by NMP solution followed by a BSA blocking step. Notice that despite greatly reduced background fluorescence, artefacts still occurred such as that seen in the top-left of scan in (C).

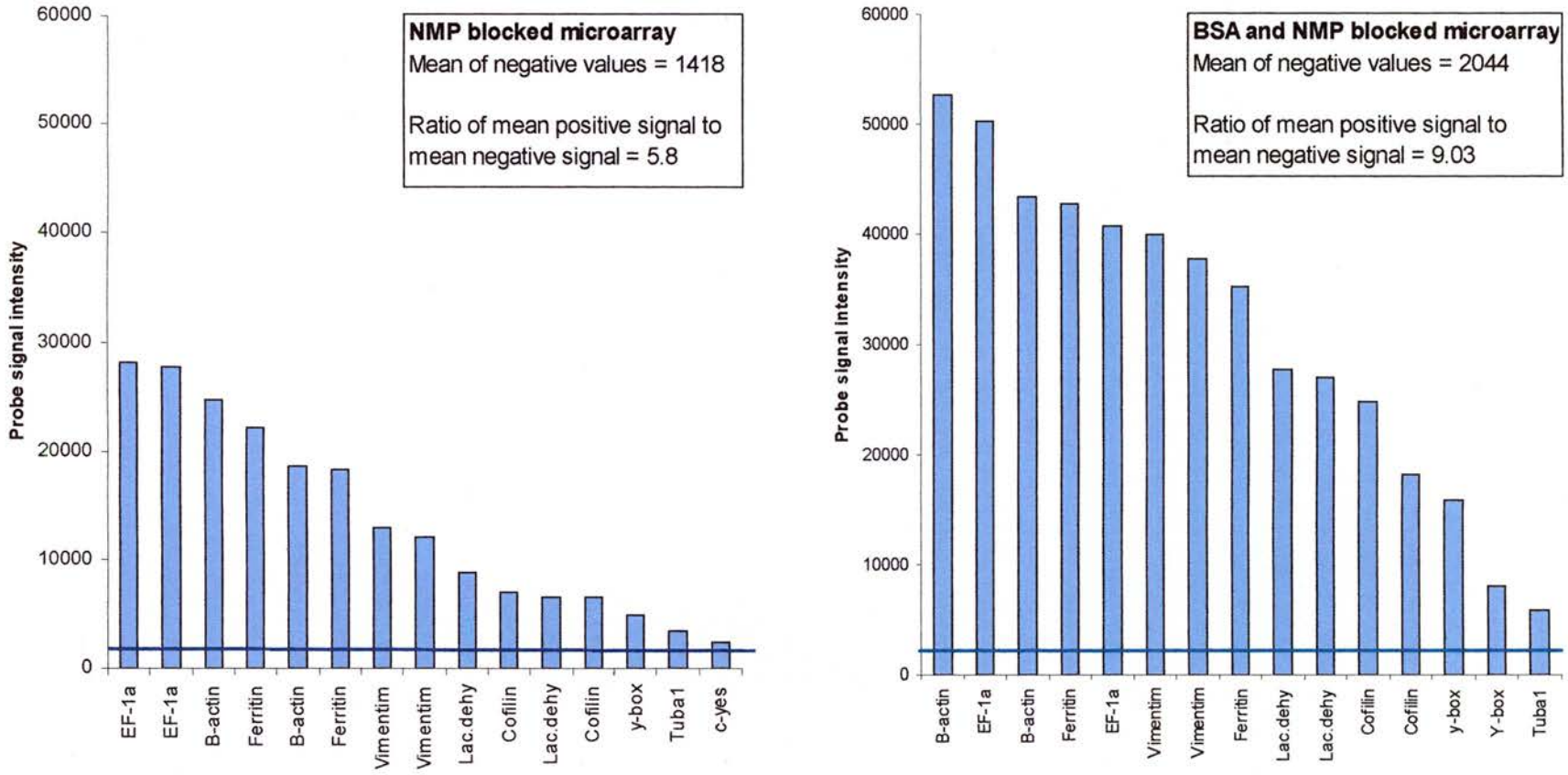

Figure 13, BSA blocking increased the positive to negative signal ratio. Shown are the 15 highest positive control probes plotted against arbitrary signal values. The dark blue line indicates the mean value of all negative control probes.

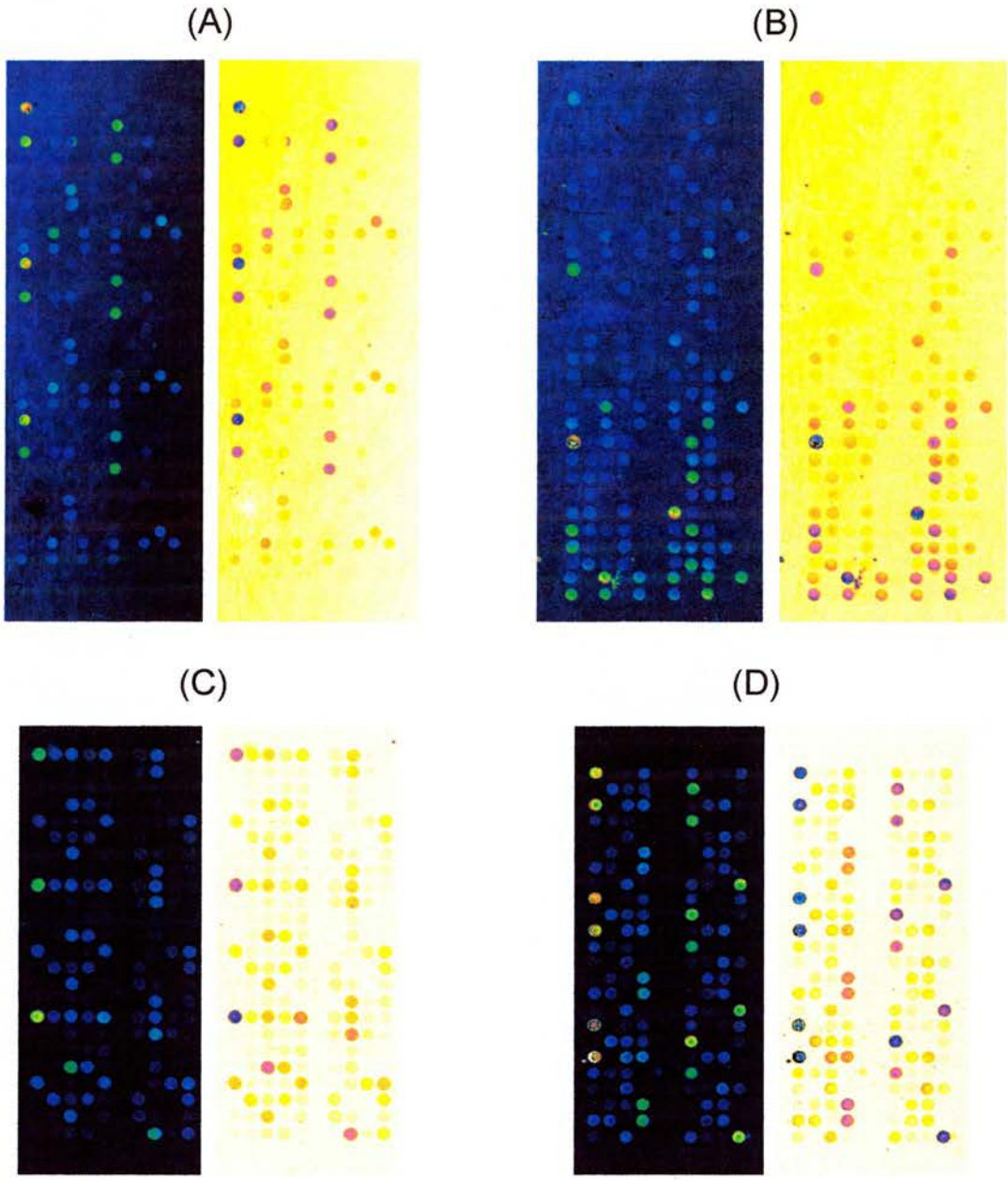

Figure 14, Corning Gap slides exhibit a low level of background signal. Two in-house poly-L-lysine slides (A and B) and two corning gap slides (C and D) were compared as substrates for microarray hybridisation. The four microarrays were blocked concurrently in the same NMP/succinic solution and the two in-house slides were subjected to a further block in BSA. N9 microglia RNA was labelled and hybridised to these arrays and scanned. Shown above are representative sections of each array scanned at the same PMT level, displayed both in "raw image" format (left-hand side) and in a format in which the colours have been inverted to better demonstrate background signal (right-hand side). The in-house slides clearly have a higher background signal as shown by the blue colour in the raw image format and the darker yellow colour in the inverted format. Conversely, the Corning Gap slides exhibit little background signal as shown by the black on the raw image format and the pale yellow on the inverted format. Signal intensity was visualised in the raw image as a colour scale with increasing intensity denoted from black to, blue, green,yellow red and white (maximal signal intensity). The scale is inverted for the other images (i.e. white is minimum signal intensity and black is maximum signal intensity).

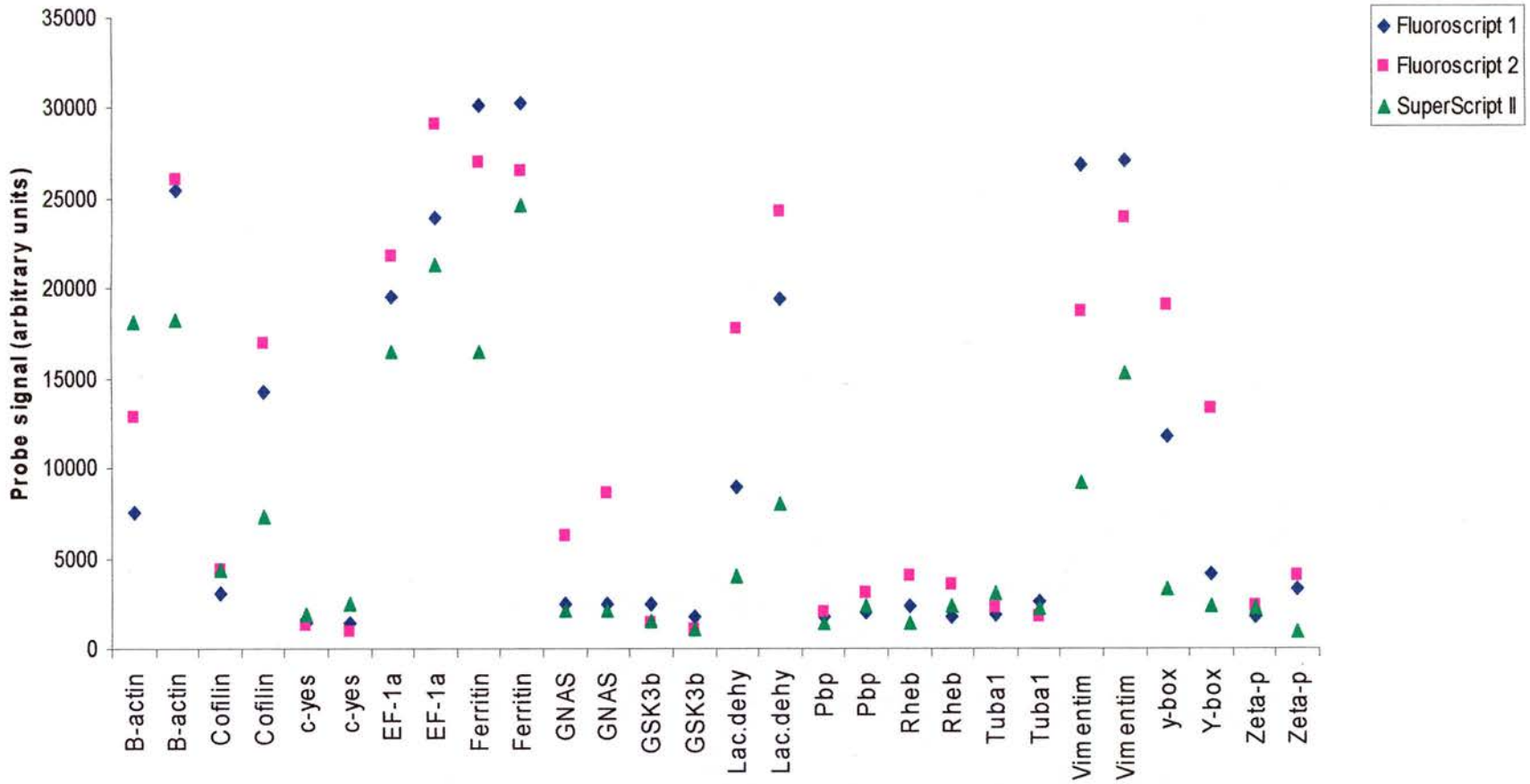

Figure 15 the signal intensities on the array were higher following labelling with fluoroscript enzyme relative to SuperScript II. Shown are the median signal intensities for all 30 positive control probes. The superscript II labelled sample produces a consistently lower signal for each probe than its fluoroscript counterparts. Values have been normalised to the fluoroscript 1 array using global normalisation.

surface in an otherwise identical manner. Following scanning and data acquisition the probe signals were normalised to one another using global normalisation to correct for differing hybridisation efficiencies and scan settings (this method of normalisation was chosen since it takes into account the overall signal intensity of the array and was influenced by all probe signal intensities). Since the hybridisations were undertaken using the same RNA sample, differences in signal intensity were minimal and reflected differences in the labelling strategy. Figure 15 shows the signal intensities of all 30 positive control probes for two arrays that utilised the new fluoroscript enzyme and a third array that utilised Superscript II to label the cDNA. The signal intensity for the fluoroscript-labelled arrays appeared to not only be adequate compared to the superscript-labelled array, but also more efficient despite using less Cy3-dCTP in the labelling master mix. In addition, visualisation of the array surface revealed that fluoroscript labelled arrays had a lower level of non-specific signal, resulting in a higher specific signal: background ratio (figure 16). This may be due to a reduction in the amount of unlabelled Cy3-dye present. In addition, the higher signal: background ratio on the fluoroscript arrays may be due to the production of more full-length cDNA that generate specific signals. (Note that this experiment used in-house poly-lysine coated slides and not the corning gap slides that give more optimal background and so cannot be directly compared to figure 14).

3.3.3 An initial assessment of replicate variability / reproducibility

To determine the reproducibility of the microarray platform an experiment was undertaken to measure inter-array variability independent of sample variation. Total RNA from J774.1 macrophages sufficient for five microarrays was labeled in a single reaction and prepared for hybridisation to five microarray chips that were prepared and blocked concurrently, using the same conditions and reagents. The data was analysed as detailed in section 3.3.5. Briefly, the median of each probe (printed in triplicate) was taken and the other replicates for each probe discarded. Using these values each array was normalised relative to the first array. Normalisation was essential since each array was scanned at a differing sensitivity and produced different global signal intensities. Normalisation is a data transformation that adjusts values and allows the data from any two or more groups to be appropriately compared. In this experiment, each array was globally normalised by comparing the 75^{th} percentile of all probes on the array to each other to generate a normalisation factor. The 75^{th} percentile has the advantage of being relatively insensitive to outliers, compared to the mean average, and accurately reflects the signal intensity of any given population of probes (Forster et al., 2003). The normalisation factor was used to adjust the data to compensate for

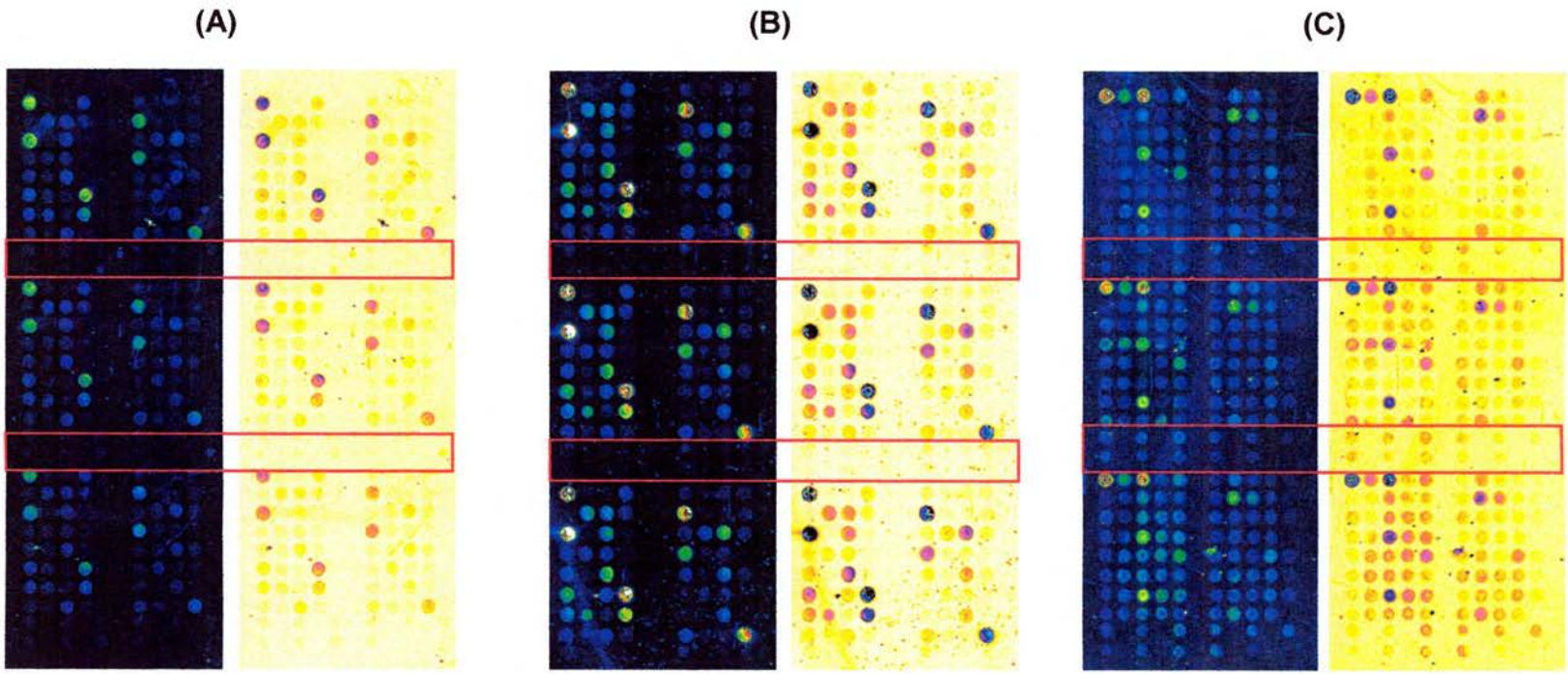

Figure 16, fluoroscript labelling results in less non-specific binding of cDNA to probes complementary to *A.thaliana* transcripts. (A and B) Two separate arrays hybridised to cDNA made by fluoroscript. (C) Representative array labelled using cDNA made by SuperScript II (RNA was sourced from the same sample). Each image was obtained using the same scanning sensitivity setting (PMT=52). The images demonstrate that the fluoroscript-labelled arrays have less background signal and that the probe signals are more specific. Note that the superscript-labelled array possesses probes that have bound labelled cDNA in an apparent non-specific manner. In particular, the probes marked in the red box are specific to *A.thaliana* transcripts and should not be labelled. Nevertheless, there was a noticeable signal for these probes in the superscript-labelled array compared to the fluoroscript-labelled arrays. Signal intensity was visualised in the raw image as a colour scale with increasing intensity denoted from black to, blue, green,yellow red and white (maximal signal intensity). The scale is inverted for the other images (i.e. white is minimum signal intensity and black is maximum signal intensity).

the observed inter-array variability and so balance the fluorescence signal. Global normalisation is advantageous in this experiment since there will not be large differences in overall signal, since the same labeled cDNA substrate has been used in each case. Despite global normalisation probe signal can still vary substantially.

Figure 17 shows the spread of probe signals for all the housekeeping genes for all five arrays. This population of genes was chosen to determine inter-array variability since they represent a group of genes known to be expressed in the cell line and to be present at varying levels, enabling determination of the extent of variability for highly and lowly expressed transcripts. Figure 17 demonstrates that whilst the arrays showed some consistency there was also a large amount of variability for both high and low expressed transcripts. For example, the probes complementary to EF-1 and ferritin generated a consistent signal on all five arrays, whilst the probe complementary to cofilin and lactate dehydrogenase generated a signal that was highly variable between arrays. The introduction of error during data analysis was unlikely since the values had simply been adjusted using one normalising value and whilst the second array (pink squares on figure 17) produced the lowest signal for several probes it also generated some of the highest signals for other probes, indicating that the normalisation process had not consistently skewed the signals from this array in any particular direction. This implies that variation was occurring across the array surface irrespective of the normalisation procedure i.e. one part of the array was brighter/produced a stronger probe signal than other parts of the array. Indeed, figure 18 shows the signal for selected probe replicates varied across the array. This finding has implications for further work when analysing *different* cDNA samples. Indeed, the ability of the array to discriminate subtle changes in gene expression from one biological sample to the next is questionable considering the extent of the variation shown in figures 17 and 18. Thus, there was a clear need for a system to efficiently measure signal differences across the array surface and correct for this.

3.3.4 The SpotReport™ system can efficiently normalise probe signal across the microarray surface (intra-array normalisation)

The SpotReport system (Stratagene) is a useful tool in facilitating the optimisation, validation and standardisation of microarray data. The system consists of ten *A.thaliana* genes that have been cloned and characterized for use as exogenous nucleic acid controls for non-plant microarrays. Supplied with the system are ten mRNA "spikes" each of which represents an *A.thaliana* transcript and ten 70-mer oligonucleotides that are complementary to an individual spike. The ten 70-mers were arrayed along with the rest of the 50-mers.

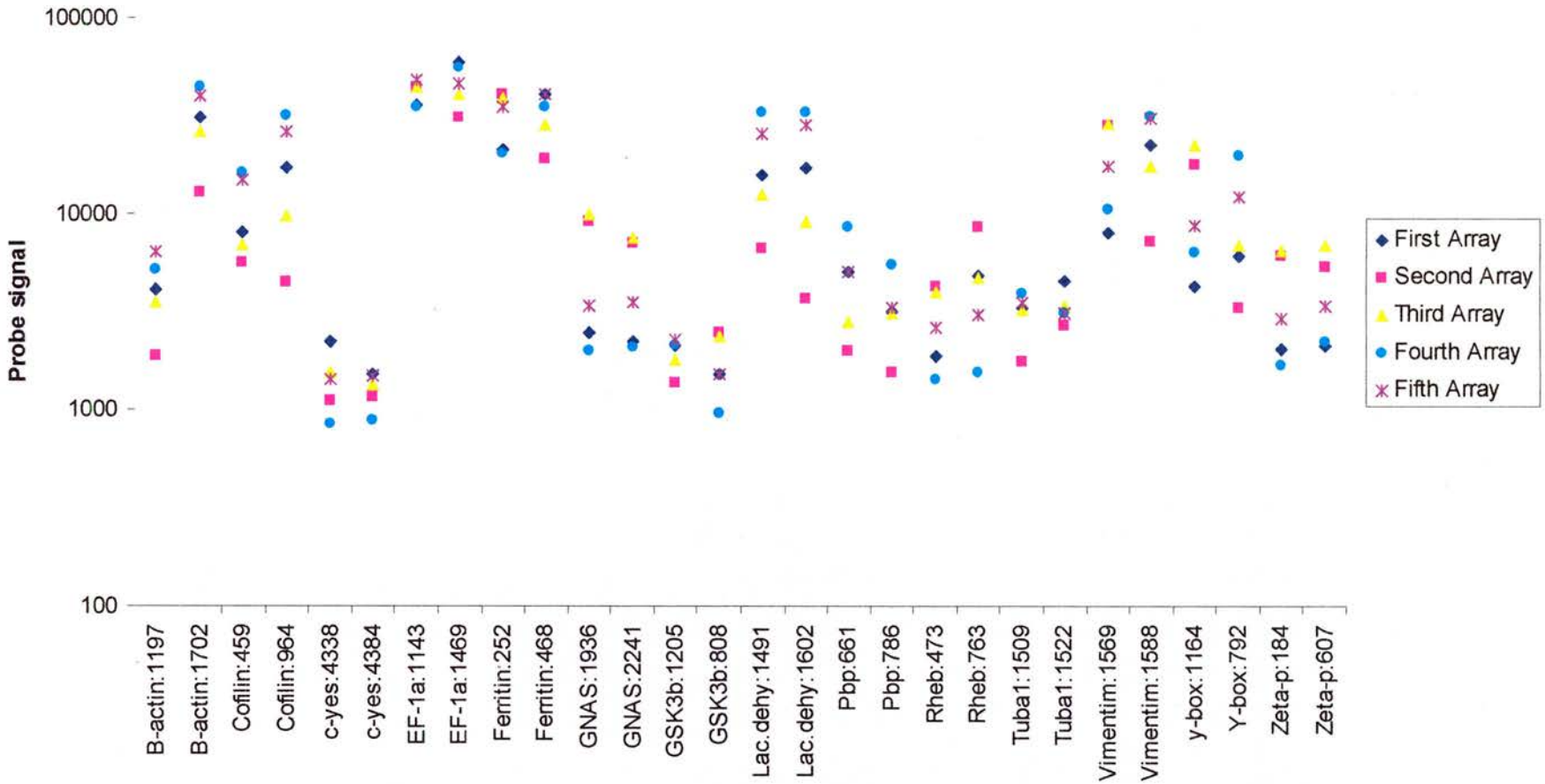

Figure 17, the signal intensity of all 30 housekeeping probes on five microarrays hybridised to the same cDNA source. The median probe signal for each array is plotted following inter-array global normalisation. The graph demonstrates considerable variability in the magnitude of an individual probe signal between arrays and suggests that the hybridisation procedure generated substantial error.

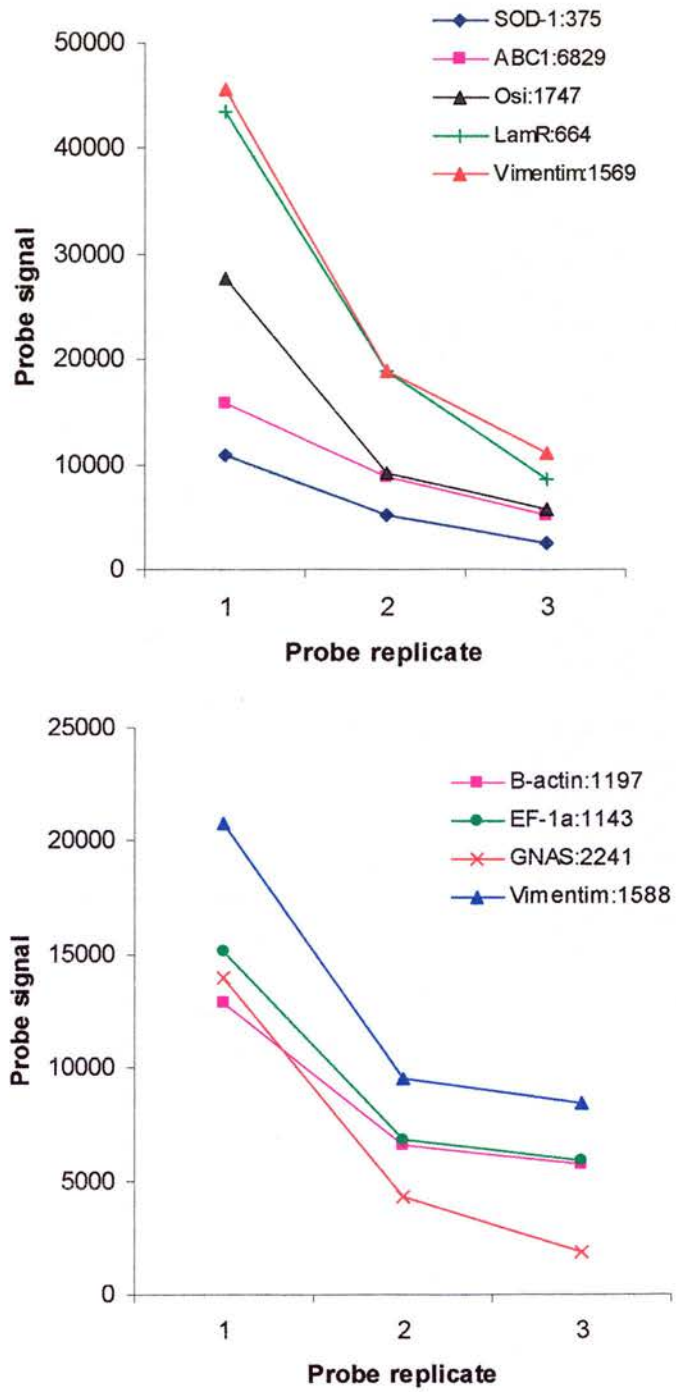

Figure 18, probe replicates generated different levels signal intensity that depended on their position on the array surface. Non-normalised values for specific probe replicates have been plotted from the third array (top graph) and fifth array (bottom graph), and both show that the signal decreases from replicate 1 (located at the top of its sub-array) to replicate 3 (located at the bottom of its sub-array).

The mRNA spikes are added to the experimental RNA and utilised to synthesize labeled cDNA as usual. The hybridisation signals from the SpotReport probes on the array can be evaluated to determine the sensitivity, specificity, signal linearity and consistency of the microarray (for example, whether signal varies across the array surface). Importantly, this system can also be used as a basis for normalising the signal intensity across the array surface (intra-assay normalisation) and as method to normalise signal intensity between arrays (inter-assay normalisation) (Causton et al., 2003).

To incorporate the SpotReport system a second-generation array was designed and printed. This had several changes compared to the first-generation array. These changes are summarised in figure 19. Most importantly the ten SpotReport probes were spotted in triplicate in each of the four sub-arrays so that in total each array possessed a total of 120 spots from the SpotReport system. In addition, 50-mer probes complementary to housekeeping genes that were shown to give a strong signal upon binding from the previous hybridisations were spotted in the top-left hand corner of each sub-array. This positioning was undertaken to aid orientation upon image capture, to enable quick evaluation that the entire array is present and to ensure that the hybridisation solution has been in contact with the whole array surface (figure 19A).

There were several factors that affected the ability of the SpotReport system to function. Firstly, the SpotReport probes arrayed onto the microarray were 70 nucleotides long whilst all the other probes were 50 nucleotides long. These two populations of probes have very different thermodynamics and do not hybridise to complementary sequences to the same extent at any given temperature. Theoretically, 70-mer probes possess a Tm that is higher than the smaller 50-mer probes. Thus hybridisation to cDNA at temperatures optimal for 50-mer probes (shown in section 3.3.1 to be 57.5°C) may have resulted in non-specific binding of cDNA to the longer 70-mer probes. Figure 19B shows that upon hybridisation to murine cDNA alone, the SpotReport probes did not bind non-specifically to murine cDNA at 57.5°C. This suggests that the 70-mer and 50-mer probes can be used concurrently on the same array and that the array platform as whole exhibits high specificity to the probes intended cDNA targets.

To determine the amount of mRNA spike required, an experiment was undertaken whereby differing amounts of mRNA spike were added to J774.1 RNA prior to synthesis of labeled cDNA. Each spike was diluted in water containing 10 ng/μl yeast tRNA as a carrier to prevent loss of specific spike mRNA at low concentrations. Two microarrays were hybridised to cDNA spiked with 5 ng of each mRNA, two microarrays were hybridised to

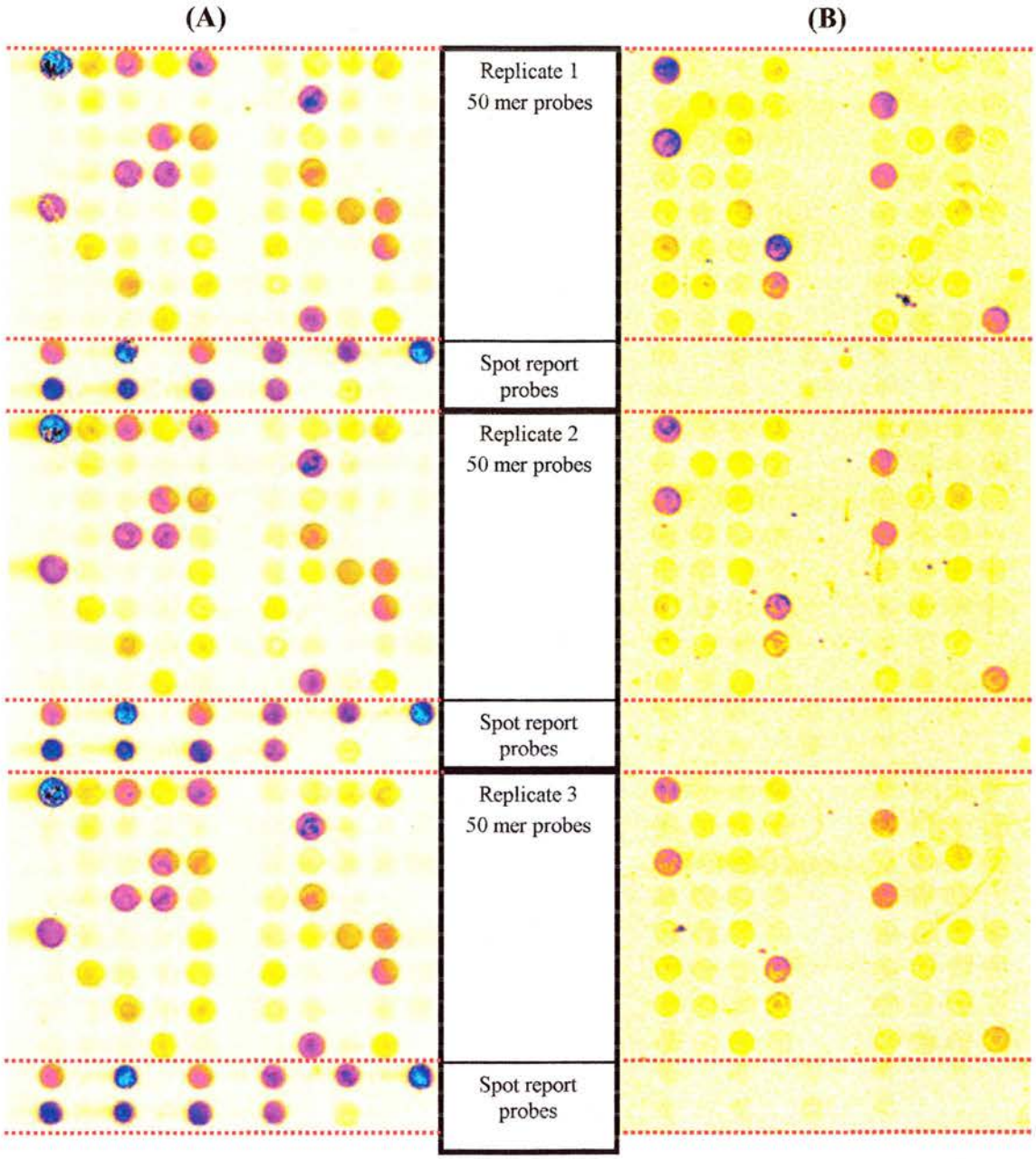

Figure 19, layout of a sub-array on the second generation microarray. **(A)** Representative portion of the second generation microarray with SpotReport™ spikes added to RNA prior to labelling. The major difference between the previous microarray was the inclusion of SpotReport™ probes. These 70-mer oligonucleotide probes were arrayed at the bottom of each replicate. There were 10 different SpotReport probes used in triplicate across each sub-array, which makes a total of 30 spots per sub-array and a total of 120 spots across all four sub-arrays. The positioning of the probes has also been subtly changed so that a positive control probe known to give to generate a strong signal was included in the top-left hand corner of each sub-array (Ferritin:252, Ferritin:468, EF-1a:1143 and EF-1a:1469). This aids in orientation of the array upon scanning. **(B)** Representative portion of the second generation array following hybridisation to cDNA that was not spiked with SpotReport prior to labelling. Signal intensity was visualised in these inverted images as a colour scale with increasing intensity denoted from white to red, green, blue, and black (maximal signal intensity)

cDNA spiked with 1 ng of each mRNA and two microarrays were hybridised to cDNA spiked with 0.2 ng of each mRNA (figure 20). Ideally, the signal intensity of the SpotReport probes should be similar to that of the 50-mer probes so that the signal from the SpotReport probes can be measured at the same scan settings (PMT setting) as the 50-mer probes. In addition, the signal from the SpotReport probes should not be saturated. Figure 20 shows representative sections of one array at each of the spike concentrations and demonstrates that the addition of either 5 ng or 1 ng of spike saturated the scan. In addition to saturation, large smears were apparent that blocked the signal from other probes on the array. This occurred since a small amount of oligonucleotide probe often binds to the array surface when the microarray is blocked with the NMP/succinic anhydride solution, but is not normally detected. However, since the amount of cDNA species that was specific for these probes was present in such amounts, these smears have been labeled. The addition of 0.2 ng of each spike did not saturate the spot report probes at a scanning setting that was also appropriate for the 50-mer probes, indicating that this was a suitable working concentration of spike. Notice that the intensity of the SpotReport probes was between that of the highly expressed housekeeping gene probe located on the very top-left of the array and other 50-mer probes that gave lower signals.

In addition, notice that the SpotReport probes individually differed in their signal intensity. This was advantageous since it can be used to demonstrate the variability of signal across the array for cDNA species that bind at high levels and at low levels (the signal intensity of each probe is product of cDNA level and of probe/cDNA affinity).

The SpotReport system was used to both highlight signal variation across the array and to correct any signal bias by normalising the sub-arrays; figure 21 demonstrates an example of this. Total RNA from J774.1 cells was spiked with 0.2 ng spike and hybridised to the array surface. The top graph of figure 21 shows the signal intensities for all 120 spot report probes, and demonstrates that there is a modest but clear increase in signal on the bottom right sub-array (D) for this particular hybridisation (as represented by the last three data points for each probe on the right of the graph). To correct for this bias, the 75^{th} percentile of all 30 SpotReport probes from each sub array was calculated to generate a normalisation factor and used to adjust the data to compensate for the observed intra-subarray variability (Table 6). The resulting normalised signal intensity of each probe was plotted (bottom graph of figure 21). This shows the normalised probe signal intensities, as a population are consistent across the array.

This process successfully normalised signal between sub-arrays. However, as figure 21 demonstrates, within any given triplicate in a sub-array the probe signal can vary as well.

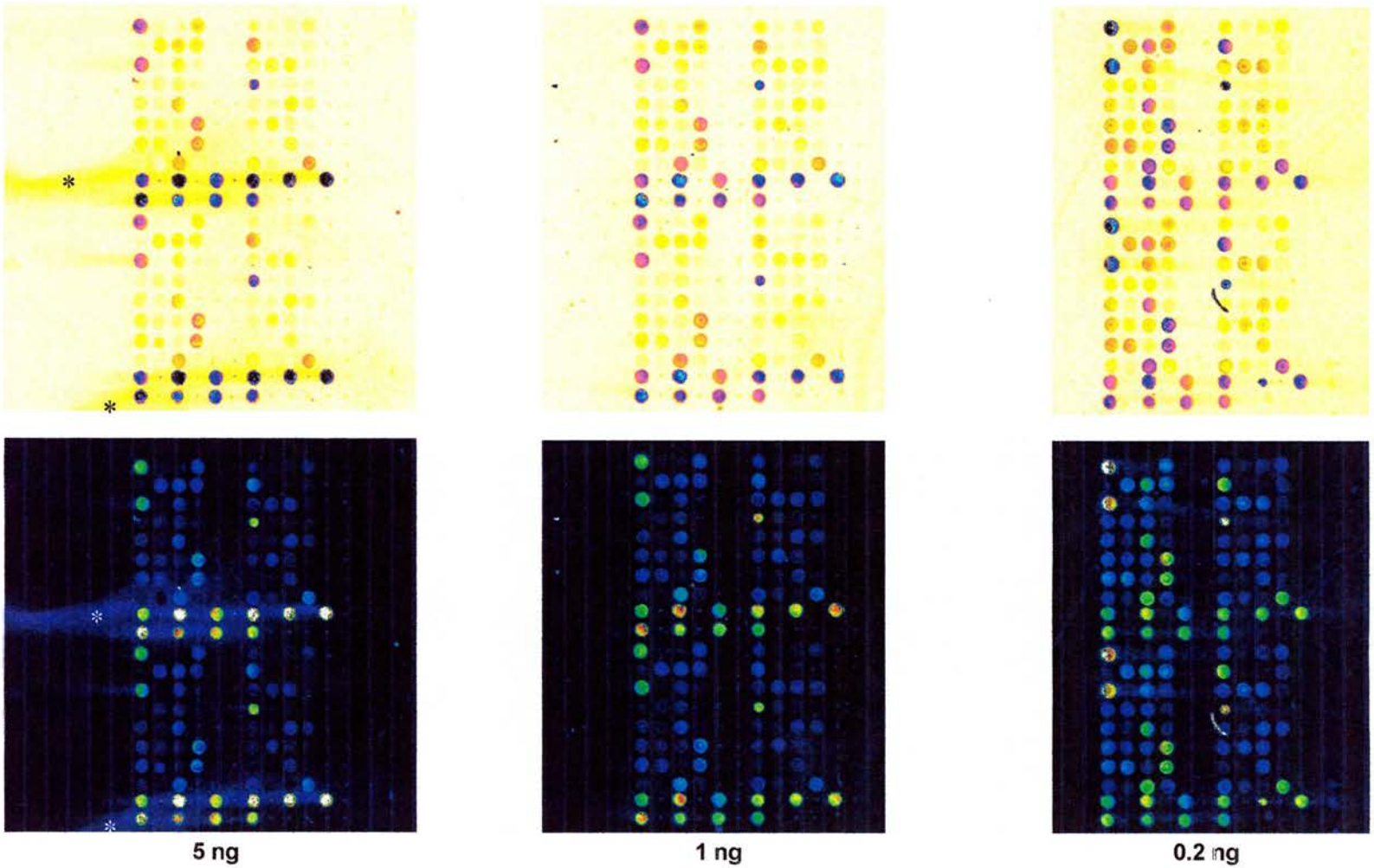

Figure 20, the optimal amount of mRNA spike was 0.2 ng. Shown are the same sections of the microarray in both its unadjusted format (bottom) and in a format in which the colours have been inverted to better illustrate the spot morphology (above). The addition of 5 ng of each mRNA spike saturated the SpotReport probes arrayed onto the microarray and even bound to the small amount of probe that had washed off and rebound to microarray surface, creating a smear (labelled *) that masks the signals of other spots (rebinding of washed probe can occur during the blocking process of the array immediately prior to hybridisation). The intensity of the SpotReport signal was also too high when 1 ng of each spike was added compared to the majority of the 50-mer probes. Smearing also occurred on other areas of the array not shown here. The intensity of the SpotReport probes with 0.2 ng was relatively similar to the population of 50-mer probes and no smearing of saturated probe occurred. Each hybridisation was undertaken twice at each spike dilution and shown are representative sections.

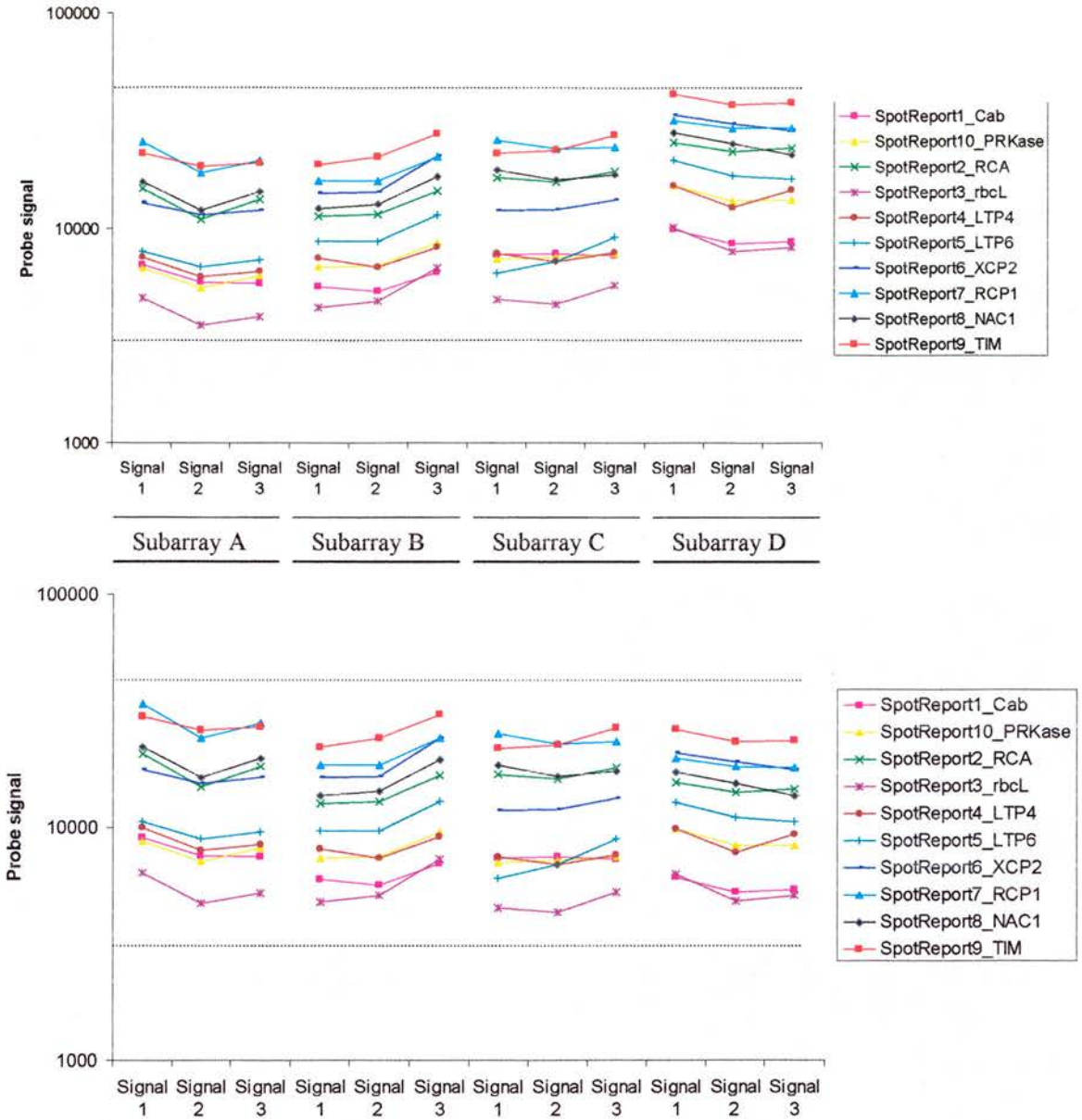

Figure 21, differences in probe signal corrected by SpotReport. Shown are the probe signal intensities for all SpotReport spots across the microarray surface. The top graph shows the signal intensities as scanned, whilst the lower graph demonstrates the signal intensities post-normalisation. The first three triplicates (A) represent the top left sub-array, the second set (B) the top right, the third set (C) the bottom left and the fourth set (D) the bottom right. Theoretically, an ideal hybridisation to an ideally printed microarray would produce signals from SpotReport probes that were identical across the array surface for each particular probe. The top graph demonstrates that the bottom right hand-side of the microarray produced a higher signal. To correct for this bias, each sub array was normalised to the mean of the 75th percentile (see section 3.3.7 for more details on intra-normalisation) and then the resulting SpotReport signals plotted (bottom graph). The process of normalisation, although not perfect, has modified the signals so that as a population they are more homogenous. This has corrected the signal bias introduced by the hybridisation process.

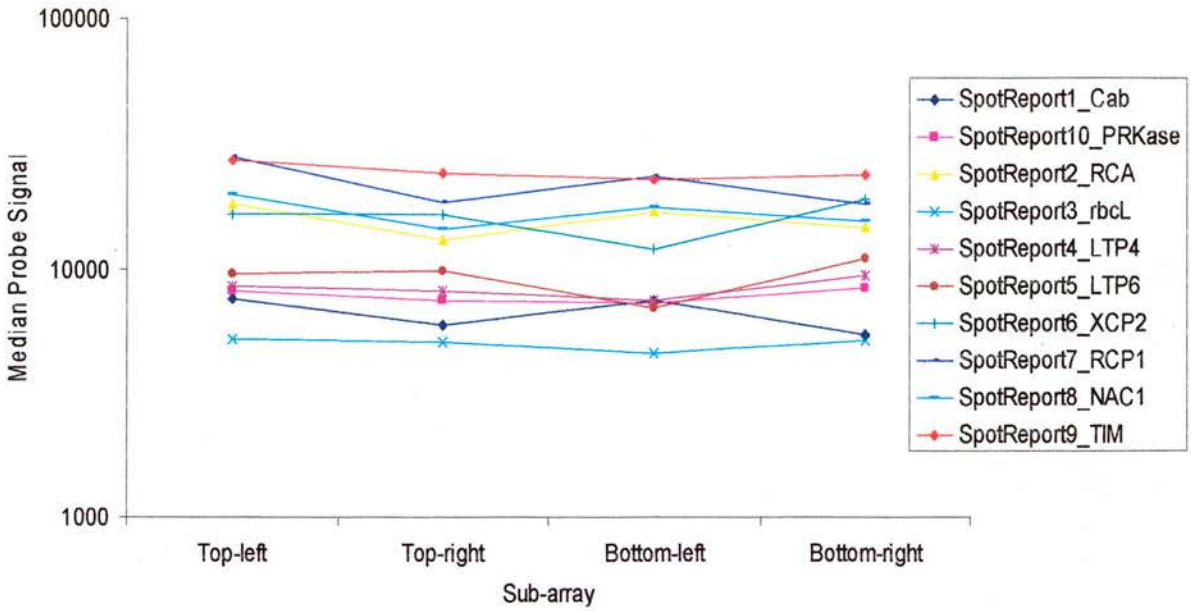

Figure 22, selection of the median from each triplicate reduces probe signal variation. The normalised values plotted in figure 20 were taken and the median from each triplicate plotted. The graph demonstrates that by using a combination of normalisation and restricted selection of the median, the final signal intensity values are consistent across the array surface. From this detailed analysis of ten genes, it can be assumed that a similar processing of the signal values for the genes of interest and positive controls will also generate robust reproducible results. The lines that connect each data point have been included to better demonstrate the consistency of each probe signal across the array surface.

However, the process of data analysis negates the need for intra sub-array normalisation, because only the median signal intensity for each probe triplicate is used. The median has the advantage of being relatively insensitive to outlying, high intensity spot signals (which can be caused by dust, unincorporated dye, or other artifacts that cause a small number of saturated pixels within a spot area). By taking the median value the variation within the sub-array is negated. For example, the normalised data from figure 21 was taken and the medians calculated for each SpotReport probe. These probe signal medians were then plotted (figure 22) and demonstrate that individual probes generated a similar signal across the array surface when only the median value was taken into account.

The ability of the second-generation platform to account for signal variation across the array surface is important since this reduces the variability *between* arrays. Indeed, the ability of the system to normalise probe signal across the array reduces the array-to-array variability considerably and is illustrated in figure 24. This shows that the inter-array variability of housekeeping probe signals is far less following intra-array normalisation (figure 24 compared to figure 17, where intra-normalisation had not been applied). Moreover, the data in figure 24 was generated using different flasks of microglia cultures, and thus also was affected by inter-flask biological variation, whilst the data in figure 17 was generated by using a single cDNA source. There has been a clear improvement in the ability of the array platform to repeatedly generate a consistent signal for a particular probe.

3.3.5 Probes complementary to house keeping genes can be effectively utilised to normalise probe signal intensity between arrays (inter-array normalisation)

Individual hybridisations tend to vary in the intensity of signal they generate due to factors that cannot be easily controlled, such as; quality and amount of starting RNA; reverse transcriptase efficiency; cDNA purification; microarray slide blocking efficiency, defects in the microarray such as cracks and scratches in the slide coating, and subtle differences in hybridisation conditions such as salt concentration and minor temperature differences (e.g. the center of the hybridisation oven can be slightly hotter than the sides). In addition, differing microarrays were scanned at differing levels of sensitivity depending on the overall signal intensity of the array and an optimal scan chosen (see section 3.3.8 for more details). Thus, hybridisations were represented by scans of differing signal intensity, which complicates the comparison of absolute probe signals from one array to the next. However, despite all these factors, the signal intensity of the housekeeping and SpotReport probes should be equivalent. The non-variable nature of these probes enables their use as reference

Sub-array position		75 Percentile	Ratio to Mean
Top	Left	10502	0.821
Top	Right	12106	0.946
Bottom	Left	13024	1.018
Bottom	Right	15560	1.216
	Mean Value	12798	

Table 6, the determination of the normalisation factor for each sub-array. The SpotReport values for each sub array were analysed and the 75 th percentile calculated (30 spots in each sub-array). The ratio between each 75 th percentile and the mean average 75 th percentile value was determined. The signal intensity of every s pot in each respective sub-array was divided by this ratio. This modification normalised si gnal across the array. In this case the bottom-right of the array has a higher signal than elsewhere on the arr ay. This bias is negated by dividing each probe signal by the respective ratio .

population of probes to normalise between hybridisations, and thus allow effective comparison of absolute probe signal.

The SpotReport probes cannot control for the level and quality of starting RNA. The housekeeping probes can control for all the factors listed above. Conversely, housekeeping genes may be differentially modulated in some experimental conditions such as *in vitro* virus infection whilst SpotReport probes will be unaffected by this (Causton et al., 2003). However, if the number of housekeeping probes is sufficiently large and experimental-induced expression changes affect only a few of these genes, housekeeping probes could remain valid for normalisation. Global normalisation was considered to be unsuitable since a large number of genes were expected to be altered during biological stimulation or infection. This would result in differing global signals between control array and test array. To determine the most effective strategy for inter-array normalisation five cultures of N9 microglia were grown until semi-confluent and RNA individually extracted. Each sample was spiked with SpotReport RNA and cDNA synthesised separately and hybridised to the second-generation microarray. The arrays were scanned and signal variation across individual arrays was negated by intra-array normalisation using the SpotReport system (as described above in section 3.3.4). The data was then normalised between arrays using one of two methods. The first method involved determining the 75th percentile of all SpotReport probes for all five arrays. A ratio was generated by comparing the five 75th percentile values to the mean average 75th percentile and then used to adjust all other probes signals on each respective array. Thus all probes were normalised to a reference value, the mean 75th percentile. The second method was identical except that it involved determining the 75th percentile of all 30 housekeeping probes (including all probe replicates so that 30 x 3 = 90 signals in total). To assess the success of each normalisation method the variation in absolute probe signal intensity between arrays was compared for a set of probes chosen at random (figure 23). Probe signal variation was a product of both biological and technological variation. Figure 23 demonstrates that the method that utilises the housekeeping probes as references for inter-array normalisation generates a lower degree of inter-array variability. Note that not all error can be accounted for since the normalisation procedure can only reduce error introduced by the microarray platform and cannot influence variation of gene expression that occurs between differing cultures. The standard error of the mean (SEM) of each probe was ascertained for each method and the difference between each SEM plotted (figure 23C). Figure 23 shows that the method that utilises housekeeping genes produces a lower SEM value for most probes, indicating that this method produced the least error. This analysis was repeated and assessed by determining the spread of housekeeping probe signals

themselves (figure 24) and again the SpotReport probes when used as reference probes for normalising produces a higher SEM value for all but three probes. These three probes possessed the three highest signals and may represent probes that saturated the scan. The signal from probes that were saturated would not equate with the level of starting cDNA, which means normalisation have little effect on reducing its variation between arrays. This suggests the variation in probe signal for these three probes should not be used as a measure for judging the relative success of each normalisation protocol.

Interestingly, those probes that generate a signal intensity that is close to the background level such as the two probes for c-yes are more highly influenced by the background noise. Consequently, the signal from these probes are more prone to error and do not reflect a failing in the ability of the system to normalise signal intensity between arrays. An example of inter-array normalisation can be found in appendix 8 (found as a Microsoft Excel file on the attached IBM PC formatted CD-ROM).

Housekeeping probes may be more accurate at determining and correcting inter-array variability because these levels accurately reflected the amount of starting RNA whilst the SpotReport probes did not inform on the starting RNA levels. This factor was particularly relevant since the amount of RNA added to each reverse transcription was prone to a 30% error (Agilent Bioanalyser). Nevertheless, the results demonstrate that this microarray platform can accurately quantify gene transcript levels in a reproducible manner.

3.3.6 Estimation of dynamic range

The dynamic range of the microarray can be calculated by comparing the background signal to the signal generated by housekeeping probes. The signal generated by the 50-mer negative control probes that are 100% complementary to only non-animal gene sequences represents the level of non-specific interaction between a 50-mer probe and a murine cDNA. Any probe generating a signal at this level or below does not bind to a sufficient quantity of specific cDNA to be above the detection threshold. The microarray platform must be able to differentiate between probes that generate signal resulting from specific probe-cDNA interaction and probes where signal results from non-specific interactions. For genes that are lowly expressed this difference may be very small. To ensure that there is clear distinction between these two categories of probes, the detection threshold was set high so that any probe generating a signal above this level can be confidently considered a specific interaction between probe and its target cDNA. Setting a high detection threshold meant lowly expressed genes weren't detected but it ensured that transcripts detected were unlikely to be the product of background noise.

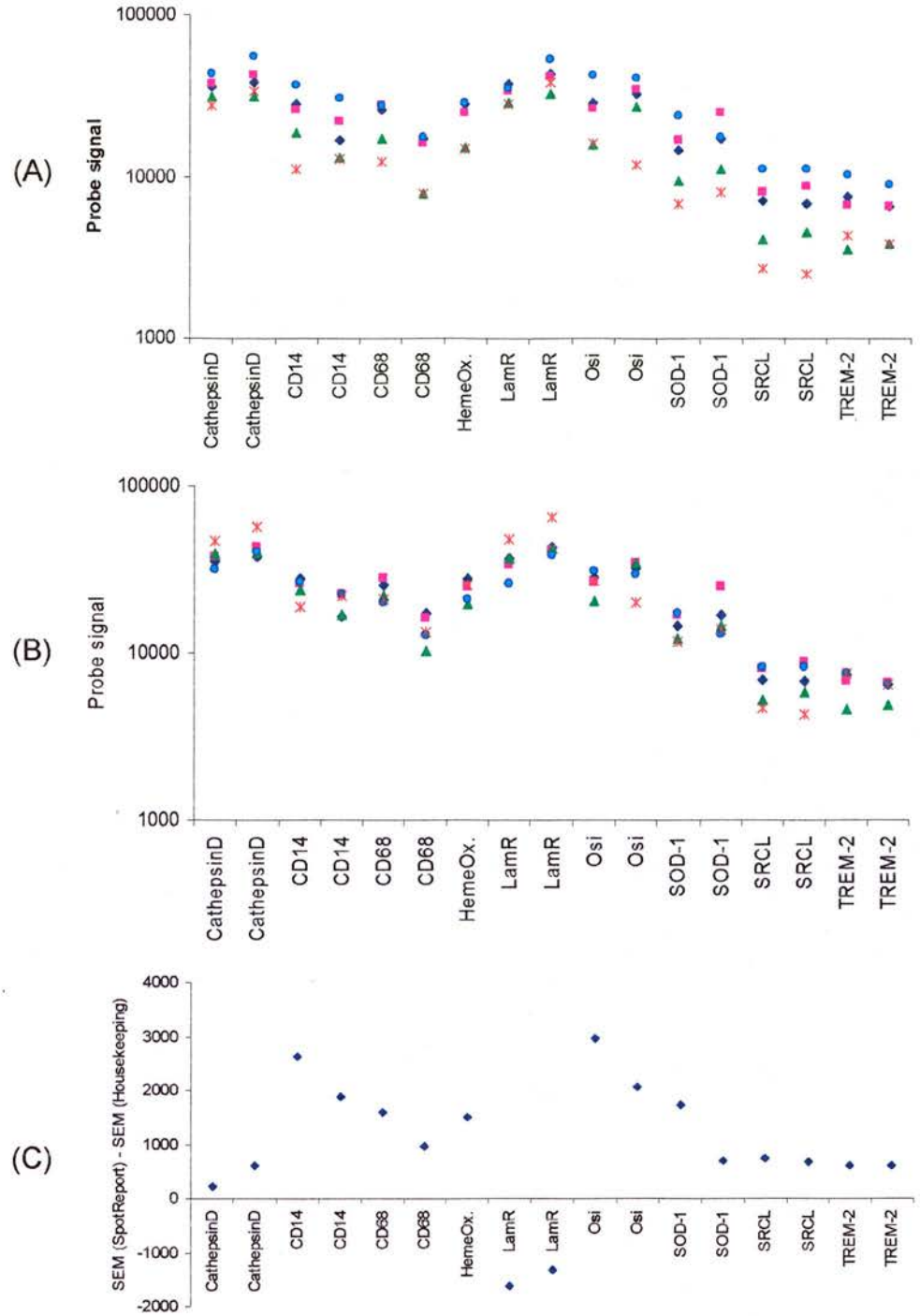

Figure 23, probes complementary to housekeeping probes are more effective than the SpotReport probes at normalising signal between arrays. (A) The signal intensity of several probes following inter-array normalisation using SpotReport probes. (B) The signal intensity of the same probes following inter-array normalisation using housekeeping probe signal intensities. (C) The SEM for each probe for each normalisation method (A and B) were calculated and the difference between the SEM calculated. A positive value indicates that the SpotReport normalised probes exhibit a higher SEM value.

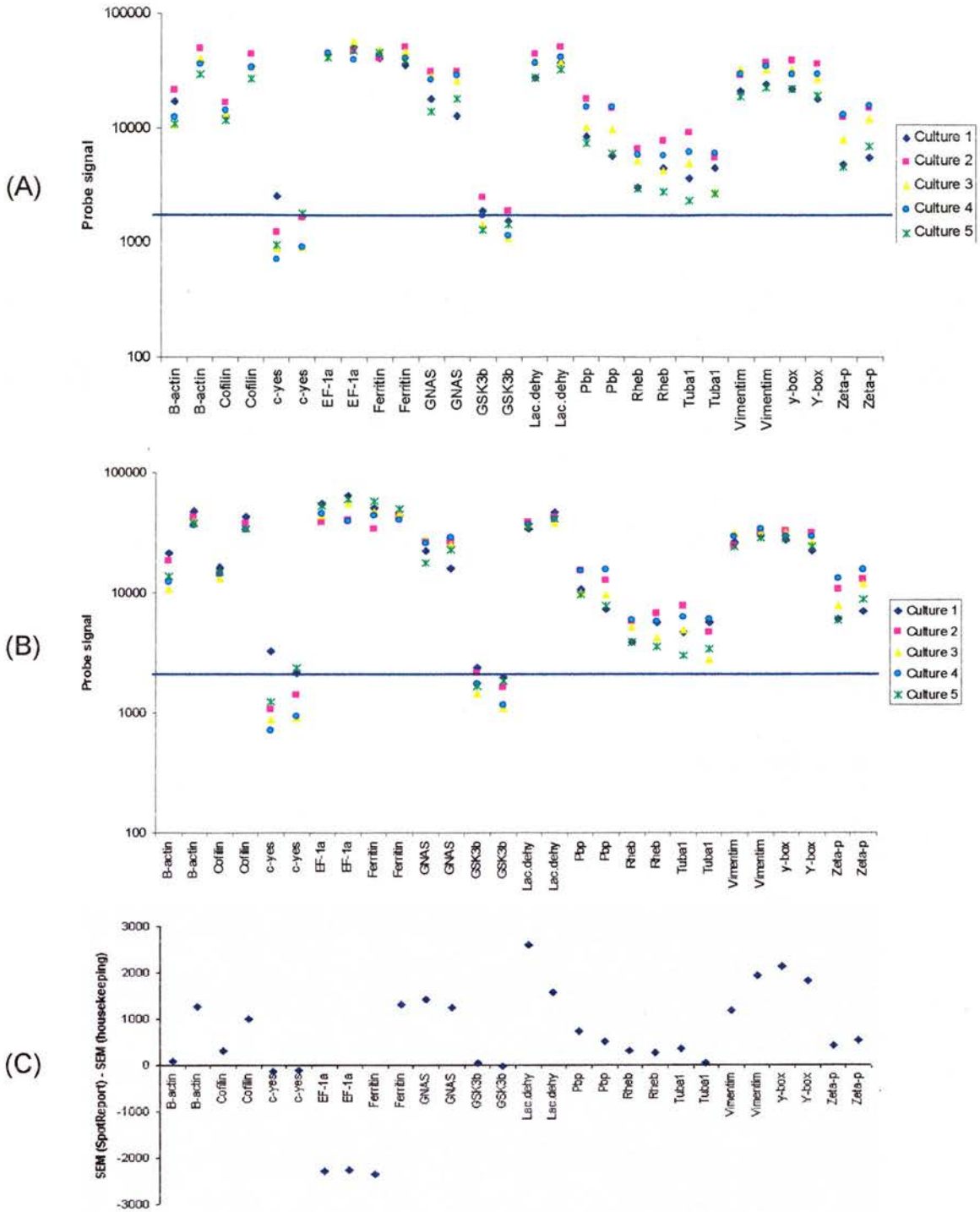

Figure 24, probes complementary to housekeeping probes are more effective than SpotReport probes at normalising between arrays. (A) The signal intensity of all housekeeping probes following inter-array normalisation that utilised the SpotReport probes. (B) The signal intensity of all housekeeping probes following inter-array normalisation that utilised housekeeping signal intensities. The blue line represents the detection threshold (mean + 2 standard deviation). (C) The SEM for each probe for each normalisation method (A and B) were calculated and the difference between the SEM calculated. A positive value indicates that the SpotReport normalised probes exhibit a higher SEM value. N.B. A reciprocal plotting of SpotReport probes normalised by these two methods also demonstrated that the normalisation method based on housekeeping genes was less error-prone.

The background level was calculated for each array as being the product of the mean signal of all negative control probes plus two standard deviations i.e. mean + (2 x SD). Figure 24B shows the mean detection threshold for five arrays hybridised to N9 microglia cDNA. The mean value of all negative control probes for these arrays was 2,370 arbitrary signal units whilst the standard deviation of all the negative probes was 582 units. Thus the detection threshold was calculated to be: 2,370 + 1164 = 3,534 units, and is plotted as a blue line on figure 24B. All but two housekeeping genes were expressed at a sufficiently high level for detection. Several housekeeping probes, including those for EF-1, generated a near maximal signal and almost saturated the scan. The signal from these probes represents the highest possible signal the microarray platform can measure. The probes that detect EF-1 transcripts generated a signal of roughly 55,000 units. Therefore the dynamic range of the platform is between 2,370 and 55,000 units and all gene products detected by the array will fall in this range. Theoretically, if the dynamic range is linear, the largest fold increases detected will be in the order of 55,000 / 3,534 = 15.6 fold change. However, the linearity of the microarray platform has yet to be fully examined, and is explored further in chapter four.

3.3.7 Scan selection, image processing and an overview of data analysis

For clarity the complete methodology of microarray data manipulation is summarised below.

1. Image processing. The first step of image processing involved identifying the spots on the array from spurious signals resulting from precipitated dye or other hybridisation artefacts, contaminants such as dust on the surface of the slide or other sources of non-specific background. This undertaking was greatly simplified by the regular arrangement of features on the array surface as rectangular grids of sub-arrays. The QuantArray^{Tm} image analysis package was used to identify each spot. This software required the user to identify approximately where each sub-array lies along with other parameters, such as number of array rows, array columns and spot size. "Nominal location" was used to identify each spot and its local region used to estimate background signal (figure 25). The placement of the grid is extremely important since the grid coordinates are used to identify each spot. To facilitate grid placement "landing lights" were utilised on the second-generation array. These were specific housekeeping probes that generated strong fluorescent signal regardless of the quality of the hybridisation and were spotted at the very start and end of each sub-array to facilitate unambiguous placement of the array grid.
2. Determination of local background. This microarray platform utilised a local estimate of the background, a sophisticated technique that identified the number of

pixels surrounding each spot to calculate a median background value. This process involved determining the precise spot boundary and measuring the spot signal by including only those pixels within the boundary. Accordingly the background signal for each spot was determined by the number of pixels lying outside the spot boundary but within the spots local region identified by the "nominal location". Before any of the data was analysed further, the "true" signal of the spot was calculated by subtracting the local background signal from the spot signal. All spots underwent this process including positive and negative probes. Note that the background signal described here is separate to the background signal of negative control probes that represent the amount of labelled cDNA that binds non-specifically to a 50-mer oligonucleotide probe.

3. PMT scanning value. The microarray was scanned using a 16-bit analogue-to-digital converter that converts the signal from the photomultiplier tubes (PMT), which measured fluorescence, to a digital value for each pixel in the resulting image. This process generates relative intensity levels that are reported in a range from 0 to 65,535 arbitrary units. Differing intensities of image were captured by using differing PMT values whilst keeping the level of laser intensity the same. Typically, when the array was scanned at sensitivity of PMT 43 and below the probe signal intensities were mostly at background level. As the sensitivity was increased by increasing PMT, the signal intensity of the probes increased disproportionably to the background signal. The optimal scanned image was one in which as many spot signal intensities were as high as possible whilst avoiding saturation of any of the spots. To determine the optimal scan, arrays were routinely scanned from PMT 43 to PMT 61 and each image processed as detailed above. The signal intensities were then plotted as scatter diagrams in which each scan is compared to the next (figure 26). Saturation of signal was evident by a curvature of the scatter plot and lowering of the correlation coefficient (r^2).
4. Normalisation. Once an optimal scan was identified the resultant signal intensities could not be directly compared from array to array. There are a variety of reasons why the raw measurements for two samples may not be directly comparable: the quantity of staring RNA may not be equal, there may be differences in labelling and each sample may generate a signal that is optimally scanned at differing PMT settings. This microarray platform utilised two steps for normalisation: the first step was to normalise signal across the array surface. This utilised the SpotReport system as (detailed in section 3.3.4). The second was to normalise signal between arrays,

this utilised housekeeping genes (detailed in section 3.3.5). In addition, the probe signals from the SpotReport probes were used as basis for validating each hybridisation. Hybridisations in which the signals varied dramatically across the array surface were rejected as where hybridisations that generated little global signal. Hybridisations that exhibited moderate variation of signal across the image where successfully utilised once corrected by SpotReport and the data refined by utilising only the median signal intensity from each probe triplicate. An example of inter-array normalisation can be found in appendix 8 (found as a Microsoft Excel file on the IBM PC formatted CD-ROM).

3.4 A study to investigate the effect of probe design on hybridisation signal

The design of microarray probes is still one of trial and error. In this study the probes were designed using a series of strict criteria detailed in section 3.2.2. Despite the implementation of these strict criteria the probes as a population exhibited some diversity in respect to their Tm values, ΔG value, probability of forming hairpin loops and their distance between site of complementation and the cDNA polyT tail. Each gene was assayed by at least two probes and examination of the data shows that each probe bound to a particular cDNA at differing levels, reaffirming that probe signal intensity was a product of cDNA levels and sequence specific probe affinity. For some probe pairs, such as the probes complementary to MARCO, one probe bound with high affinity and generated substantial signal whilst the other probe generated signal at background levels. Within a given hybridization the amount of cDNA for any given transcript is the same. Thus, such discrepancies must be due to probe sequence differences. To investigate this phenomenon all probe pairs that generated substantially different signal intensities were examined in an attempt to identify which, if any of the probe characteristics may be responsible. The ability of a probe to bind to cDNA and generate signal was almost certainly due to a combination of all these factors. However, it was possible to group probe pairs into categories; i) probe pairs that bind at least 400 bp apart on the cDNA strand and don't have divergent probe Tm values; ii) probe pairs that have divergent Tm values and bind within 400 bp of each other; and iii) probes pairs in which at least one has substantial hairpin prediction (Tm of hairpin above 26°C).

Figure 27A demonstrates that the Tm of the probe did not correlate with probe signal divergence. For example, the two probes for CD68 each possessed highly similar Tm values and yet each probe generated substantially different signal intensities. The two probes for Tuba1 exhibited more similar signal intensities than the CD68 probes and yet possessed

markedly different Tm values. Therefore, the small difference in predicted probe Tm value had little impact on probe pair signal differences. Likewise, figure 27B demonstrates that predicted Tm of hairpin loops does not correlate with signal difference between probe pairs. Figure 27B shows the Tm of the most stable hairpin for each probe. If the predicted hairpin impacted on probe signal intensity, one would observe the signal intensity to be less for probes that had high hairpin Tm values compared to its probe pair that has a less stable hairpin. However, probe 1 for CD68 possessed the highest hairpin Tm and yet it is this probe that possessed the highest signal. Whilst the probe pair for Scyb10 possess markedly differing hairpin Tm values and yet each produced a signal that was equivalent. Therefore it would appear that predicted hairpin formation has no obvious impact on the ability of a probe to generate differing signal intensities.

In contrast the site of probe complementation on the cDNA strand did affect the signal intensity. Figure 28 shows the differences in signal intensities for probes that bind at least 400 bp apart on the cDNA strand but have similar Tm values. The signal intensity of the most 3' probe was subtracted from the signal intensity of the probe that binds closer to the 5'polyT tail. A positive value indicates the 5' binding probe generated a stronger signal. The graphs shows that the majority of 5' probes generated more signal than their more 3' counterparts. In particular the probes for β-actin and MARCO exhibited substantial signal differences. However, it must be noted that not all probe pairs that bound at least 400 bp pairs apart exhibited substantial signal differences, suggesting that as yet undefined factors influence signal intensity between probe pairs.

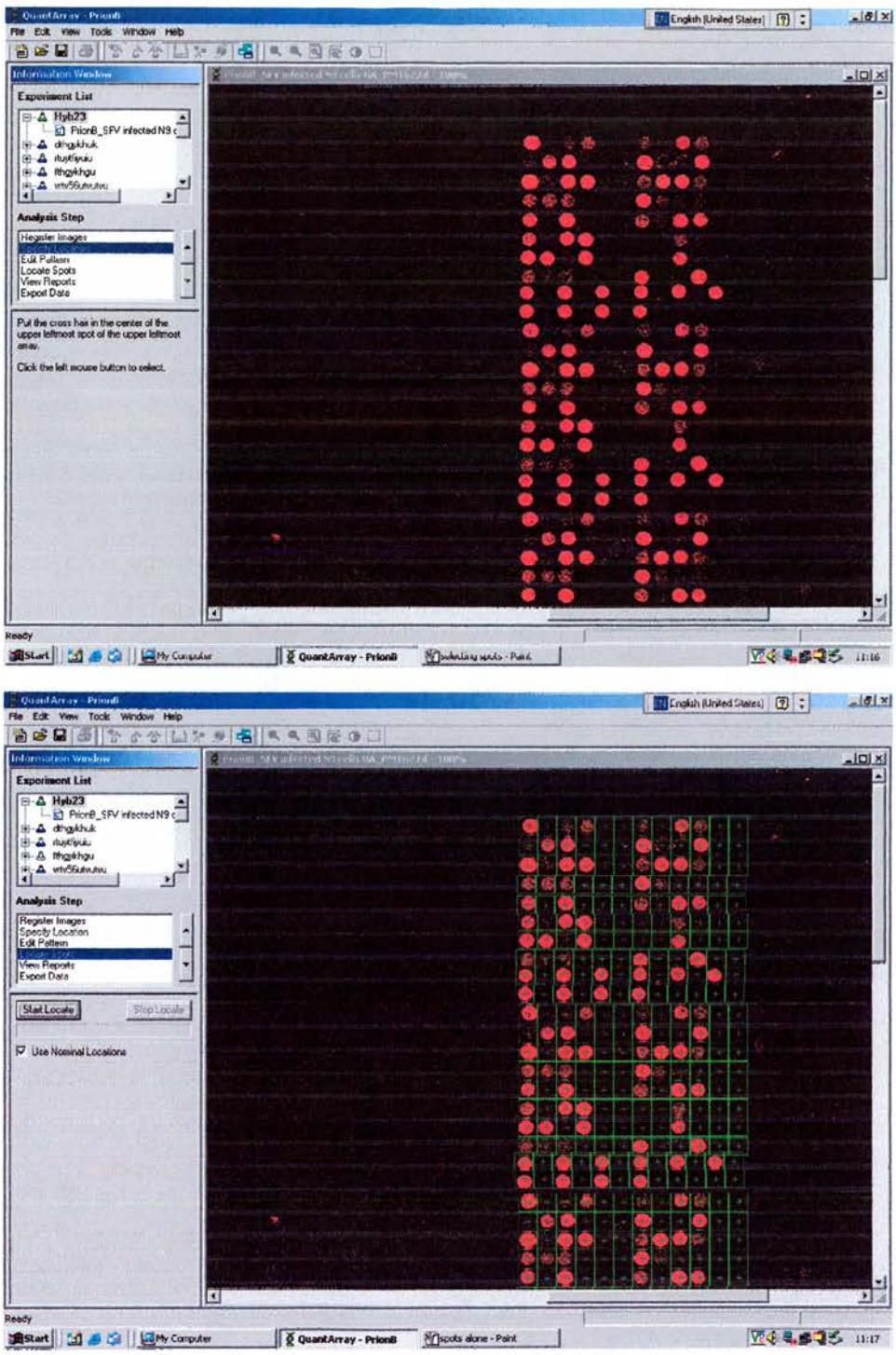

Figure 25, screen shots of a computer running QuantArray™. The top image shows the raw image for a section of the microarray. Each spot fluoresced red due to the presence of Cy3-labelled cDNA. The software locates each spot using "nominal location", bottom image. The number of pixels within a spot was converted into signal intensity. The level of background signal on the array surface was measured individually for each spot (the area in each box surrounding a spot).

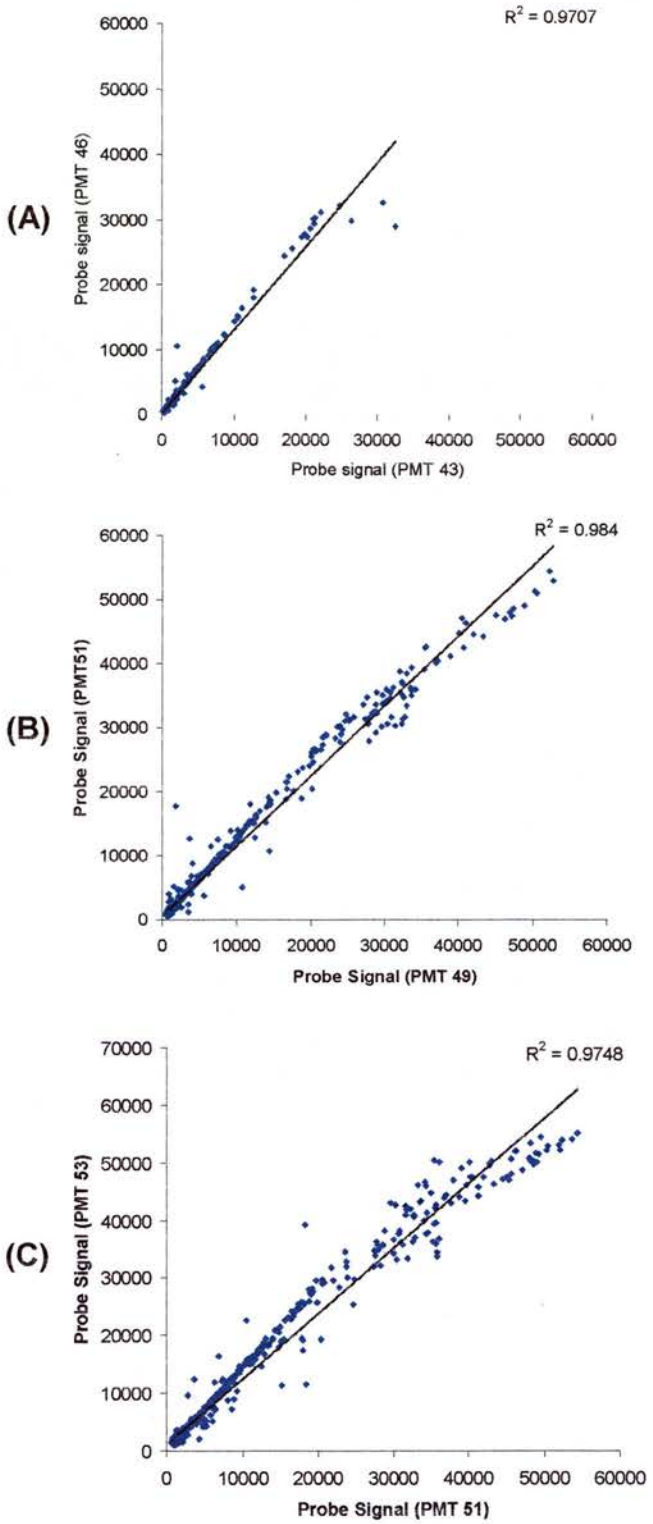

Figure 26, a scan was selected that detected as many spots as possible but did not contain spots that were saturated.

Graph A shows a scatter diagram plotting the probe signal intensities generated from two scans of the same array set at PMT 43 and PMT 46 (the higher the PMT value, the more sensitive the scan). This graph demonstrates that most probes produced a low signal in both scans and few were substantially above background levels.

Graph B shows an ideal scatter plot in which there are many probes that have high signal and yet there is no evidence of probe saturation. The scatter plot is relatively straight and demonstrates good correlation ($r^2 = 0.984$), since the increase in signal intensity from one scan to the next was linear. Consequently, the scan at PMT 51 was selected to represent this hybridisation.

Graph C demonstrates that the next more sensitive scan (PMT 53) generated saturated spots, evident as a curving of the line i.e. the increase in signal intensity from PMT 51 to PMT 53 was not linear for some of the probes. Accordingly the correlation between the two scans was not as high as that found in graph B.

All probe signal intensities were plotted excluding negative control probes.

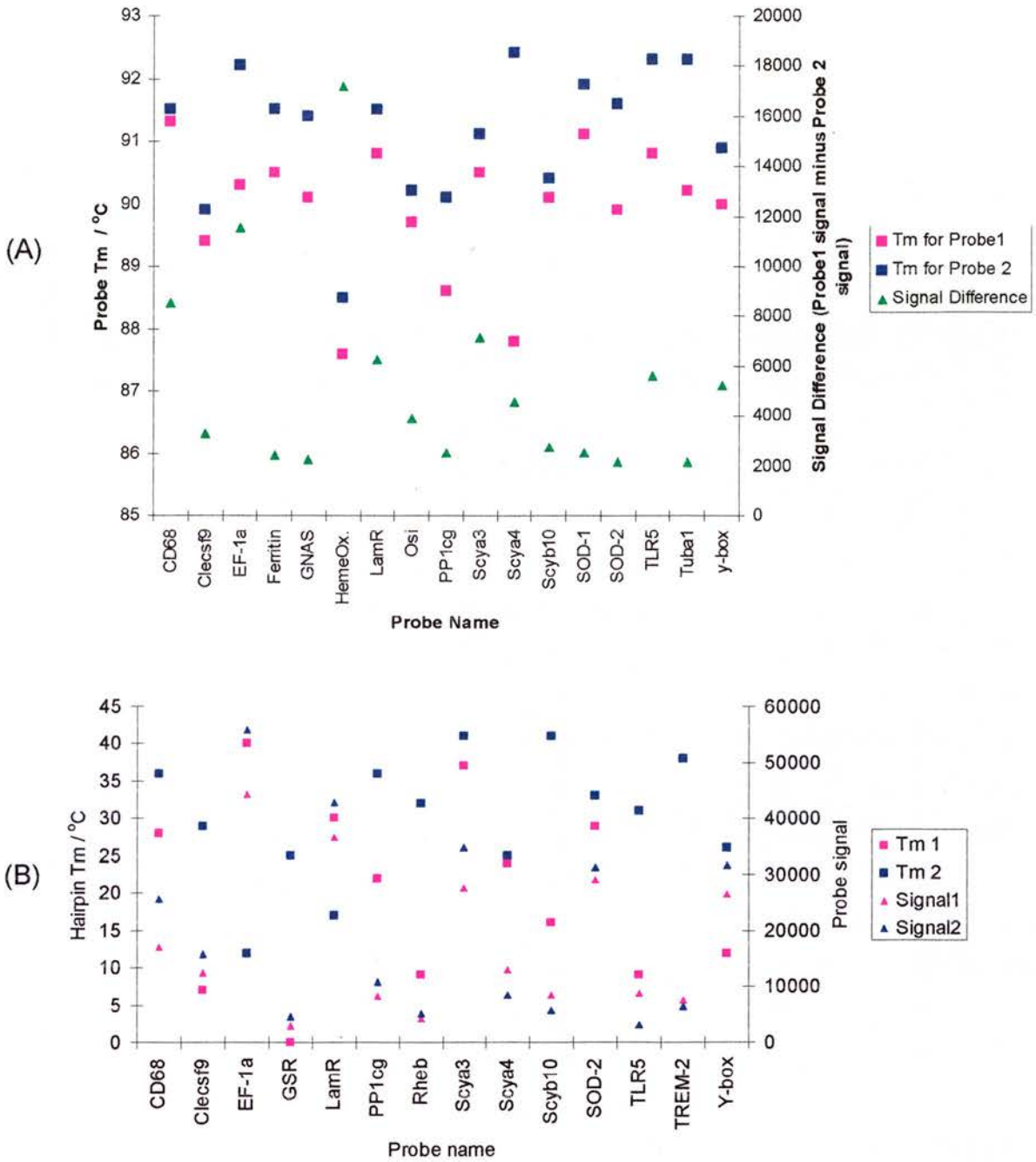

Figure 27, differences in probe Tm values and hairpin Tm values did not correlate with signal difference between probe pairs. (A) Probe pairs that generate a signal difference of at least 2,000 units and bound within 400 bp of the polyT tail have been plotted. The Tm of each probe has been plotted on the left hand y-axis (squares) and the signal difference between each probe has been plotted in respect to the right-hand y-axis (green triangle). The degree of signal difference did not correlate with differences in probe Tm variation. (B) Probe pairs that bound within 400 bp of the polyT tail and in which at least one probe possessed a predicted hairpin Tm of at least 26°C have been plotted. The Tm of each probe's hairpin has been plotted on the left-hand y-axis (squares) and the absolute signal generated by each probe has been plotted in respect to the right-hand axis (triangles). The Tm of hairpin loops did not correlate with a difference in signal intensity, suggesting that this probe characteristic had little to do with probe pair signal differences

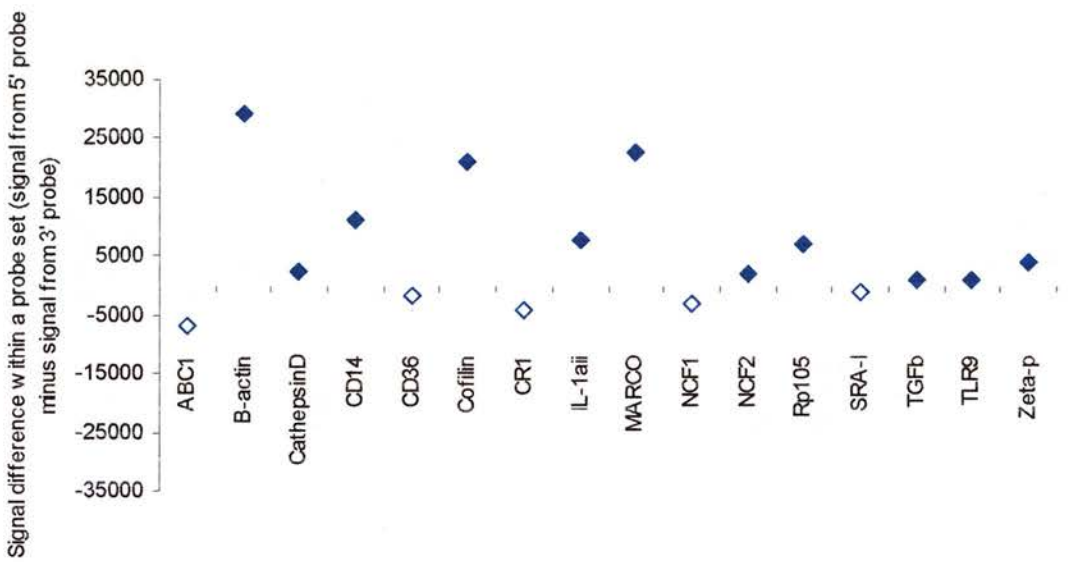

Figure 28, probes that bound closer to the 5'polyT tail produced more signal than probes that bound at least 400 bp more 3'. Probe pairs that were separated by more than 400 bp were selected and the difference between their signal intensities plotted. The signal of the probe that bound more 3' on the cDNA strand was subtracted from the signal of the the more 5' probe. A positive value indicates the 5' probe generated a more intense signal. The graph demonstrates that for the majority of probe pairs, it is the 5' probe that generated a higher signal intensity (blue diamonds). However, this was not the case for all probe pairs (empty diamonds).

3.5 Summary

This chapter has reported the development of a novel custom microarray platform. This platform can effectively and repeatedly measure the expression of a multitude of genes of interest. Probes have been designed to assay the expression of several key genes, including; PRRs such as the TLR and scavenger receptor families; cytokines; chemokines; stress-associated genes; and other genes of interest. These probes form a relatively thermodynamically homogenous population of probes that hybridise optimally at 57.5°C. At this temperature negative probes produce relatively little non-specific signal whilst positive control probes produce a strong signal that can be readily detected. The glass surface, to which the probes are spotted, bound DNA with high affinity and required blocking prior to hybridisation. In house poly-lysine coated slides required two stages of blocking with NMP/succinic anhydride followed by BSA. However, commercially available Corning Gap slides blocked with NMP/succinic anhydride alone were found to generate the lowest background signal in a reproducible manner. The cDNA labeling reaction was studied and it was found that the reverse transcriptase enzyme Fluoroscript labeled cDNA more efficiently and more cheaply than Superscript II.

This chapter also reported that the signal from probe replicates varied across the array and was hampering effective inter-array comparisons. To address this issue the RNA was spiked with exogenous *A.thaliana* mRNA controls that bound to specifically designed probes spotted extensively across the array surface (SpotReport system). By normalising the signal of each sub-array using the *A.thaliana* probes as references the variation in signal intensity was controlled.

To examine gene expression in test and control samples, effective inter-array comparison is critical. This chapter has shown that housekeeping probes can effectively be used as a population of reference probes to normalise microarray signal intensities. Once normalised the probe signal intensities can be effectively compared between arrays and replicate cultures of resting N9 microglia. This demonstrated that the entire process of RNA extraction, cDNA labeling, microarray printing, blocking, hybridisation, image processing and data analysis resulted in a reproducible signal for transcripts that do not vary considerably between resting cultures of microglia.

The exact criteria that are critical for microarray probe design are still not well defined. This study investigated which probe characteristics were responsible for a probe's failure to generate signal. Several transcripts possessed probe pairs in which one generated signal and the other did not. Investigation of probe pairs that generated divergent signal intensities demonstrated that probe Tm or their predicted ability to form hairpin secondary structures

did not correlate with probe signal intensity. This suggests that the strict rules imposed on probe design had prevented the design of inappropriate probes for these two criteria. It was determined that probes that bound at least 400 bp apart produced divergent signal, with the more 3' probe generating less signal. This can be explained by the reported relative inefficiency of reverse transcriptase activity when incorporating bulky Cy dyes, which limits the production of long cDNA strands and enriches the number of short cDNA strands (Causton et al., 2003). Despite this finding, a number of probe pairs generated different signal intensities for unknown reasons. Conceivably, the oligonucelotide probes may have been synthesised incorrectly by the manufacturer. More work needs to be done to better understand which probe characteristics are responsible for affecting the level of probe binding at a given hyrbidisation condition.

Chapter 4. Validation of the custom microarray and characterisation of gene transcript levels in microglia at rest, upon LPS stimulation and upon infection with SFV.

Contents

4.1.1 Introduction

In the previous chapter a novel custom microarray was designed and developed to assay gene transcripts associated with innate immune responses. Methods to accurately normalise and analyse the data were optimised to provide consistent reproducible results for biological replicates. The ability of the microarray to produce a reproducible signal was demonstrated in chapter 3 but not its ability to accurately discern gene expression changes. This chapter exploits the microarray platform to characterise the levels of gene transcripts involved in innate immune responses of microglia.

The N9 microglia cell line was first characterised due to its ability to respond to LPS and has since been extensively used as a cell line representative of resting microglia (Ferrari et al., 1996; Meda et al., 1995). In this study the cell line was used to ascertain whether the microarray could describe changes in several key immune gene transcripts upon exposure to LPS or infection with SFV. LPS is a potent stimulator of the innate immune response in microglia and upregulates several transcripts, including the pro-inflammatory cytokines (Olson and Miller, 2004). SFV is a neuroinvasive virus that initiates encephalitis and activates glial cells *in vivo*. Microglia play an important role in the initiation of CNS immune responses and possess an ability to trigger processes that are destructive to neurones, yet the innate immune response of microglia to SFV infection has been little studied. This chapter investigates the ability of the microarray platform to discern changes in microglial transcripts under two different forms of innate immune stimulus; LPS stimulation and infection with SFV. In addition, this chapter examines the qualitative and quantitative differences in microglial responses to these two stimuli. The initial response of innate immune cells, such as microglia, is pivotal in initiating appropriate adaptive immune responses that act to clear microbes. In particular, dendritic cells can activate differing adaptive immune responses to differing pathogens (Re and Strominger, 2001; Qi et al., 2003). This chapter aims to determine whether microglia, the only cell in the CNS capable of activating T-cells, have the capacity to trigger different and appropriate responses to different innate immune stimuli. Control, LPS stimulated and SFV infected microglia cDNA were hybridised to microarrays and gene transcript levels determined using the techniques developed in chapter 3. To validate changes in transcript levels a robust quantitative PCR (QPCR) technique, able to accurately measure transcript levels was developed.

4.1.2 Objectives

1. To discern the expression profile of several key genes involved in innate immune responses in resting N9 microglia with use of the custom microarray
2. To investigate changes in gene transcript levels in N9 microglia upon stimulation with LPS with use of the microarray
3. To utilise the microarray to assay gene transcript changes of microglia upon infection with SFV
4. To develop QPCR assays for several key genes; including the TLRs and other gene transcripts such as IFN-α
5. To validate the results of the microarray by assaying key gene transcript changes with the use of the QPCR platform

4.2 Resting N9 microglia express a multitude of genes involved in innate immune responses

To determine the expression profile of resting N9 microglia, four cultures were grown for 48 hours until semi-confluent and harvested for RNA extraction. cDNA from individual cultures grown in parallel were hybridised to the microarray and transcript levels determined as detailed in chapter 3 (figure 29). All probes that generated a signal greater than the detection threshold (see section 3.3.6) are plotted in figure 29. Since the signal intensity generated by a particular probe is a product of both the amount of transcript present and the degree to which the hybridisation conditions allow probe binding, it cannot be firmly inferred that differing signal intensity between differing probes accurately reflects the starting amount of cellular transcript. Indeed, each probe must be treated independently; for example most probe pairs give differing signal intensities despite the amount of a specific transcript being uniform e.g. the two probes for β-actin differed substantially in their signal intensity.

Figure 29 demonstrates that resting N9 microglia expressed a range of genes including all housekeeping genes with the exception of c-yes, a gene previously shown to be lowly expressed in some tissue types, and one probe for GSK-3 (Warrington et al., 2000). That probes did not generate a signal above the threshold of detection may be due to several factors including; low level of gene transcript; unfavourable hybridisation conditions; probe secondary structure; or erroneous oligonucleotide synthesis by the manufacturer. Since c-yes is known to be lowly expressed and both probes generated minimal signal it is likely that transcript levels were below the level of detection. Conversely, one of the GSK-3 probes was the only probe that unexpectedly failed to produce a positive signal whilst the other GSK-3

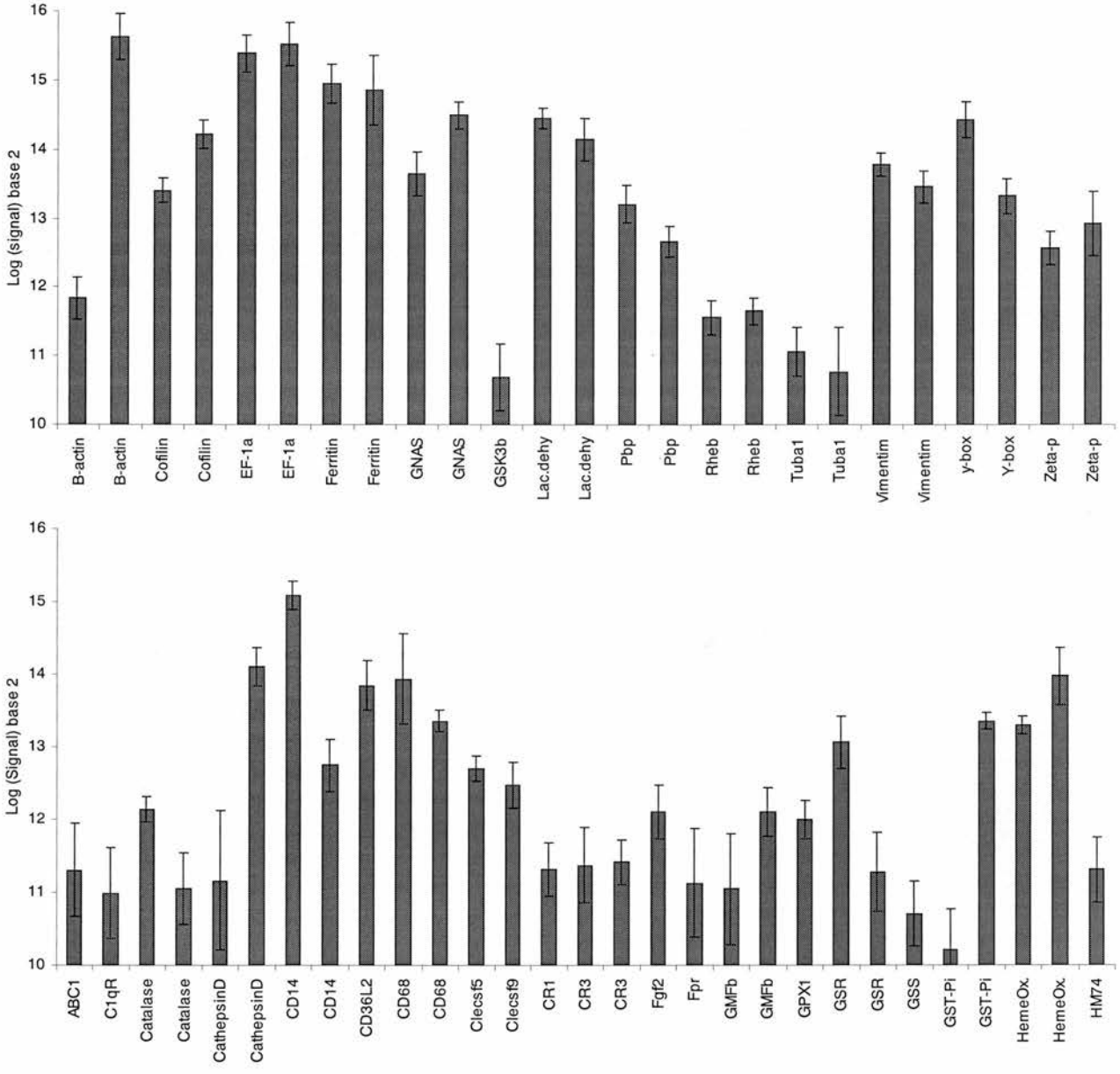

Figure 29, signal intensity of probes above background level indicate those genes expressed by resting N9 microglia. Four cultures of resting N9 microglia were hybridised to four separate arrays and data analysed as detailed in chapter 3. The signal intensity from probes designed to be complementary to transcripts of non-animal origin indicated the level of non-specific hybridisation. The threshold for a positive signal was set as the mean plus two standard deviations of the average signal of 12 negative control probes (each spotted 3 times). Those probes generating a signal higher than this threshold value in at least three of the four arrays are plotted here. Error bars indicate ± SEM from four arrays. In some cases only one probe out of a prob e pair generated a signal higher than background. In the case of both probes generating a positive signal (such as CD14), the probe that bound closest to the 5' poly T tail is plotted after the more 3' probe. This figure is continued on the next page.

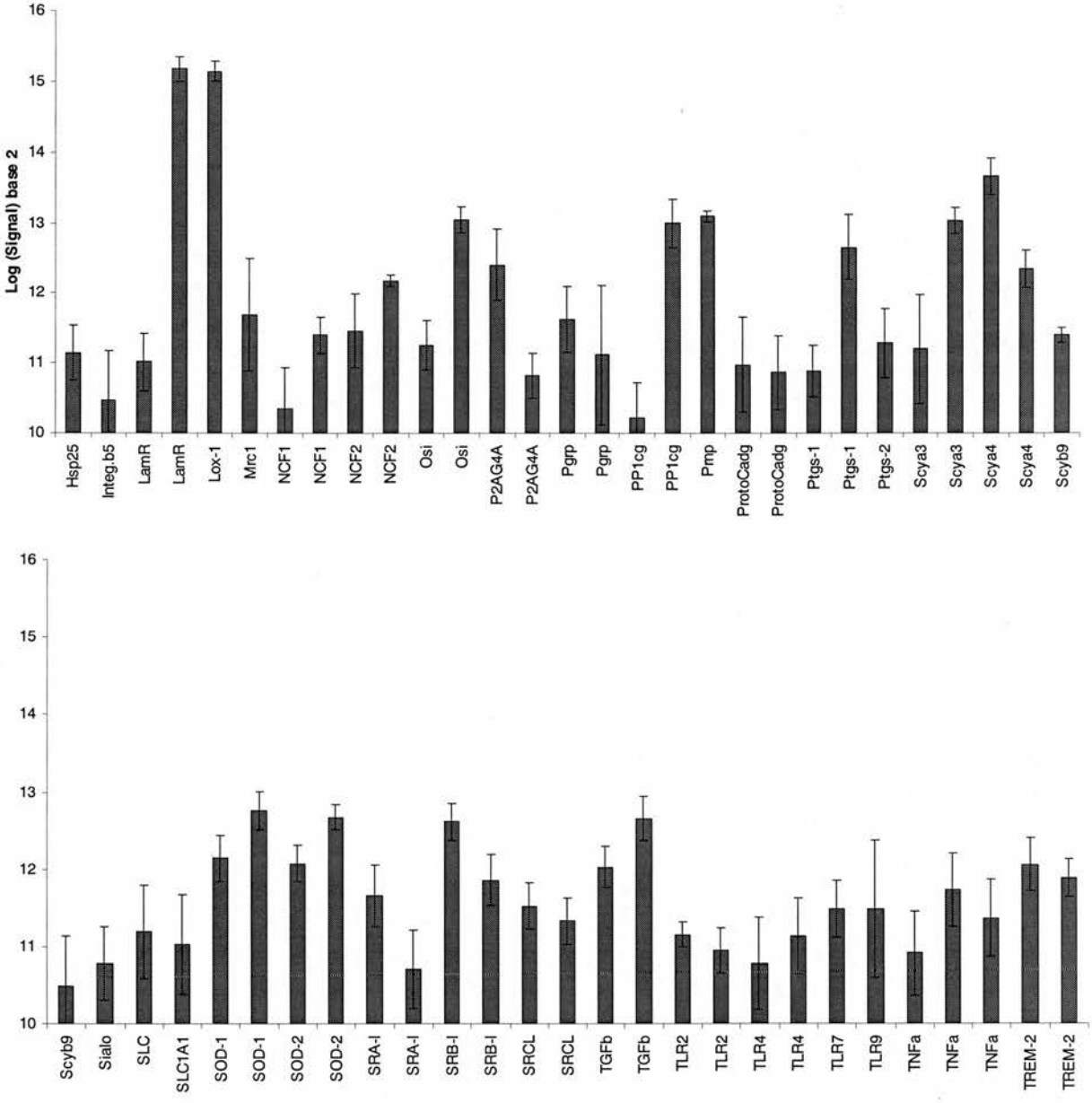

Figure 29 (continued).

probe generated substantial signal. This failure to generate signal was therefore most likely due to factors other than transcript levels. This single example indicates that the numbers of probes failing to hybridise was very low. This suggests the probe design criteria had successfully generated a population of homogenous probes that hybridised under similar conditions.

Figure 29 demonstrates that a wide variety of gene transcripts were detected in resting N9 microglia, including typical markers of microglia/macrophages such as CD14, CD68, complement receptors 1 and 3, and scavenger receptors. Additional cell surface markers whose probes generated signal included CD36-like 2, formyl-peptide receptor, HM74, laminin receptor, peptidoglycan receptor protein (pgrp), TLR 2, 4, 7 and 9 and TREM-2 amongst others. Figure 29 also demonstrates that N9 microglia constitutively expressed transcripts for cytokines such as TGF-β, chemokines such as MIP-1α and MIP-1β (whose probe names are Scya3 and Scya4 respectively), gene associated with phagocytic responses such as NCF 1 and 2 (part of the NAPDH-oxidase system that generates toxic free radicals), Cathepsin D (a lysosomal protease) and Ptgs-1 and Ptgs-2 (also known as COX-1 and COX-2 that mediate prostaglandin synthesis). Finally, probes complementary to transcripts associated with responses to stress were also expressed, such as Osi (induced by stress in macrophages), SOD-1 and SOD-2 (scavengers of free radicals), genes involved in glutathione synthesis (such as GSS that acts to protect against free radicals) and heat shock proteins hsp25 and heme oxygenase 1. The functions of all gene transcripts assayed by the microarray are briefly summarised in appendix 2.

4.3 The microarray was able to discern gene transcript changes in N9 microglia following LPS stimulation

In parallel, ten cultures of N9 microglia were grown until semi-confluent and then treated with either LPS in PBS or PBS alone for 18 hours and harvested for RNA extraction. The resultant cDNA was hybridised to the microarray platform and data analysed as detailed in chapter 3. During RNA extraction one control sample was degraded and a further control sample failed to hybridise effectively to the microarray, such that the final data represented three cultures of PBS exposed microglia and five cultures of LPS stimulated microglia (figure 30). The microarray data demonstrates that a multitude of probes gave significantly differing signal intensities when hybridised to cDNA from LPS stimulated N9 cells compared to cDNA from resting cultures, indicating transcript levels were altered. In particular, a series of cytokines were significantly upregulated following LPS stimulation including TNF-α, IL-1α and IL-1β, as were the chemokines MIP-1α, MIP-1β and IP10 (also

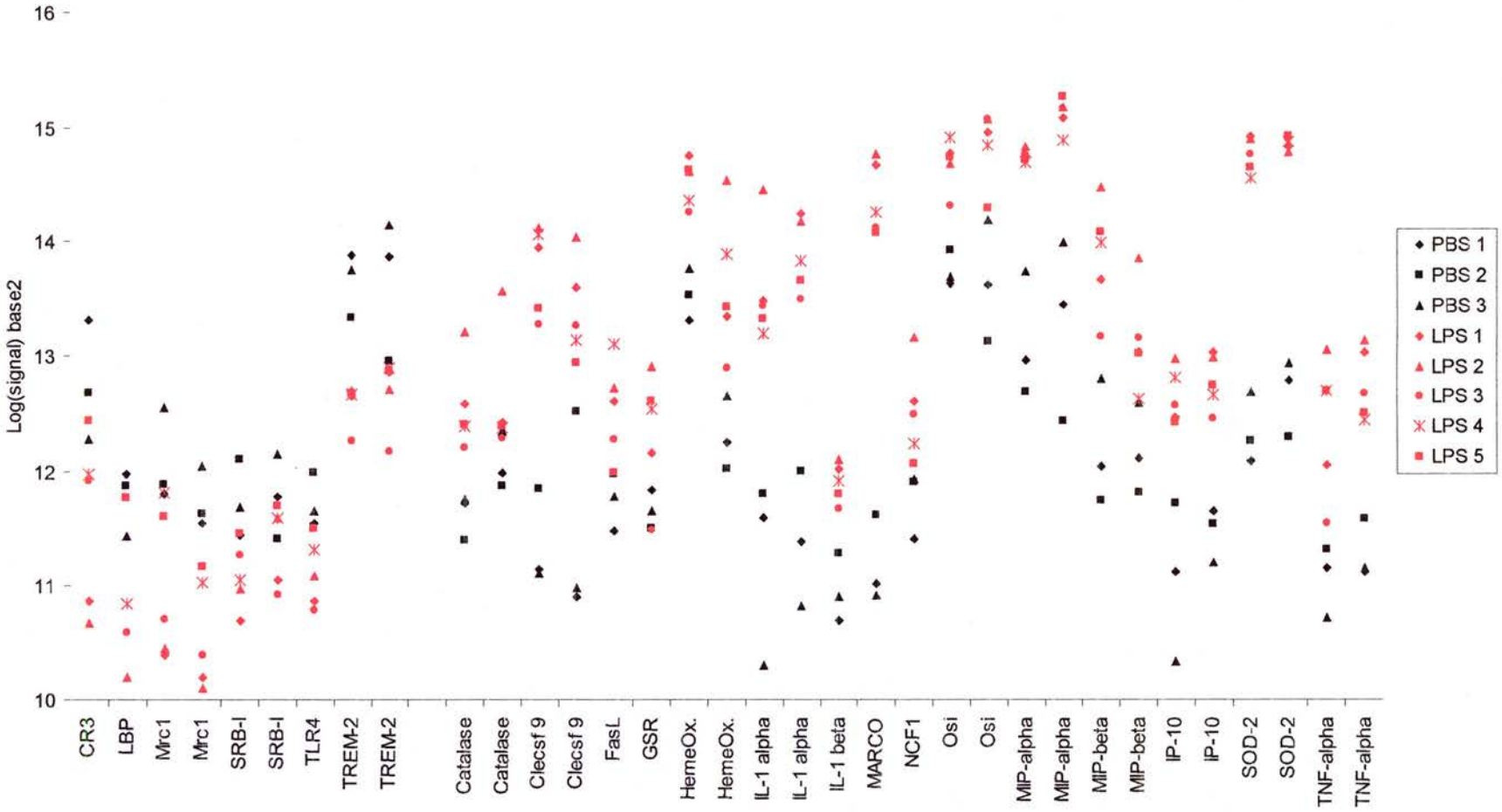

Figure 30, probes generated significantly different signal intensities when hybridised to cDNA from LPS stimulated N9 microglia, compared to unstimulated control cells. Parallel cultures of N9 microglia were grown until semi-confluent and then treated with either LPS in PBS or PBS alone for 18 hours. In parallel, cDNAs prepared from these cultures (PBS n=3; LPS n=5) were hybridised to separate microarrays and the data sets normalised as specified in Chapter 3. Those probes that generated a significantly different signal in LPS stimulated cells (Students t-test $p<0.05$) compared to PBS treated cells are shown here. Those probes that gave a significantly decreased mean signal are plotted on the left of the graph (probes for CR3 to TREM-2),whilst those probes that gave a significantly increased mean signal are plotted on the right hand-side (probes for catalase to TNF-alpha).

referred to as Scyb10). Several transcripts associated with stress were also upregulated. The free-radical scavenger SOD-2 exhibited the largest increase. Significant increases were also seen for heme oxygenase, catalase, GSR, Osi, and free radical generator NCF1. The lectin Clecsf 9 (also known as Mincle) was also upregulated in cDNA from LPS cells. Conversely, several transcripts that encode cellular receptors were down-regulated in LPS stimulated samples, such as TREM-2, TLR 4, scavenger receptor B-I and mannose receptor 1. The analysis of microarray data for this experiment can be found in appendix 9, a Microsoft Excel™ file, on the IBM PC formatted CD-ROM.

4.4 A separate population of gene transcripts were altered in N9 microglia following infection with SFV4

Parallel cultures of N9 microglia were grown until semi-confluent and infected with SFV (MOI=0.1) and harvested for RNA extraction at 3, 12 and 24 hours post infection. The resultant cDNA were hybridised to the microarray platform and data analysed as detailed in chapter 3. It has been reported that infection with virus can decrease the level of housekeeping genes during the course of infection and in the process render them inappropriate for normalisation purposes (Goodbourn et al., 2000). However, the infection of glial cultures with a HSV at a low MOI has been shown to have minimal effect on housekeeping transcript levels (Michael Buchmeier, Scripps Research Institute – personal communication). To determine if any housekeeping transcript were altered by SFV infection, the signal intensities of all housekeeping probes post normalisation were plotted for uninfected samples (0 hour) and for samples 12 hours post infection (figure 32). This graph indicates that housekeeping transcript were unaffected by SFV infection at 12 hours. Note that these probe signals have been normalised to a value generated by the levels of housekeeping transcripts. In effect, this graph shows levels of transcripts normalised to them. Thus, individual probes that are affected by SFV infection would be identified, although a generalised down-regulation of all transcripts to an equal extent would not be identified by this plot. However, further analysis of housekeeping transcripts β-actin and GAPDH by QPCR demonstrated levels were not significantly altered by SFV infection (Figure 41A). Consequently housekeeping probe signals were used to normalise the array data. A similar analysis was undertaken for samples 24 hours post infection and housekeeping genes were similarly unaffected (data not shown).

Following SFV infection, there were no significant changes in gene transcript levels at 3 hours. Changes were observed at 12 hours and are shown in figure 33. Down regulated transcripts included the complement receptors C1qR and CR1, scavenger receptors CD68

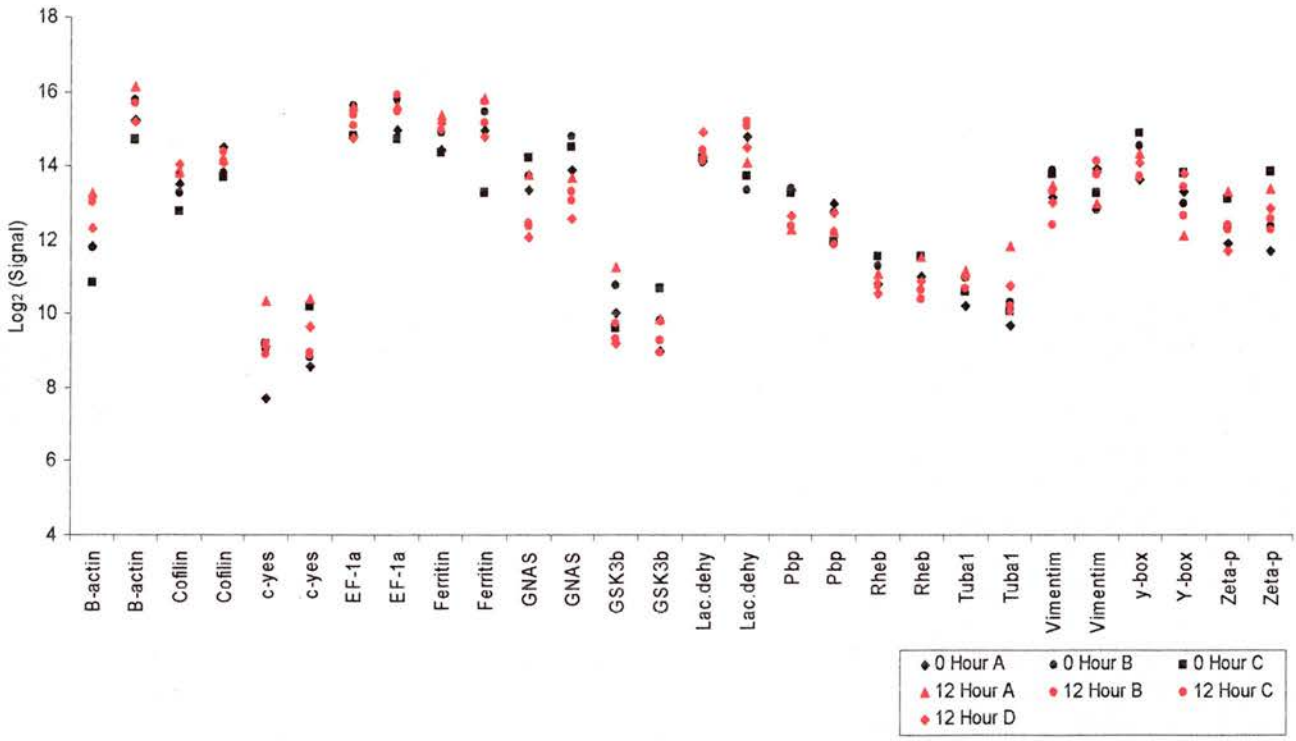

Figure 32, housekeeping transcripts levels were unaffected by infection with SFV4. cDNA from N9 microglia at 0 hour post infection of 12 hours post infection were hybridised to microarrays and data analysed and normalised as detailed in chapter 3. To demonstrate that the normalisation process had worked, the signal intensities of the housekeeping transcripts are plotted above. None of the probes, with the exception of the one of the Pbs probes, appeared to generate substantially different signal upon hybridisation to cDNA from uninfected or SFV infected cells

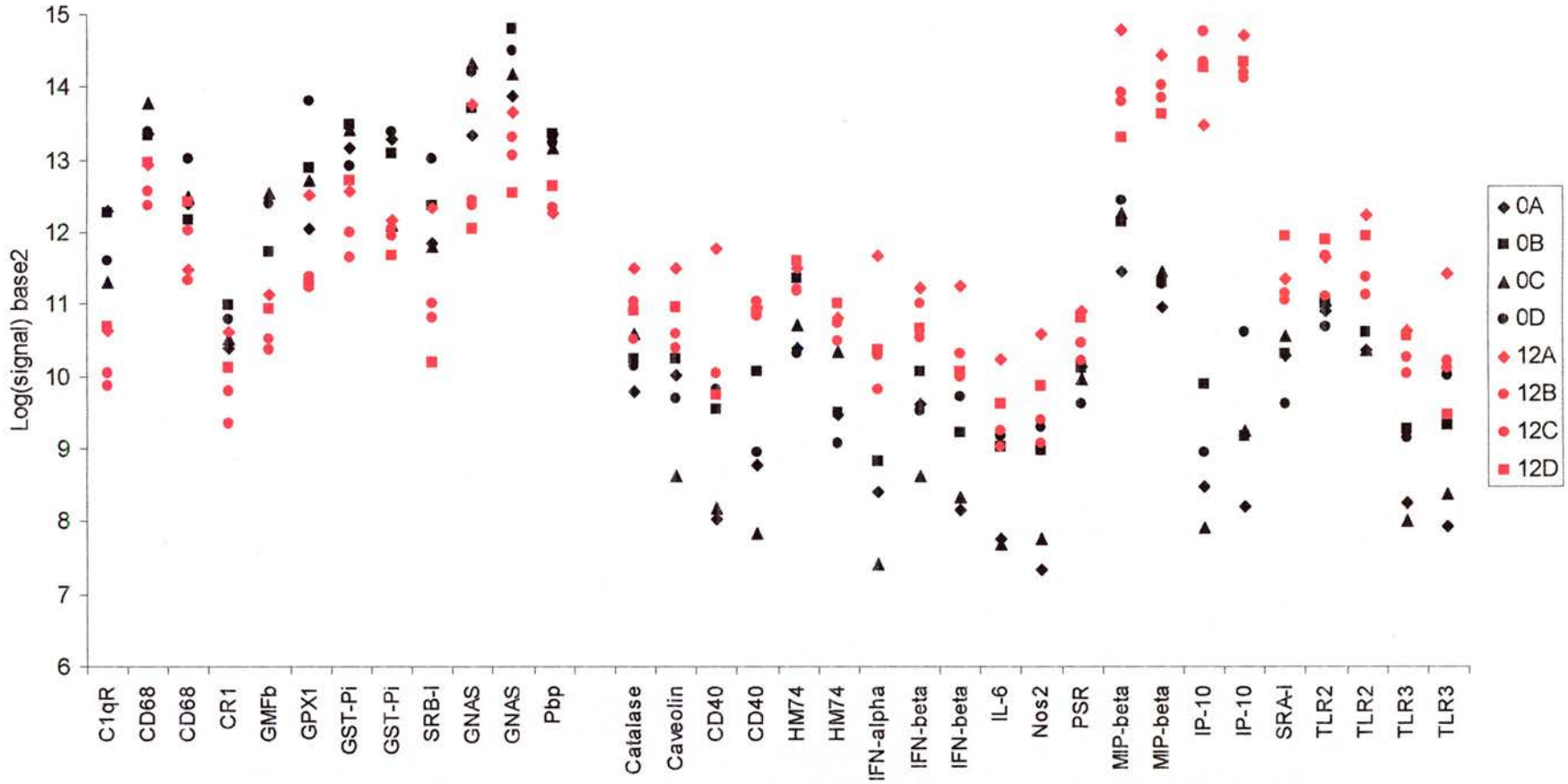

Figure 33, probes that gave significantly different signal intensities at 12 hours post infection with SFV4 compared to uninfected cells. Parallel cultures (n = 8) of N9 microglia were grown until semi-confluent and half were infected with SFV4 for 12 hours. cDNA was hybridised to the microarray and data normalised as specified in Chapter 3. Those probes that generated a significantly different signal in SFV infected samples compared to uninfected are shown here (Student's t-test $p<0.05$). Those probes that give a significantly decreased mean signal are plotted on the left of the graph (probes for C1qR to Pbp), whilst those probes that give a significantly increased mean signal are plotted on the right hand-side (probes for catalase to TLR3).

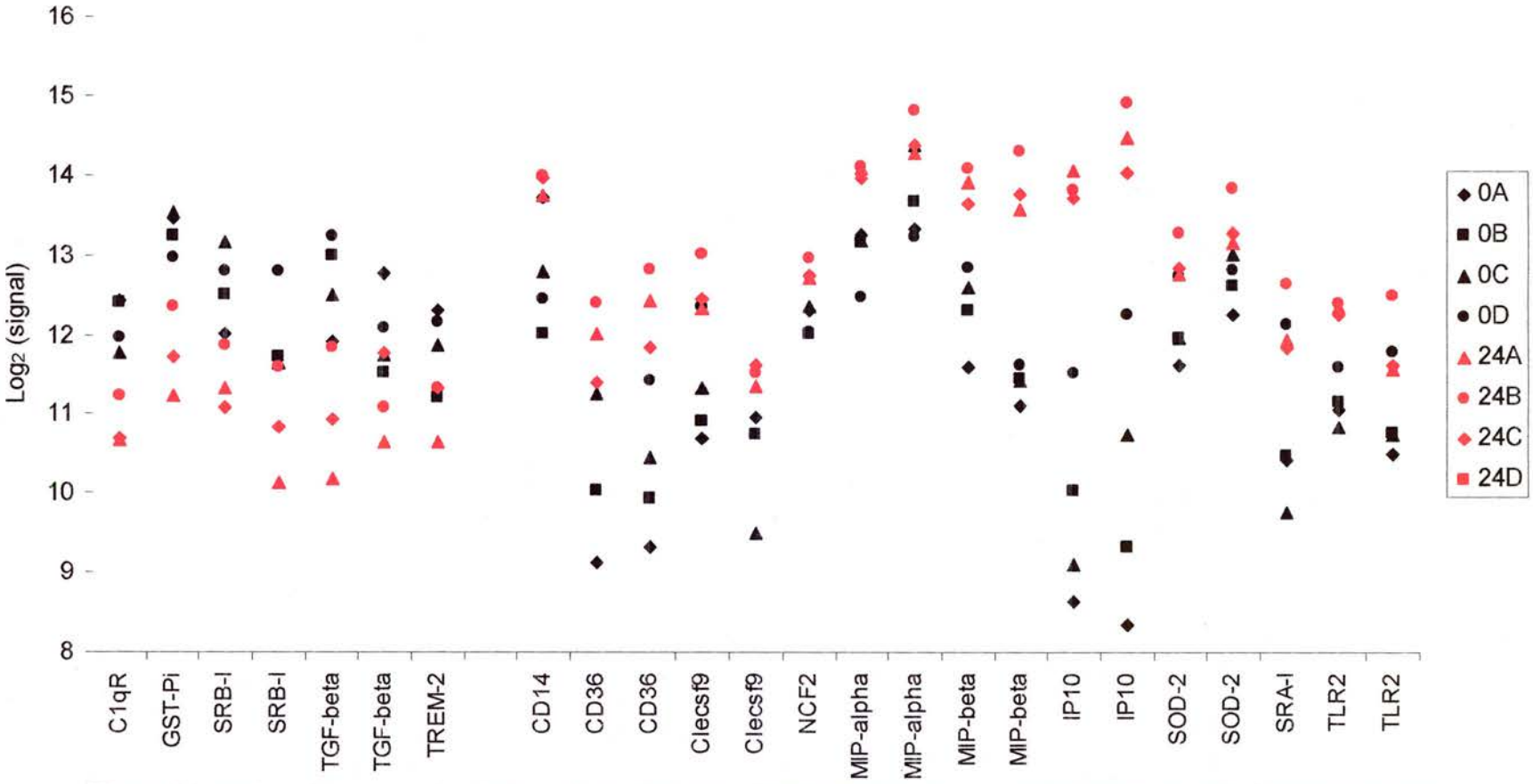

Figure 34, probes that gave significantly different signal intensities at 24 hours post infection with SFV4 compared to uninfected cells. Parallel cultures (n = 8) of N9 microglia were grown until semi-confluent and half were infected with SFV4 for 24 hours. cDNA was hybridised to the microarray and data normalised as specified in Chapter 3. Those probes that generated a significantly different signal in SFV infected samples compared to uninfected are shown here (Student's t-test $p<0.05$). Those probes that gave a significantly decreased mean signal are plotted on the left of the graph (probes for C1qR to TREM-2), whilst those probes that gave a significantly increased mean signal are plotted on the right hand-side (probes for CD14 to TLR 2).

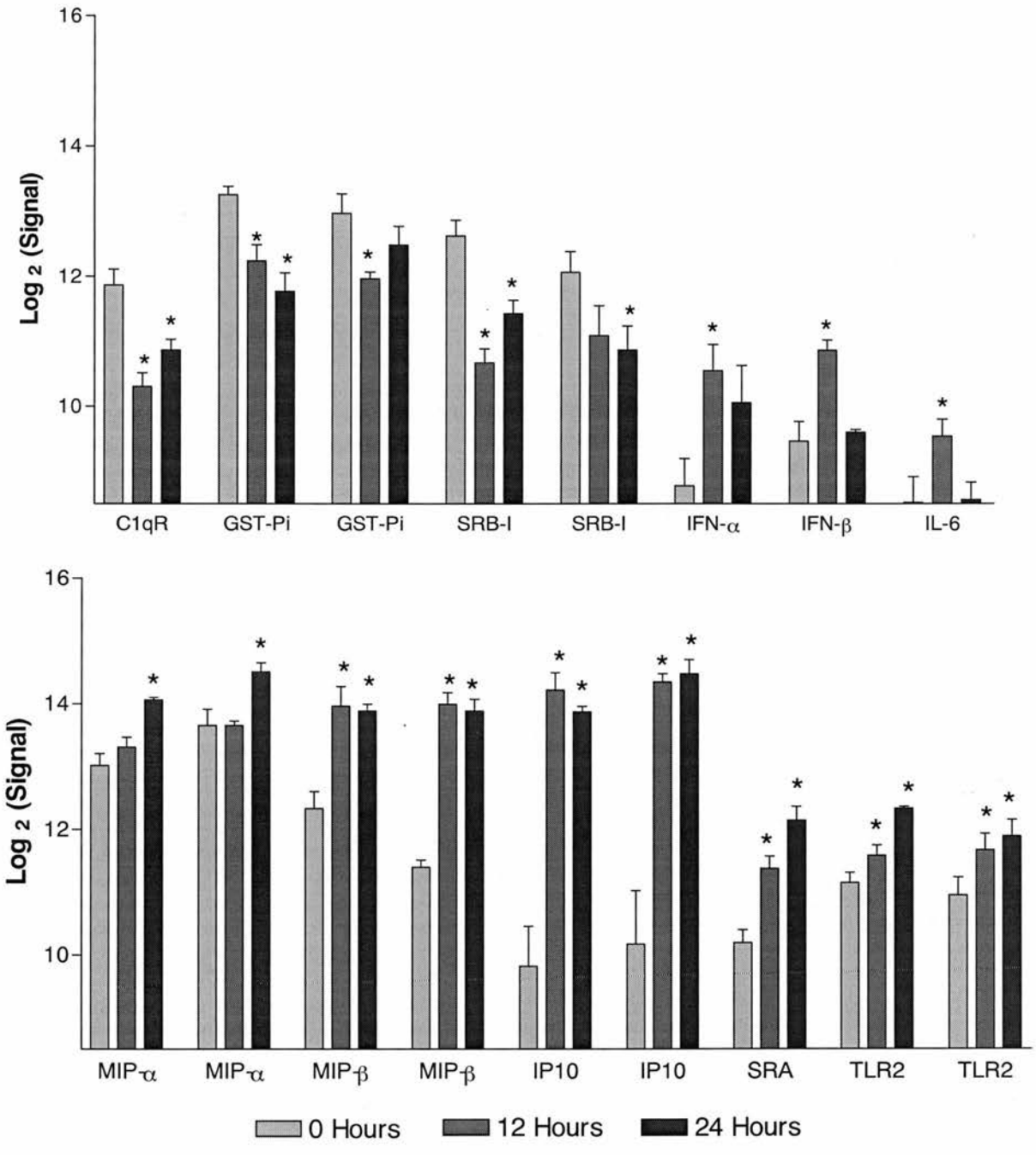

Figure 35, mean probe signal intensities at 0, 12 and 24 hours post infection with SFV4. Some probes that gave signal intensities that were significantly different at 12 or 24 hours post infection compared to the 0 hour time point are plotted here as a time course to show how transcript levels varied over time. The bars marked with an asterisk indicate that the probe signal intensity was significantly different from 0 hour time point (Student's t-test, $p<0.05$). All cultures ($n = 12$) were grown in parallel.

and SR-BI and GST-Pi (involved in glutathione synthesis). Despite the majority of housekeeping probes being unaffected two were marginally down regulated, GNAS and Pbp. Several transcripts were upregulated including some that mediate responses to viruses. These included; IFN-α and IFN-β; IL-6; chemokines MIP-1β and IP10; scavenger receptor A-I; HM74; TLR 2 and 3; CD40 and Nos2 (the gene product responsible for inducible nitric oxide synthesis in macrophages). There was no marked increase in the gene expression of pro-inflammatory cytokines IL-1α, IL-1β or TNF-α or in genes associated with cellular stress such as heat shock proteins, Osi or SOD-2. The greatest fold increases were observed for the chemokines MIP-1β and IP-10 followed by IFN-α.

Figure 34 shows the probes that gave significantly different signal intensities at 24 hours post infection. Some of these were different to those identified at 12 hours post infection, but many were the same. By 24 hours, the immunosuppressive cytokine TGF-β was down regulated, as was TREM-2. Several cell surface receptors were upregulated such as CD14, CD36 and TLR 2. TLR 3 was no longer significantly different from controls. Several chemokines were upregulated including MIP-1α (which was at basal levels at 12 hours post infection). The highest fold increases were again observed with the chemokines MIP-1β and IP-10. Both probes for the free-radical scavenger SOD-2 also gave a marginal but significant higher signal at 24 hours.

Figure 35 summarises some of the changes in probe signal intensities over the course of infection. The graph shows that most of the probes with decreased signal at 12 hours remain depressed at 24 hours. Meanwhile, the probes for the type-I IFNs and IL-6 appear to peak at 12 hours post infection and then decrease. Conversely, the chemokines that are upregulated at 12 hours remain at these higher levels or continue to increase. Finally, the probe signal intensities for scavenger receptor A and TLR 2 progressively increase with time post infection.

4.5 A series of QPCRs were designed and optimised to validate microarray results and further explore gene transcript levels

To verify the microarray results another method of gene transcript quantification was used. QPCR was developed for selected genes. A series of primers were designed and QPCRs optimised as described in chapter 2. The QPCR could detect transcripts that were present below the threshold of detection on the microarray. For example, on the microarray the majority of probes complementary to the TLR transcripts were at or below the threshold of detection. This meant that changes in TLR expression might not be adequately described. The one exception was TLR 2 where signal was high enough to be detected at rest and was

upregulated at 12 and 24 hours post infection with SFV. Nevertheless, a major aim of this thesis was to describe TLR expression in cells of the CNS and the microarray platform appeared to lack the sensitivity required to assay TLR transcripts in cultured N9 microglia. The probability of the array platform being able to assay TLR transcripts in CNS tissue was even less likely, due to the presence of numerous cell types in the CNS unlikely to express TLRs that would dilute TLR transcripts from expressing cells. Thus, primers for all TLR members were designed and TLR QPCRs optimised.

There are several methodologies that can be used to detect PCR amplification in real time that rely on the production of a fluorescent signal once a PCR product is formed. These techniques include the use of probes conjugated to a fluorophore, which directly label the specific PCR product (a technique first developed by TaqMan^{TM}). This technique, whilst highly sensitive, is prohibitively expensive and therefore inappropriate for extensive research work. Alternatively, the PCR product can be labelled in real-time with SYBR-green dye, a molecule that is only fluorescent upon intercalation into the double stranded DNA PCR product. This method is considerably less expensive but requires greater optimisation of PCR conditions, primarily because the non-specific nature of this dye means the PCR itself must be highly specific. To ensure primers were specific, a set of strict criteria was used to design primers and limit primer-dimer formation (see chapter 2 for criteria). Each QPCR was based on the amplification of DNA by a set of "inner primers". To quantify transcript levels a standard DNA template was assayed concurrently with samples of interest. Each specific DNA template was generated in a standard PCR using a set of "outer" primers that encompassed the region amplified by the inner primers (more details are found in chapter 2).

Figure 36A and B demonstrates the large dynamic range that the QPCR platform affords. This figure shows the amplification of a DNA template present at a variety of concentrations. The DNA template diluted 1 in 100 ($1x10^{-2}$) was amplified first and each subsequent ten-fold dilution was amplified at intervals of 3.3 cycles until the DNA template was diluted by 10 orders of magnitude. Software analysis located a threshold at which all curves represented logarithmic growth, and the point at which the curve intersected this threshold determined the C_T value given in PCR cycles (see figure 36 for more details). Each QPCR experiment included a series of diluted DNA template so that a standard curve could be constructed in each case. The inclusion of a standard curve in each QPCR assay enabled the determination of the threshold of detection, and demonstrated the ability of the platform to accurately quantify starting DNA levels.

Figures 37, 38, and 39 demonstrate the specificity of each PCR primer set. Figure 37A demonstrates the use of capillary electrophoresis to show the production of a single PCR

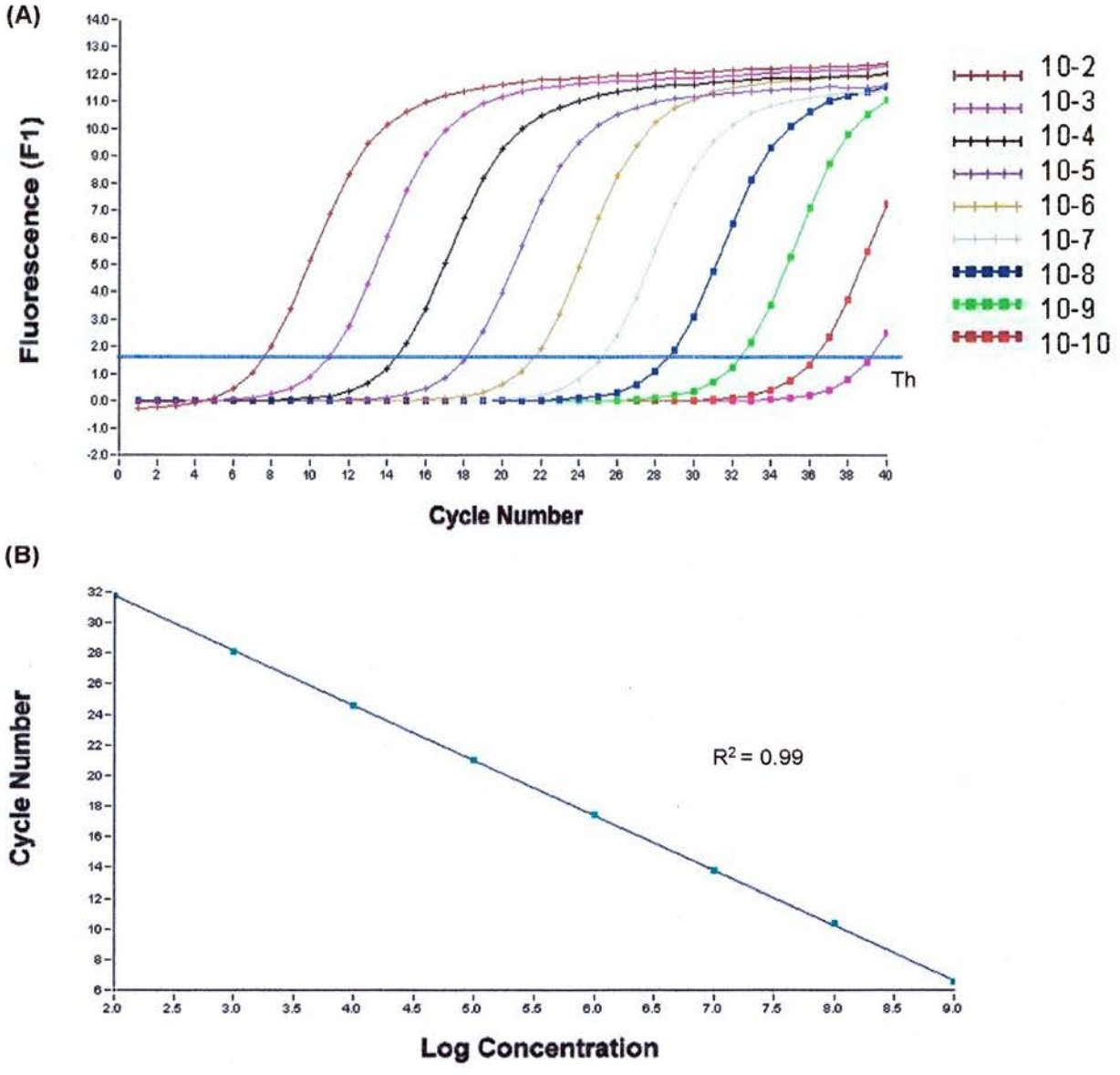

Figure 36, DNA standards were used to determine PCR sensitivity and quantify levels of transcripts. (A) The TNF-α DNA template standard was diluted in ten-fold serial dilutions and 10^{-2} to 10^{-10} was used as a template in QPCR reactions along with a negative control in which there was no template. Software analysis calculated the level of fluorescence at which all curves were representative of logarithmic growth, known as the threshold value (shown here as a blue line labelled "Th"). The number of cycles completed by each PCR at the intersection of each curve with this threshold was measured and is know as the C_T value (given in cycle numbers). **(B)** This graph plots the log of DNA template concentration against the C_T values to create a standard curve and thus equate PCR cycle number with starting DNA concentration. Note that the correlation of this graph was high with R^2=0.99 (1 = perfect correlation whilst 0 = no relationship). The standard curve was used to quantify unknown transcript levels. Each QPCR experiment included a standard curve along with samples of interest.

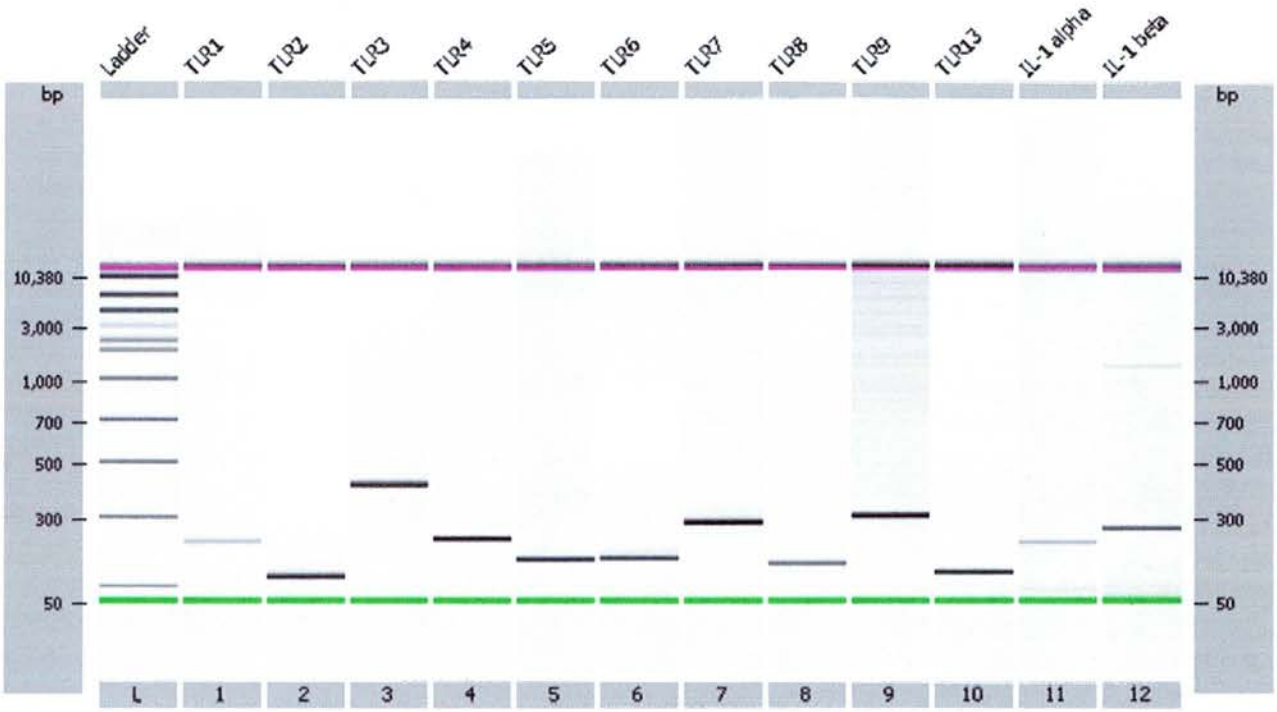

Gene	Genbank	PCR product size (in base pair (bp))
TLR1	NM_030682	216
TLR2	NM_011905	119
TLR3	NM_126166	406
TLR4	NM_021297	225
TLR5	NM_016928	169
TLR6	NM_011604	170
TLR7	NM_133211	270
TLR8	NM_133212	156
TLR9	NM_031178	304
TLR13	NM_205820	131
IL-1 alpha	NM_010554	228
IL-1 beta	NM_008361	269

Figure 37A, primers designed for use in quantitative PCR were specific. PCR products were generated by amplifying cDNA from LPS stimulated N9 microglia. The resulting reactions were analysed on an Agilent DNA chip using capillary electrophoresis; the single band demonstrates the specificity of each primer pair. The estimated PCR product size is shown in the table.

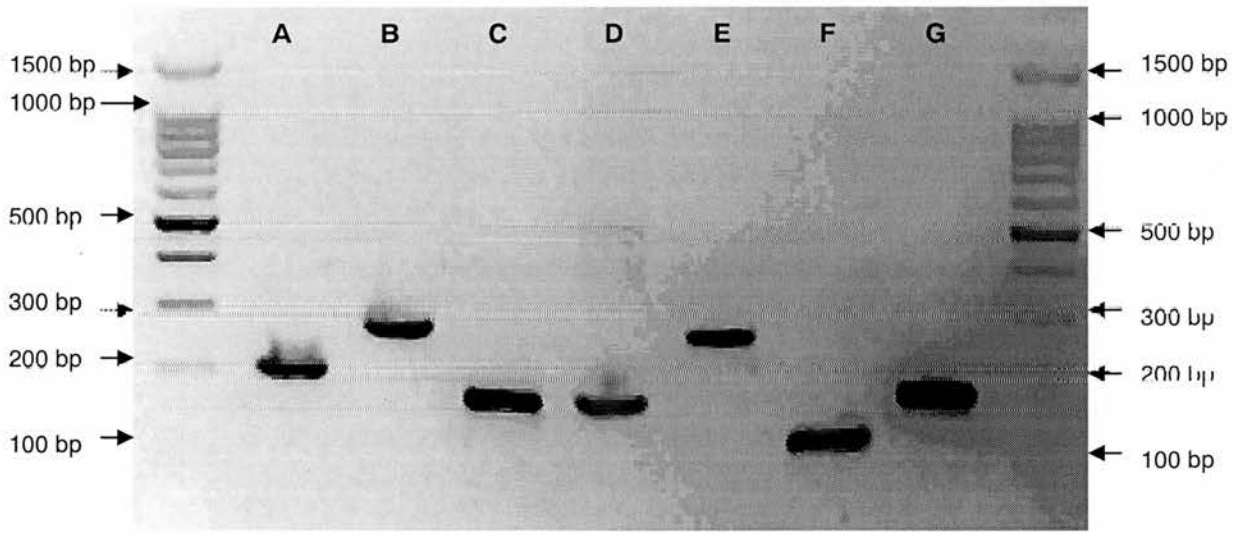

Column	Gene	Genbank	PCR product size (in base pair (bp))
A	Beta-actin	NM_007393	202
B	GAPDH	NM_001001303	269
C	IL-6	NM_031168	171
D	SFV E1	X74491	173
E	TNF-alpha	NM_013693	260
F	GFAP	NM_010277	128
G	IFN-alpha	NM_010504	186

Figure 37B, primers designed for use in quantitative PCR were specific. PCR products were generated by amplifying cDNA from LPS stimulated N9 microglia. The resulting reactions were analysed by standard agarose gel electrophoresis; the single band demonstrates the specificity of each primer pair. The estimated PCR product size is shown in the table.

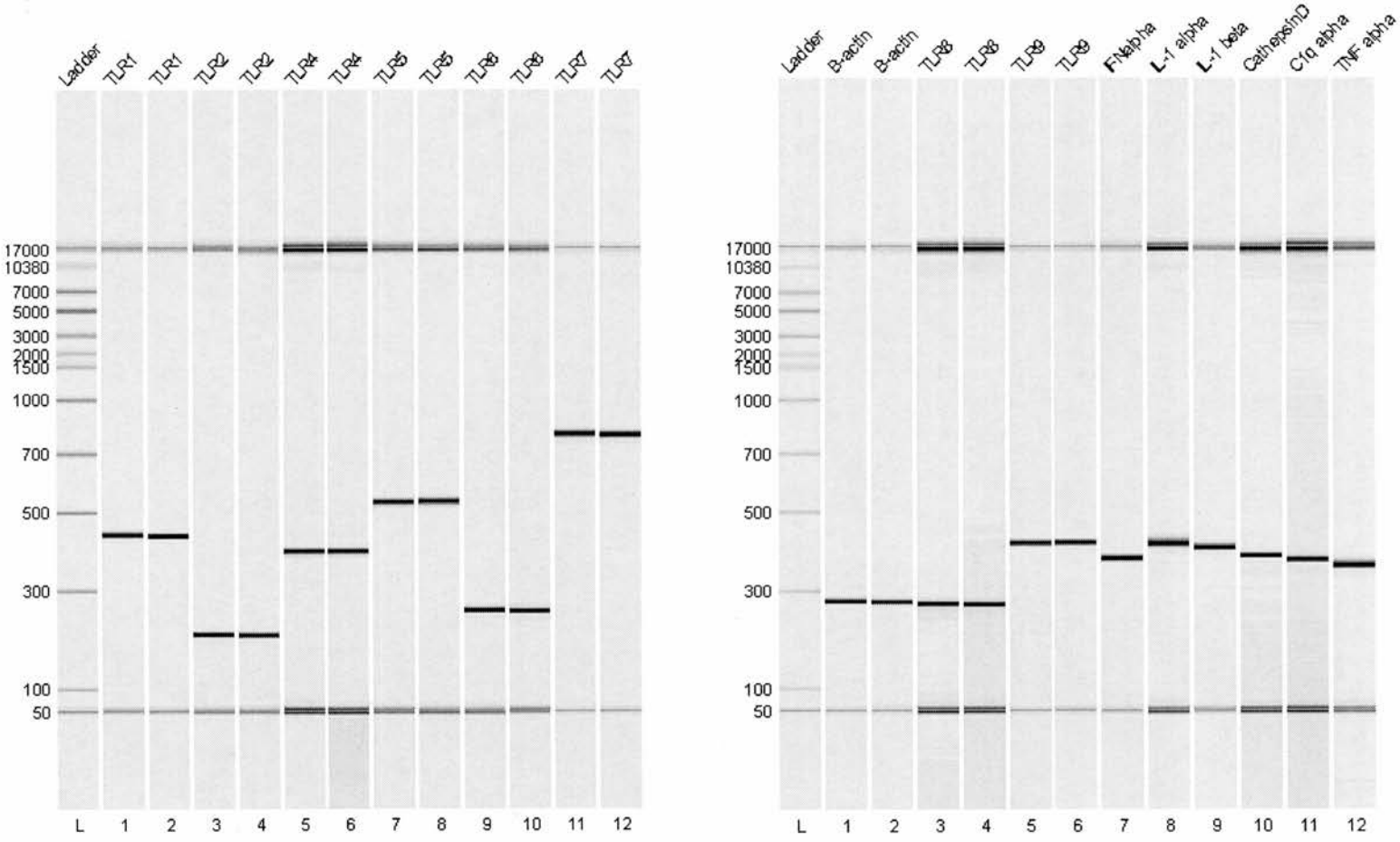

Figure 38, the "outer" primers were used to generate PCR products to act as standards for the QPCR. PCR products were amplified using a mixed cDNA substrate sourced from LPS stimulated and SFV infected N9 microglia. The resultant PCR products were analysed on an Agilent DNA chip using capillary electrophoresis. The single bands generated in each reaction indicate its specificity (the predicted PCR product sizes can be found in chapter 2, table 4). The ladder sizes are given in base pair (bp) and the mass of each PCR was determined (for details of calculations see section 2.12.3). These PCR products were utilised as reference standards for QPCR.

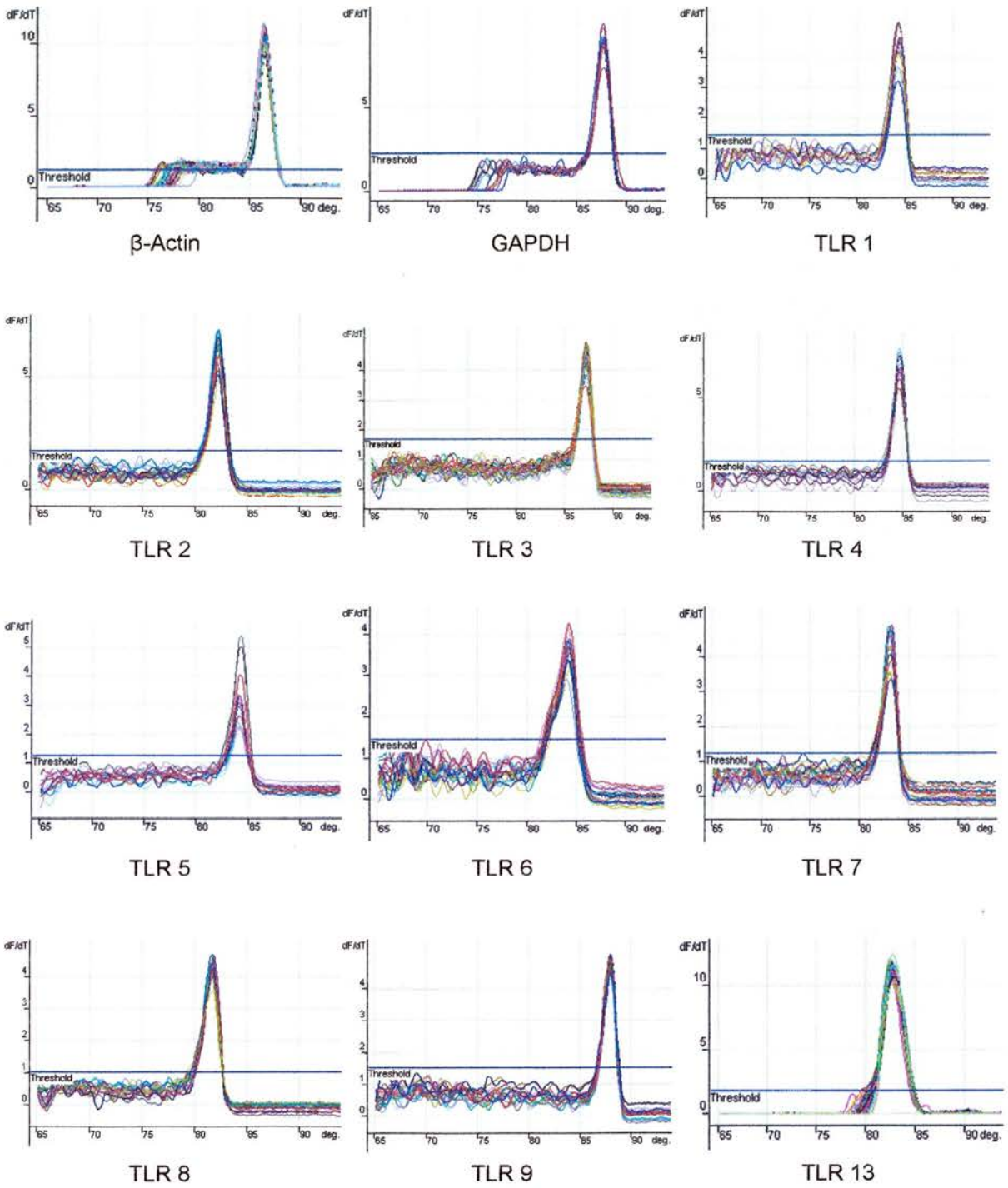

Figure 39, melt-curve analysis was used to determine the specificity of all QPCRs. Following optimisation of PCR conditions, the specificity was ascertained by undertaking a melt curve analysis for all primer sets. Each graph shows the change in fluorescence over time (dF/dT) on the y-axis, as the PCR mixture is heated from 65 to 93°C. The presence of a single peak demonstrates the production of a single PCR product that represents a homogeneous species of DNA that melts at a given temperature This figure is continued on the next page.

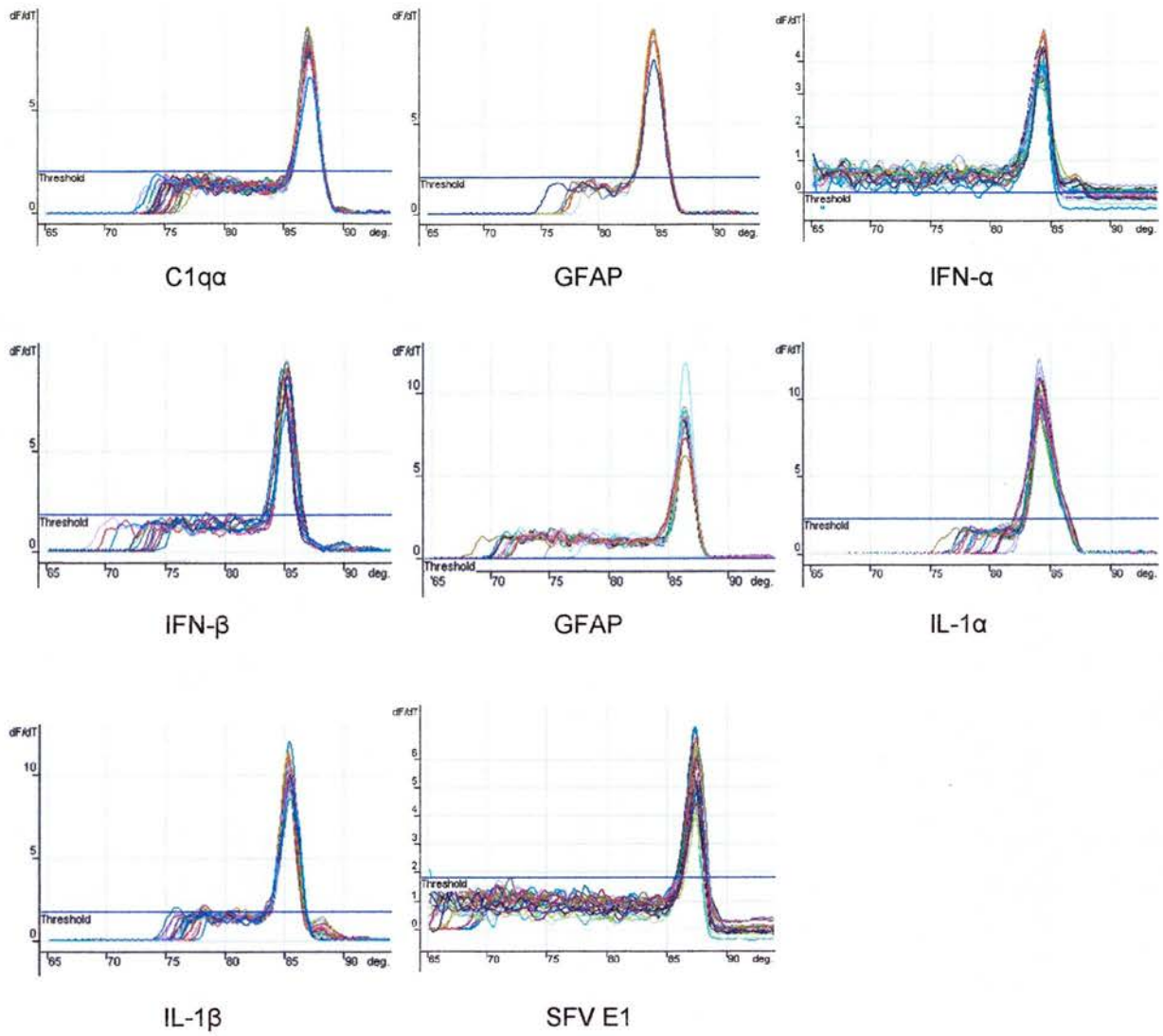

Figure 39, (continued).

product for inner QPCR primers. Notice the absence of bands indicative of primer dimer or other non-specific products. Figure 37B continued this analysis using standard gel electrophoresis for inner QPCR primers. Figure 38 demonstrates the specificity of the outer primers used to generate DNA templates. In addition to gel electrophoresis melt-curve analysis was used to determine the specificity of each QPCR. Melt-curve analysis exploits the thermodynamics of DNA complementation by assuming that at a given salt concentration the amount of dsDNA present is dependent on temperature. Thus, following QPCR amplification the mixture was heated from 63 to 93°C and the level of fluorescence measured at 0.2°C increments. At 63°C fluorescence was high since at this temperature most PCR product was present as dsDNA, whilst at 93°C almost all DNA had melted and fluorescence was therefore minimal. The presence of specific PCR product was detected by a sudden loss of fluorescence as the population of homogenous DNA strands melted. Non-specific products of differing sizes could be detected as irregular decreases in fluorescence (figure 39). In practice the specificity of each QPCR was undertaken without exception by melt curve analysis, rather than gel electrophoresis. Gel electrophoresis is relatively time intensive whilst melt-curve analysis is a technique that can be programmed into the QPCR machine to occur automatically at the end of each PCR.

To determine the reproducibility of the QPCR platform, 18 cDNA samples were assayed for β-actin content. Each cDNA sample was assayed twice and the standard deviation of the two C_T values calculated for each cDNA sample. The smallest standard deviation observed for two samples was 0.0007 (mean = 13.325) whist the largest was 0.17 (mean = 13.22), whilst the average standard deviation for all 18 samples was 0.049 (mean = 13.61). In addition, the technique was developed and validated on two differing QPCR machines: the Rotor gene 3000 (Corbett Research) and the Lightcycler II (Roche). The Lightcyler offered the advantage of being particularly quick and robust whilst the Rotor gene 3000 allowed a larger number of samples to be assayed concurrently in a significantly less expensive manner.

4.6 QPCR was used to validate gene expression changes observed by the microarray in LPS stimulated and SFV infected N9 microglia

The microarray results demonstrated several probe signal intensities were significantly increased in LPS treated microglia, indicating that their complementary gene transcripts were elevated. To validate this and more accurately determine changes, QPCR was undertaken on two gene transcript: IL-1α and IL-1β. In addition, although LPS stimulation is known to upregulate IL-6 in primary microglia (Godbout et al., 2004), the microarray identified no significant differences; to determine if the array results represented a false

(A)

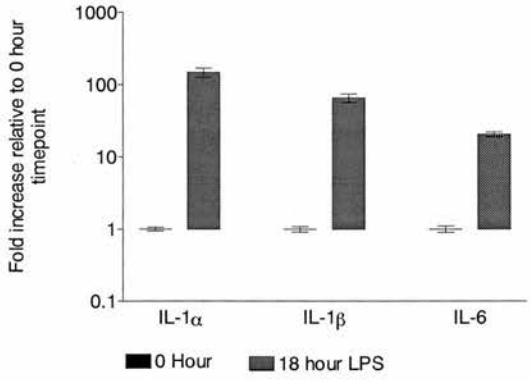

(B)

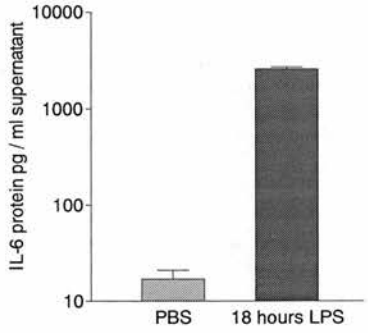

(C)

	Probe 1	Probe 2	QPCR
IL-1α	5.06*	5.57*	148.9*
IL-1β	1.92*	1.14	66.87*
IL-6	0.99	0.87	20.68*

Figure 40, validation of microarray results using QPCR and ELISA. The LPS stimulated N9 RNA samples that generated the cDNA used for the microarray hybridisations were also used to generate full-length cDNA for validation purposes. (A) The transcript levels for IL-1α, IL-1β and IL-6 were measured using QPCR. (B) The levels of IL-6 in the tissue culture supernatant of the PBS and LPS stimulated N9 microglia were measured using an ELISA and expressed as pg per ml tissue culture supernatant. (C) A comparison of the estimates of fold change in transcript levels in LPS stimulated microglia, as determined by probes on the microarray and the QPCR platform. Those values marked with an asterisk were significantly different from respective controls (Student's t-test, $p<0.05$).

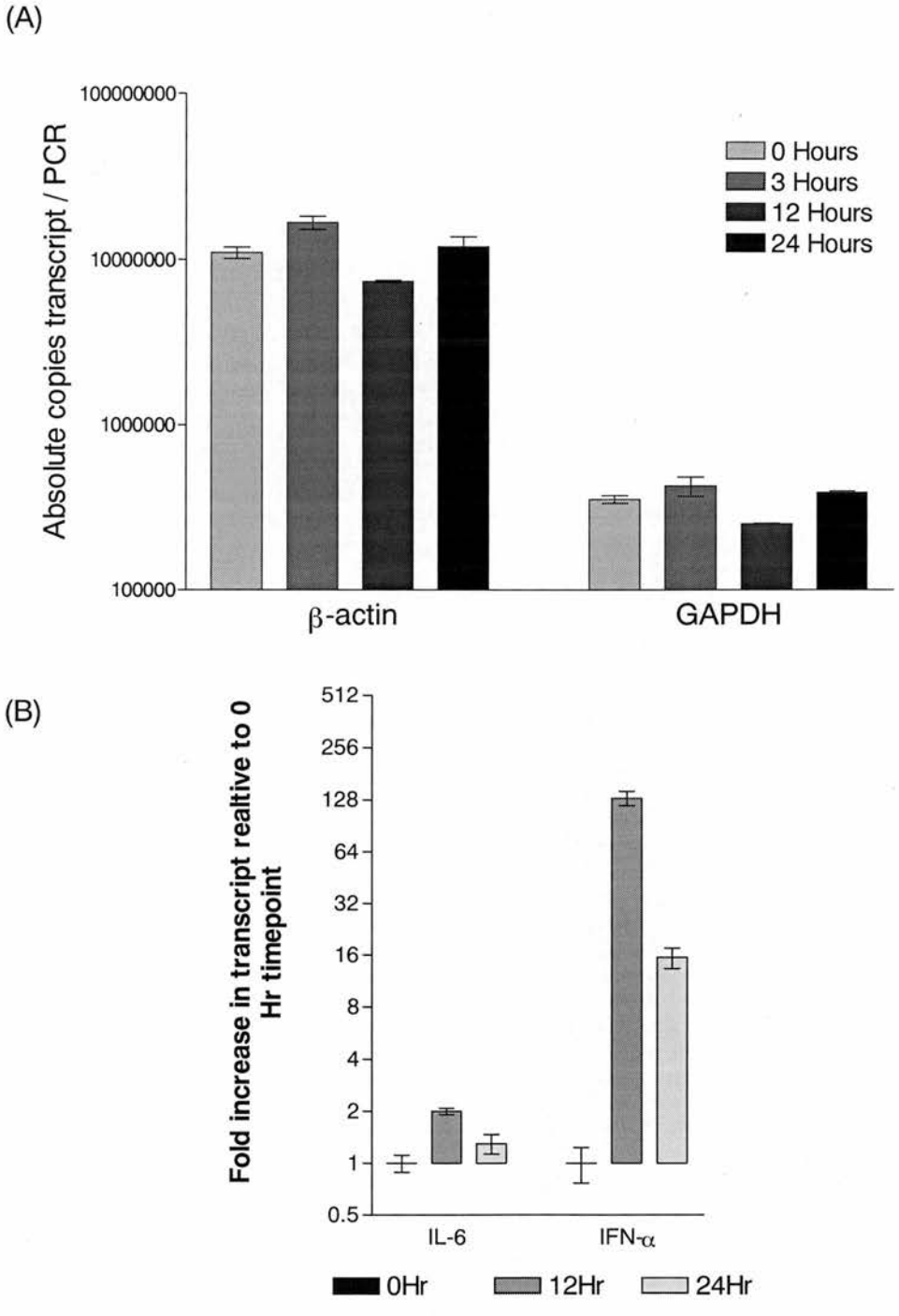

Figure 41, QPCR analysis of SFV4 infected N9 cDNA. Transcript levels were determined by QPCR as previously described. (A) Housekeeping gene transcripts were assayed and absolute levels determined.(B) Genes of interest were assayed and expressed as fold increase relative to the 0 hour time point. Error bars indicate ± SEM (n=4).

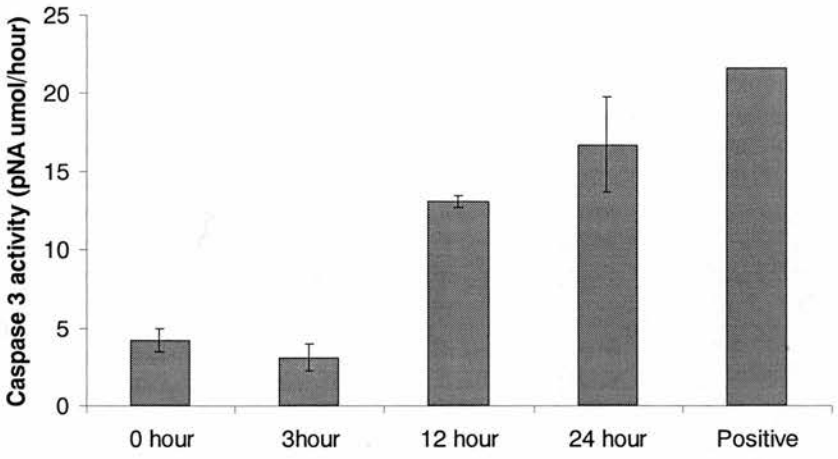

Figure 42, infection of microglia with SFV4 increased levels of active caspase 3. The level of caspase 3 activity was determined by assaying the cleavage of a caspase-specific substrate, with and without the presence of a caspase 3 inhibitor. Cleavage of the substrate by caspase 3 released the colourimetric compound pNA. The level of non-specific conversion undertaken in the presence of the caspase 3 inhibitor was subtracted to reveal the level of specific caspase 3 activity. Microglia were infected with SFV4 and sampled at 0, 3, 12 and 24 hours post infection. A culture of microglia exposed to staurosporin was included as a positive control. Error bars indicate ± SEM.

negative, the levels of this cytokine transcript were also determined by QPCR (Figure 40A). QPCR confirmed significant upregulation of both IL-1α and IL-1β indicating that the microarray correctly reported the increased expression of these two gene transcripts. QPCR analysis also revealed a significant increase in IL-6 transcripts, a finding not observed by the microarray. To confirm that expression of IL-6 resulted in de novo protein production, the tissue culture supernatant of the LPS stimulated microglia was assayed by ELISA and revealed significant IL-6 protein production (Figure 40B).

The level of upregulation on the array and on the QPCR platform was compared (Figure 40C). The fold increase in mean signal intensity for each microarray probe is shown along with the fold increase of transcripts as determined by the QPCR platform. This table shows that the fold increases estimated by the array platform were substantially lower than those estimated by the QPCR platform. For example, the array indicated an increase in IL-1α transcripts of 5 fold, whilst the QPCR platform determined this increase to be 149 fold.

QPCR validation of SFV infected microglia was also undertaken (Figure 41). The microarray results indicated a marginal increase in IL-6 transcripts at 12 hours post infection, whilst IFN-α levels were clearly increased at 12 hours. QPCR analysis confirmed this pattern of upregulation, and showed IFN-α to be also significantly upregulated at 24 hours. Furthermore, the magnitude of fold increase for IFN-α at 12 hours was substantially higher by QPCR than by array. Note that the level of housekeeping genes β-actin and GAPDH were unaffected by SFV infection.

To further investigate the effects of SFV infection on N9 microglia, levels of apoptosis were measured (figure 42). Cultures of N9 microglia were infected with SFV4 concurrent with those used for gene expression studies. At 3, 12 and 24 hours post infection; the cells and tissue culture supernatant were harvested, lysed and assayed for caspase 3 activity, a marker of late-stage apoptosis. At 3 hours no significant increase was seen in caspase 3 activity, by 12 hours a substantial increase in activity was observed that was maintained at 24 hours post infection. Levels of caspase 3 activity did not reach that observed in staurosporin treated (positive control) cultures of N9 cells.

4.7 Discussion

This chapter aimed to determine the ability of the custom microarray to detect gene transcripts and discern changes in transcript levels between control and test samples. An experiment was undertaken to determine whether the microarray could discern changes in transcript levels following stimulation with LPS, a potent stimulant of the innate immune system. This generated clear differences in a multitude of gene transcripts assayed by the

array platform. A QPCR technique was developed for selected genes to quantitatively determine transcript levels. The first part of this discussion examines the success of the microarray and QPCR platform to discern transcript changes, whilst the second half examines the biological meaning of the data.

4.7.1 The custom microarray can discern changes in gene transcripts

The microarray not only successfully characterised the transcript profile of resting N9 microglia but also was also able to discern changes in a multitude of transcripts following LPS stimulation. Selected changes were validated by QPCR. Array analysis indicated that following LPS stimulation, gene transcripts were both up and down-regulated, demonstrating that the array platform can detect both increases and decreases in transcript levels. The signal for individual probes demonstrated only a small variation between arrays hybridised to biological replicates, a consequence of both biological variation and error introduced by the experimental system and normalisation protocols. The small variation observed did not confound the ability of the platform to generate statistically significant results. The differences in probe signal intensities were subjected to Student's t-test and numerous probe sets were significantly altered when hybridised to LPS stimulated samples. However, the variation in probe signal between arrays may have been of sufficient magnitude to hide more subtle changes in gene transcript levels. This could be overcome by increasing replicate number to highlight trends in the changes of transcript levels.

The QPCR technique was developed for a panel of genes studied here and in later chapters. This technique was highly sensitive and accurately distinguished changes in transcript levels in a DNA template diluted from 1×10^{-2} to 1×10^{-10}. The technique was highly reproducible and generated only very marginal differences in cT values for replicates of the same DNA sample. The QPCR assay was also very specific and following PCR amplification lacked primer or other non-specific products.

The microarray demonstrated that LPS induced the upregulation of IL-1α and IL-1β in microglia, a finding validated by QPCR analysis. The degree of upregulation estimated by the array and QPCR platforms differed. In addition, the microarray did not report IL-6 expression following LPS stimulation, despite confirmation of IL-6 synthesis by QPCR and ELISA. It is perhaps inappropriate to directly compare the exact quantifiable nature of these two techniques since they are based on very different chemistries; hybridisation of DNA probes verses amplification-based technology. Nevertheless, QPCR was the more sensitive technique by several orders of magnitude as demonstrated by the dilution of DNA templates, and as shown by analysis of IL-6 levels (and TLR analysis in chapter 5). It is highly likely

that QPCR more accurately discerned basal levels of transcripts in resting microglia. Consequently, the degree of fold increase in stimulated cells was more substantial than that described by the microarray. Several gene transcripts were below the threshold of detection on the array in resting cultures, but upon LPS-induced upregulation became detectable. An example is MARCO; MARCO may well be expressed at low levels in resting N9 microglia but was not detected by the array. QPCR would better describe the basal levels of MARCO expression in unstimulated microglia.

The QPCR work did accurately validate the changes in expression of IL-6 and IFN-α 12 hours after SFV infection of microglia. Again the fold increase was underestimated by the array in the case of IFN-α, presumably because the starting signal on the array was high compared to the basal transcript level determined by the QPCR platform. The ability of the array to detect upregulated IL-6 transcripts in the case of SFV infected N9 cells but not in the case of LPS stimulated N9 cells is puzzling, but probably reflects the differing level of background that exists between microarray hybridisations. In summary, direct comparison of transcript levels reported by the microarray and QPCR platforms do not agree. Almost certainly, the QPCR values are the most accurate. The microarray can therefore distinguish up or down regulation, but the fold changes should not be relied upon. Further development to increase the sensitivity of the microarray platform would be a productive future strategy. The current system relies on a rather inefficient reverse transcription reaction that directly labels cDNA with Cy3 dye. This system results in the generation of many short cDNA strands and few full-length cDNA strands. There now exists a method that indirectly labels cDNA that is substantially more efficient and critically produces full-length cDNA. Conceivably, this labelling system may increase the sensitivity of the platform by; increasing the number of target labelled cDNA strands; reducing the number of non-specific small cDNA that represent the region proximal to the 3' of the mRNA; reducing the level of unincorporated Cy3 dye in the hybridisation mixture.

It was not possible to validate the upregulation of all transcripts identified by the array. To be definitively certain of all transcript levels required validation by QPCR and preferably quantification of protein levels in each case. Developing individual assays for each gene transcript/product would take considerable time and the feasibility of undertaking this analysis for each transcript was beyond the scope of this investigation. In addition, it has been assumed that altered levels of transcripts observed by either the array or QPCR leads to a respective change in protein levels and hence function. Whilst this is likely to be the case for the vast majority of transcripts, it cannot be guaranteed.

The detection of transcript levels in a population of unsynchronised cells does not imply all cells altered their transcript levels. For example, SOD-2 transcripts were marginally increased in SFV infected N9 microglia. Potentially infected cells could have down regulated SOD-2 whilst uninfected cells could have upregulated SOD-2 in response to the cytokine milieu. The overall change in transcript levels would not have reflected this diversity of expression. Indeed, it is impossible to determine the exact phenotype of each cell in culture using microarrays or QPCR. Methodologies such as immunocytochemistry would be necessary to further describe gene expression at the cellular level.

The microarray demonstrated that two housekeeping genes, GNAS and Pbp, were marginally down-regulated 12 hours post infection with SFV. These transcripts may be inappropriate for normalisation purposes in SFV infected N9 cells when used in isolation. The use of multiple housekeeping genes on the array for normalisation purposes likely negated the marginal decreases observed in these transcripts. This finding further underscores the necessity of using two or more housekeeping genes when normalising transcript levels.

4.7.2 Resting N9 microglia express a broad range of PPRs

Several gene transcripts not previously associated with microglia were shown to be constitutively expressed on N9 microglia in culture. These include two lectins. Clecsf 5 and 9, HM74, pgrp, SRCL and TLR 2, 4, 7 and 9. Lectins are sugar-binding proteins that can mediate both pathogen recognition and cell-cell interactions. Clecsf 5, also known as myeloid DAP-12-associated lectin (MDL)-1, is expressed in peripheral blood monocytes and macrophages and together with DAP-12 may signal to initiate an oxidative burst, cytokine production and induction of co-stimulatory molecules (Bakker et al., 1999). Clecsf 9, also known as mincle, is strongly induced in murine peritoneal macrophages in response to several inflammatory stimuli such as LPS and TNF-α and may play a role in the function of macrophages infiltrating sites of inflammation (Matsumoto et al., 1999). The upregulation of clecsf 5 and 9 reported here suggests these lectins may have similar functions in microglia. HM74, also known as PUMA-G in mice, is a novel chemokine receptor that is best known as a nicotinic receptor in adipose tissue. Its potential role in the CNS remains to be elucidated (Tunaru et al., 2003). Pgrp, also known as peptidoglycan recognition protein (PGRP)-S is a member of a family of pattern recognition molecules conserved from insects to mammals that bind to bacteria and their peptidoglycan components. Mice deficient in pgrp have increased susceptibility to intraperitoneal infection with some gram-positive bacteria and possess neutrophils that exhibit defective intracellular killing of pathogens (Dziarski et al., 2003; Dziarski, 2004). SRCL, also known as scavenger receptor with C-type lectin, is a

novel member of scavenger family expressed in the macrophage cell line J774A.1 and can bind gram-negative bacteria when transfected into CHO-K1 cells (Nakamura et al., 2001). In addition, TLR 2, 4, 7 and 9 have not been previously reported in N9 microglia. Together these results demonstrate that microglia express a wide variety of PRRs that have not been previously associated with these cells. In addition to these transcripts a variety of other PRRs were detected in resting N9 microglia that have previously been associated with microglia including; mannose receptor 1; scavenger receptor-AI (SR-AI), scavenger receptor-BI (SR-BI), triggering receptor expressed on myeloid cells (TREM)-2 and, CD14. These results suggest N9 microglia are able to detect the presence of a considerable range of pathogen-associated molecules and endogenous altered or oxidised proteins that require clearing. In addition, the expression of prostaglandin synthase 1 and 2 (also known as COX-1 and COX-2) suggests these cells have an innate capability to generate pro-inflammatory prostaglandins.

4.7.3 LPS stimulation and SFV infection invoked qualitatively and quantitatively different gene expression changes

Microarray analysis revealed that LPS stimulation and infection with SFV invoked qualitatively and quantitatively different changes in gene expression in N9 microglia. Importantly, these gene transcript changes appeared to be appropriate to the pathogen; LPS invoked substantial pro-inflammatory cytokine gene expression whilst SFV infection induced type-I IFN transcripts. Specifically, N9 microglia reacted to LPS with the upregulation of a several pro-inflammatory cytokines and chemokines. Were this to occur *in vivo* microglia would actively induce an inflammatory response in the brain and recruit blood-borne leukocytes. MIP-1α, MIP-1β and IP-10 are well characterised potent attractants of monocytes and other leukocytes. The proinflammatory cytokines TNF-α and IL-1α/β are known to activate leukocytes and are pro-active in the induction of immune responses. These cytokines are also actively neurotoxic and may contribute towards neuronal damage and death that can be observed during inflammatory responses of the brain (Kielian, 2004; Streit, 2002; Wang et al., 2004). Conversely, during SFV infection microglia exhibited a less pronounced pro-inflammatory response, with no increases seen in TNF-α, IL-1α, IL-1β and only a slight increase in IL-6 production. However, the expression of the anti-inflammatory cytokine TGF-β was reduced. TGF-β directs gene expression of activated microglia by primarily preventing the induction of chemokines and genes involved in cell migration (Paglinawan et al., 2003). The reduction of this cytokine suggests the threshold for induction of these genes was reduced. Indeed, these cells demonstrated large increases in chemokine

production. In addition, SFV infection induced large fold increases in the levels of both IFN-α and IFN-β, both of which exert powerful anti-viral effects in an auto- and paracrine fashion. Nos2, also known as iNOS, was also uniquely upregulated by SFV. This inducible gene product mediates the production of anti-microbial nitric oxide and whose expression is detectable in embryonic microglia, but is suppressed in microglia derived from the adult brain. This is unlike peripheral macrophages that readily synthesise NO following stimulation with a range of microbial products (Brannan and Roberts, 2004). Primary microglia derived from embryonic CNS cultures can increase iNOS expression following infection with another RNA virus, TMEV, or stimulation with LPS, peptidoglycan and CpG motifs (Olson and Miller, 2004). In light of these reports, careful validation of the microarray data will be required before N9 microglia can be considered active producers of NO upon SFV infection. If substantiated, the ability of N9 cells to upregulate iNOS suggests this cell line possessed a phenotype more analogous to embryonic microglia than adult microglia.

LPS stimulation increased the transcript levels of NCF1 (also known as p47phox). The NCF1 gene product activates the phagocyte NADPH oxidase system that generates superoxide anions, a precursor of microbicidal oxidants (Tsunawaki et al., 1996). Perhaps in response to the increased production of free radicals, N9 microglia upregulated several transcripts known to counteract the damaging actions of free radicals such as SOD-2 and catalase. SOD-2 acts to convert oxygen free radical to less reactive compounds (Zelko et al., 2002), whilst catalase plays a major role in cellular antioxidant defence by decomposing hydrogen peroxide and preventing the generation of the highly reactive hydroxyl radical (Ho et al., 2004). In addition several heat shock protein transcripts were increased, indicating LPS exposure or cellular responses to this compound are harmful to the cell. In comparison, at least by 24 hours, SFV infection did not upregulate these stress-associated gene transcripts, with exception of a marginal increase in SOD-2.

Infection by SFV uniquely initiated the upregulation of CD40. Expression of this molecule has previously been reported in microglia in two disease states: in inflammatory lesions of demyelination observed in multiple sclerosis and in activated microglia of Alzheimer's disease. Importantly, ablation of CD40L or pharmacological intervention ameliorates pathology or attenuates progression in models of both disease states (Howard et al., 1999; Tan et al., 2002). It has been suggested that interaction of CD40 on microglia with its ligands, expressed on CD4+ T-cells, may enhance inflammation through the production of cytokines, chemokines, prostaglandins and NO (D'Aversa et al., 2002; Jana et al., 2001; Okuno et al., 2004). The data here suggests SFV infection upregulated microglial CD40 and

as such may represent a new mechanism in which SFV infection induces inflammation by activated microglia.

Stimulation with LPS and infection with SFV altered the expression of several key scavenger receptors (SRs). SRs are defined by their ability to bind chemically modified low density lipoprotein but can also bind a variety of other ligands that are either poly-anionic or possess cross pleated β-sheets and can function as PRRs (Krieger and Stern, 2001; Franc et al., 1999). Reports suggest the expression of SR-AI is restricted to peripheral macrophages at sites of important immunosurveillance, such as the spleen. However, the receptor is expressed in microglia of the embryonic brain, and is lost as the brain develops (Honda et al., 1998; El Khoury et al., 1996). This receptor can recognise a variety of ligands such as modified lipoproteins, apoptotic cells and gram-negative bacteria (Husemann et al., 2002). Following LPS exposure SR-AI can induce the production of pro-inflammatory cytokines and acts to clear LPS *in vivo* (Hampton et al., 1991; Ashkenas et al., 1993). The upregulation of SR-A seen in the present study in N9 microglia agrees with previous work that characterised increased expression in primary rat microglia following LPS stimulation (Grewal et al., 1997). The upregulation of SR-AI during SFV infection is a novel finding and may represent a response to either direct SFV infection or the effect of SFV infection on neighbouring cells. The cytokine milieu of the infected tissue culture may well alert non-infected cells to the infection and stimulate upregulation of receptors that detect infection such as SR-AI. Alternatively, the level of caspase 3 activity was high following SFV infection, suggesting a large number of apoptotic cells were present. This may have driven upregulation of SR-AI that, among many functions, mediates the uptake of dying cells. Furthermore, PSR the receptor for phosphatidylserine (a lipid that is uniquely expressed on apoptotic cells) was also upregulated. This may reflect the extent of apoptosis that occurred in these cultures. Microglia are capable of recognising and engulfing apoptotic cells. Indeed, the phagocytosis of apoptotic lymphocytes makes microglia refractory to further pro-inflammatory cytokine release, if further stimulated with LPS (Magnus et al., 2002). Conceivably, the absence of pro-inflammatory cytokine release in these cultures; concurrent with substantial chemokine release, may partly be a product of the anti-inflammatory action of apoptotic cell engulfment.

SR-BI is expressed on macrophages and endothelia in cholesterol rich tissues and participates in reverse cholesterol transport to the liver (Hirano et al., 1999; Krieger, 1999). Like SR-AI, SR-BI appears to be developmentally regulated being expressed at high levels in the immature brain and at low levels in the adult brain (Husemann et al., 2001). The function of this receptor in the brain is yet to be fully elucidated however it has a putative

function in lipid metabolism and the clearance of apoptotic cells and denatured proteins (Husemann et al., 2002). SR-BI is down-regulated in macrophages following exposure to TNF-α, although there is no work reporting transcript levels in microglia (Buechler et al., 1999). The results here suggest that either the LPS stimulus or subsequent TNF-α production acts to down-regulate this receptor in N9 microglia. However, since SR-BI down-regulation occurred during SFV infection in the absence of LPS or significant TNF-α production, molecules other than these two can modulate its expression. In addition, the expression of both SR-AI and SR-BI in resting cultures of N9 microglia further highlights the likely embryonic origin and phenotype of this cell line.

CD36 is another SR related to SR-BI that is expressed in both macrophages and vascular endothelium (Febbraio et al., 2001). CD36 protein is expressed in human microglia *in vivo* and on N9 microglia. This receptor has the capacity to recognise β-amyloid and initiate the production of reactive oxygen species, and may play role in the pathogenesis of Alzheimer's disease (Coraci et al., 2002; El Khoury et al., 2003). The finding that CD36 is highly upregulated in N9 microglia 24 hours post infection with SFV is a novel finding, although the exact functional significance of this is not clear due to the scarcity of reports on the innate immune functions of CD36 (Husemann et al., 2002).

MARCO, also known as macrophage receptor with collagenous structure, is a scavenger receptor expressed in a limited sub-set of macrophages and in granulocyte-macrophage-colony stimulating factor (GM-CSF)-treated microglia. LPS stimulation can induce MARCO expression in most other macrophage populations and dendritic cells (van der Laan et al., 1999; Palecanda et al., 1999). The results here suggest N9 microglia also dramatically upregulate this receptor upon LPS exposure. This receptor can bind both gram-positive and negative bacteria but not yeast, and its expression correlates with profound changes in actin-cytoskeleton organisation and decrease in antigen uptake in dendritic cells and microglia (Granucci et al., 2003).

TREM-2 is expressed on monocyte-derived dendritic cells and upon activation dramatically increases the expression of molecules associated with antigen presentation to T-cells (Bouchon et al., 2001). Whilst TREM-2 expression is lacking on monocytes and macrophages, the receptor was among the few mRNAs identified as being expressed by resting microglia and down regulated by LPS. Thus, TREM-2 is considered a marker of resting microglia *in vivo*, and brain regions with incomplete blood-brain barrier exhibit reduced expression. Indeed, regional variations in TREM-2 CNS expression may contribute to the varying sensitivities of different brain regions to pathogenic signals (Schmid et al., 2002). The work here confirms that TREM-2 down-regulation occurs in N9 microglia

following LPS stimulation and following SFV infection. Further work would be required to determine if concurrent changes in co-stimulatory molecules occurs. In addition, the expression of TREM-2 in resting N9 cultures further underscores their phenotype as a resting microglial cell line.

The upregulation of TLR 2 and 3 during SFV infection suggests that these two receptors may function to recognise virus infection in N9 microglia. However, the sensitivity of the microarray precluded any substantial analysis of TLR expression. The analysis of these transcripts by the more sensitive QPCR technique would provide a more comprehensive description of expression levels during SFV infection.

4.7.4 Summary

This chapter has successfully proven the ability of the microarray to assay key gene transcripts of interest in cultured N9 microglia and discern changes in gene transcript levels. The microarray has comprehensively described the expression of a multitude of genes involved in innate immune responses of cultured N9 microglia, several of which have not been previously associated with this cell type. This work has demonstrated N9 microglia express a broad range of PRRs that were differentially modulated upon stimulation with LPS or infection with SFV. The expression of many of these receptors suggested N9 microglia possessed an embryonic (i.e. SR-AI), unactivated (i.e. TREM-2) phenotype, which suggests they are functionally equivalent to microglia found in the developing brain. In addition, key differences in the form of innate immune response generated by N9 microglia in response to LPS stimulation verses SFV infection was observed. LPS stimulation generated a substantial pro-inflammatory response with the induction of several stress-associated genes, whilst SFV infection induced substantial increases in type-I interferons and chemokines. The feasibility of utilising this microarray platform for the characterisation of further innate immune responses is substantial and includes characterising the responses of; primary microglia to SFV infection; microglia to amyloid fibrils formed by either PrP^{Sc} or β-amyloid; and astrocytes to LPS or SFV infection.

Chapter 5. In response to LPS and virus infection, neural cells dynamically and differentially regulate toll-like receptor gene expression

Contents

5.1 Introduction

Toll-like receptors (TLR) are an expanding family of receptors that recognise unique molecular patterns characteristic of different types of pathogen. A growing consensus suggests they are key to the initiation of innate immune responses (Akira and Takeda, 2004). Thirteen TLR are now recognised. These are predominantly expressed on cell types likely to be the first to encounter antigen such as phagocytic cells. TLR 1 to 9 are expressed in both mice and humans. TLR 10 is present in mice only as a degenerate pseudogene. TLR 11, 12 and 13 are expressed in mice but lack human orthologs (Medzhitov et al., 1997; Rock et al., 1998; Takeuchi et al., 1999b; Chuang and Ulevitch, 2000; Chuang and Ulevitch, 2001; Du et al., 2000; Tabeta et al., 2004). All TLR share a similar structure with extracellular leucine rich repeat (LRR) motifs and an intracellular Toll/IL-1 receptor domain. TLR 1, 2, 4, 5 and 6 appear to recognise the repeating patterns on the structural components of pathogens, principally bacteria. TLR 2 is known to be involved in the recognition of bacterial peptidoglycan, fungal components and viral glycoproteins (Takeuchi et al., 1999a; Underhill et al., 1999a; Bieback et al., 2002). TLR 4 is involved in the recognition of lipopolysacharide (LPS) and viral envelope proteins (Poltorak et al., 1998; Rassa et al., 2002). TLR 5 can recognise bacterial flagellin (Hayashi et al., 2001) whilst TLR 11 is involved in the recognition of uropathogenic bacteria (Zhang et al., 2004). TLR 1, 2 and 6 appear to act together to discriminate between bacterial lipoproteins (Takeuchi et al., 2001; Wyllie et al., 2000). Pathogen nucleic acids are also recognised by several TLR. In contrast to TLR that recognise structural components these TLR have also been observed in intracellular compartments (Matsumoto et al., 2003). TLR 3 can recognise dsRNA (Alexopoulou et al., 2001), TLR 7 and 8 can recognise ssRNA (Heil et al., 2004; Diebold et al., 2004) and TLR 9 is involved in the recognition of CpG motifs present in bacterial and viral DNA (Hemmi et al., 2000; Tabeta et al., 2004).

There is little information on TLR expression and function in CNS cells. In response to a variety of pathogens both microglia and astrocytes can undergo hypertrophy and hyperplasia and express cytokines. Astrocytes can initiate the production of complement proteins and microglia can become active phagocytes, capable of producing many of the same anti-microbial molecules as activated macrophages and capable of activating T cells (Mack et al., 2003; Olson and Miller, 2004), but it remains unclear how this early glial cell response is activated. The putative expression of TLR on glial cells may provide one mechanism by which these specialised cells are stimulated. Previous work has shown cultured primary microglia from SJL/J mice were shown to express TLR 1 to 9 (Olson and Miller, 2004)

whilst a more limited study demonstrated primary cultures of astrocytes from Balb/c mice express TLR 2, 4, 5 and 9. TLR levels in neurones have not been investigated.

Virus-like particle (VLPs) are infectious agents that upon entry to a cell can initiate genomic replication, but lack structural genes necessary to form nascent mature virus. Since VLPs cannot produce mature virus they cannot spread from cell-to-cell. As with the virus, VLPs can fuse with the plasma membrane and initiate viral genome replication and synthesis of sub genomic RNA; however, VLPs cannot express structural proteins and replicated viral RNA remains unpackaged in the cytoplasm.

The previous two chapters successfully explored the expression patterns of several key genes involved in innate immune responses in N9 microglia following LPS stimulation and SFV infection. However, the microarray was unable to adequately assay TLR expression. This study has examined TLR expression using quantitative real time PCR developed in chapter 4. Cultures of microglia, astrocyte and neuroblastoma cells were analysed to determine constitutive levels of TLR transcripts and their differential regulation according to the microbial stimulus.

5.2 Objectives

To determine TLR expression in microglia, astrocyte and neurones

To describe TLR expression changes in response to

- LPS stimulation
- SFV infection

To describe cytokine and type-I interferon expression in response to LPS and SFV

To describe levels apoptosis of CNS cells in response to SFV

5.3 Absolute levels of transcripts were assayed by determining copies of DNA molecules in DNA standards

The level of TLR expression in cultured cells was determined by QPCR using DNA standards. To assay the absolute level of TLR transcript it was necessary to determine the absolute amount of DNA copies in the standards. The DNA standards constituted PCR products amplified by outer primers that encompassed the region amplified by the inner primers. To effectively assay the amount of each standard, samples were diluted 4-fold in water and were analysed on an Agilent Bioanalyser (see methods section for more details). The amount of DNA copies for each standard was then calculated (Table 7). In contrast, absolute value of SFV RNA was calculated by using a plasmid that contained the SFV gene assayed (the structural gene E1). The plasmid had been previously amplified in bacteria and

quantified by optical density. Subsequently, each QPCR experiment assayed absolute levels of transcripts by correlating amplification levels of DNA standards with copy number.

5.4 CNS cells express a broad repertoire of TLR at rest

RNA was prepared from N9 microglia, differentiated primary astrocyte cultures and N2a neuroblastoma cells. At the time of sampling the microglia had been cultured for 48 hours and had a semi-amoeboid morphology with occasional processes. The primary astrocyte cultures were grown from neonatal brains. Fibroblasts, microglia and oligodendrocytes were excluded or removed from the cultures. The cultures were differentiated with dibutyryl cyclic adenosine monophosphate (dbcAMP) and the cells exhibited a mature phenotype analogous to the type 1 astrocytes found in adult brain (Raff et al., 1983) (Figure 43). The cultures lacked microglial or myeloid contaminants as determined by glial fibrillary acidic protein (GFAP) and CD11b staining (>99% cells were GFAP positive). Cells of the N2a neuroblastoma cells were grown for 48 hours by which time the majority of cells possessed multiple, short processes as previously described (Shea and Beermann, 1994). Analysis of resting microglia revealed the presence of TLR 1, 2, 3, 4, 6, 7, 8 and 9 (Figure 44A). TLR 2 transcripts were most abundant, followed by TLR 4 and TLR 7. TLR 1, 3, 6 and 9 were expressed at moderate levels, whilst TLR 8 was expressed at very low but reproducibly detectable levels. TLR 5 was not detected. Analysis of astrocytes demonstrated overall TLR transcript expression at a level comparable to the microglia cells (Figure 44B). TLR 7 had the highest expression, with TLR 2, 3, 8 and 9 also expressed at high levels. TLR 1, 4, 5 and 6 were expressed at low but detectable levels. N2a cells expressed TLR 3 transcripts at a level comparable to microglia but TLR 1, 2, 4 and 6 transcripts were at levels considerable below those described in either of the glial cultures and transcripts for TLR 5, 7, 8 and 9 could not be detected (Figure 44C).

5.5 CNS cells differentially regulate TLR expression upon stimulation with LPS or infection with SFV

N9 microglia were grown for 48 hours and then exposed to LPS for 0, 3, 6 or 12 hours. Within 3 hours the cells increased their levels of TNF-α and IL-6 transcripts; in the case of IL-6 by 190 fold, demonstrating their ability to be activated by this microbial component (Figure 45). TLR 4 is well known to be involved in LPS recognition (Poltorak et al., 1998). Given that N9 microglial cells express TLR 4 (Figure 44A), activation could be occurring via this pathway. As expected, LPS exposure did not induce high levels of IFN-α transcripts. LPS activation of N9 cells resulted within 3 hours in 3-fold increased expression of TLR 2,

PCR product	Size (bp)	Avergae Mass	Molecular weight (Daltons)	Daltons per mole	Copies /ul
TLR1	436	4.08E-08	2.878E+05	2.878E+05	8.54E+10
TLR2	211	2.93E-08	1.393E+05	1.393E+05	1.27E+11
TLR3	849	4.04E-08	5.603E+05	5.603E+05	4.34E+10
TLR4	393	3.15E-08	2.594E+05	2.594E+05	7.31E+10
TLR5	535	1.77E-08	3.531E+05	3.531E+05	3.02E+10
TLR6	262	2.18E-08	1.729E+05	1.729E+05	7.58E+10
TLR7	844	7.67E-08	5.570E+05	5.570E+05	8.29E+10
TLR8	269	1.01E-08	1.775E+05	1.775E+05	3.41E+10
TLR9	423	7.97E-08	2.792E+05	2.792E+05	1.72E+11
B-actin	278	7.04E-08	1.835E+05	1.835E+05	2.31E+11
IFN alpha	382	1.82E-08	2.521E+05	2.521E+05	4.35E+10
IL-1 alpha	419	5.60E-09	2.765E+05	2.765E+05	1.22E+10
IL-1 beta	409	1.22E-08	2.699E+05	2.699E+05	2.72E+10
CathespinD	389	3.80E-09	2.567E+05	2.567E+05	8.91E+09
C1q alpha	378	2.40E-09	2.495E+05	2.495E+05	5.79E+09
TNF alpha	365	8.00E-09	2.409E+05	2.409E+05	2.00E+10

Table 7, the absolute amount of DNA in undiluted standard was calculated as detailed in methods section.

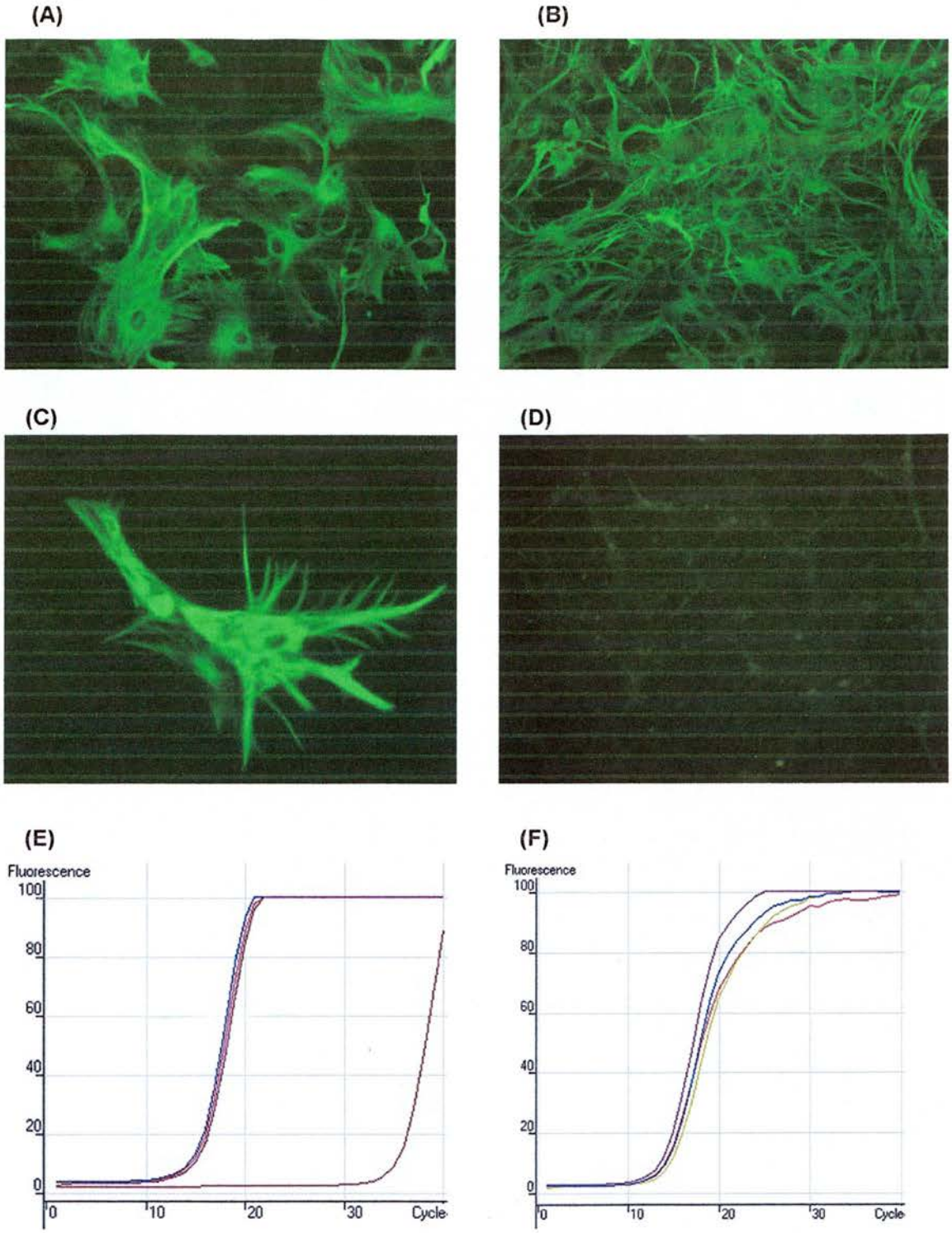

Figure 43, primary astrocytes were positive for GFAP and lacked myeloid contaminants. (A,B,C) Representative pictures of astrocyte cultures stained for GFAP. (D) Representative picture of astrocyte culture stained for CD11b. (E) QPCR of resting astrocyte cultures for GFAP transcripts.Included is a QPCR negative control that amplified at a high cycle number. (F) QPCR of resting astrocyte cultures for β-actin transcripts. Note that the level of GFAP transcripts was comparable to that of β-actin transcripts.

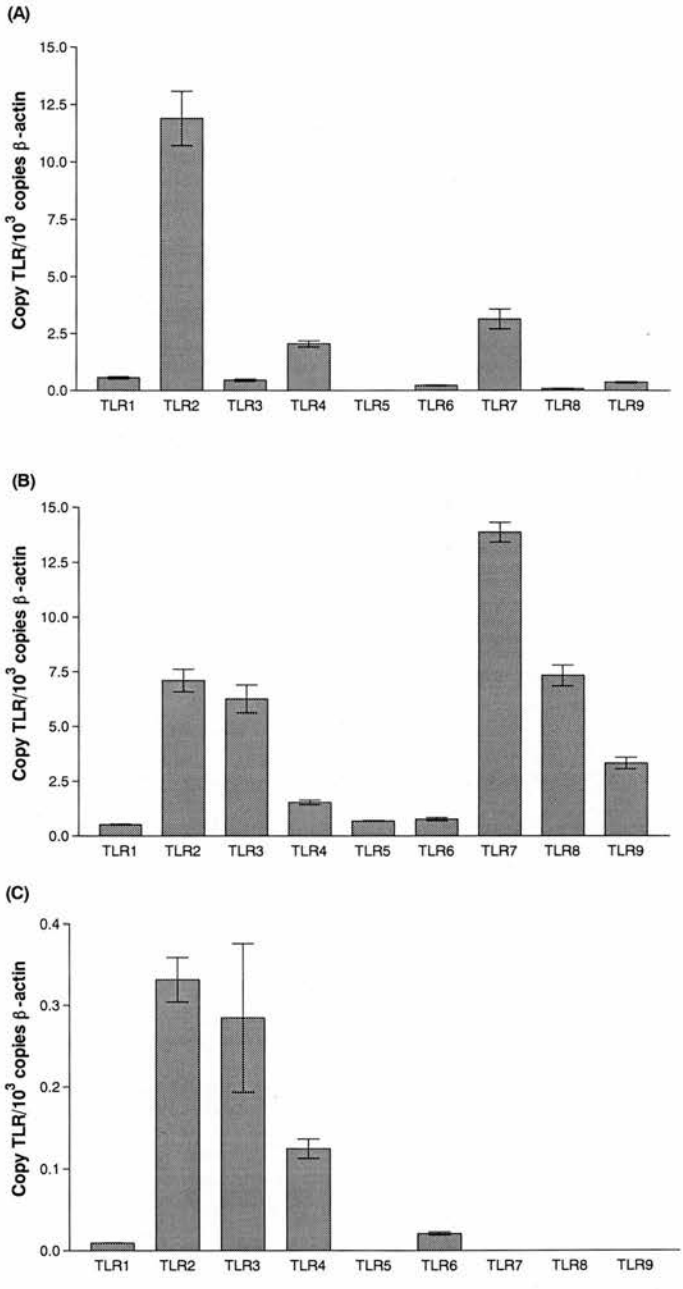

Figure 44, glial cells and neurones express TLR. Copy numbers of β - actin and TLR 1 to 9 were determined using quantitative RT-PCR and expressed as copies per 1,000 copies β-actin. (A) N9 microglia grown for 48 hours until semi-confluent. (B) Expression in cultures of primary astrocytes, 3 weeks post-creation. (C) Expression in cultures of N2a neuroblastoma cells grown for 48 hours until semi-confluent. The bars are mean of 4 replicate samples. The error bars are ± SEM.

whilst TLR 3 was also upregulated, though more slowly. In contrast, all other TLR were either unaffected or even down-regulated. TLR 8 exhibited the most profound decrease whilst TLR 4 and 7 were also consistently down-regulated in a consistent manner. Astrocyte cultures exhibited more pronounced changes in TLR expression in response to LPS (Figure 46). In common with microglia, TLR 2 and 3 exhibited the largest increases, whilst sizeable decreases were observed for other TLRs. In contrast to microglia, astrocytes upregulated TLR 1 and down-regulated TLR 5. Neuroblastoma cells showed no change in TLR expression upon LPS stimulation (Table 8). In addition, astrocytes down-regulated transcripts of GFAP four-fold. Neuroblastoma cells showed no change in TLR expression upon LPS stimulation.

5.6 SFV infection of CNS cells triggered substantial changes in TLR transcripts

To determine whether neural cells support SFV replication in culture, cultures were infected with virus and levels of virus RNA determined over time by QPCR (Figure 47). The MOI used was low and is analogous to virus infection *in vivo* in which few cells within a given population are infected. Infection of mice with virulent strains of SFV results in infection of neurones and glial cells to a higher degree than avirulent strains. (Fazakerley et al., 1993; Smyth et al., 1990; Balluz et al., 1993). To ensure efficient infection in the present study, cells were infected with the virulent SFV 4 strain. The virus was able to replicate and induce caspase 3 activity, indicative of late stage apoptosis, in all three types of culture (Figure 47). In contrast to LPS, virus infection microglia resulted in a large increase in IFN-α transcripts. Virus infection also dramatically altered TLR expression profiles with strong upregulation of several TLR. The largest increase was observed with TLR 3 but TLR 8 and 9 also demonstrated high fold increases (Figure 48A). However, TLR 8 upregulation was from a very low basal level (Figure 43A). TLR 4 was significantly and consistently down-regulated. Furthermore, in contrast to LPS stimulation, pro-inflammatory cytokines IL-6 and TNF-α were only marginally increased by 12 hours. Infection of astrocyte cultures resulted in high levels of viral RNA molecules; an order of magnitude higher than in microglia (Figure 47). Interestingly, the microglia had a stronger IFN-α response than the astrocytes (Figures 48A and 48B). More efficient IFN-α production in microglial cells than astrocytes could have reduced virus replication in microglial cells relative to astrocytes. In astrocytes, TLR 3 and TLR 9 upregulation was not as great as that observed in microglial cells, although TLR 2 upregulation was greater. Unlike microglia infection, astrocytes dramatically down-regulated most other TLR transcripts (Figure 48B).

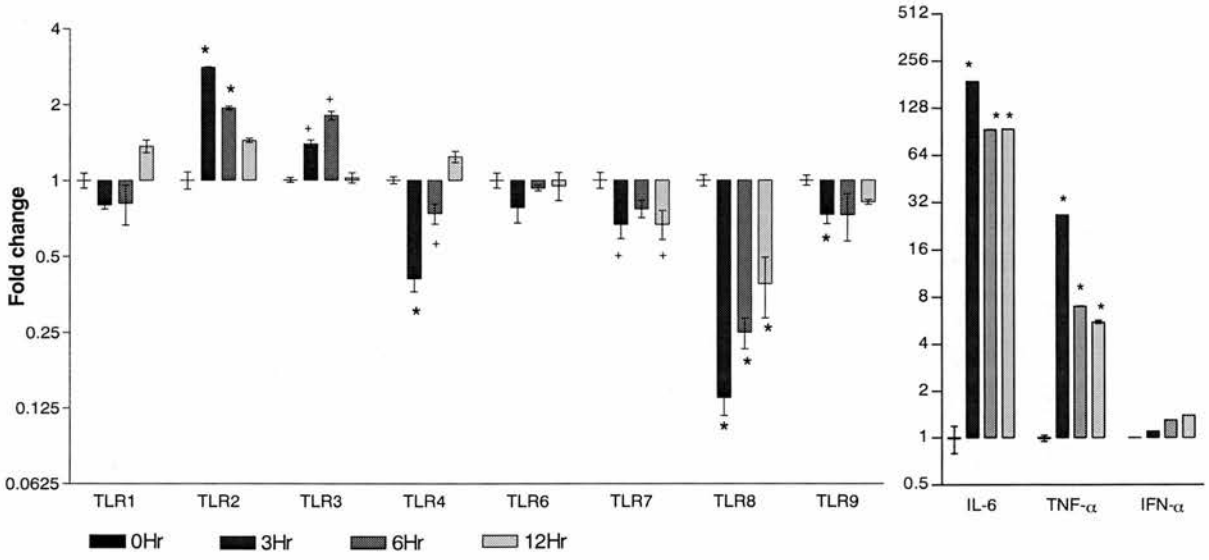

Figure 45, TLR transcripts were dynamically regulated by microglia in response to stimulation with LPS. N9 cells were stimulated with LPS for 3, 6 and 12 hours and transcript levels expressed relative to unstimulated cells. cDNA levels were normalised relative to . -actin. Bars show the mean of 4 replicates ± SEM. Marked bars are statistically different from the respective 0 hour time-point (Student's t-test; +p<0.05 *p<0.01, n=4)..

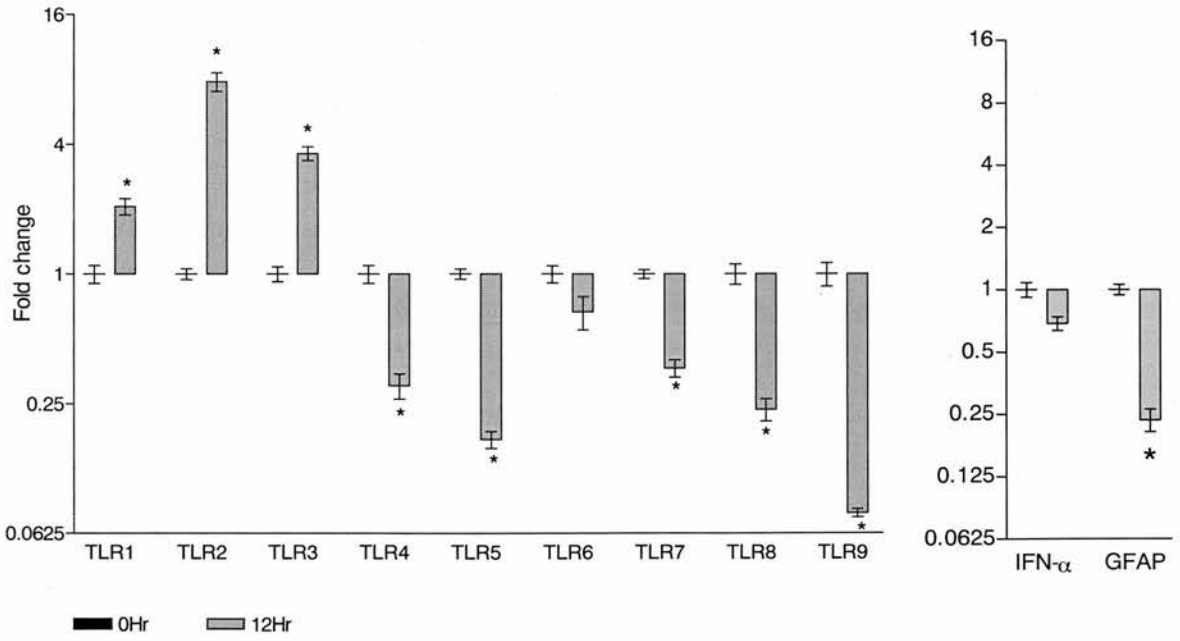

Figure 46, TLR transcripts were dynamically regulated by astrocytes in response to stimulation with LPS. Astrocytes were stimulated with LPS for 12 hours and transcript levels expressed relative to unstimulated cells. cDNA levels were normalised relative to . -actin. Bars show the mean of 5 replicates ± SEM. Marked bars are statistically different from the respective 0 hour time-point (Student's t-test; +p<0.05 *p<0.01, n=5).

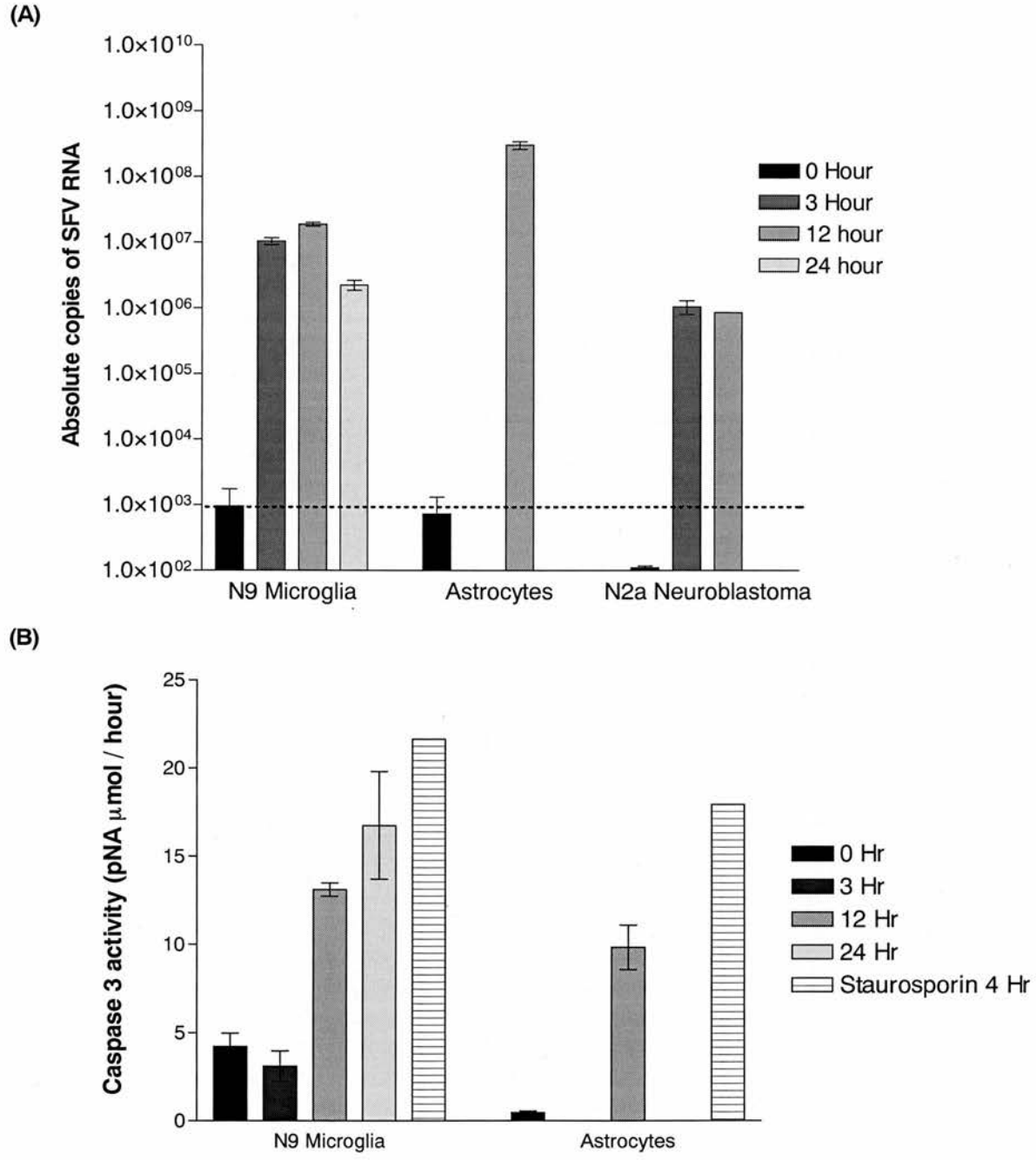

Figure 47, SFV replicates in cultured CNS cells and induces caspase 3 activity. (A) SFV RNA copies were determined by QPCR. Notice that astrocytes were only sampled at 0 and 12 hours whilst neuroblastoma cells were sampled at 0, 3 and 12 hours only. Bars show the mean of 3 replicates ± SEM. Dotted line indicates the level of detection of this assay. (B) Caspase 3 activity was determined in cultures of microglia and astrocytes following SFV infection. For a positive control, cells were treated with staurosporin for 4 hours to induce apoptosis. Note astrocytes were only sampled at 0 and 12 hours following SFV infection. Caspase activity was not measured in neuroblastoma cells following SFV infection. Bars show the mean of 3 replicates ± SEM.

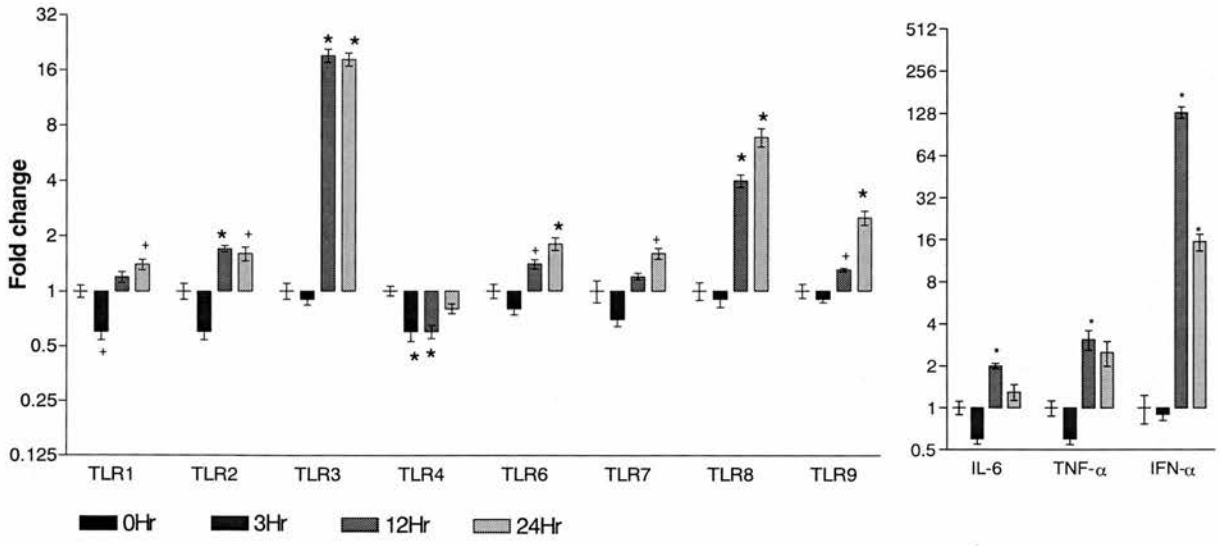

Figure 48A, TLR transcripts were dynamically regulated by microglia in response to infection with SFV. N9 cells were infected with SFV4 (MOI = 0.1) and gene expression assayed at 3, 12 and 24 hours post-infection and expressed relative to uninfected cells. cDNA levels were normalised relative to . -actin. Bars show the mean of 4 replicates ± SEM. Marked bars are statistically different from the respective 0 hour time-point (Student's t-test; +p<0.05 *p<0.01, n=4).

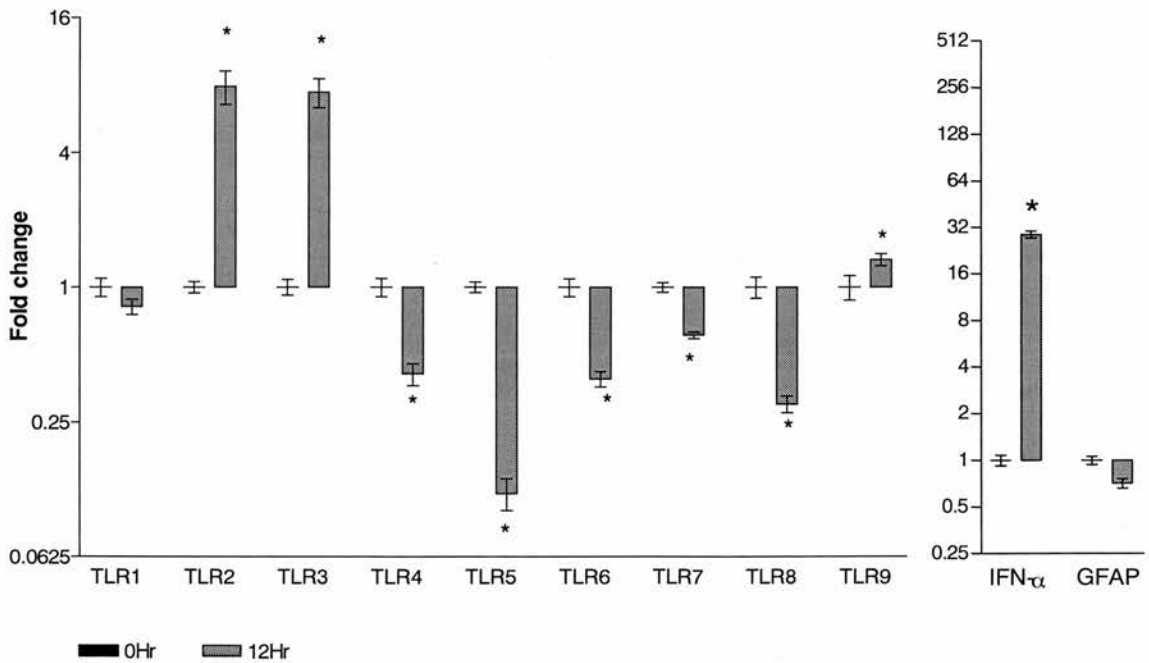

Figure 48B, TLR transcripts were dynamically regulated by astrocytes in response to infection with SFV. Astrocytes were infected with SFV4 and gene expression assayed at 12 hours post-infection and expressed relative to uninfected cells. Bars show the mean of 5 replicates ± SEM. Marked bars are statistically different from the respective 0 hour time-point (Student's t-test; *p<0.05, n=5).

As with LPS stimulation, the neuroblastoma cell line did not alter TLR expression despite active viral replication as determined by high levels of viral RNA (Figure 47). IFN-α expression could not be detected in these cells at 0, 3, 6 or 12 hours post-infection.

A summary of TLR, IFN-α and SFV transcript levels is given in table 8.

5.7 Infection of microglia with virus-like particles caused TLR 3 upregulation

Infection of microglia with SFV was further dissected by infection with virus-like particles (VLPs). VLPs attach to and enter host cells and replicate virus RNA exactly as for virus; however, replacement of structural genes with eGFP precludes the production of mature virus and labels infected cells with eGFP. eGFP is highly expressed upon infection in a variety of cells and in the CNS upon inoculation (personal communication-Audrey Graham). VLPs used here were based on the SFV 4 strain and were synthesised by Audrey Graham, Centre for Infectious Disease, University of Edinburgh, UK. This system was used to determine whether attachment, entry and viral RNA replication were sufficient to induce TLR 3 upregulation. Microglia were infected with VLPs (1% cells infected as measured by eGFP expression) and TLR 3 transcripts measured. Transcripts were significantly upregulated by 24 hours infection (Figure 49).

	LPS					SFV		
	N9	**N9**	**Astrocyte**	**N2a**		**N9**	**Astrocyte**	**N2a**
	3 Hr	12 Hr	12 Hr	12 Hr		12 Hr	12 Hr	12 Hr
TLR1	0.80	1.37	2.1*	1.00		1.20	0.82*	1.00
TLR2	2.80*	1.44*	7.8*	1.00		1.7*	7.92*	1.00
TLR3	1.39*	1.02	3.6*	1.00		19.2*	7.46*	1.00
TLR4	0.41*	1.24	0.3*	1.00		0.59*	0.41*	1.00
TLR5	ND	ND	0.17*	ND		9.6*	0.12*	ND
TLR6	0.78	0.95	0.66*	1.00		1.4*	0.39*	1.00
TLR7	0.67*	0.67*	0.36*	ND		1.20	0.61*	ND
TLR8	0.14*	0.39*	0.23*	ND		4.0*	0.30*	ND
TLR9	0.732	0.82	0.08*	ND		1.3*	1.33	ND
IFN-α	1.01	1.05	0.70	ND		130*	28.7*	**ND**
SFV	NA	NA	NA	NA		$1.87x10^{07}$	$2.97x10^{08}$	$8.47x10^{05}$

Table 8, mean (n=4) fold changes of TLR, IFN-α, and absolute copies of SFV transcripts 3 or 12 hours post stimulation with LPS or post infection with SFV. Values a re normalised to β-actin. Levels significantly different from controls are marked with an asterisk (Student's t-test; $p < 0.05$). SFV RNA values are given as absolute levels rather than fold increases, otherwise values are relative to 0 hour time point. ND=Not detected, NA=Not applicable.

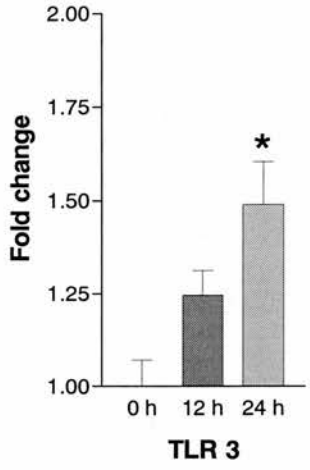

Figure 49, infection of microglia with virus like particles upregulated TLR 3. Virus like particles are infectious agents that upon entry to a cell can initiate genomic replication, but lack structural components that enable the production of mature virus and spread from cell-to-cell. N9 microglia were infected with a low MOI (MOI=0.1) and TLR 3 transcripts assyed at 0, 12 and 24 hours post infection. Bars represent mean of five cultures ± SEM. Bars marked with an asterisk are significantly different from 0 hour time point (Student's t-test, $p<0.05$).

5.8 Discussion

5.8.1 Expression of TLR on glia indicates they can recognise a multitude of microbial components

This thesis reports the first systematic comparison of TLR gene expression in cultured neural cells. The finding that cells of the CNS have the ability via TLR expression to detect infection and discern its type provides an important contribution to understanding pathological processes of this tissue. Parenchymal microglia populate the CNS during embryogenesis and are not derived from circulating monocytes (Streit, 2002; Hickey and Kimura, 1988; Ford et al., 1995). They have a multitude of roles involved in neuronal support and they function to synergise immune responses once initiated. Two previous reports have documented extensive expression of TLR transcripts in cultured human microglia (Bsibsi et al., 2002), and in primary cultures of murine microglia (Olson and Miller, 2004). The present quantitative study reveals that TLR 2 is the most highly expressed TLR on N9 microglia. TLR 2 is also high expressed on circulating human monocytes (Hornung et al., 2002), which underscores the phenotypic similarity of microglia to blood-borne myeloid cells despite their differing lineages. Astrocytes predominantly function as support cells for neurones but also have a documented role in immune function *in vitro*, being able to react to several prototypic microbial components such as LPS and CpG motifs (Lieberman et al., 1989; Schluesener et al., 2001). This study demonstrates that primary cultures of astrocytes express levels of TLR comparable to the immortalised N9 microglial cell line, suggesting that astrocytes are well endowed with the ability to detect a variety of pathogens. Unlike microglia, astrocytes express high levels of TLR 3, 7, 8 and 9; a TLR subfamily well known to recognise microbial nucleic acids (Kadowaki et al., 2001c; Hornung et al., 2002). Astrocytes were of embryonic origin and were cultured for several weeks *in vitro* that included maturation with dbcAMP. This compound is known to increase GFAP expression in primary astrocytes and generates cells with a more mature phenotype that is representative of adult astrocyte populations (Murphy, Jr. et al., 1993). The effect dbcAMP treatment had on TLR expression was not explored. Conceivably dbcAMP treatment could modulate TLR expression and may explain why a previous study, which used embryonic astrocytes, failed to detect TLR 7, 8 and 9 in astrocytes (Carpentier et al., 2005). N2a neuroblastoma cells expressed TLR 1, 2, 3, 4 and 6, albeit at low levels and it was notable that TLR 3 expression was comparable to that observed in microglial cells. This expression may indicate that neurones are able to recognise some forms of infection, perhaps particularly viral dsRNA via TLR 3. The ability of both microglia and astrocytes to express

all nine TLR assayed suggests they are capable of recognising a vast array of microbial associated molecules, *a strategy that may be an essential requirement for a tissue mostly devoid of recognisable immune processes.*

Microglia are the principal phagocyte of the CNS and have the potential to release large amounts of inflammatory mediators, whilst astrocytes appear primarily to act as support cells for neurones. TLR expression by these cell types may function to induce an inflammatory reaction upon infection. However, TLR expression on astrocytes may be a later event requiring activation by other processes in this regard. TLR expression by microglia may initiate responses whereas TLR expression by activated astrocytes may function to perpetuate or amplifying them. Another possibility is that TLR expression allows activation of astrocytes to augment their neuroprotective functions. In this scenario astrocyte TLR primarily acts to protect neurones rather than initiate immune responses.

5.8.2 TLR transcripts are differentially modulated on glia in a manner appropriate to the innate immune stimuli

5.8.2.1 Response of glia to LPS stimulation

The level of TLR expression affects macrophage responses to microbial stimuli. Macrophage responses have been correlated with levels TLR expression. TLR 4 ligands appear to induce an early TNF-α response, whilst TLR 2 ligands generate a later TNF-α response. These responses correlate with the timing of TLR expression; TLR 4 ligands induce a response until TLR 4 has become down-regulated; whilst TLR 2 ligands only induce cytokine release once TLR 2 is upregulated (Weiss et al., 2004). Furthermore, monocyte-derived dendritic cells induced to upregulate TLR 7 expression have increased sensitivity to the TLR 7 ligand imiquimod (Mohty et al., 2003). Together these data suggest that TLR expression change can have dramatic effect on the responsiveness of macrophages to microbial stimuli.

Stimulation of microglia with LPS upregulated TLR 2. This parallels the increase in TLR 2 observed following exposure of microglia to *Staphylococcus aureus* (Kielian et al., 2002). . LPS down-regulated several TLR including TLR 4. This has also been reported for murine LPS-stimulated macrophages *in vitro* (Nomura et al., 2000), and may represent a mechanism to prevent over stimulation of innate immune responses. Indeed, LPS exposure is known to sensitises the rat brain to ischaemic injury (Eklind et al., 2001), whilst work investigating LPS-induced injury of oligodendrocytes in mice has documented a pro-active role for TLR4 expressing microglia (Lehnardt et al., 2002; Lehnardt et al., 2003). Circulating LPS is the major cause of sepsis and initiates a systemic release of pro-inflammatory cytokines that can

lead to organ failure and death (Beutler, 2002). LPS-stimulated macrophages become tolerant to further LPS exposure and fail to express additional pro-inflammatory cytokine. This phenomena is known as endotoxin tolerance and represents a mechanism by which the host attempts to protect itself from endotoxin shock. This partly occurs through down-regulation of TLR 4 and adaptor molecules that signal from this receptor, such as IRAK and MyD88 (Fan and Cook, 2004). The present study suggests a similar mechanism may occur in glial cells to limit damaging pro-inflammatory responses in response to LPS.

However, a recent report has suggested primary microglia derived from SJL/J mice react differently to LPS (Olson and Miller, 2004). This study stimulated microglia with a dose of LPS 50-fold higher than that used here and transcript levels were measured 24 hours post stimulation. In agreement with the present study, TLR 2 and 3 were upregulated. In contrast, the study also reported upregulation of type-I interferons and TLR 4, 6, 8 and 9 with no TLR transcripts down-regulated. These conflicting results can almost certainly be explained due to differences in experimental conditions and sampling times. The present study has shown transcript levels fluctuate overtime following LPS stimulation and that the time of analysis is critical. The Olson and Miller study recorded TLR transcripts levels at 24 hours only, whilst the present study reports transcript levels at 3, 6 and 12 hours (since some TLR trasmcripts returned to base line by 18 hours, data not shown). In addition, the Olson and Miller report is not directly comparable to the present study since N9 microglia represent a cell line derived from CD1 mice whilst the Olson and Miller study utilised primary cultures from embryonic SJL/J mice. Differing strains of mice are well-known to respond differently to microbial stimulus and immune responses between strains cannot be directly compared (Smyth et al., 1990; Tabeta et al., 2004). In addition, whereas LPS is known to induce type-I IFN synthesis *in vitro*, a comprehensive study has also demonstrated that activation of IRF3 (necessary for type-I IFN transcription) is more potent and rapid through dsRNA/TLR 3 signalling than that triggered through LPS/TLR 4 signalling, and it is likely that LPS-induced IFN-β synthesis in the present study was too little and too late to trigger a detectable increase in IFN-α transcripts at the time points investigated.

The intermediate filament protein GFAP is a specific marker of astrocytes, is important in modulating astrocyte motility and shape by providing structural stability to astrocytic processes (Eng et al., 2000) and is upregulated during maturation with dbcAMP. In agreement with previous data (Letournel-Boulland et al., 1994), astrocytes down-regulated GFAP in response to LPS. Housekeeping genes β-actin and GAPDH were unaffected. These cultures had been aged and differentiated *in vitro* and were likely to be highly activated. LPS stimulation upregulated TLR 2 and 3 but down-regulated all other TLR. This is in

comparison to embryonic cultures of undifferentiated astrocytes that demonstrate upregulation of TLR 2, 4, 5 and 9 (Bowman et al., 2003). Note that the Bowman *et al.* study utilised end-product PCR analysis on agarose gels, a less sensitive, accurate and quantitative technique than used here. In addition, the strain from which the astrocyte culture was derived may have had some impact on these divergent results.

5.8.2.2 Response of glia to infection with SFV

In microglia, infection with SFV resulted in increases of gene transcripts for TLR 2, 3, 6, 8 and 9. TLR 3, 8 and 9 had the greatest increases; these TLR each have been linked to sensing viral nucleic acid sequences. The response of astrocytes to SFV infection was similar in that TLR 2, 3 and 9 were upregulated but dissimilar in that expression of all other TLR genes were severely curtailed. Upregulation of TLR 2 occurred in both astrocytes and microglia in response to both LPS and SFV. The amount of IFN-α produced by astrocyte cultures was far lower than microglial cultures despite a higher level of SFV replication. More efficient IFN-α production in microglial cells than astrocytes could have reduced virus replication in microglial cells relative to astrocytes, although levels of caspase 3 activity was similar in both SFV infected glial cultures. A recent report has shown infection of primary microglia with TMEV selectively upregulates TLR 2, 3 and 9, with TLR 3 upregulation being greatest (Olson and Miller, 2004). Together with the present data this suggests upregulation of TLR 2, 3 and 9 by cultured microglia and astrocytes may be a common response to several RNA viruses. TLR 3 is a well-described sensor of virus infection and recognises dsRNA whilst TLR 9 recognises viral CpG motifs of DNA viruses. In mice, deficiency of TLR 3 or 9 dramatically increases susceptibility to CMV infection (Tabeta et al., 2004). Selective upregulation of TLR 3 and 9 is therefore a highly appropriate response to a virus infection and upregulation of these molecules would act to increase the sensitivity of the tissues to respond to any spread of infection.

Infection of microglia with VLPs initiated significant increase in TLR 3 expression. The upregulation of TLR 3 transcripts suggests that either virus entry or virus RNA replication was sufficient to induce an increase in TLR 3 expression and consequently increase the sensitivity of the detection system that senses virus dsRNA. This informs us that neither viral structural proteins nor virus particle assembly are required for TLR 3 upregulation, although the enhancement of upregulation by virus structural proteins cannot be excluded. VLPs lack the ability to spread from cell to cell and consequently the dynamics of infection compared to SFV infection were highly divergent. Microglia infected with SFV4 would have been subjected to several waves of infection as cells were lysed and new infectious virus released.

In comparison VLPs cannot spread from cell to cell and so the total number of cells infected at 12 and 24 hours would be significantly less. Accordingly, TLR 3 transcripts were not as dramatically upregulated in VLP infected cultures compared to SFV 4 infected cultures.

The mechanisms that modulate TLR expression are yet to be determined. In the case of SFV infection, direct recognition of virus glycoproteins by TLR 2 is a distinct possibility since the hemagglutinin protein of the measles virus signals through TLR 2 (Bieback et al., 2002) as may glycoproteins of the Herpes Simplex virus (Kurt-Jones et al., 2004b). In addition, responses of microglia to poly (I:C), a stimulator of the dsRNA sensor TLR 3, are very different to microglial responses to TMEV and that described here to SFV, suggesting virus may activate innate immunity via multiple TLR such as TLR 2 in addition to TLR 3. However, this activation may not necessarily represent a direct recognition of viral components by TLR 2, since a variety of pathogens as well as cytokines alone can upregulate TLR 2 expression (Liu et al., 2000; Kirschning and Schumann, 2002; Matsuguchi et al., 2000; Wang et al., 2000) as does sterile inflammatory events such as rheumatoid arthritis *in vivo* (Seibl et al., 2003). Thus, upregulation of TLR 2 may represent a general maker of inflammation in both peripheral and CNS settings or may represent a direct recognition of viral components. Further study will be required to clarify the exact nature of this interaction. SFV infection down-regulated TLR 4 in both microglia and astrocytes. Since activation of TLR 4 by LPS similarly down-regulates TLR 4 expression, TLR 4 itself may have been activated during SFV infection, perhaps via recognition of viral glycoproteins, as occurs for the respiratory syncytial virus and the mouse mammary-tumour virus (Kurt-Jones et al., 2000; Rassa et al., 2002). Alternatively, TLR 4 down-regulation may represent a generalised mechanism in response to stimulation by a variety of microbial components. In contrast to glial cells, neuroblastoma cells did not dynamically regulate TLR levels in response to either LPS stimulation or SFV infection, but neither did they express cytokines or IFN.

5.8.3 Summary

This chapter has demonstrated that cultured glial cells expressed a multitude of TLR that were differentially modulated in an appropriate manner in response to microbial stimuli. Microglia reacted to LPS stimulation with the expression of pro-inflammatory cytokines, whilst infection with SFV predominantly induced the expression of type-I interferon. These divergent responses underlie the capability of glial cells to determine the type of pathogen and initiate an innate response that differs in its form and effect. These findings are in agreement with the microarray data presented in chapter 4. LPS stimulation resulted in the

down-regulation of several TLR and may contribute to a localised state of endotoxin tolerance, whilst TLR 2 and 3 were upregulated. SFV infection specifically upregulated TLR known to be involved in virus sensing whilst other TLR where either unaffected or down regulated. Whether this upregulation occurs in infected cells, in adjacent uninfected cells, or in both, remains to be determined. The mechanisms that mediate TLR up and down-regulation are still to be clarified. Potentially, direct exposure to either SFV itself or components of SFV, such as dsRNA, may modulate TLR gene expression. Alternatively, signalling in response to extracellular molecules such as cytokines and interferon may contribute to the modulation of TLR expression. These issues are further investigated in chapter 6.

Chapter 6. An investigation of TLR expression in the CNS at rest, in viral encephalitis and in encephalopathy.

Contents

6.1 Introduction

The mechanisms that mediate the detection of infection in the immunospecialised environment of the CNS are poorly characterised. CNS immune responses are crucial to the control of infections, disease such as bacterial meningitis and viral encephalitis, but are also important in neuroinflammatory diseases such as multiple sclerosis. More recently, innate immune responses have been suggested to be important in the pathogenesis of neurodegenerative diseases such as Alzheimer's disease and the transmissible spongiform encephalopathies. Whilst there is growing information on the expression and function of TLR in the lymphoid system, there is little information on TLR expression and function in the CNS; indeed the profile of TLR expression in the brain remains undefined. The CNS is the most complex organ in the mammalian body. Specific neuronal nuclei and circuits are vital and cannot be replaced if damaged or lost and inflammatory and immune responses are tightly controlled. Lymphocytes, antibodies, complement and MHC-I expression are generally absent, and consequently the CNS is often described as an immunologically privileged site. Immunospecialised may be more appropriate since specialised glial cells can fulfil some of the functions of the innate immune system (Streit, 2002) and even florid inflammatory responses with highly active immune responses can develop.

The results from previous chapters of this thesis have demonstrated that cultured glial cells were capable of responding appropriately to differing microbial stimuli. These cells were also found to express a broad range of TLR suggesting they are well endowed with the ability to detect infection and discern its type. However, the situation *in vivo* could be quite different. N9 microglia represent an embryonic immortalised cell line selected for its responsiveness to LPS and its resting phenotype; whilst the astrocyte cultures were of embryonic origin and were treated to several weeks of culture that included maturation with dbcAMP. Whether either of these cell types adequately begins to describe *in vivo* expression is a matter of debate. Expression of TLR was therefore investigated in the brain at rest and during infection with two neuroinvasive viruses and with a strain of transmissible spongiform encephalopathy (TSE).

To, avoid the trauma and glial cell activation that can be associated with intracerebral inoculation, a neuroinvasive virus, SFV, was principally used in these studies. SFV is a positive-stranded RNA virus that generates an exceptionally high viremia following extraneural inoculation, and is efficiently neuroinvasive (Fazakerley, 2002). Upon entry into the brain SFV initiates encephalitis characterised by activation of endogenous glial cells and a later infiltrate of T- and B- cells. To determine the extent of TLR expression by endogenous glial cells, TLR transcript levels were compared in both immunocompetent

Balb/c mice and *nu/nu* Balb/c mice. The *nu/nu* Balb/c mice are athymic, lack T-cells, and do not exhibit an inflammatory leukocyte infiltrate in the brain. The levels of TLR transcripts during SFV infection of the brain in these two groups of mice were studied in detail. Standard immunocytochemistry has so far failed to identify TLR protein expression in the resting brain primarily due to a lack of sensitivity and of good quality commercial antibodies for murine TLR. This study has examined TLR expression using quantitative real time PCR developed in chapter 4.

To determine whether transcript changes during SFV encephalitis were unique to this positive-stranded RNA virus, gene expression changes were also studied in rabies virus (RABV) encephalitis. RABV is a negative stranded RNA virus that remains a significant cause of human mortality in the developing world for which there is no treatment following the development of symptoms. Exposure to the virus, principally through a bite from an infected animal, enables the virus to infect sensory neurons, with or without local replication in muscle tissue (Shankar et al., 1991). The virus rapidly ascends the central nervous system to the brain where uncontrolled viral replication and a prominent pro-inflammatory response lead to the inevitable death of the host (Theerasurakarn and Ubol, 1998). This work was undertaken in collaboration with Nick Johnson of the Veterinary Laboratory agency who infected the animals and sampled whole brains for RNA. Nick and I jointly undertook QPCR analysis at the University of Edinburgh.

Type-I IFN is a potent anti-viral extracellular messenger that has multiple dramatic effects on cellular metabolism and antigen presentation, as well as possessing immunomodulatory effects (Goodbourn et al., 2000). The ability of this messenger to sensitise cells to and resist virus infection is well described. TLR expression was examined in the CNS of mice lacking a functional IFN system.

The TSEs represent a unique group of chronic neurodegenerative diseases that are caused by an infectious protein component, termed prions (PrP^{Sc}). The TSE-infected CNS does not exhibit typical signs of inflammation and most immune processes are absent. However, the TSE-infected CNS is characterised by a strong glial reaction, with significant activation of microglia and astrocytes (Williams et al., 1997a). During infection with the ME7 strain of scrapie, CV mice exhibit pronounced activation of microglia that precedes significant neuronal loss in the hippocampus and may contribute indirectly to the neurodegeneration observed in this model (Brown et al., 2003). This chapter explores whether glial cells in the TSE-infected CNS exhibit altered levels of TLR transcripts. The differences and similarities of glial reactions during viral encephalitis and prion encephalopathy are discussed.

6.2 Objectives

To determine TLR expression in the resting CNS of several mouse strains

To compare CNS TLR expression in different strains of mice

To compare TLR levels in the spleen and CNS

To determine TLR expression in the SFV infected CNS

To determine TLR expression in the RABV infected CNS

To determine TLR expression in the scrapie infected CNS

To examine the dependence of any TLR transcription change on:

- the presence of lymphocytes
- interferon signalling

6.3 The resting mouse brain demonstrates extensive expression of TLR

To determine levels of TLR transcripts in the resting mouse brain four strains of mice, Balb/c, athymic Balb/c (*nu/nu*) CBA and 129 were investigated. TLR transcripts were detectable in the PBS perfused brains of all four strains. As expected the Balb/c mice and *nu/nu* (Balb/c background) mice exhibited similar levels of TLR expression. Substantial differences existed between the Balb/c and the other two strains (Figure 50A). Most strikingly, 129 mice expressed significantly higher levels of TLR 2, 3, 5, 7, 8 and 9 than Balb/c mice, whilst CBA mice expressed significantly higher TLR 9 than Balb/c mice. Furthermore, both CBA and 129 mice demonstrated a significantly lower expression of TLR 1 and 6 compared to Balb/c mice (Figure 50A). For Balb/c mice, TLR transcripts in the brain were compared to those in the spleen (Figure 50B). Generally, as normalised to either β-actin or GAPDH housekeeping genes, the CNS expressed far fewer TLR transcripts than the spleen. The single exception to this was TLR 3, where transcript levels were comparable between the two organs.

6.4 Infection with SFV A7(74) triggers profound changes in CNS TLR expression

To determine the response of the TLR expression profile of the CNS to virus infection and to distinguish whether changes were due to inflammatory infiltrates, Balb/c and Balb/c *nu/nu* mice were infected with the A7(74) strain of SFV. Intraperitoneal infection of Balb/c mice with SFV A7(74) results in virus invasion of the brain within 48 hours followed by a predominantly mononuclear inflammatory infiltrate starting at around 4 days (Fazakerley and Webb, 1987c). In contrast athymic *nu/nu* Balb/c mice infected with SFV A7(74) have no

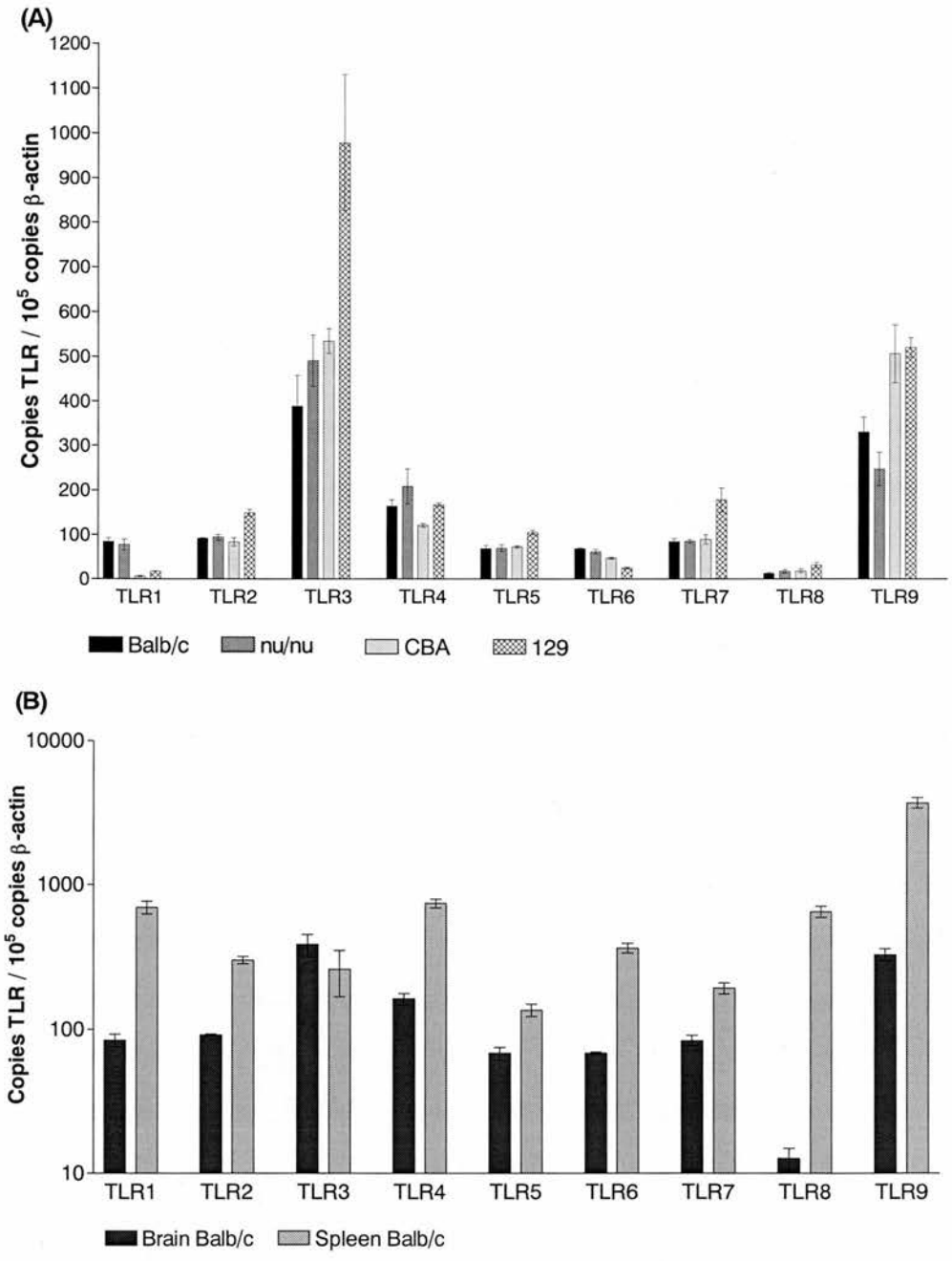

Figure 50, TLR transcript levels in the brain and spleen. Groups of four six-week old mice were perfused with PBS to remove blood-borne leukocytes and their brains and spleens immediately processed for RNA extraction. Absolute levels of β -actin and TLR 1 to 9 were assayed by QPCR. The data is expressed as a ratio of copies of TLR per 100,000 copies β -actin. (A) TLR transcripts in the resting CNS of Balb/c, Balb/c *nu/nu*, CBA and 129 mice, expressed as copy number per copy β-actin. Levels of β-actin transcripts per . g brain RNA were equivalent in all four mouse strains. (B) Comparison of TLR transcript levels in brains and spleens of Balb/c mice. Analysis comparing TLR copy number per GAPDH copy number (data not shown) revealed marginally higher TLR expression in the spleen. All bars show mean value of 4 mice ± SEM.

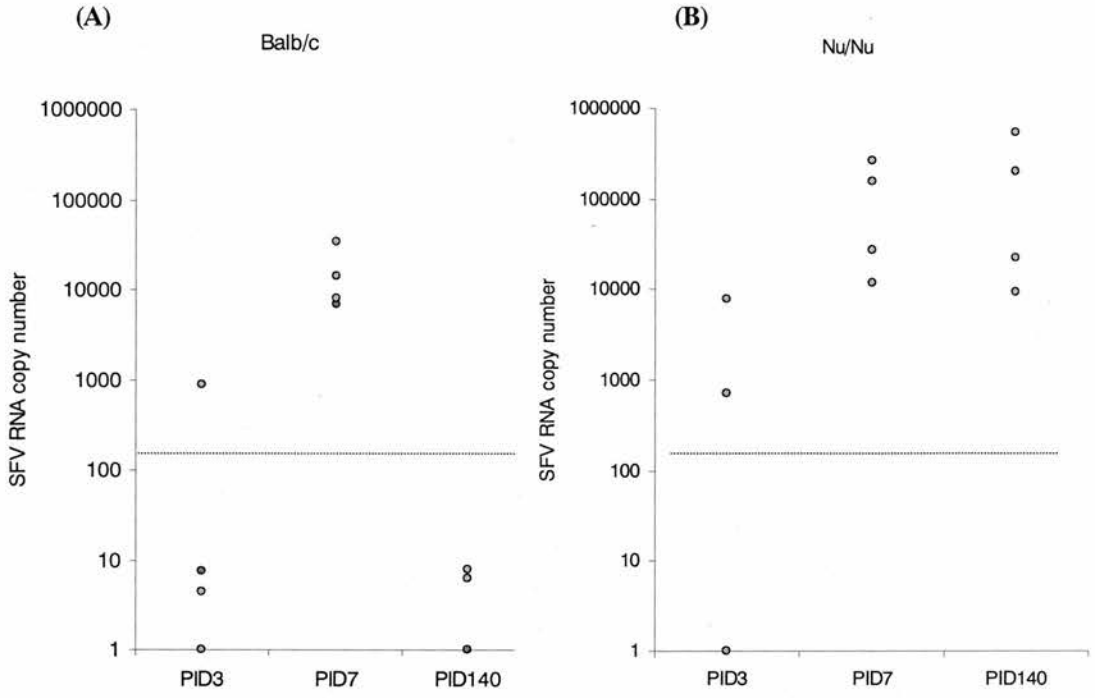

Figure 51, SFV RNA levels in the brain during infection. Mice were inoculated intraperitoneally with either PBSA or SFV A7(74) and sampled on post infection day 3, 7 or 140 (PID). SFV RNA copy number was determined by QPCR using primers to E1 gene sequences. (A) Balb/c mice (B) *nu/nu* Balb/c mice.

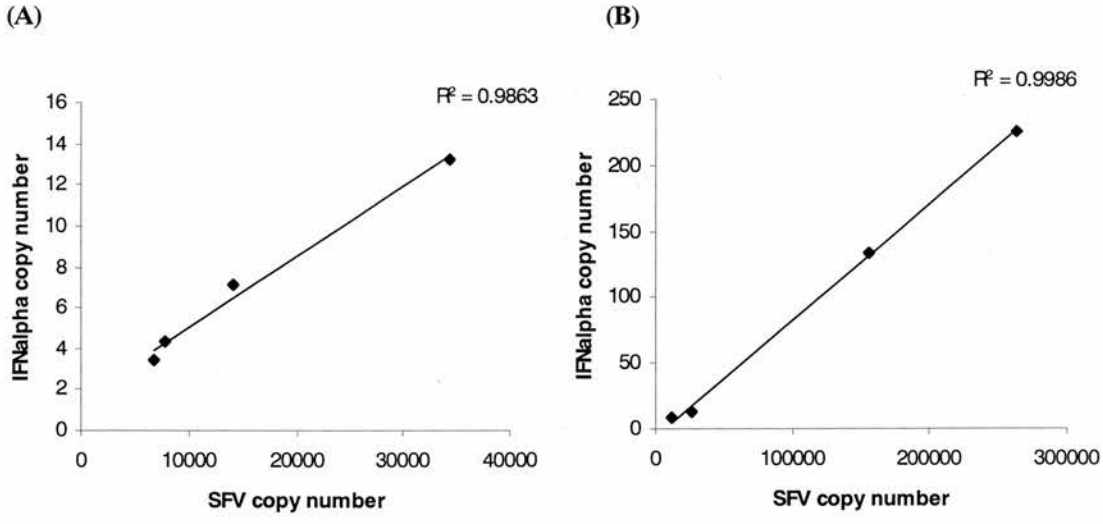

Figure 52, IFN-α transcripts correlate with SFV RNA levels. Mice infected intraperitoneally with SFV A7(74) were sampled on PID 7. (A) Balb/c mice. (B) *nu/nu* Balb/c mice. R^2 values indicate relative correlation efficiency (1 = perfect correlation and 0 = no correlation).

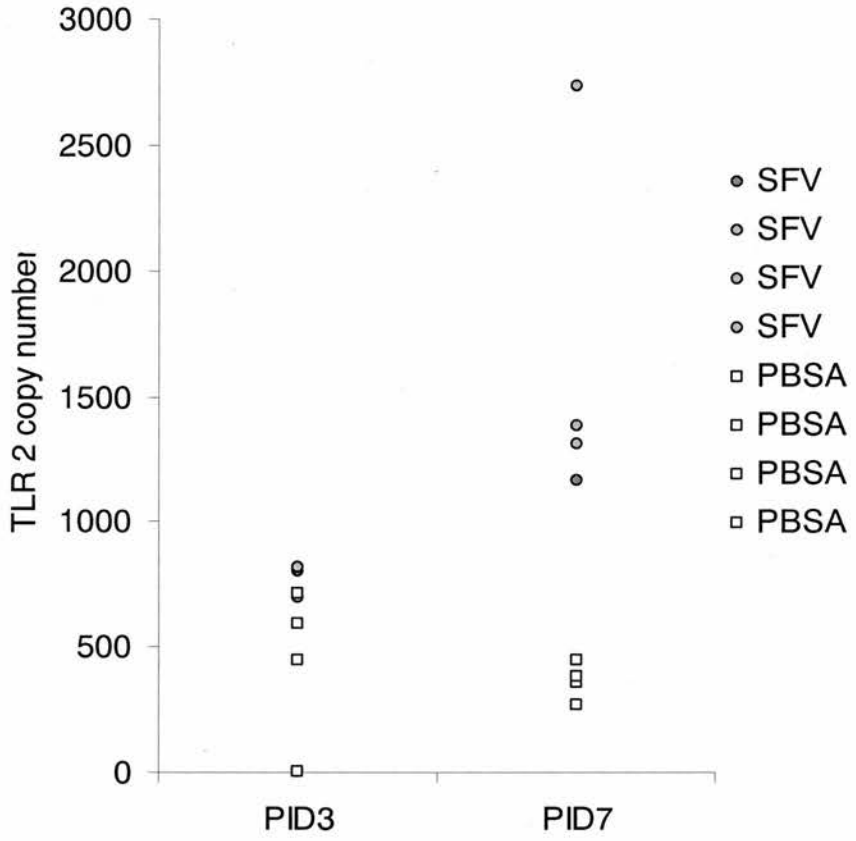

Figure 53, TLR 2 transcripts are elevated in SFV A7(74) infected brains of Balb/c mice. TLR 2 transcript were assayed by QPCR and absolute levels calculated and normalised to β-actin transcripts. Shown above are the amounts of TLR 2 in the cDNA samples from SFV-infected brain (grey circle) and brains inoculated with PBSA alone (empty squares). A slight but non-significant increase in TLR 2 expression was observed in SFV infected brain at PID 3. Levels of TLR 2 were significantly higher in SFV infected brain by PID 7.

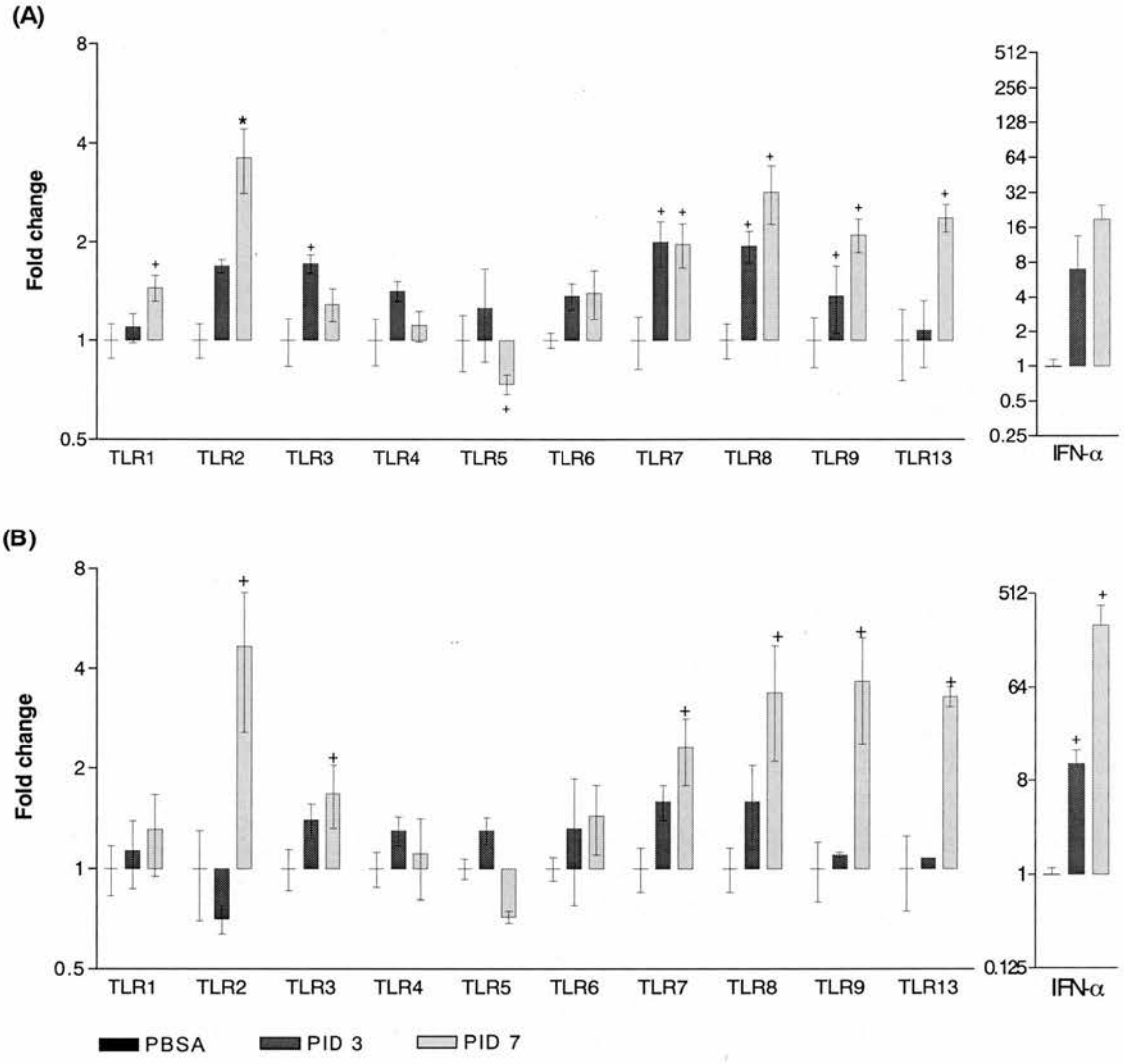

Figure 54, TLRs are differentially regulated in the CNS during SFV infection. Mice were inoculated intraperitoneally with either PBSA or SFV A7(74) and sampled on post inoculation day 3 or 7 (PID). (A) Balb/c mice (B) *nu/nu* Balb/c mice. Each bar represents the mean fold increase of 4 mice ± SEM relative to PBSA inoculated mice. Marked bars are statistically different from the respective 0 hour time-point (Mann Whitney; +$p<0.05$ *$p<0.01$).

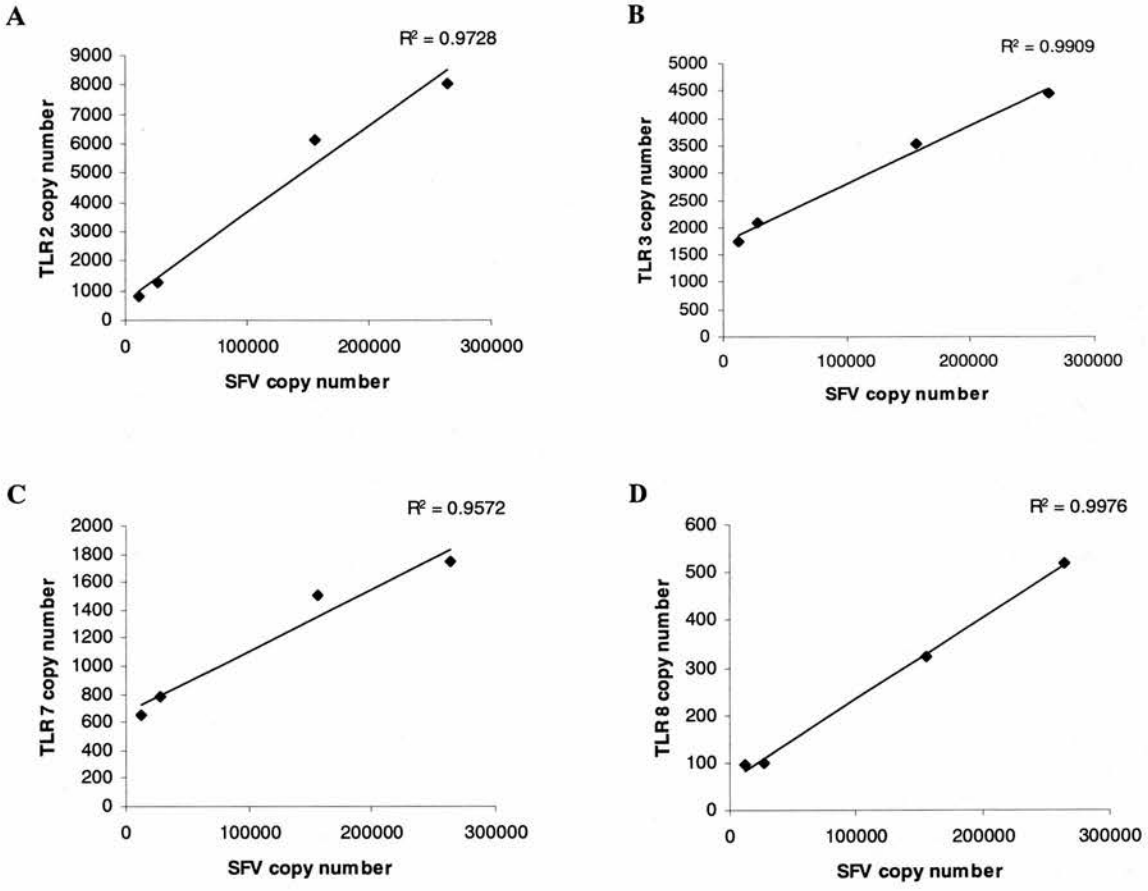

Figure 55, TLR 2 (A), 3 (B), 7 (C), and 8 (D) transcripts correlate with SFV RNA levels in *nu/nu* mice at PID 7. Correlation was also found for TLRs 4,6 and 9 (data not shown).

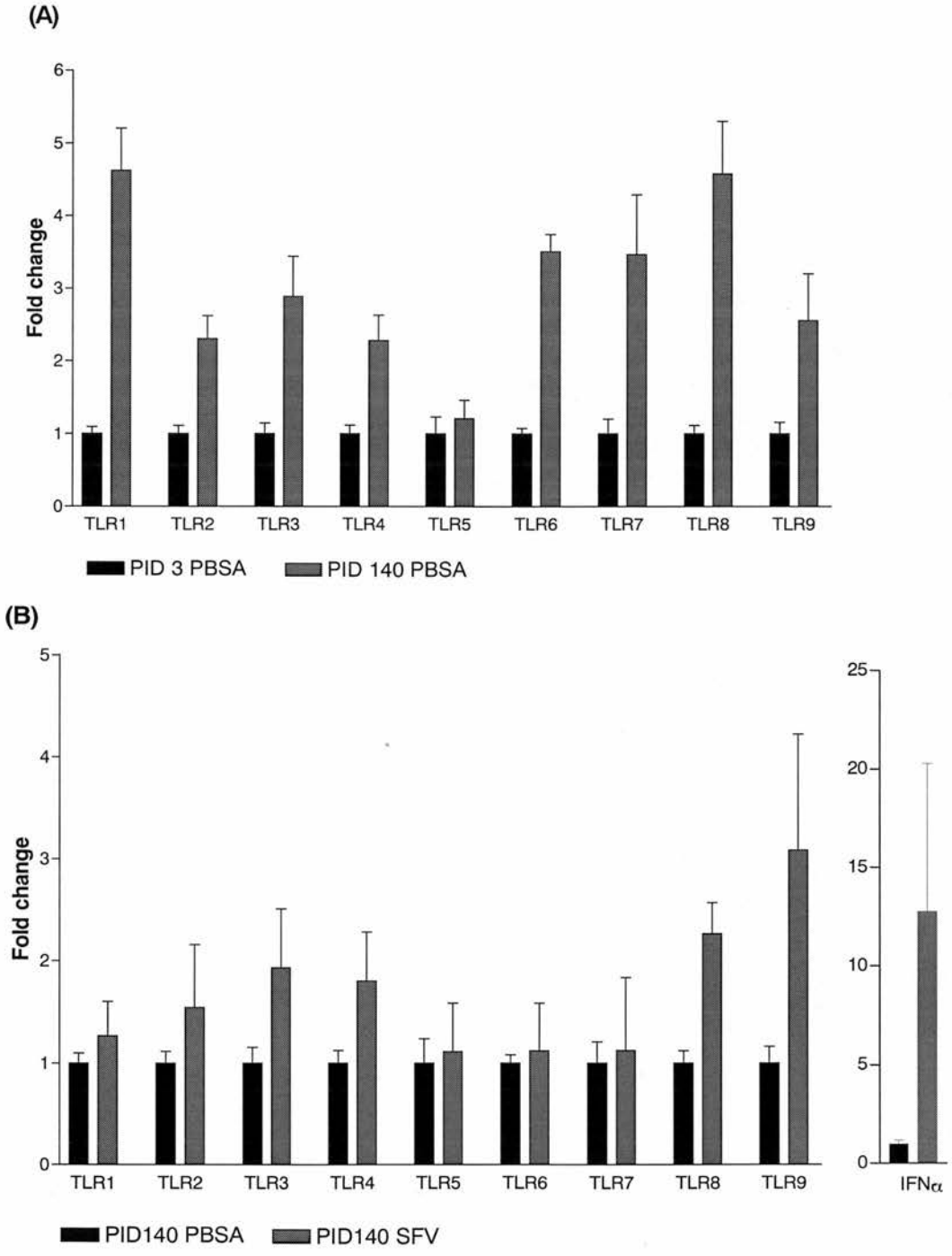

Figure 56, TLR transcripts were elevated in both uninfected and SFV infected brain of *nu/nu* Balb/c mice at PID 140. Mice were inoculated intraperitoneally with either PBSA or SFV A7(74) and sampled on post infection day 3 or 140 (PID). (A) Fold increase of TLR transcripts at PID 140 relative to levels at PID 3 in PBSA inoculated mice ± SEM. (B) Fold increase of TLR transcripts in SFV infected mice at PID 140 relative to levels in mice inoculated with PBSA at PID140 ± SEM.

invading mononuclear cell response (Jagelman et al., 1978). All mice were infected via the intraperitoneal route, avoiding CNS trauma, and CNS gene expression in the PBS perfused brain was assayed on post infection days (PID) 3 and 7. SFV and IFN-α levels in the CNS were determined by QPCR (Figure 51 and 52). SFV levels peaked at PID 7 and were significantly higher in *nu/nu* mice. SFV RNA was detectable at PID 140 only in the *nu/nu* mice, suggesting that virus had persisted. Both groups of mice demonstrated increased IFN-α transcripts; the levels of which correlated with levels of virus RNA (Figure 52).

SFV infection upregulated TLR transcripts with clear variation between individual mice (Figure 53). Balb/c mice exhibited a broad increase in TLR expression, with TLR 2, 3, 7, 8, 9 and 13 significantly upregulated. TLR 2 upregulation was greatest at 3.6 fold (Figure 54A). Athymic *nu/nu* mice had a more extensive infection as determined by viral RNA levels (Figure 51) and greater increases in TLR transcripts were observed (Figure 54B). Qualitatively, TLR changes were similar in both strains of mice with TLR 2, 3, 7, 8, 9 and 13 upregulated. TLR 2 and 9 showed the greatest fold-change. As with IFN-α (Figure 52), TLR 2, 3, 7, 8 and 9 showed good correlation with virus RNA levels in *nu/nu* mice at PID 7, suggesting virus levels were driving TLR upregulation (Figure 55). TLR upregulation did not correlate with SFV levels in Balb/c mice.

TLR transcripts were also analysed at PID 140. Surprisingly, PBSA inoculated mice exhibited TLR levels that were elevated compared to their littermates sampled 137 days previously (Figure 56A). All TLR assayed, except TLR 5, were shown to be elevated, suggesting the aged mice possessed more TLR transcripts in general. To determine whether persistently infected *nu/nu* mice exhibited chronically elevated TLR transcripts, the levels of TLR were examined and compared to age matched controls (figure 56B). Upregulation was highly variable with no significant differences between the groups. However, the results suggest that TLR 2, 3, 4, 8 and 9 may be elevated by the persistent virus infection. This profile is different to that observed at PID 7. Elevated levels of IFN-α transcripts were detected (figure 56B) and similarly to PID 7 correlated with viral load (data not shown).

6.5 TLR levels are altered during rabies encephalitis

To determine whether TLR expression changes were unique to SFV infection, mice were infected intracerebrally with the rabies virus (RABV). Intracerebral inoculation was utilised since this generates a reproducible CNS infection. In this study, inoculation resulted in uncontrolled viral replication, a prominent pro-inflammatory response and death of the host. All mice had reached defined clinically terminal end points or were dead by 6 days post infection. QPCR analysis revealed extensive upregulation of several pro-inflammatory

cytokines and type-I IFN, with IL-6 and TNF-α demonstrating the greatest fold-increases (figure 57B). Concurrent with this rampant pro-inflammatory response, RABV infection resulted in substantial upregulation of most TLR transcripts, with TLR 2, 3 and 9 demonstrating the greatest fold-increases. TLR 3 was uniquely upregulated at both PID 2, 4 and 6 (Figure 57A). Mice sampled at PID 0, before virus had time to replicate but had experienced the trauma of a needle-stick injury, demonstrated transcript levels that were not significantly different from uninoculated mice (data not shown).

6.6 Mice lacking a functional IFN system cannot upregulate TLR 3 or TLR 9 upon SFV infection

To determine whether the correlation between SFV RNA and TLR transcripts levels in the brain was dependent on, or independent of the type-I interferon response, 129 mice possessing a functional type-I IFN system and 129 mice lacing a functional type-I IFN system (IFN-α/β-$R^{-/-}$) were infected with either avirulent SFV A7(74) or virulent SFV4 via the intracerebral route. For these studies mice could not be inoculated intraperitoneally as they die of peripheral pathology prior to neuroinvasion. All IFN-α/β-$R^{-/-}$ mice had reached clinically defined terminal end points or were dead by 42 hours; gene expression was therefore only analysed at 24 hours. In comparison, 129 mice demonstrated no or only mild clinical signs 42 hours following SFV A7(74) infection, but 50% mice had reached terminal disease or were dead 42 hours post SFV4 infection.

A7(74) infection of 129 mice produced no or minimal changes in TLR, IL-1α or TNF-α transcripts at 24 hours. However, by 42 hours there was upregulation of TLR 1, 2, 3, 7, 8, 9 and 13 with TNF-α, IL-1α, TLR 3 and 9 demonstrating the greatest fold-increases. TLR transcripts in sham-infected brain were equivalent to uninoculated brains at this time. In contrast, IFN-α/β-$R^{-/-}$ mice demonstrated large increases in proinflammatory IL-1α and TNF-α cytokine transcripts by 24 hours (Figure 58). This earlier increase most likely reflects the increased virus loads in these mice, which were an order of magnitude higher in IFN-α/β-$R^{-/-}$ than 129 mice (Table 9). Transcripts for TLR 1, 2, 4, 6, 7, 8, and 13 showed greatest upregulation at 24 hours, with TLR 2 and 8 exhibiting the largest increases. Strikingly, despite higher levels of viral RNA and transcripts for IL-1α, TNF-α , and TLR 1, 2, 7, 8 and 13, levels of expression of TLR 3 and 9 transcripts showed no increase in the IFN-α/β-$R^{-/-}$ mice.

Intracerebral inoculation with virulent SFV4 produced similar results with even greater changes in TLR expression (Figure 59). Again this correlated with virus titres (Table 9).

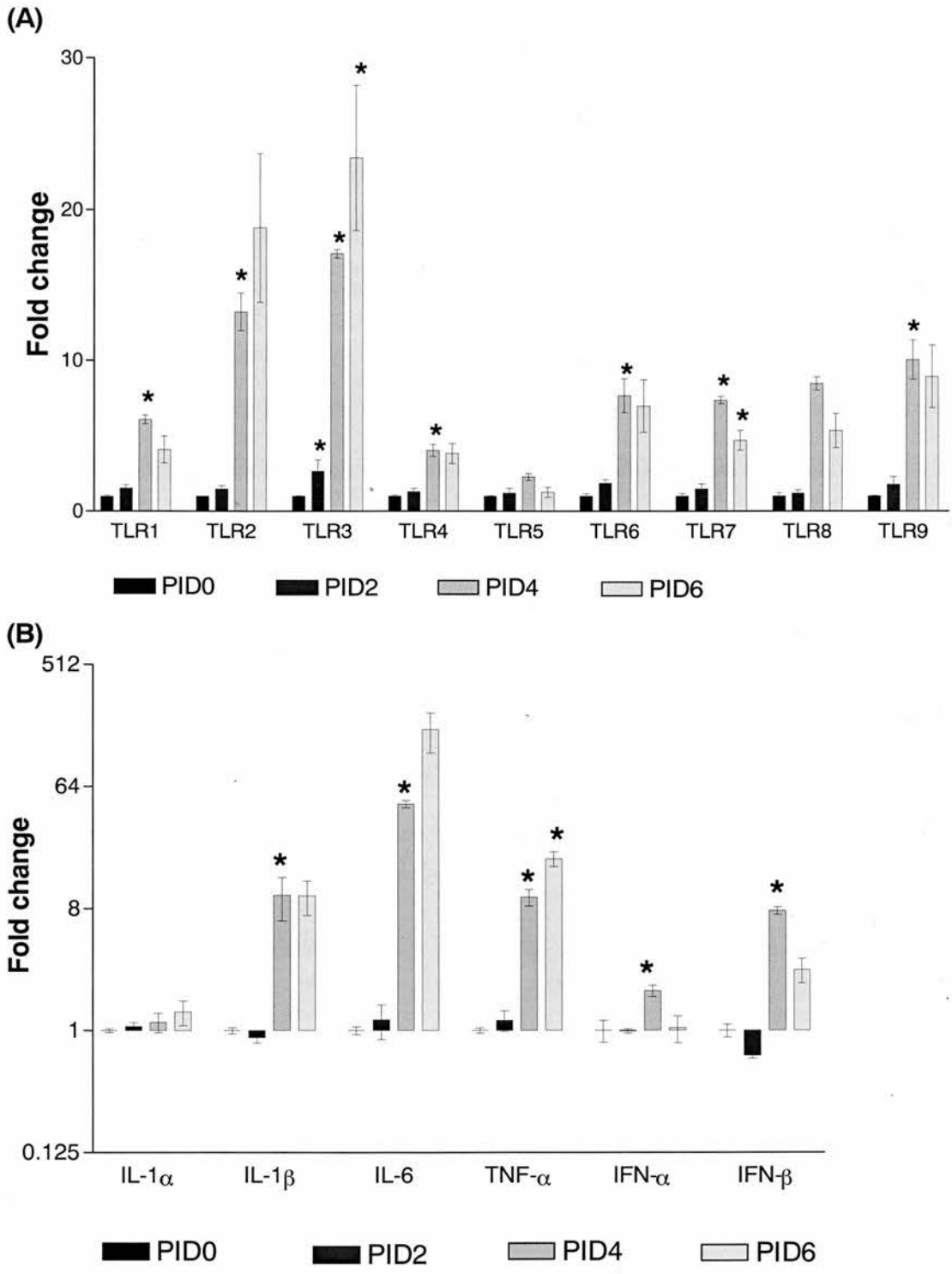

Figure 57. RABV infection elicits large changes in TLR and cytokine transcripts. Mice were inoculated intracerebrally with RABV and sampled on post infection day (PID) 0, 2, 4 and 6. (A) TLR transcripts (B) Cytokine and type-I IFN transcripts. Each bar represents the mean fold increase of 3 mice ± SEM relative to PID 0 time point. Marked bars are statistically different from control (Student's t-test, n=3, $p<0.05$).

Higher levels of virus RNA in SFV4 infected mice than in SFV A7(74) infected mice produced greater fold increases in TLR and IFN-α. Upon infection, 129 mice upregulated TLR 1, 2, 3, 4, 6, 7, 8, 9 and 13, with TLR 2, 3 and 9 exhibiting the largest increases (29 fold for TLR 2 and 16 fold for TLR 9 at 42 hours). Proinflammatory cytokines were detected by 24 hours and continued to rise at 42 hours. IFN-α/β-R$^{-/-}$ mice also exhibited high levels of cytokine transcripts at 24 hours and exhibited levels of SFV RNA that was equivalent to the levels in SFV4 infection of 129 mice at the later time-point of 42 hours. Interestingly, TLR 1, 2, 4 and 7 were upregulated in IFN-α/β-R $^{-/-}$ mice to a similar extent to 129 mice at 24 hours post infection, whilst TLR 6, 8 and 13 and the cytokines were more substantially upregulated. As with A7(74) infection, there was a striking failure of IFN-α/β-R $^{-/-}$ mice to upregulate TLR 3 and 9. Expression levels were not significantly different from uninfected littermates despite a high virus load, and a substantial pro-inflammatory response. These results demonstrate that an intact type-I IFN system is critical for upregulation of TLR 3 and 9, whereas upregulation of other TLR is independent of type-I IFN.

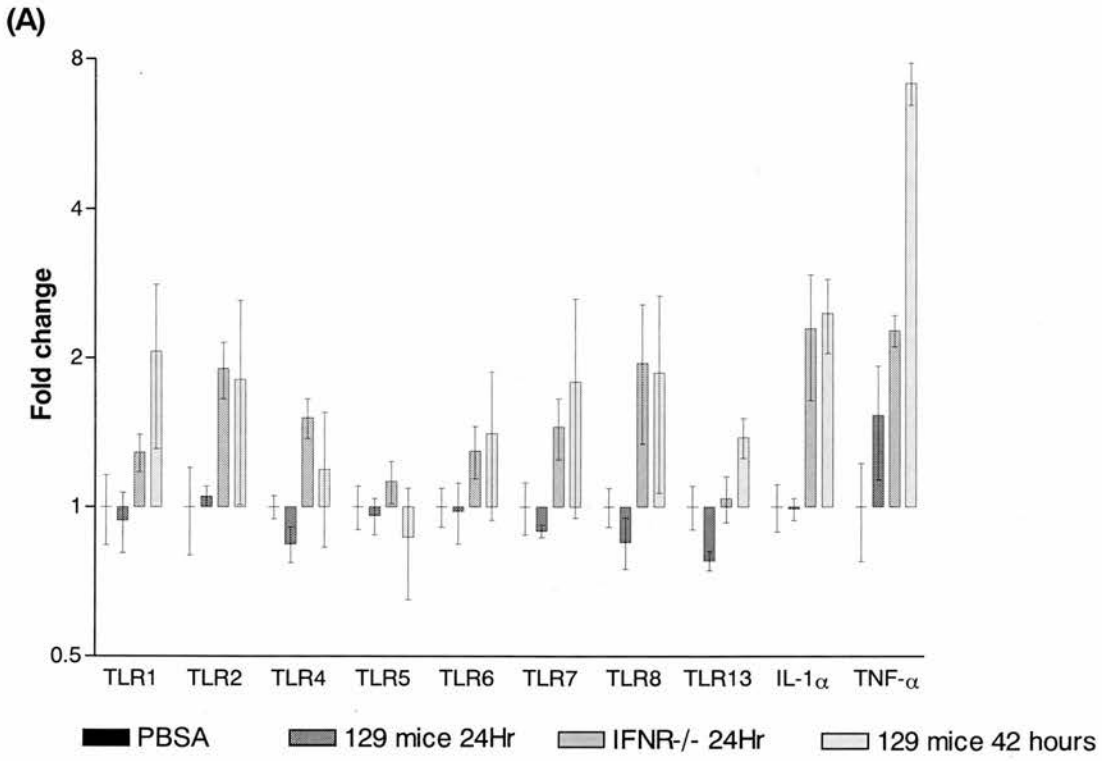

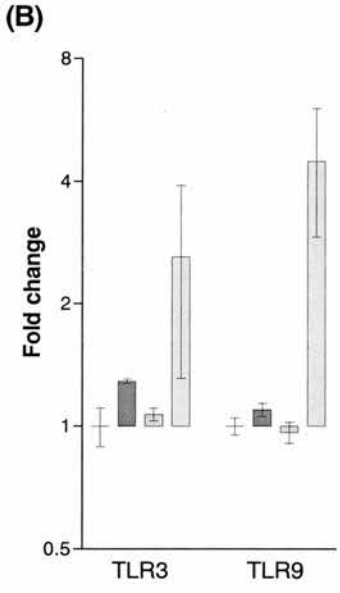

Figure 58, Infection of 129 mice and IFN-αβ-R deficient mice with avirulent SFV A7(74). 129 and 129 IFN-αβ-R$^{-/-}$ mice were infected intracerebrally with either PBSA or SFV and sampled at 24 hours or 42 hours post infection. By 42 hours all IFN-αβ-R$^{-/-}$ mice had died. Mice inoculated with PBSA alone demonstrated no TLR up-regulation compared to the resting brain. 129 mice sampled at 42 hours exhibited markedly varied levels of SFV RNA. (A) Transcripts expressed at a higher level in IFN-αβ-R$^{-/-}$ compared to 129 at 24 hours post infection. (B) Transcripts up-regulated in 129 mice but not in IFN-αβ-R$^{-/-}$ mice.

Table 9 SFV RNA transcripts per ng total RNA

	24 hours		42 hours
	SFV A7(74)	SFV4	SFV4
129 mice	37	4,956	17,420
IFN-α/β-R -/- mice	351	17,718	N/A

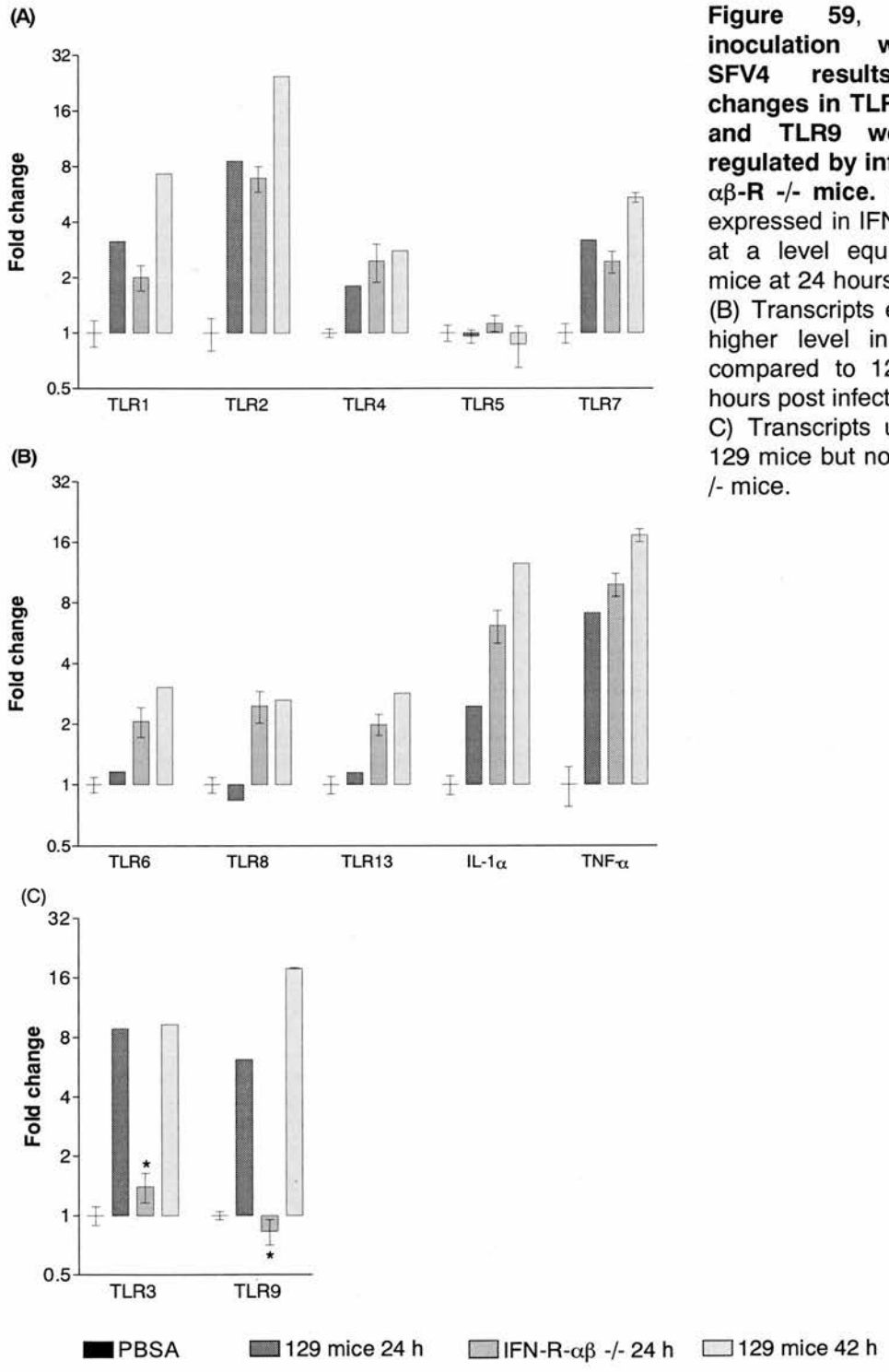

Figure 59, Intracerebral inoculation with virulent SFV4 results in large changes in TLR levels. TLR3 and TLR9 were not up-regulated by infection in IFN-αβ-R -/- mice. (A) Transcripts expressed in IFN-αβ-R -/- mice at a level equivalent to 129 mice at 24 hours post infection. (B) Transcripts expressed at a higher level in IFN-αβ-R -/- compared to 129 mice at 24 hours post infection.
C) Transcripts up-regulated in 129 mice but not in IFN-αβ-R -/- mice.

6.7 TLR expression is modulated during scrapie neuropathogenesis

In contrast to viral encephalitis TSEs exhibits no obvious inflammatory infiltrates or BBB permeability. Lymphocytes and other immune cells such as natural killer cells are absent despite a prominent glial reaction. During scrapie pathogenesis glial cells undergo hyperplasia and hypertrophy, and yet the level of pro-inflammatory cytokine release relative to the degree of reactive gliosis is highly restricted, temporally late and disproportionately low (Brown et al., 2003). The work above has described large changes in TLR expression during viral infection of the brain. To determine whether the glial activation that occurs in the scrapie brain is associated with TLR expression change, samples of ME7 scrapie infected hippocampus and age matched control hippocampus were examined. These samples were taken from a library of samples available in the Fazakerley laboratory (Brown et al., 2003). The dynamics of TSE infection and onset of clinical disease, along with levels of glial activation and neuronal death in these samples have been previously reported (Brown et al., 2003). The ME7 hippocampus was chosen since this area of the brain has particularly well described pathological changes. PrP^{Sc} deposition and glial activation are evident from 100 days post infection (dpi) and increase until terminal disease. In addition, between 160 and 180 dpi 50% of the CA1 neurones of the hippocampus are lost. Accordingly, TLR transcript levels were assayed at 169 dpi, 180 dpi and 237 dpi (approaching terminal disease). Fold increases of TLR transcripts were calculated relative to age matched controls inoculated with normal brain homogenate; this negated any possible effect of age related changes due to the phenomenon of age-related increases in TLR expression, described in section 6.4. Increases in TLR 2, 3, 7, 8 and 9 were seen at 169 dpi, whilst TLR 2, 7 and 9 were in addition significantly elevated at 237 dpi (Figure 60). To determine whether increases in TLR 2 continued to terminal disease, a second set of hippocampus samples were examined which included mice sampled beyond 237 dpi at the time at which they reached a clinically defined terminal end point of disease (Figure 60B). TLR 2 transcripts continued to increase towards terminal disease by which time levels had increased by 10-fold relative to controls.

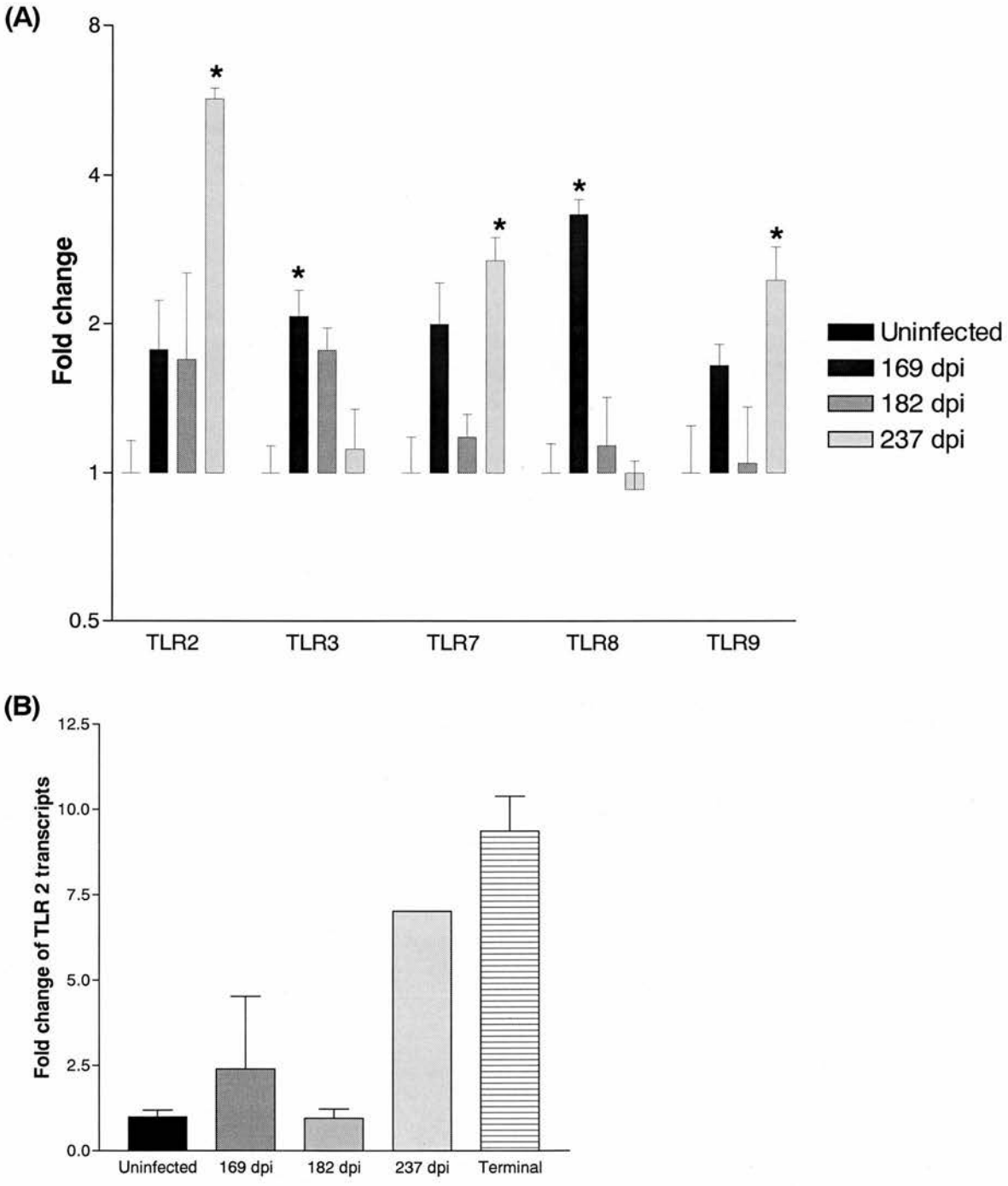

Figure 60, TLR transcripts are up-regulated during scrapie infection of the hippocampus. Mice were inoculated with either ME7 scrapie brain homogenate or normal brain homogenate and hippocampal samples taken at 169, 182 and 237 days post infection (dpi). (A) Fold increase of TLR transcripts significantly altered relative to uninfected controls. Bars represent the mean fold change in transcript level of the infected mice relative to age matched controls. Bars marked with an asterisk are statistically different from control (Student's t-test, n=3, $p<0.05$). (B) TLR 2 transcripts were analysed in more detail and revealed higher TLR 2 expression at terminal disease.

6.8 Discussion

This chapter reports the first systematic analysis of TLR gene expression in the CNS. It reveals extensive expression in the resting CNS and differential modulation during viral encephalitis. The finding that the brain has the ability via TLR expression to detect infection and discern its type provides an important contribution to understanding pathological processes in this organ. This chapter also demonstrates for the first time that upregulation of transcription for TLR 3 and 9 is dependent upon type-I IFN responses whereas for other TLR, increased expression is proportional to virus load but is independent of type I interferon. TLR expression has also been described for the first time during scrapie infection and suggests an interaction between innate immune processes and infection with PrP^{Sc}.

6.8.1 TLR expression in the uninfected brain indicates endogenous CNS cells can sense infection at rest

This is the first comprehensive *in vivo* analysis of TLR gene expression in the mouse brain. TLR 1 to 9 and TLR 13 were all expressed but at levels lower than immunological organs such as the spleen. An exception to this was TLR 3, which was uniquely expressed in the brain at a level comparable to that of the spleen. This novel finding could reflect an evolutionary history of RNA virus infection as the major pathogen selective pressure in the CNS. Indeed, on a worldwide basis, RNA virus infections remain the most common type of pathogen infecting the CNS. Viruses such as polio, rabies, West Nile and Japanese encephalitis, are all important causes of human morbidity and mortality. The relatively high CNS expression of TLR 3 may be an evolutionary selected response to the pressure of RNA virus infections. The finding that astrocytes express TLR 3 at relatively high levels (chapter 5) suggests that most of the TLR 3 detected in whole brain may be of astrocyte origin in addition to microglia.

It is interesting to note that differing strains of inbred mice exhibited differing TLR expression levels in the brain. 129 and CBA mice are both derived from the C57Bl/6 mice and would be expected to exhibit some of their characteristics. The more substantial expression of TLR 2, 3, 5, 7 8 and 9 in 129 mice compared to Balb/c mice and of TLR 9 in CBA mice compared to Balb/c mice is interesting in the knowledge that these strains differ in their susceptibility to a variety of microrganisms. Differential TLR gene expression could contribute to some of these susceptibility differences. For example, in C576Bl/6 mice, absence of TLR 3 and particularly TLR 9 renders them as susceptible to CMV-associated morbidity as the susceptible Balb/c strain (Tabeta et al., 2004). Unlike all other TLR, CBA and 129 mice exhibited lower levels of TLR 1 and 6 compared to Balb/c mice. The

concurrent lowly expressed nature of both TLR 1 and TLR 6 in both CBA and 129 mice suggest these two highly related TLR members are expressed in a coordinate manner.

6.8.2 Virus infection selectively and appropriately upregulates Toll-like receptor gene expression in the central nervous system

Upregulation of TLR expression can increase a cell's sensitivity to microbial components and infection. Macrophages can upregulate TLR 2 in response to stimulation with a variety of microbial components. Upregulation of TLR 2 correlates with increased responsiveness to further microbial challenge (Nilsen et al., 2004), whilst down-regulation of TLR 4 correlates with decreased responsiveness to LPS (Nomura et al., 2000). Dendritic cells induced to express high levels of TLR 7 makes them more sensitive to challenge with TLR 7 ligand imiquimod (Mohty et al., 2003). Together this data indicates changes in TLR transcript levels modulate responsiveness to innate immune stimuli.

The data reported here show for the first time that TLR are upregulated during viral encephalitis and presumably increase the tissues sensitivity to microbial components. Furthermore, the response is appropriate to the pathogen. During SFV infection, TLR 2, 3, 7, 8 and 9 were significantly upregulated while TLR 1, 4, 5 and 6 were not. TLR 2 may a have role in detecting viral glycoproteins (Bieback et al., 2002; Kurt-Jones et al., 2004a), whilst TLR 3, 7, 8 and 9 are all critical for recognising viral nucleic acid sequences and TLR 1, 4, 5 and 6, which were not upregulated, are principally associated with bacterial infections (Takeda et al., 2003). This selective upregulation does not require lymphocytes, as demonstrated by infection of the *nu/nu* mice. In these mice the IFN response was able to control the infection; levels of IFN-α correlated with levels of virus and increases in TLR transcripts. These results demonstrate that either a direct effect of virus replication or an indirect effect, mediated perhaps by interferon, results in a selective increase in gene expression for those TLR able to sense virus infection. This would increase the sensitivity of the system to detect spread of infection and presumably allow cells to react more rapidly to infection. Infection of the CNS with RABV resulted in TLR transcript changes that were qualitatively similar to that which occurred during SFV infection. Indeed, the substantial upregulation of TLR 2, 3 and 9 was a response common to both intracerebral inoculation with SFV and RABV, suggesting upregulation of these three TLR is a response common to several types of neuroinvasive RNA virus. Upregulation of TLR 3 may be a particularly early response to RNA infection of the brain, since TLR 3 alone was significantly upregulated at PID 2 with RABV. Events were further dissected by the analysis of IFN-αβ-R -/- mice infected with SFV. These mice showed no defect in the upregulation of

proinflammatory cytokines or TLR 2, 7 or 8 but were unable to upregulate gene expression of TLR 3 and 9.

An interferon independent mechanism mediated the substantial upregulation of TLR 2 following SFV infection in a manner proportional to the virus load. Cell stress responses such as induction of heat shock proteins, direct viral glycoprotein-mediated activation of TLR 2 or the presence of cytokines could be responsible for this. Cytokines have been shown to upregulate TLR 2 in other settings whilst TLR 2 is well known to be upregulated in myeloid cells in response to a variety of pathogens (Matsuguchi et al., 2000) and during sterile inflammatory events such as rheumatoid arthritis *in vivo* (Seibl et al., 2003), and thus may represent a general maker of inflammation in both peripheral and CNS settings. Similarly, in both Balb/c and 129 mice, SFV infection with either avirulent or virulent SFV triggered moderate increases in TLR 7 and 8 expression, which did not require IFN-α/β signalling. TLR 13 is a newly described member of the family whose function is uncharacterised but possesses sequence similarities to TLR 3 (Tabeta et al., 2004). TLR 13 was examined here to determine whether its expression was, as with TLR 3, controlled by IFN. Moderate up regulation of TLR 13 was observed in the infected CNS that was not dependent on IFN.

Two previous studies have linked TLR 3 upregulation to IFN-α/β production in cultured monocyte-derived macrophages (Doyle et al., 2003; Miettinen et al., 2001). This report demonstrates for the first time that this occurs *in vivo*, in this case, during viral encephalitis, and in addition informs us TLR 9 is also under IFN control. It is likely that by upregulating TLR 3 and 9, IFN-α/β acts to increase the sensitivity of cells in the vicinity of virally infected cells. This parallels events with PKR another interferon inducible activator of innate cellular defences (Meurs et al., 1992; Tanaka et al., 1998; Goodbourn et al., 2000). Basal levels of PKR detect viral RNA and induce type-I IFN synthesis. This IFN acts in both an autocrine and paracrine way to upregulate a number of genes including PKR itself (Meurs et al., 1990). In this way cells in the vicinity of virally infected cells have their virus sensing mechanisms upregulated. The finding here, is that this also applies to the two TLR most associated with recognition of virus nucleic acids, TLR 3 and 9.

6.8.3 Functional significance of *in vivo* TLR 3 expression

Several reports have begun to address the functional significance of TLR 3 expression *in vivo*. TLR 3 is necessary and sufficient for responses to poly(I:C) and reovirus RNA *in vitro* (Alexopoulou et al., 2001). However, recent reports have questioned the *in vivo* relevance of these findings. The ability of TLR 3 deficient mice to resist infection with several viruses

including, CMV, reovirus and LCMV were investigated. This report found the outcome of infection was independent of TLR 3 (Edelmann et al., 2004), although this report did not examine innate immune responses. In comparison, innate immune responses are significantly curtailed in TLR 3 deficient mice following CMV infection and demonstrate increased mortality (Tabeta et al., 2004). Furthermore, mice deficient in a downstream component of TLR 3 signalling, TRIF, are more susceptible to infection with CMV when given at higher doses (Hoebe et al., 2003) than that used in the report by Edelmann *et al.* In addition, TLR 3 deficient mice have significantly elevated levels of spleen virus following infection with WNV and decreased cytokine production (Wang et al., 2004). Together this suggests TLR 3 expression does impart some function to viral immune responses. In addition, TLR 3 deficient mice are protected from shock induced by poly(I:C) treatment, suggesting the receptor has an *in vivo* role in the recognition of and responses to extracellular dsRNA (Alexopoulou et al., 2001).

It has been suggested that the concentrations of dsRNA made during some natural infections may not be sufficient to bind to and significantly influence TLR 3 signalling, when compared to the high concentrations used for *in vitro* studies (Edelmann et al., 2004). However, the amount of dsRNA generated during the course of infection with several viruses may well be sufficient to activate TLR 3. This may be the case following infection with SFV. SFV is a positive-stranded RNA virus that replicates very rapidly upon infection and initiates high levels of viremia within 24 hours of infection (Fazakerley, 2002). The present study demonstrates intra-peritoneal infection with SFV generates relatively low levels of brain virus levels at PID 3 and 7, and appropriately TLR 3 upregulation was minimal. Conversely, in mice infected with SFV intracerebrally, transcripts were assayed far earlier at 24 and 42 hours post infection. These inoculations resulted in several orders of magnitude higher levels of brain virus by compared to intraperitoneal inoculation and appropriately exhibited dramatic upregulation of TLR 3. In addition, RABV infection given by the intracerebral route resulted in very high levels of viral replication (Theerasurakarn and Ubol, 1998), and the data here shows it was TLR 3 that was upregulated first at PID 2 and to high levels by PID 4 and 6, suggesting that TLR 3 function may be important during the early stage of infection. However, whether TLR 3 expression is a critical component of CNS immune responses to viruses remain to be determined. Investigating the course of infection and host immune responses during infection of TLR 3 deficient mice with SFV would be one way to enhance our understanding of the *in vivo* significance of TLR 3 expression.

6.8.4 Elevated TLR expression in the CNS of aged mice may partly explain the increased sensitivity of the brain to infection

TLR upregulation during the initial stages of SFV infection in both Balb/c and *nu/nu* was appropriate and specific. This perceived specificity is maintained following persistent infection of the brain as seen in *nu/nu* mice sampled 140 days post infection with SFV, with TLR 3 and 9 most substantially upregulated. In addition, Balb/c mice that were inoculated with PBSA alone upregulated most TLR transcripts by PID 140 despite the absence of infection. This would suggest glial cells exhibit higher levels of TLR expression as the brain ages. Age related increases in TLR expression would parallel the higher expression of other markers of activated microglia such as MHC-II and F4/80 in the aged human brain. Infant humans have few if any activated microglia in resting brain tissue and the number of activated microglia gradually increases with age (Streit et al., 1999). Alternatively, the increased level of TLR transcripts in the older mice may have represented expression by circulating monocytes that gradually infiltrate the brain as it matures. Unlike endogenously derived microglia, these infiltrating cells are known to express high levels of MHC and CD45 (Ford et al., 1995), and undergo cytoskeletal rearrangements so that they possess a morphology reminiscent of endogenous microglia (Streit et al., 1999). Nevertheless, TLR transcripts in the brain appeared to be higher in older mice. The brain is well known to become more sensitive to infection and prone to neurodegeneration as it ages; a phenomenon that could in part be a consequence of higher TLR expression that lowers the threshold for glial activation. In elderly humans, peripheral infections often result in the onset of dementia and putative glial cell activation. This suggests microbial components or extracellular messengers, induced by peripheral infection, trigger inflammatory processes in the brain that become clinically apparent as an episode of dementia (Perry, 2004; Perry et al., 2003; Holmes et al., 2003). In addition, the elderly are more susceptible to a range of neuroinvasive viruses such a West Nile virus and Japanese encephalitis virus, again perhaps a consequence of excessive glial activation (Solomon, 2004). Microglial activation and inflammatory reactions co-localise with viral antigen in the brain, and several reports have linked neuronal damage and dysfunction with microglial activation during viral encephalitis (Wang et al., 2003; Xiao et al., 2001; Shrestha et al., 2003). The production of several inflammatory mediators including TNF-α and IL-6 appear necessary and sufficient to induce neuronal death (Jeohn et al., 1998; Meda et al., 1995; Wang et al., 2004), whilst an absence of TLR 3 protects the brain from the counterproductive immune responses relating to infection with West Nile virus infection (Wang et al., 2004). TLR 9 signalling in microglia has also been shown to induce neuronal injury *in vitro* (Iliev et al., 2004). Taken together this would

suggest increased TLR expression in glial cells may partly contribute to the increased sensitivity of the aged brain to infection and enhance the susceptibility of the organ to inflammatory processes associated with viral infection.

6.8.5 Increased TLR expression in scrapie-infected brain indicates an involvement of innate immune processes

The form of glial activation observed during viral encephalitis could differ from that in scrapie. During viral encephalitis glial activation is rapid and associated with substantial cytokine and chemokine production. An inflammatory infiltrate of mononuclear cells and serum proteins develops which may contribute to the destruction of neural cells (Morris et al., 1997; Mack et al., 2003; Olson and Miller, 2004; Amor et al., 1996). Conversely, glial activation in scrapie is prominent but there is little associated production of inflammatory mediators and it occurs over a considerably longer period of time. An influx of inflammatory mononuclear cells is not evident in scrapie (Williams et al., 1997a; Brown et al., 2003). Appropriately the dynamics of TLR expression have been shown here to be different in each case, with the exception of TLR 2 upregulation that was prominent in both conditions.

TLR 2 upregulation was substantial and significant towards terminal disease during scrapie neuropathogenesis. This correlates with increased levels of several glial-associated transcripts such as CD68, complement components and GFAP (Brown et al., 2004; Eikelenboom et al., 2002). As described above, TLR 2 upregulation may represent a non-specific marker of innate immune activation. Alternatively, the substantial upregulation of TLR 2 may represent a mechanism by which the innate immune system senses infection. Indeed, small but physiologically relevant levels of bacterial lipoproteins upregulate TLR 2 expression in macrophages. This upregulation causes an increase in the cell's sensitivity to further challenge with TLR 2 ligands, and may represent an important mechanism by which the immune system boosts its response during the beginning of an immune response (Nilsen et al., 2004). Conceivably the upregulation of TLR 2 in the scrapie brain may represent a response by glial cells to determine the source and type of infection in a tissue undergoing extraordinary levels of neuronal damage and death.

These findings are relevant for our understanding of scrapie neuropathogenesis, since unlike viral encephalitis, few immune processes are observed and cytokine production is minimal. The data here suggests that activation of innate immunity in the brain, as demonstrated by TLR upregulation, occurred before clinical disease and was substantial at terminal disease. Upregulation of several TLR transcripts at 169 dpi correlated with neuronal loss in the hippocampus and may reflect activated glial processes that are toxic to resident neurones. In

comparison, upregulation of TLR at terminal disease occurred in a tissue demonstrating severe pathology that included; cell death, destruction of tissue architecture in addition to chronic glial activation (Brown et al., 2003). Further work will be required to determine the identities of the cell types exhibiting TLR upregulation. In addition, the number of mice sampled was small and the upregulation at 169 dpi for all TLR was variable. More work will be required to clarify whether the transcript changes described here can be repeated in both ME7 scrapie and in other TSE models.

It will be interesting to determine whether the upregulation of TLR in the scrapie brain is a reaction to neuronal damage or a contributor to that damage. Mice deficient in the TLR signalling adaptor Myd88 exhibit the same classic neuropathological changes that occur in wild type mice following infection with scrapie, suggesting TLR signalling is dispensable for disease progression (Prinz et al., 2003). However, it is now clear that some TLR can signal independently of MyD88 and so these results do not preclude the possibility that TLR have a role to play during scrapie neuropathogenesis. The increased level of TLR may explain why patients suffering from neurodegeneration are more sensitive to cognitive dysfunction following peripheral infection. Microglia are capable of releasing a wide barrage of neurotoxic mediators and have been implicated as a major determinant factor in the progression of neurodegeneration in TSE and AD (Eikelenboom et al., 2002). Marked activation of microglia occurs in close parallel to the deposition of amyloid fibrils, such as PrP^{Sc} in TSEs and β-amyloid in AD. In TSE, microglial activation is not only strictly associated with neurodegeneration (Williams et al., 1994; Muhleisen et al., 1995), but precedes neuronal death in the hippocampus of mice and is prior to the onset of clinical symptoms (Williams et al., 1997a; Giese et al., 1998). Several *in vitro* models have also implicated microglial processes as the major contributory factor in the death of PrP^{Sc}-infected neurones (Bate et al., 2001; Brown et al., 1996). These findings suggest activation of microglia may contribute to neuronal damage rather than be a reaction to it.

The initial stimulus that activates microglia in TSEs is likely to be the abnormal form of the prion protein, PrP^{Sc}. This agent is directly toxic to neurones, although significant neuronal death only occurs in the presence of glial cells (Brown et al., 1996). In the TSE-infected brain, PrP^{Sc} can be found as polymers of repeating units in the form of amyloid fibrils (Wille et al., 2002). Potentially these abnormal repeating patterns may be recognised by PRRs such as TLR and trigger a response more appropriate for defence against pathogens than endogenously derived protein, be they infections in the case of TSE, or non-infections as in the case of AD. Several studies have suggested PRRs are involved in the recognition of amyloid and the pathogenesis of neurodegeneration; CD14 binds β-amyloid and is

upregulated in mouse models of AD (Fassbender et al., 2004), whilst microglia deficient in CD14 cannot kill neurones through β-amyloid induced inflammation (Bate et al., 2004); and mice deficient in CD36 have marked reductions in the recruitment of microglia following β-amyloid injections and secrete lower levels of neurotoxic, inflammatory mediators (El Khoury et al., 2003). Together this suggests that PRRs may recognise amyloid and trigger an innate immune response that is damaging to CNS tissue.

Animal models of AD suggest that when activated microglia are stimulated by a systemic infection this results in significantly raised levels of IL-1β within the CNS, which may in turn potentiate neurodegeneration. In addition, humans suffering from AD are more prone to CNS complications and demonstrate decreased cognitive functions following systemic infection (Holmes et al., 2003; Perry et al., 2003). A mouse model of motor neurone disease suggests activation of innate immunity through TLR signalling in the brain exacerbates neurodegeneration (Nguyen et al., 2004). The present study suggests TLR may be upregulated during scrapie neurodegeneration and during the course of normal aging. TLR impart the ability to recognise infectious agents and increased TLR expression correlates with increased cytokine release upon TLR activation (Weiss et al., 2004). One can speculate that TLR may also be upregulated in other types of neurodegeneration such as AD, and may in part explain the more sensitive nature of degenerating CNS tissue to infection.

The innate activation of glia in neurodegeneration appears non-productive, i.e. neither is the adaptive immune system engaged nor is the stimulatory agent effectively removed, perhaps because the stimulus does not represent an immunogen of significant strength to activate T-cell responses. Indeed, models of TSE and AD in which adaptive immune responses are induced experimentally; demonstrate clearance of amyloid, reduced neuropathology and less severe cognitive dysfunction (Heppner et al., 2001; Enari et al., 2001; Janus et al., 2000). This would suggest that therapeutic intervention that translates the initial innate immune response of glia into an adaptive immune response may help resolve disease or slow disease progression. Indeed, several large scale clinical trials are currently underway to determine the efficacy of vaccines in the treatment of AD (Nitsch and Hock, 2004). Arguably, a better understanding of TLR function in neurodegeneration would enable more effective design of therapeutics in this emerging area.

Chapter 7 Overall discussion

This thesis has examined innate immune responses of CNS cells upon stimulation with LPS, infection with virus, and during the chronic neurodegeneration of TSE. The ability of the immunospecialised CNS environment to detect infection despite the absence of any recognisable immune process remains puzzling. This project aimed to explore the capability of CNS cells to express key PRRs and in more detail TLRs that function to recognise a variety of pathogen associated molecules. In addition, key genes involved in innate immune responses to pathogens were assayed. The results provide a new understanding of the innate capability of CNS cells to detect and respond to infection and are relevant not only to the acute stage of infection but also to our understanding of the neuropathogenesis of neurodegeneration, such as that exemplified by TSEs and AD.

Several techniques exist to describe gene expression at both the transcript and protein level. The approach taken here to utilise microarray technology was chosen since this permits the simultaneous analysis of many gene transcripts in one experimental sample. Using such an approach provided information on a whole host of genes that could not have been gained through analysis of each gene in isolation. Chapter 3 reports the development and validation of a novel custom microarray that assayed the expression of a multitude of key gene transcripts involved in innate immune responses. This technique required considerable development to obtain optimal conditions for hybridisation and minimise non-specific background signal. The process of hybridisation was found to generate considerable signal variation across the array surface and a methodology to correct for this experimental bias was introduced and developed. Several methodologies for normalising data sets between arrays were investigated. Probe design demonstrated that the distance from where the probe binds to from the 5'polyT cDNA tail had an impact on probe signal intensity. Future microarray design should take into account these findings, by either using alternative labelling strategies or limiting probe complementation to the extreme 5' end of the cDNA sequence.

The microarray platform was successfully utilised to characterise gene expression in resting, LPS-stimulated and SFV infected N9 microglia and responses generated were appropriate to the pathogen. The analysis revealed that resting N9 microglia expressed a multitude of gene transcripts involved in innate immune responses. These included; inflammatory mediators such as cytokines and chemokines; markers of activated phagocytes such as the cyloxygenases and the free radical generator NCF1 (p47phox); and pattern recognition receptors such as scavenger receptors. Notably the level of TLR expression was not adequately described by the microarray due to the inadequate sensitivity of the array

platform to detect these lowly expressed transcripts. Indeed, other work has shown that even in purified populations of macrophages TLR expression is barely detectable at the transcript and protein level (Weiss et al., 2004). TLR 2 was, however, consistently detected by the array. LPS stimulation profoundly changed N9 microglia gene transcript levels, underlying the potent nature of this component of gram-negative bacterial infection. LPS induced large changes in both proinflammatory cytokines and chemokines and several novel changes in scavenger receptor expression. Comparison of samples assayed by both microarray and QPCR indicated that the array could be relied upon qualitatively (if not quantitatively) to observe up or down-regulation of transcripts. These array findings therefore need to be validated using an alternative technique such as QPCR analysis of transcript levels or FACS analysis of protein expression.

Microarray analysis demonstrated that SFV infection of microglia initiated a different and appropriate response. This neuroinvasive virus is a well-established model of viral encephalitis that has also been used extensively to describe other aspects of virus biology such as virus-cell fusion (Gibbons et al., 2004) and has more recently been developed as a vector for the delivery of vaccines and as a tool for gene therapy (Atkins et al., 1999; Fazakerley, 2004). Despite the ability of microglia to respond to viral infection, activate T-cells *in vitro*, express pro-inflammatory mediators and generate many of the microbicidal molecules produced by activated macrophages; little work has been done to study the response of microglia to virus infection. The present study provides new insight into the nature of innate immune responses of N9 microglia at the transcript level. SFV infection initiated substantial upregulation of several chemokines and type-I IFN, although cytokine expression was minimal. Some of these findings were confirmed and further investigated by QPCR analysis in chapter 5.

These microarray results demonstrated the capability of microglia to respond in a distinct and appropriate manner to differing microbial stimuli. The rapid initiation of innate immune responses is critical to limit the spread of infection before adaptive immune responses can be generated. Innate immune responses can also modulate the form of adaptive immune response. The production of pro-inflammatory cytokines in response to LPS is a typical response of many leukocytes and serves to rapidly induce an inflammatory response that acts to clear gram-negative bacterial infection. Indeed, gram-negative bacteria provide a considerable challenge to the immune system due to the ability of LPS to inhibit phagocytosis. Conversely, the production of type-I IFN is critical for effective innate immune responses to virus infection and serves to exert potent anti-viral effects on surrounding cells, making them refractory to active viral replication. These findings confirm

the ability of microglia to respond to differing microbial stimuli and demonstrate microglia possess a capability to sense infection using a series of pattern recognition receptors.

QPCRs were developed that sensitively and accurately assayed the level of gene transcripts for the entire TLR family, several key cytokines and IFN. Glial cells expressed a multitude of TLRs, suggesting they can recognise a wide range of microbial associated molecules. Few other leukocytes in the body express such a broad repertoire of TLR; the extensive expression demonstrated by glia may be an essential strategy for a tissue that at rest is otherwise devoid of any recognisable immune process. Specificity of innate immune responses are possible through the differential use of TIR-containing adaptors molecules such as MyD88 and TRIF. Activation of differing TLR pathways results in the induction of distinct patterns of gene expression that are appropriate to control the infectious agent. The present study informs us that this model of innate immune specificity may apply to glial cells. In addition, the expression of TLR can confer the ability to directly kill pathogens. Macrophages deficient in TLR cannot kill phagocytosed bacteria or synthesis NO to the same extent as wild-type cells, and this may apply to microglia as well (Weiss et al., 2004).

The implicit appropriate nature of glial responses to infectious agents was underlined by the finding that in addition to cytokine transcripts, TLR transcript levels were also dynamically regulated in an appropriate and specific manner. In N9 microglia, LPS stimulation resulted in down-regulation of several TLR and upregulation of TLR 2 and 3, a response previously described in cultured macrophages (Sweet et al., 2002; Doyle et al., 2003). This response may serve to both limit over-excessive production of cytokines to a highly potent stimulator of the innate immune system, whilst TLR 2 and 3 upregulation has been suggested to provide specificity to innate immune responses. This hypothesis suggests microbe-stimulated macrophages upregulate both TLR 2 and 3 followed by differential TLR activation; with TLR 2 activation occurring if infection is bacterial and TLR 3 activation occurring if infection is viral (Weiss et al., 2004). In comparison to LPS stimulation, SFV infection of microglia upregulated several TLR, with TLR 3 exhibiting the largest increase. TLR 3 functions to recognise viral dsRNA and initiate type-I IFN responses, hence this response is appropriate.

This thesis has explored *in vivo* TLR expression in the resting and virally infected CNS for the first time. This provides us with a new insight into the innate immune capability of this important tissue to respond to infection. Several TLRs associated with responses to either viral structural components or viral nucleic acids were upregulated by RNA virus infection, whilst TLRs associated with sensing bacterial components were either unaffected, or not upregulated to a similar magnitude. TLR 2, 3 and 9 were significantly and most substantially

upregulated during infection with either a positive-stranded RNA virus, SFV, or a negative-stranded virus, RABV. The nature of this CNS reaction suggests upregulation of these three TLRs may be a response common to all RNA viruses. Whether DNA viruses such as *Herpes simplex* initiate similar TLR transcript level changes during CNS infection remains to be determined. Importantly, the type of cell that contributes to these changes remains to be determined. This thesis has shown microglia and astrocytes expressed TLRs at a comparable level *in vitro* and were capable of dynamically regulating TLRs upon SFV infection. The majority of publications have assumed the functional significance of TLR expression in microglia is paramount due to the ability of microglia to express higher levels of inflammatory mediators such as cytokines (Wang et al., 2004; Kurt-Jones et al., 2004b; Iliev et al., 2004; Kielian et al., 2002; Laflamme et al., 2001; Lee and Lee, 2002; Lehnardt et al., 2003). However, astrocytes are capable of producing cytokines and chemokines following TMEV infection, and can activate T-cells *in vitro* following IFN-γ stimulation (Carpentier et al., 2005). Importantly, astrocytes play a vital role as support cells to neurones. They have a multitude of functions that neutralise neurotoxic compounds and become activated upon neuronal injury in numerous conditions including acute ischaemic insult, virus infection and during chronic neurodegeneration (Liberto et al., 2004). Arguably, the ability of astrocytes to detect infection so that they can support neurones and prevent excessive neuronal damage associated with CNS infection may be more important than their ability to generate immune responses. Thus TLR expression on astrocytes may not necessarily suggest a role for this cell type in the generation of brain inflammation, but rather may further underlie the ability of these support cells to detect situations in which neuronal damage can occur. Indeed, the activation of astrocytes during the early stages of an immune response could be advantageous in limiting neuronal dysfunction that occurs as a secondary process to CNS immune responses. Thus, astrocytes may conceivably contribute to the TLR upregulation described *in vivo* during SFV and RABV infection. In particular, TLR 2 upregulation was far more substantial in astrocyte cultures, compared to microglia infected with SFV and this may be reflected *in vivo*. To determine the exact cellular identity of TLR expression *in vivo*, techniques must be developed that are sensitive enough to work on tissue sections. Few commercial antibodies exist that can detect TLR expression in the CNS and work undertaken in this laboratory (not shown here) using TLR monoclonal antibodies has failed to generate adequate signal on cryostat sections. In addition, polyclonal antibodies appear to lack the specificity required to label specific TLRs, presumably due to the highly conserved and repetitive nature of TLR sequences. Conceivably, TLR transcripts could be detected *in situ*

by hybridisation RNA probes. Nevertheless, further work will be required to clarify exactly which cell types contributes to the majority of TLR expression in the brain.

The relative importance of each TLR in sensing infections and generating immune responses remains to be clarified, however some work has begun to address this. Infection of mice deficient in TLR 2 with *Herpes simplex* exhibit markedly lower levels of brain inflammation and higher CNS titres (Kurt-Jones et al., 2004b), which suggests TLR 2 may be key to initiating CNS immune responses to DNA viruses, whilst similar experiments demonstrated TLR 4 expression was dispensable. TLR 2 expression is complex and not well understood (Nilsen et al., 2004) and the results here show it is independent of type-I IFN in the case of viral encephalitis. TLR 2 up regulation was also observed during scrapie pathogenesis, and occurs in a variety of other model systems that involve inflammation. The functional significance of TLR 2 upregulation during SFV or scrapie infection remains to be determined. TLR 3 plays an important role *in vivo* during WNV infection to initiate brain inflammation, whilst *in vitro* cultures of TLR 3 deficient microglia cannot kill neurones upon infection with WNV, unlike their wild-type counterparts (Wang et al., 2004). This suggests TLR 3 is important for both the initiation of immune responses and for generating responses that are harmful to neurones. These studies have shown the power of utilising knockout mice to elucidate the functional significance of TLR expression during CNS infection. Insight would be gained by investigating the course of CNS SFV infection in mice deficient in either TLRs or adaptor molecules such as MyD88.

Type-I IFN is a potent anti-viral system critical for early innate immune responses that limit viral replication *in vivo*. The dependence of TLR 3 and 9 upregulation during virus infection of the CNS on type-I IFN is a novel finding and further describes the effects of this potent anti-viral messenger. Two previous studies have linked TLR 3 upregulation to IFN-α/β production in cultured macrophages (Doyle et al., 2003; Miettinen et al., 2001). This present report demonstrates that this occurs *in vivo*, in this case during viral encephalitis, and in addition informs us TLR 9 expression is under IFN-mediated control. We propose that by upregulating TLR 3 and 9, IFN-α/β acts to increase the sensitivity of cells in the vicinity of virally infected cells. This parallels events with PKR another interferon inducible activator of innate cellular defences (Meurs et al., 1992; Tanaka et al., 1998; Goodbourn et al., 2000). Basal levels of PKR detect viral RNA and induce type-I IFN synthesis. This IFN acts in both an autocrine and paracrine way to upregulate a number of genes including PKR itself (Meurs et al., 1990). In this way cells in the vicinity of virally infected cells have their virus sensing mechanisms upregulated. Here we demonstrate that this also applies to two TLR associated with virus nucleic acid recognition, TLR 3 and 9.

To clear an actively replicating agent requires a robust immune response to limit microbial infection. Paradoxically, activation of glia and the production of inflammatory mediators result in the acute injury of neurones that may be vital for life-critical processes. In addition, inflammatory processes are also involved in the generation of neurological sequeale that can remain for the lifetime of the individual. The activation of microglia has been linked with neuronal damage in the case of HIV-associated dementia. Apoptotic neurones are closely associated with activated microglia (Adle-Biassette et al., 1999), whilst neurobehavioral abnormalities in infected primates correlate with the degree of microglial activation (Berman et al., 1999). The mechanisms that mediate glial activation are still to be clarified. However, the expression of TLR on microglia may be one route by which these cells are activated. In addition, the present study has reinforced the idea that microglia are capable of producing a wide variety of inflammatory cytokines, chemokines, and the enzymes necessary for the production of prostaglandins and microbicidal molecules such as reactive oxygen species. However, whilst studies such as this one and others have greatly increased our understanding on the capabilities and function of glia, the *in* vivo relevance of these findings during the course of CNS virus infection are still to be convincingly demonstrated.

Viral encephalitis is a disease that kills many thousands each year and leaves surviving patients with severe neurological sequelae. It can be caused by a variety of viruses endemic to various regions of the world, such as Japanese encephalitis virus and Venezuelan equine encephalitis virus. In both cases, the highest mortality is observed in immunologically naive children and the elderly (Solomon, 2004). Little can be done for patients presenting with viral encephalitis apart from basic bed rest and support. RABV is another important cause of death in the developing world and invariably leads to death once the virus has infected the nervous system. The lack of therapeutics for these diseases reflects our lack of understanding of the pathogenic mechanisms at play. Understandably, therapeutic trials are difficult to undertake due to the unpredictable nature of viral encephalitis incidence, and the reluctance of clinicians to use therapeutics that may worsen the condition of patients. Alternatively, work can be undertaken in animal models of viral encephalitis, such as that represented by SFV infection of the laboratory mouse. This system provides a useful way of better understanding these diseases and the fundamental interactions between host immune system, CNS and neuroinvasive viruses. Whilst it is too early to determine whether the findings of the present study can inform us of possible therapeutics, they do constitute a novel description of early innate immune responses. A better understating of TLR signalling and function in the CNS will undoubtedly increase our understanding of pathogenic mechanisms

of viral encephalitis and enable the development of rationales for the application of novel therapeutics.

Furthermore the expression of TLRs on glial cells has implications for a variety of other diseases that lack an obvious infectious component. Activated microglia are associated with a variety of neurodegenerative diseases such as Alzheimer's disease, motor neurone disease, TSE and multiple sclerosis. Many studies have highlighted the strict association of activated glia with neuronal dysfunction and death in these diseases, whilst *in vitro* models have implicated a pro-active role for microglia in neuronal damage. The mechanism that activates microglia in each case remains elusive. It will be interesting to investigate whether TLR function has a role to play in the activation of glia in these diseases. Together the diseases of chronic neurodegeneration affect a sizeable proportion of the population and are likely to contribute a growing burden on an increasingly elderly population. Therefore work that increases our understanding of these diseases is clearly a priority.

Reference list

Abraham,N., Stojdl,D.F., Duncan,P.I., Methot,N., Ishii,T., Dube,M., Vanderhyden,B.C., Atkins,H.L., Gray,D.A., McBurney,M.W., Koromilas,A.E., Brown,E.G., Sonenberg,N., and Bell,J.C. (1999). Characterization of transgenic mice with targeted disruption of the catalytic domain of the double-stranded RNA-dependent protein kinase, PKR. J. Biol. Chem. *274*, 5953-5962.

Adachi,O., Kawai,T., Takeda,K., Matsumoto,M., Tsutsui,H., Sakagami,M., Nakanishi,K., and Akira,S. (1998). Targeted disruption of the MyD88 gene results in loss of IL-1- and IL-18-mediated function. Immunity. *9*, 143-150.

Adle-Biassette,H., Chretien,F., Wingertsmann,L., Hery,C., Ereau,T., Scaravilli,F., Tardieu,M., and Gray,F. (1999). Neuronal apoptosis does not cor relate with dementia in HIV infection but is related to microglial activation and axonal damage. Neuropathol. Appl. Neurobiol. *25*, 123-133.

Ahmad-Nejad,P., Hacker,H., Rutz,M., Bauer,S., Vabulas,R.M., and Wagner,H. (2002). Bacterial CpG-DNA and lipopolysaccharides activate Toll-like receptors at distinct cellular compartments. Eur. J. Immunol. *32*, 1958-1968.

Akashi,S., Nagai,Y., Ogata,H., Oikawa,M., Fukase,K., Kusumoto,S., Kawasaki,K., Nishijima,M., Hayashi,S., Kimoto,M., and Miyake,K. (2001). Human MD-2 confers on mouse Toll-like receptor 4 species-specific lipopolysaccharide recognition. Int. Immunol. *13*, 1595-1599.

Akira,S. and Takeda,K. (2004). Toll-like receptor signalling. Nat. Rev. Immunol. *4*, 499-511.

Albrecht,P.J., Murtie,J.C., Ness,J.K., Redwine,J.M., Enterline,J.R., Armstrong,R.C., and Levison,S.W. (2003). Astrocytes produce CNTF during the remyelination phase of viral-induced spinal cord demyelination to stimulate FGF-2 production. Neurobiol. Dis. *13*, 89-101.

Alexopoulou,L., Holt,A.C., Medzhitov,R., and Flavell,R.A. (2001). Recognition of double-stranded RNA and activation of NF-kappaB by Toll-like receptor 3. Nature *413*, 732-738.

Aliprantis,A.O., Yang,R.B., Mark,M.R., Suggett,S., Devaux,B., Radolf,J.D., Klimpel,G.R., Godowski,P., and Zychlinsky,A. (1999). Cell activation and apoptosis by bacterial lipoproteins through toll-like receptor-2. Science *285*, 736-739.

Allsopp,T.E. and Fazakerley,J.K. (2000). Altruistic cell suicide and the specialized case of the virus-infected nervous system. Trends Neurosci. *23*, 284-290.

Allsopp,T.E., Scallan,M.F., Williams,A., and Fazakerley,J.K. (1998). Virus infection induces neuronal apoptosis: A comparison with trophic factor withdrawal. Cell Death. Differ. *5*, 50-59.

Aloisi,F., Ria,F., and Adorini,L. (2000). Regulation of T-cell responses by CNS antigen-presenting cells: different roles for microglia and astrocytes. Immunol. Today *21*, 141-147.

Amor,S., Scallan,M.F., Morris,M.M., Dyson,H., and Fazakerley,J.K. (1996). Role of immune responses in protection and pathogenesis during Semliki Forest virus encephalitis. J Gen Virol *77 (Pt 2)*, 281-291.

Amor,S. and Webb,H.E. (1987). The effect of cycloleucine on SFV A7(74) infection in mice. Br. J. Exp. Pathol. *68*, 225-235.

Amor,S. and Webb,H.E. (1988). CNS pathogenesis following a dual viral infection with Semliki Forest (alphavirus) and Langat (flavivirus). Br. J. Exp. Pathol. *69*, 197-208.

Anderson,K.V., Bokla,L., and Nusslein-Volhard,C. (1985). Establishment of dorsal-ventral polarity in the Drosophila embryo: the induction of polarity by the Toll gene product. Cell *42*, 791-798.

Asai,T., Tena,G., Plotnikova,J., Willmann,M.R., Chiu,W.L., Gomez-Gomez,L., Boller,T., Ausubel,F.M., and Sheen,J. (2002). MAP kinase signalling cascade in Arabidopsis innate immunity. Nature *415*, 977-983.

Ashkenas,J., Penman,M., Vasile,E., Acton,S., Freeman,M., and Krieger,M. (1993). Structures and high and low affinity ligand binding properties of murine type I and type II macrophage scavenger receptors. J. Lipid Res. *34*, 983-1000.

Asselin-Paturel,C., Boonstra,A., Dalod,M., Durand,I., Yessaad,N., Dezutter-Dambuyant,C., Vicari,A., O'Garra,A., Biron,C., Briere,F., and Trinchieri,G. (2001). Mouse type I IFN-producing cells are immature APCs with plasmacytoid morphology. Nat. Immunol. *2*, 1144-1150.

Atkins,G.J., Sheahan,B.J., and Liljestrom,P. (1999). The molecular pathogenesis of Semliki Forest virus: a model virus made useful? J Gen Virol *80 (Pt 9)*, 2287-2297.

Au,W.C., Moore,P.A., LaFleur,D.W., Tombal,B., and Pitha,P.M. (1998). Characterization of the interferon regulatory factor-7 and its potential role in the transcription activation of interferon A genes. J. Biol. Chem. *273*, 29210-29217.

Bafica,A., Scanga,C.A., Schito,M., Chaussabel,D., and Sher,A. (2004). Influence of coinfecting pathogens on HIV expression: evidence for a role of Toll-like receptors. J. Immunol. *172*, 7229-7234.

Bafica,A., Scanga,C.A., Schito,M.L., Hieny,S., and Sher,A. (2003). Cutting edge: in vivo induction of integrated HIV-1 expression by mycobacteria is critically dependent on Toll-like receptor 2. J. Immunol. *171*, 1123-1127.

Bakker,A.B., Baker,E., Sutherland,G.R., Phillips,J.H., and Lanier,L.L. (1999). Myeloid DAP12-associating lectin (MDL)-1 is a cell surface receptor involved in the activation of myeloid cells. Proc. Natl. Acad. Sci. U. S. A *96*, 9792-9796.

Balachandran,S., Roberts,P.C., Brown,L.E., Truong,H., Pattnaik,A.K., Archer,D.R., and Barber,G.N. (2000a). Essential role for the dsRNA-dependent protein kinase PKR in innate immunity to viral infection. Immunity. *13*, 129-141.

Balachandran,S., Roberts,P.C., Kipperman,T., Bhalla,K.N., Compans,R.W., Archer,D.R., and Barber,G.N. (2000b). Alpha/beta interferons potentiate virus-induced apoptosis through activation of the FADD/Caspase-8 death signaling pathway. J. Virol. *74*, 1513-1523.

Balluz,I.M., Glasgow,G.M., Killen,H.M., Mabruk,M.J., Sheahan,B.J., and Atkins,G.J. (1993). Virulent and avirulent strains of Semliki Forest virus show similar cell tropism for the murine central nervous system but differ in the severity and rate of induction of cytolytic damage. Neuropathol. Appl. Neurobiol. *19*, 233-239.

Banchereau,J. and Steinman,R.M. (1998). Dendritic cells and the control of immunity. Nature *392*, 245-252.

Barron,K.D., Marciano,F.F., Amundson,R., and Mankes,R. (1990). Perineuronal glial responses after axotomy of central and peripheral axons. A comparison. Brain Res. *523*, 219-229.

Bartlett,N., Symons,J.A., Tscharke,D.C., and Smith,G.L. (2002). The vaccinia virus N1L protein is an intracellular homodimer that promotes virulence. J. Gen. Virol. *83*, 1965-1976.

Bate,C., Boshuizen,R.S., Langeveld,J.P., and Williams,A. (2002). Temporal and spatial relationship between the death of PrP-damaged neurones and microglial activation. Neuroreport *13*, 1695-1700.

Bate,C., Reid,S., and Williams,A. (2001). Killing of prion-damaged neurones by microglia. Neuroreport *12*, 2589-2594.

Bate,C., Veerhuis,R., Eikelenboom,P., and Williams,A. (2004). Microglia kill amyloid -beta1-42 damaged neurons by a CD14-dependent process. Neuroreport *15*, 1427-1430.

Bauer,S., Kirschning,C.J., Hacker,H., Redecke,V., Hausmann,S., Akira,S., Wagner,H., and Lipford,G.B. (2001). Human TLR9 confers responsiveness to bacterial DNA via species -specific CpG motif recognition. Proc. Natl. Acad. Sci. U. S. A *98*, 9237-9242.

Bell,J.K., Mullen,G.E., Leifer,C.A., Mazzoni,A., Davies,D.R., and Segal,D.M. (2003). Leucine -rich repeats and pathogen recognition in Toll-like receptors. Trends Immunol. *24*, 528-533.

Belvin,M.P. and Anderson,K.V. (1996). A conserved signaling pathway: the Drosophila toll-dorsal pathway. Annu. Rev. Cell Dev. Biol. *12*, 393-416.

Benveniste,E.N., Nguyen,V.T., and O'Keefe,G.M. (2001). Immunological aspects of microglia: relevance to Alzheimer's disease. Neurochem. Int. *39*, 381-391.

Bergeron,J., Mabrouk,T., Garzon,S., and Lemay,G. (1998). Characterization of the thermosensitive ts453 reovirus mutant: increased dsRNA binding of sigma 3 protein correlates with interferon resistance. Virology *246*, 199-210.

Berglund,P., Tubulekas,I., and Liljestrom,P. (1996). Alphaviruses as vectors for gene delivery. Trends Biotechnol. *14*, 130-134.

Berman,N.E., Marcario,J.K., Yong,C., Raghavan,R., Raymond,L.A., Joag,S.V., Narayan,O., and Cheney,P.D. (1999). Microglial activation and neurological symptoms in the SIV model of NeuroAIDS: association of MHC-II and MMP-9 expression with behavioral deficits and evoked potential changes. Neurobiol. Dis. *6*, 486-498.

Beutler,B. (2002). LPS in microbial pathogenesis: promise and fulfilment. J. Endotoxin. Res. *8*, 329-335.

Bieback,K., Lien,E., Klagge,I.M., Avota,E., Schneider-Schaulies,J., Duprex,W.P., Wagner,H., Kirschning,C.J., ter,M., V, and Schneider-Schaulies,S. (2002). Hemagglutinin protein of wild-type measles virus activates toll-like receptor 2 signaling. J. Virol. *76*, 8729-8736.

Birchler,T., Seibl,R., Buchner,K., Loeliger,S., Seger,R., Hossle,J.P., Aguzzi,A., and Lauener,R.P. (2001). Human Toll-like receptor 2 mediates induction of the antimicrobial peptide human beta-defensin 2 in response to bacterial lipoprotein. Eur. J. Immunol. *31*, 3131-3137.

Bjorkbacka,H., Kunjathoor,V.V., Moore,K.J., Koehn,S., Ordija,C.M., Lee,M.A., Means,T., Halmen,K., Luster,A.D., Golenbock,D.T., and Freeman,M.W. (2004). Reduced atherosclerosis in MyD88-null mice links elevated serum cholesterol levels to activation of innate immunity signaling pathways. Nat. Med. *10*, 416-421.

Boehme,K.W. and Compton,T. (2004). Innate sensing of viruses by toll-like receptors. J. Virol. *78*, 7867-7873.

Boehme,K.W., Singh,J., Perry,S.T., and Compton,T. (2004). Human cytomegalovirus elicits a coordinated cellular antiviral response via envelope glycoprotein B. J. Virol. *78*, 1202-1211.

Bosisio,D., Polentarutti,N., Sironi,M., Bernasconi,S., Miyake,K., Webb,G.R., Martin,M.U., Mantovani,A., and Muzio,M. (2002). Stimulation of toll-like receptor 4 expression in human mononuclear phagocytes by interferon-gamma: a molecular basis for priming and synergism with bacterial lipopolysaccharide. Blood *99*, 3427-3431.

Bouchon,A., Hernandez-Munain,C., Cella,M., and Colonna,M. (2001). A DAP12-mediated pathway regulates expression of CC chemokine receptor 7 and maturation of human dendritic cells. J. Exp. Med. *194*, 1111-1122.

Bourke,E., Bosisio,D., Golay,J., Polentarutti,N., and Mantovani,A. (2003). The toll-like receptor repertoire of human B lymphocytes: inducible and selective expression of TLR9 and TLR10 in normal and transformed cells. Blood *102*, 956-963.

Bowie,A., Kiss-Toth,E., Symons,J.A., Smith,G.L., Dower,S.K., and O'Neill,L.A. (2000). A46R and A52R from vaccinia virus are antagonists of host IL-1 and toll-like receptor signaling. Proc. Natl. Acad. Sci. U. S. A *97*, 10162-10167.

Bowman,C.C., Rasley,A., Tranguch,S.L., and Marriott,I. (2003). Cultured astrocytes express toll-like receptors for bacterial products. Glia *43*, 281-291.

Bozza,M., Satoskar,A.R., Lin,G., Lu,B., Humbles,A.A., Gerard,C., and David,J.R. (1999). Targeted disruption of migration inhibitory factor gene reveals its critical role in sepsis. J. Exp. Med. *189*, 341-346.

Bradish,C.J., Allner,K., and Fitzgeorge,R. (1975). Immunomodification and the expression of virulence in mice by defined strains of Semliki Forest virus: the effects of cyclophosphamide. J. Gen. Virol. *28*, 225-237.

Bradish,C.J., Allner,K., and Maber,H.B. (1971). The virulence of original and derived strains of Semliki forest virus for mice, guinea-pigs and rabbits. J. Gen. Virol. *12*, 141-160.

Bradley,J.R. and Pober,J.S. (2001). Tumor necrosis factor receptor-associated factors (TRAFs). Oncogene *20*, 6482-6491.

Brannan,C.A. and Roberts,M.R. (2004). Resident microglia from adult mice are refractory to nitric oxide-inducing stimuli due to impaired NOS2 gene expression. Glia *48*, 120-131.

Brightbill,H.D., Libraty,D.H., Krutzik,S.R., Yang,R.B., Belisle,J.T., Bleharski,J.R., Maitland,M., Norgard,M.V., Plevy,S.E., Smale,S.T., Brennan,P.J., Bloom,B.R., Godowski,P.J., and Modlin,R.L. (1999). Host defense mechanisms triggered by microbial lipoproteins through toll-like receptors. Science *285*, 732-736.

Brochu,S., Olivier,M., and Rivest,S. (1999). Neuronal activity and transcription of proinflammatory cytokines, IkappaBalpha, and iNOS in the mouse brain during acute endotoxemia and chronic infection with Trypanosoma brucei brucei. J. Neurosci. Res. *57*, 801-816.

Brown,A.R., Webb,J., Rebus,S., Walker,R., Williams,A., and Fazakerley,J.K. (2003). Inducible cytokine gene expression in the brain in the ME7/CV mouse model of scrapie is highly restricted, is at a strikingly low level relative to the degree of gliosis and occurs only late in disease. J Gen Virol *84*, 2605-2611.

Brown,A.R., Webb,J., Rebus,S., Williams,A., and Fazakerley,J.K. (2004). Identification of up-regulated genes by array analysis in scrapie-infected mouse brains. Neuropathol. Appl. Neurobiol. *30*, 555-567.

Brown,D.R., Schmidt,B., and Kretzschmar,H.A. (1996). Role of microglia and host prion protein in neurotoxicity of a prion protein fragment. Nature *380*, 345-347.

Brown,P., Gibbs,C.J., Jr., Rodgers-Johnson,P., Asher,D.M., Sulima,M.P., Bacote,A., Goldfarb,L.G., and Gajdusek,D.C. (1994). Human spongiform encephalopathy: the National Institutes of Health series of 300 cases of experimentally transmitted disease. Ann. Neurol. *35*, 513-529.

Bruce,M.E., Will,R.G., Ironside,J.W., McConnell,I., Drummond,D., Suttie,A., McCardle,L., Chree,A., Hope,J., Birkett,C., Cousens,S., Fraser,H., and Bostock,C.J. (1997). Transmissions to mice indicate that 'new variant' CJD is caused by the BSE agent. Nature *389*, 498-501.

Bsibsi,M., Ravid,R., Gveric,D., and van Noort,J.M. (2002). Broad expression of Toll-like receptors in the human central nervous system. J. Neuropathol. Exp. Neurol. *61*, 1013-1021.

Buechler,C., Ritter,M., Quoc,C.D., Agildere,A., and Schmitz,G. (1999). Lipopolysaccharide inhibits the expression of the scavenger receptor Cla-1 in human monocytes and macrophages. Biochem. Biophys. Res. Commun. *262*, 251-254.

Bueler,H., Raeber,A., Sailer,A., Fischer,M., Aguzzi,A., and Weissmann,C. (1994). High prion and PrPSc levels but delayed onset of disease in scrapie-inoculated mice heterozygous for a disrupted PrP gene. Mol. Med. *1*, 19-30.

Burns,K., Janssens,S., Brissoni,B., Olivos,N., Beyaert,R., and Tschopp,J. (2003). Inhibition of interleukin 1 receptor/Toll-like receptor signaling through the alternatively spliced, short form of MyD88 is due to its failure to recruit IRAK-4. J. Exp. Med. *197*, 263-268.

Burzyn,D., Rassa,J.C., Kim,D., Nepomnaschy,I., Ross,S.R., and Piazzon,I. (2004). Toll-like receptor 4-dependent activation of dendritic cells by a retrovirus. J. Virol. *78*, 576-584.

Cario,E. and Podolsky,D.K. (2000). Differential alteration in intestinal epithelial cell expression of toll-like receptor 3 (TLR3) and TLR4 in inflammatory bowel disease. Infect. Immun. *68*, 7010-7017.

Carpentier,P.A., Begolka,W.S., Olson,J.K., Elhofy,A., Karpus,W.J., and Miller,S.D. (2005). Differential activation of astrocytes by innate and adaptive immune stimuli. Glia *49*, 360-374.

Carson,M.J., Reilly,C.R., Sutcliffe,J.G., and Lo,D. (1998). Mature microglia resemble immature antigen-presenting cells. Glia *22*, 72-85.

Causton,H.C., Quackenbush,J., and Brazma,A. (2003). Microarray Gene Expression and Data Analysis: a beginner's guide. (United Kingdom: Blackwell Publishing), pp. 1-150.

Chang,H.W., Watson,J.C., and Jacobs,B.L. (1992). The E3L gene of vaccinia virus encodes an inhibitor of the interferon-induced, double-stranded RNA-dependent protein kinase. Proc. Natl. Acad. Sci. U. S. A *89*, 4825-4829.

Chapman,G.A., Moores,K., Harrison,D., Campbell,C.A., Stewart,B.R., and Strijbos,P.J. (2000). Fractalkine cleavage from neuronal membranes represents an acute event in the inflammatory response to excitotoxic brain damage. J. Neurosci. *20*, RC87.

Chin,Y.E., Kitagawa,M., Kuida,K., Flavell,R.A., and Fu,X.Y. (1997). Activation of the STAT signaling pathway can cause expression of caspase 1 and apoptosis. Mol. Cell Biol. *17*, 5328-5337.

Choe,K.M., Werner,T., Stoven,S., Hultmark,D., and Anderson,K.V. (2002). Requirement for a peptidoglycan recognition protein (PGRP) in Relish activation and antibacterial immune responses in Drosophila. Science *296*, 359-362.

Chu,W.M., Ostertag,D., Li,Z.W., Chang,L., Chen,Y., Hu,Y., Williams,B., Perrault,J., and Karin,M. (1999). JNK2 and IKKbeta are required for activating the innate response to viral infection. Immunity. *11*, 721-731.

Chuang,T. and Ulevitch,R.J. (2001). Identification of hTLR10: a novel human Toll-like receptor preferentially expressed in immune cells. Biochim. Biophys. Acta *1518*, 157-161.

Chuang,T.H. and Ulevitch,R.J. (2000). Cloning and characterization of a sub-family of human toll-like receptors: hTLR7, hTLR8 and hTLR9. Eur. Cytokine Netw. *11*, 372-378.

Coelho,P.S., Klein,A., Talvani,A., Coutinho,S.F., Takeuchi,O., Akira,S., Silva,J.S., Canizzaro,H., Gazzinelli,R.T., and Teixeira,M.M. (2002). Glycosylphosphatidylinositol-anchored mucin-like glycoproteins isolated from Trypanosoma cruzi trypomastigotes induce in vivo le ukocyte recruitment dependent on MCP-1 production by IFN-gamma-primed-macrophages. J. Leukoc. Biol. *71*, 837-844.

Compton,T., Kurt-Jones,E.A., Boehme,K.W., Belko,J., Latz,E., Golenbock,D.T., and Finberg,R.W. (2003). Human cytomegalovirus activates inflammatory cytokine responses via CD14 and Toll-like receptor 2. J. Virol. *77*, 4588-4596.

Coraci,I.S., Husemann,J., Berman,J.W., Hulette,C., Dufour,J.H., Campanella,G.K., Luster,A.D., Silverstein,S.C., and El Khoury,J.B. (2002). CD36, a class B scavenger receptor, is expressed on microglia in Alzheimer's disease brains and can mediate production of reactive oxygen species in response to beta-amyloid fibrils. Am. J. Pathol. *160*, 101-112.

Cotran,R.S.K.V.a.C.T. (2004). Robbins pathologic basis of disease. (Philadelphia, USA.: *Saunders*), pp. 251-257.

Cuadros,M.A. and Navascues,J. (1998). The origin and differentiation of microglial cells during development. Prog. Neurobiol. *56*, 173-189.

Cuadros,M.A. and Navascues,J. (2001). Early origin and colonization of the developing central nervous system by microglial precursors. Prog. Brain Res. *132*, 51-59.

D'Aversa,T.G., Weidenheim,K.M., and Berman,J.W. (2002). CD40-CD40L interactions induce chemokine expression by human microglia: implications for human immunodeficiency virus encephalitis and multiple sclerosis. Am. J. Pathol. *160*, 559-567.

Da Silva,C.J., Soldau,K., Christen,U., Tobias,P.S., and Ulevitch,R.J. (2001). Lipopolysaccharide is in close proximity to each of the proteins in its membrane receptor complex. transfer from CD14 to TLR4 and MD-2. J. Biol. Chem. *276*, 21129-21135.

Dalpke,A.H., Opper,S., Zimmermann,S., and Heeg,K. (2001). Suppressors of cytokine signaling (SOCS)-1 and SOCS-3 are induced by CpG-DNA and modulate cytokine responses in APCs. J. Immunol. *166*, 7082-7089.

Dalpke,A.H., Schafer,M.K., Frey,M., Zimmermann,S., Tebbe,J., Weihe,E., and Heeg,K. (2002). Immunostimulatory CpG-DNA activates murine microglia. J. Immunol. *168*, 4854-4863.

Deller,J.J., Jr. and Russell,P.K. (1968). Chikungunya disease. Am. J. Trop. Med. Hyg. *17*, 107-111.

Diebold,S.S., Kaisho,T., Hemmi,H., Akira,S., and Reis e Sousa (2004). Innate antiviral responses by means of TLR7-mediated recognition of single-stranded RNA. Science *303*, 1529-1531.

DiPerna,G., Stack,J., Bowie,A.G., Boyd,A., Kotwal,G., Zhang,Z., Arvikar,S., Latz,E., Fitzgerald,K.A., and Marshall,W.L. (2004). Poxvirus protein N1L targets the I-kappa B kinase complex, inhibits signaling to NF-kappa B by the tumor necrosis factor superfamily of receptors, and inhibits NF-kappa B and IRF3 signaling by toll-like receptors. J. Biol. Chem.

Donnelly,S.M., Sheahan,B.J., and Atkins,G.J. (1997). Long-term effects of Semliki Forest virus infection in the mouse central nervous system. Neuropathol. Appl. Neurobiol. *23*, 235-241.

Doyle,S., Vaidya,S., O'Connell,R., Dadgostar,H., Dempsey,P., Wu,T., Rao,G., Sun,R., Haberland,M., Modlin,R., and Cheng,G. (2002). IRF3 mediates a TLR3/TLR4-specific antiviral gene program. Immunity. *17*, 251-263.

Doyle,S.E., O'Connell,R., Vaidya,S.A., Chow,E.K., Yee,K., and Cheng ,G. (2003). Toll-like receptor 3 mediates a more potent antiviral response than Toll-like receptor 4. J. Immunol. *170*, 3565-3571.

Dreyfus,C.F. (1998). Neurotransmitters and neurotrophins collaborate to influence brain development. Perspect. Dev. Neurobiol. *5*, 389-399.

Du,X., Poltorak,A., Wei,Y., and Beutler,B. (2000). Three novel mammalian toll-like receptors: gene structure, expression, and evolution. Eur. Cytokine Netw. *11*, 362-371.

Dunne,A., Ejdeback,M., Ludidi,P.L., O'Neill,L.A., and Gay,N.J. (2003). Structural complementarity of Toll/interleukin-1 receptor domains in Toll-like receptors and the adaptors Mal and MyD88. J. Biol. Chem. *278*, 41443-41451.

Dziarski,R. (2004). Peptidoglycan recognition proteins (PGRPs). Mol. Immunol. *40*, 877-886.

Dziarski,R., Platt,K.A., Gelius,E., Steiner,H., and Gupta,D. (2003). Defect in neutrophil killing and increased susceptibility to infection with nonpathogenic gram-positive bacteria in peptidoglycan recognition protein-S (PGRP-S)-deficient mice. Blood *102*, 689-697.

Eaves-Pyles,T., Murthy,K., Liaudet,L., Virag,L., Ross,G., Soriano,F.G., Szabo,C., and Salzman,A.L. (2001). Flagellin, a novel mediator of Salmonella-induced epithelial activation and systemic inflammation: I kappa B alpha degradation, induction of nitric oxide synthase, induction of proinflammatory mediators, and cardiovascular dysfunction. J. Immunol. *166*, 1248-1260.

Ebrahimi,B., Dutia,B.M., Roberts,K.L., Garcia-Ramirez,J.J., Dickinson,P., Stewart,J.P., Ghazal,P., Roy,D.J., and Nash,A.A. (2003). Transcriptome profile of murine gammaherpesvirus-68 lytic infection. J. Gen. Virol. *84*, 99-109.

Edelmann,K.H., Richardson-Burns,S., Alexopoulou,L., Tyler,K.L., Flavell,R.A., and Oldstone,M.B. (2004). Does Toll-like receptor 3 play a biological role in virus infections? Virology *322*, 231-238.

Edfeldt,K., Swedenborg,J., Hansson,G.K., and Yan,Z.Q. (2002). Expression of toll-like receptors in human atherosclerotic lesions: a possible pathway for plaque activation. Circulation *105*, 1158-1161.

Edwards,J.A., Denis,F., and Talbot,P.J. (2000). Activation of glial cells by human coronavirus OC43 infection. J. Neuroimmunol. *108*, 73-81.

Eikelenboom,P., Bate,C., Van Gool,W.A., Hoozemans,J.J., Rozemuller,J.M., Veerhuis,R., and Williams,A. (2002). Neuroinflammation in Alzheimer's disease and prion disease. Glia *40*, 232-239.

Eklind,S., Mallard,C., Leverin,A.L., Gilland,E., Blomgren,K., Mattsby-Baltzer,I., and Hagberg,H. (2001). Bacterial endotoxin sensitizes the immature brain to hypoxic--ischaemic injury. Eur. J. Neurosci. *13*, 1101-1106.

El Khoury,J., Hickman,S.E., Thomas,C.A., Cao,L., Silverstein,S.C., and Loike,J.D. (1996). Scavenger receptor-mediated adhesion of microglia to beta-amyloid fibrils. Nature *382*, 716-719.

El Khoury,J.B., Moore,K.J., Means,T.K., Leung,J., Terada,K., Toft,M., Freeman,M.W., and Luster,A.D. (2003). CD36 mediates the innate host response to beta -amyloid. J. Exp. Med. *197*, 1657-1666.

Enari,M., Flechsig,E., and Weissmann,C. (2001). Scrapie prion protein accumulation by scrapie-infected neuroblastoma cells abrogated by exposure to a prion protein antibody. Proc. Natl. Acad. Sci. U. S. A *98*, 9295-9299.

Eng,L.F. (1985). Glial fibrillary acidic protein (GFAP): the major protein of glial intermediate filaments in differentiated astrocytes. J. Neuroimmunol. *8*, 203-214.

Eng,L.F., Ghirnikar,R.S., and Lee,Y.L. (2000). Glial fibrillary acidic protein: GFAP-thirty-one years (1969-2000). Neurochem. Res. *25*, 1439-1451.

Erlandsson,L., Blumenthal,R., Eloranta,M.L., Engel,H., Alm,G., Weiss,S., and Leanderson,T. (1998). Interferon-beta is required for interferon-alpha production in mouse fibroblasts. Curr. Biol. *8*, 223-226.

Esen,N., Tanga,F.Y., DeLeo,J.A., and Kielian,T. (2004). Toll-like receptor 2 (TLR2) mediates astrocyte activation in response to the Gram-positive bacterium Staphylococcus aureus. J. Neurochem. *88*, 746-758.

Fan,H. and Cook,J.A. (2004). Molecular mechanisms of endotoxin tolerance. J. Endotoxin. Res. *10*, 71-84.

Fassbender,K., Walter,S., Kuhl,S., Landmann,R., Ishii,K., Bertsch,T., Stalder,A.K., Muehlhauser,F., Liu,Y., Ulmer,A.J., Rivest,S., Lentschat,A., Gulbins,E., Jucker,M., Staufenbiel,M., Brechtel,K., Walter,J., Multhaup,G., Penke,B., Adachi,Y., Hartmann,T., and Beyreuther,K. (2004). The LPS receptor (CD14) links innate immunity with Alzheimer's disease. FASEB J. *18*, 203-205.

Fawaz,L.M., Sharif-Askari,E., and Menezes,J. (1999). Up-regulation of NK cytotoxic activity via IL-15 induction by different viruses: a comparative study. J. Immunol. *163*, 4473-4480.

Fazakerley,J.K. (2002). Pathogenesis of Semliki Forest virus encephalitis. J Neurovirol. *8 Suppl 2*, 66-74.

Fazakerley,J.K. (2004). Semliki forest virus infection of laboratory mice: a model to study the pathogenesis of viral encephalitis. Arch. Virol. Suppl 179-190.

Fazakerley,J.K., Boyd,A., Mikkola,M.L., and Kaaria inen,L. (2002). A single amino acid change in the nuclear localization sequence of the nsP2 protein affects the neurovirulence of Semliki Forest virus. J. Virol. *76*, 392-396.

Fazakerley,J.K., Pathak,S., Scallan,M., Amor,S., and Dyson,H. (1993). Replication of the A7(74) strain of Semliki Forest virus is restricted in neurons. Virology *195*, 627-637.

Fazakerley,J.K. and Walker,R. (2003). Virus demyelination. J. Neurovirol. *9*, 148-164.

Fazakerley,J.K. and Webb,H.E. (1987a). Cyclosporine enhances virally induced T-cell-mediated demyelination. The effect of cyclosporine on a demyelinating virus infection. J. Neurol. Sci. *78*, 35-50.

Fazakerley,J.K. and Webb,H.E. (1987b). Semliki Forest virus induced, immune mediated demyelination: the effect of irradiation. Br. J. Exp. Pathol. *68*, 101-113.

Fazakerley,J.K. and Webb,H.E. (1987c). Semliki Forest virus-induced, immune-mediated demyelination: adoptive transfer studies and viral persistence in nude mice. J. Gen. Virol. *68 (Pt 2)*, 377-385.

Febbraio,M., Hajjar,D.P., and Silverstein,R.L. (2001). CD36: a class B scavenger receptor involved in angiogenesis, atherosclerosis, inflammation, and lipid metabolism. J. Clin. Invest *108*, 785-791.

Ferrari,D., Villalba,M., Chiozzi,P., Falzoni,S., Ricciardi-Castagnoli,P., and Di Virgilio,F. (1996). Mouse microglial cells express a plasma membrane pore gated by extracellular ATP. J. Immunol. *156*, 1531-1539.

Fiette,L., Aubert,C., Muller,U., Huang,S., Aguet,M., Brahic,M., and Bureau,J.F. (1995). Theiler's virus infection of 129Sv mice that lack the interferon alpha/beta or interferon gamma receptors. J. Exp. Med. *181*, 2069-2076.

Fischer,M., Rulicke,T., Raeber,A., Sailer,A., Moser,M., Oesch,B., Brandner,S., Aguzzi,A., and Weissmann,C. (1996). Prion protein (PrP) with amino-proximal deletions restoring susceptibility of PrP knockout mice to scrapie. EMBO J. *15*, 1255-1264.

Fitzgerald,K.A., McWhirter,S.M., Faia,K.L., Rowe,D.C., Latz,E., Golenbock,D.T., Coyle,A.J., Liao,S.M., and Maniatis,T. (2003). IKKepsilon and TBK1 are essential components of the IRF3 signaling pathway. Nat. Immunol. *4*, 491-496.

Fitzgerald,K.A., Palsson-McDermott,E.M., Bowie,A.G., Jefferies,C.A., Mansell,A.S., Brady,G., Brint,E., Dunne,A., Gray,P., Harte,M.T., McMurray,D., Smith,D.E., Sims,J.E., Bird,T.A., and O'Neill,L.A. (2001). Mal (MyD88-adapter-like) is required for Toll-like receptor-4 signal transduction. Nature *413*, 78-83.

Fleeton,M.N., Chen,M., Berglund,P., Rhodes,G., Parker,S.E., Murphy,M., Atkins,G.J., and Liljestrom,P. (2001). Self-replicative RNA vaccines elicit protection against influenza A virus, respiratory syncytial virus, and a tickborne encephalitis virus. J. Infect. Dis. *183*, 1395-1398.

Fleming,P. (1977). Age-dependent and strain-related differences of virulence of Semliki Forest virus in mice. J. Gen. Virol. *37*, 93-105.

Ford,A.L., Goodsall,A.L., Hickey,W.F., and Sedgwick,J.D. (1995). Normal adult ramified microglia separated from other central nervous system macrophages by flow cytometric sorting. Phenotypic differences defined and direct ex vivo antigen presentation to myelin basic protein-reactive CD4+ T cells compared. J. Immunol. *154*, 4309-4321.

Forster,T., Roy,D., and Ghazal,P. (2003). Experiments using microarray technology: limitations and standard operating procedures. J. Endocrinol. *178*, 195-204.

Franc,N.C., White,K., and Ezekowitz,R.A. (1999). Phagocytosis and development: back to the future. Curr. Opin. Immunol. *11*, 47-52.

Fraser,I.P., Koziel,H., and Ezekowitz,R.A. (1998). The serum mannose-binding protein and the macrophage mannose receptor are pattern recognition molecules that link innate and adaptive immunity. Semin. Immunol. *10*, 363-372.

Frese,M., Kochs,G., Feldmann,H., Hertkorn,C., and Haller,O. (1996). Inhibition of bunyaviruses, phleboviruses, and hantaviruses by human MxA protein. J. Virol. *70*, 915-923.

Frolova,E.I., Fayzulin,R.Z., Cook,S.H., Griffin,D.E., Rice,C.M., and Frolov,I. (2002). Roles of nonstructural protein nsP2 and Alpha/Beta interferons in determining the outcome of Sindbis virus infection. J. Virol. *76*, 11254-11264.

Funami,K., Matsumoto,M., Oshiumi,H., Akazawa,T., Yamamoto,A., and Seya,T. (2004). The cytoplasmic 'linker region' in Toll-like receptor 3 controls receptor localization and signaling. Int. Immunol. *16*, 1143-1154.

Gallucci,S. and Matzinger,P. (2001). Danger signals: SOS to the immune system. Curr. Opin. Immunol. *13*, 114-119.

Galon,J., Franchimont,D., Hiroi,N., Frey,G., Boettner,A., Ehrhart-Bornstein,M., O'Shea,J.J., Chrousos,G.P., and Bornstein,S.R. (2002). Gene profiling reveals unknown enhancing and suppressive actions of glucocorticoids on immune cells. FASEB J. *16*, 61-71.

Garden,G.A., Budd,S.L., Tsai,E., Hanson,L., Kaul,M., D'Emilia,D.M., Friedlander,R.M., Yuan,J., Masliah,E., and Lipton,S.A. (2002). Caspase cascades in human immunodeficiency virus-associated neurodegeneration. J. Neurosci. *22*, 4015-4024.

Gewirtz,A.T., Navas,T.A., Lyons,S., Godowski,P.J., and Madara,J.L. (2001). Cutting edge: bacterial flagellin activates basolaterally expressed TLR5 to induce epithelial proinflammatory gene expression. J. Immunol. *167*, 1882-1885.

Ghani,A.C., Ferguson,N.M., Donnelly,C.A., and Anderson,R.M. (2000). Predicted vCJD mortality in Great Britain. Nature *406*, 583-584.

Gibbons,D.L., Vaney,M.C., Roussel,A., Vigouroux,A., Reilly,B., Lepault,J., Kielian,M., and Rey,F.A. (2004). Conformational change and protein-protein interactions of the fusion protein of Semliki Forest virus. Nature *427*, 320-325.

Giese,A., Brown,D.R., Groschup,M.H., Feldmann,C., Haist,I., and Kretzschmar,H.A. (1998). Role of microglia in neuronal cell death in prion disease. Brain Pathol. *8*, 449-457.

Giese,A. and Kretzschmar,H.A. (2001). Prion-induced neuronal damage--the mechanisms of neuronal destruction in the subacute spongiform encephalopathies. Curr. Top. Microbiol. Immunol. *253*, 203-217.

Girardin,S.E., Tournebize,R., Mavris,M., Page,A.L., Li,X., Stark,G.R., Bertin,J., DiStefano,P.S., Yaniv,M., Sansonetti,P.J., and Philpott,D.J. (2001). CARD4/Nod1 mediates NF-kappaB and JNK activation by invasive Shigella flexneri. EMBO Rep. *2*, 736-742.

Giulian,D., Yu,J., Li,X., Tom,D., Li,J., Wendt,E., Lin,S.N., Schwarcz,R., and Noonan,C. (1996). Study of receptor-mediated neurotoxins released by HIV-1-infected mononuclear phagocytes found in human brain. J. Neurosci. *16*, 3139-3153.

Glasgow,G.M., Sheahan,B.J., Atkins,G.J., Wahlberg,J.M., Salminen,A., and Liljestrom,P. (1991). Two mutations in the envelope glycoprotein E2 of Semliki Forest virus affecting the maturation and entry patterns of the virus alter pathogenicity for mice. Virology *185*, 741-748.

Godbout,J.P., Berg,B.M., Kelley,K.W., and Johnson,R.W. (2004). alpha-Tocopherol reduces lipopolysaccharide-induced peroxide radical formation and interleukin-6 secretion in primary murine microglia and in brain. J. Neuroimmunol. *149*, 101-109.

Gomez-Gomez,L. and Boller,T. (2002). Flagellin perception: a paradigm for innate immunity. Trends Plant Sci. *7*, 251-256.

Goodbourn,S., Didcock,L., and Randall,R.E. (2000). Interferons: cell signalling, immune modulation, antiviral response and virus countermeasures. J. Gen. Virol. *81*, 2341-2364.

Gordon,L.B., Nolan,S.C., Ksander,B.R., Knopf,P.M., and Harling-Berg,C.J. (1998). Normal cerebrospinal fluid suppresses the in vitro development of cytotoxic T cells: role of the brain microenvironment in CNS immune regulation. J. Neuroimmunol. *88*, 77-84.

Gottar,M., Gobert,V., Michel,T., Belvin,M., Duyk,G., Hoffmann,J.A., Ferrandon,D., and Royet,J. (2002). The Drosophila immune response against Gram-negative bacteria is mediated by a peptidoglycan recognition protein. Nature *416*, 640-644.

Granucci,F., Petralia,F., Urbano,M., Citterio,S., Di Tota,F., Santambrogio,L., and Ricciardi-Castagnoli,P. (2003). The scavenger receptor MARCO mediates cytoskeleton rearrangements in dendritic cells and microglia. Blood *102*, 2940-2947.

Gregory,C.D. (2000). CD14-dependent clearance of apoptotic cells: relevance to the immune system. Curr. Opin. Immunol. *12*, 27-34.

Grewal,R.P., Yoshida,T., Finch,C.E., and Morgan,T.E. (1997). Scavenger receptor mRNAs in rat brain microglia are induced by kainic acid lesioning and by cytokin es. Neuroreport *8*, 1077-1081.

Grieder,F.B. and Vogel,S.N. (1999). Role of interferon and interferon regulatory factors in early protection against Venezuelan equine encephalitis virus infection. Virology *257*, 106-118.

Griffin,D.E. (2003). Immune responses to RNA-virus infections of the CNS. Nat. Rev. Immunol *3*, 493-502.

Griffin,D.E. and Hardwick,J.M. (1997). Regulators of apoptosis on the road to persistent alphavirus infection. Annu. Rev. Microbiol. *51*, 565-592.

Griffin,D.E., Levine,B., Tyor,W.R., Tucker,P.C., and Hardwick,J.M. (1994). Age-dependent susceptibility to fatal encephalitis: alphavirus infection of neurons. Arch. Virol. Suppl *9*, 31-39.

Griffin,D.E., Ubol,S., Despres,P., Kimura,T., and Byrnes,A. (2001). Role of antibodies in controlling alphavirus infection of neurons. Curr. Top. Microbiol. Immunol. *260*, 191-200.

Grimley,P.M., Berezesky,I.K., and Friedman,R.M. (1968). Cytoplasmic structures associated with an arbovirus infection: loci of viral ribonucleic acid synthesis. J. Virol. *2*, 1326-1338.

Grimley,P.M. and Friedman,R.M. (1970). Development of Semliki forest virus in mouse brain: an electron microscopic study. Exp. Mol. Pathol. *12*, 1-13.

Habich,C., Baumgart,K., Kolb,H., and Burkart,V. (2002). The receptor for heat shock protein 60 on macrophages is saturable, specific, and distinct from receptors for other heat shock proteins. J. Immunol. *168*, 569-576.

Hailer,N.P., Heppner,F.L., Haas,D., and Nitsch,R. (1998). Astrocytic factors deactivate antigen presenting cells that invade the central nervous system. Brain Pathol. *8*, 459-474.

Hajjar,A.M., Ernst,R.K., Tsai,J.H., Wilson,C.B., and Miller,S.I. (2002). Human Toll-like receptor 4 recognizes host-specific LPS modifications. Nat. Immunol. *3*, 354-359.

Hajjar,A.M., O'Mahony,D.S., Ozinsky,A., Underhill,D.M., Aderem,A., Klebanoff,S.J., and Wilson,C.B. (2001). Cutting edge: functional interactions between toll-like receptor (TLR) 2 and TLR1 or TLR6 in response to phenol-soluble modulin. J. Immunol. *166*, 15-19.

Halevy,M., Akov,Y., Ben Nathan,D., Kobiler,D., Lachmi,B., and Lustig,S. (1994). Loss of active neuroinvasiveness in attenuated strains of West Nile virus: pathogenicity in immunocompetent and SCID mice. Arch. Virol. *137*, 355-370.

Hampton,R.Y., Golenbock,D.T., Penman,M., Krieger,M., and Raetz,C.R. (1991). Recognition and plasma clearance of endotoxin by scavenger receptors. Nature *352*, 342-344.

Hanisch,U.K. (2002). Microglia as a source and target of cytokines. Glia *40*, 140-155.

Hardy,J.A. and Higgins,G.A. (1992). Alzheimer's disease: the amyloid cascade hypothesis. Science *256*, 184-185.

Harrison,J.K., Jiang,Y., Chen,S., Xia,Y., Maciejewski,D., McNamara,R.K., Streit,W.J., Salafranca,M.N., Adhikari,S., Thompson,D.A., Botti,P., Bacon,K.B., and Feng,L. (1998). Role for neuronally derived fractalkine in mediating interactions between neurons and CX3CR1-expressing microglia. Proc. Natl. Acad. Sci. U. S. A *95*, 10896-10901.

Harte,M.T., Haga,I.R., Maloney,G., Gray,P., Reading,P.C., Bartlett,N.W., Smith,G.L., Bowie,A., and O'Neill,L.A. (2003). The poxvirus protein A52R targets Toll-like receptor signaling complexes to suppress host defense. J. Exp. Med. *197*, 343-351.

Hashimoto,C., Hudson,K.L., and Anderson,K.V. (1988). The Toll gene of Drosophila, required for dorsal-ventral embryonic polarity, appears to encode a tr ansmembrane protein. Cell *52*, 269-279.

Hayashi,F., Smith,K.D., Ozinsky,A., Hawn,T.R., Yi,E.C., Goodlett,D.R., Eng,J.K., Akira,S., Underhill,D.M., and Aderem,A. (2001). The innate immune response to bacterial flagellin is mediated by Toll-like receptor 5. Nature *410*, 1099-1103.

Hayes,G.M., Woodroofe,M.N., and Cuzner,M.L. (1988). Characterisation of microglia isolated from adult human and rat brain. J. Neuroimmunol. *19*, 177-189.

Haynes,L.M., Moore,D.D., Kurt-Jones,E.A., Finberg,R.W., Anderson,L.J., and Tripp,R.A. (2001). Involvement of toll-like receptor 4 in innate immunity to respiratory syncytial virus. J. Virol. *75*, 10730-10737.

Heggelund,L., Muller,F., Lien,E., Yndestad,A., Ueland,T., Kristiansen,K.I., Espevik,T., Aukrust,P., and FrOland,S.S. (2004). Increased expression of toll-like receptor 2 on monocytes in HIV infection: possible roles in inflammation and viral replication. Clin. Infect. Dis. *39*, 264-269.

Heil,F., Hemmi,H., Hochrein,H., Ampenberger,F., Kirschning,C., Akira,S., Lipford,G., Wagner,H., and Bauer,S. (2004). Species-specific recognition of single-stranded RNA via toll-like receptor 7 and 8. Science *303*, 1526-1529.

Heise,M.T., Simpson,D.A., and Johnston,R.E. (2000). Sindbis-group alphavirus replication in periosteum and endosteum of long bones in adult mice. J. Virol. *74*, 9294-9299.

Helenius,A., Morein,B., Fries,E., Simons,K., Robinson,P., Schirrmacher,V., Terhorst,C., and Strominger,J.L. (1978). Human (HLA-A and HLA-B) and murine (H-2K and H-2D) histocompatibility antigens are cell surface receptors for Semliki Forest virus. Proc. Natl. Acad. Sci. U. S. A *75*, 3846-3850.

Hemmi,H., Kaisho,T., Takeda,K., and Akira,S. (2003). The roles of Toll-like receptor 9, MyD88, and DNA-dependent protein kinase catalytic subunit in the effects of two distinct CpG DNAs on dendritic cell subsets. J. Immunol. *170*, 3059-3064.

Hemmi,H., Kaisho,T., Takeuchi,O., Sato,S., Sanjo,H., Hoshino,K., Horiuchi,T., Tomizawa,H., Takeda,K., and Akira,S. (2002). Small anti-viral compounds activate immune cells via the TLR7 MyD88-dependent signaling pathway. Nat. Immunol. *3*, 196-200.

Hemmi,H., Takeuchi,O., Kawai,T., Kaisho,T., Sato,S., Sanjo,H., Matsumoto,M., Hoshino,K., Wagner,H., Takeda,K., and Akira,S. (2000). A Toll-like receptor recognizes bacterial DNA. Nature *408*, 740-745.

Heppner,F.L., Musahl,C., Arrighi,I., Klein,M.A., Rulicke,T., Oesch,B., Zinkernagel,R.M., Kalinke,U., and Aguzzi,A. (2001). Prevention of scrapie pathogenesis by transgenic expression of anti-prion protein antibodies. Science *294*, 178-182.

Hertz,C.J., Kiertscher,S.M., Godowski,P.J., Bouis,D.A., Norgard,M.V., Roth,M.D., and Modlin,R.L. (2001). Microbial lipopeptides stimulate dendritic cell maturation via Toll-like receptor 2. J. Immunol. *166*, 2444-2450.

Hickey,W.F., Hsu,B.L., and Kimura,H. (1991). T-lymphocyte entry into the central nervous system. J. Neurosci. Res. *28*, 254-260.

Hickey,W.F. and Kimura,H. (1988). Perivascular microglial cells of the CNS are bone marrow-derived and present antigen in vivo. Science *239*, 290-292.

Hirano,K., Yamashita,S., Nakagawa,Y., Ohya,T., Matsuura,F., Tsukamoto,K., Okamoto,Y., Matsuyama,A., Matsumoto,K., Miyagawa,J., and Matsuzawa,Y. (1999). Expression of human scavenger receptor class B type I in cultured human monocyte-derived macrophages and atherosclerotic lesions. Circ. Res. *85*, 108-116.

Hirschfeld,M., Kirschning,C.J., Schwandner,R., Wesche,H., Weis,J.H., Wooten,R.M., and Weis,J.J. (1999). Cutting edge: inflammatory signaling by Borrelia burgdorferi lipoproteins is mediated by toll-like receptor 2. J. Immunol. *163*, 2382-2386.

Hirschfeld,M., Weis,J.J., Toshchakov,V., Salkowski,C.A., Cody,M.J., Ward,D.C., Qureshi,N., Michalek,S.M., and Vogel,S.N. (2001). Signaling by toll-like receptor 2 and 4 agonists results in differential gene expression in murine macrophages. Infect. Immun. *69*, 1477-1482.

Ho,Y.S., Xiong,Y., Ma,W., Spector,A., and Ho,D.S. (2004). Mice lacking catalase develop normally but show differential sensitivity to oxidant tissue injury. J. Biol. Chem. *279*, 32804-32812.

Hoebe,K., Du,X., Georgel,P., Janssen,E., Tabeta,K., Kim,S.O., Goode,J., Lin,P., Mann,N., Mudd,S., Crozat,K., Sovath,S., Han,J., and Beutler,B. (2003). Identification of Lps2 as a key transducer of MyD88-independent TIR signalling. Nature *424*, 743-748.

Hoek,R.M., Ruuls,S.R., Murphy,C.A., Wright,G.J., Goddard,R., Zurawski,S.M., Blom,B., Homola,M.E., Streit,W.J., Brown,M.H., Barclay,A.N., and Sedgwick,J.D. (2000). Down-regulation of the macrophage lineage through interaction with OX2 (CD200). Science *290*, 1768-1771.

Holmes,C., El Okl,M., Williams,A.L., Cunningham,C., Wilcockson,D., and Perry,V.H. (2003). Systemic infection, interleukin 1beta, and cognitive decline in Alzheimer's disease. J. Neurol. Neurosurg. Psychiatry *74*, 788-789.

Honda,M., Akiyama,H., Yamada,Y., Kondo,H., Kawabe,Y., Takeya,M., Takahashi,K., Suzuki,H., Doi,T., Sakamoto,A., Ookawara,S., Mato,M., Gough,P.J., Greaves,D.R., Gordon,S., Kodama,T., and Matsushita,M. (1998). Immunohistochemical evidence for a macrophage scavenger receptor in Mato cells and reactive microglia of ischemia and Alzheimer's disease. Biochem. Biophys. Res. Commun. *245*, 734-740.

Horng,T., Barton,G.M., and Medzhitov,R. (2001). TIRAP: an adapter molecule in the Toll signaling pathway. Nat. Immunol. *2*, 835-841.

Hornung,V., Rothenfusser,S., Britsch,S., Krug,A., Jahrsdorfer,B., Giese,T., Endres,S., and Hartmann,G. (2002). Quantitative expression of toll-like receptor 1-10 mRNA in cellular subsets of human peripheral blood mononuclear cells and sensitivity to CpG oligodeoxynucleotides. J. Immunol. *168*, 4531-4537.

Hoshino,K., Kaisho,T., Iwabe,T., Takeuchi,O., and Akira,S. (2002). Differential involvement of IFN-beta in Toll-like receptor-stimulated dendritic cell activation. Int. Immunol. *14*, 1225-1231.

Hoshino,K., Takeuchi,O., Kawai,T., Sanjo,H., Ogawa,T., Takeda,Y., Takeda,K., and Akira,S. (1999). Cutting edge: Toll-like receptor 4 (TLR4)-deficient mice are hyporesponsive to lipopolysaccharide: evidence for TLR4 as the Lps gene product. J. Immunol. *162*, 3749-3752.

Howard,L.M., Miga,A.J., Vanderlugt,C.L., Dal Canto,M.C., Laman,J.D., Noelle,R.J., and Miller,S.D. (1999). Mechanisms of immunotherapeutic intervention by anti-CD40L (CD154) antibody in an animal model of multiple sclerosis. J. Clin. Invest *103*, 281-290.

Husemann,J., Loike,J.D., Anankov,R., Febbraio,M., and Silverstein,S.C. (2002). Scavenger receptors in neurobiology and neuropathology: their role on microglia and other cells of the nervous system. Glia *40*, 195-205.

Husemann,J., Loike,J.D., Kodama,T., and Silverstein,S.C. (2001). Scavenger receptor class B type I (SR-BI) mediates adhesion of neonatal murine microglia to fibrillar beta-amyloid. J. Neuroimmunol. *114*, 142-150.

Hwang,S.Y., Hertzog,P.J., Holland,K.A., Sumarsono,S.H., Tymms,M.J., Hamilton,J.A., Whitty,G., Bertoncello,I., and Kola,I. (1995). A null mutation in the gene encoding a type I interferon receptor component eliminates antiproliferative and antiviral responses to interferons alpha and beta and alters macrophage responses. Proc. Natl. Acad. Sci. U. S. A *92*, 11284-11288.

Iliev,A.I., Stringaris,A.K., Nau,R., and Neumann,H. (2004). Neuronal injury mediated via stimulation of microglial toll-like receptor-9 (TLR9). FASEB J. *18*, 412-414.

Inohara,N., Ogura,Y., Chen,F.F., Muto,A., and Nunez,G. (2001). Human Nod1 confers responsiveness to bacterial lipopolysaccharides. J. Biol. Chem. *276*, 2551-2554.

Jacobs,B.L. and Langland,J.O. (1996). When two strands are better than one: the mediators and modulators of the cellular responses to double-stranded RNA. Virology *219*, 339-349.

Jagelman,S., Suckling,A.J., Webb,H.E., and Bowen,F.T. (1978). The pathogenesis of avirulent Semliki Forest virus infections in athymic nude mice. J. Gen. Virol. *41*, 599-607.

Jana,M., Liu,X., Koka,S., Ghosh,S., Petro,T.M., and Pahan,K. (2001). Ligation of CD40 stimulates the induction of nitric-oxide synthase in microglial cells. J. Biol. Chem. *276*, 44527-44533.

Janeway,C.A., Jr. (1989). Approaching the asymptote? Evolution and revolution in immunology. Cold Spring Harb. Symp. Quant. Biol. *54 Pt 1*, 1-13.

Jankovic,D., Kullberg,M.C., Hieny,S., Caspar,P., Collazo,C.M., and Sher,A. (2002). In the absence of IL-12, CD4(+) T cell responses to intracellular pathogens fail to default to a Th2 pattern and are host protective in an IL-10(-/-) setting. Immunity. *16*, 429-439.

Janus,C., Pearson,J., McLaurin,J., Mathews,P.M., Jiang,Y., Schmidt,S.D., Chishti,M.A., Horne,P., Heslin,D., French,J., Mount,H.T., Nixon,R.A., Mercken,M., Bergeron,C., Fraser,P.E., George-Hyslop,P., and Westaway,D. (2000). A beta peptide immunization reduces behavioural impairment and plaques in a model of Alzheimer's disease. Nature *408*, 979-982.

Janzer,R.C. and Raff,M.C. (1987). Astrocytes induce blood-brain barrier properties in endothelial cells. Nature *325*, 253-257.

Jeohn,G.H., Kong,L.Y., Wilson,B., Hudson,P., and Hong,J.S. (1998). Synergistic neurotoxic effects of combined treatments with cytokines in murine primary mixed neuron/glia cultures. J. Neuroimmunol. *85*, 1-10.

Jiang,Q., Akashi,S., Miyake,K., and Petty,H.R. (2000). Lipopolysaccharide induces physical proximity between CD14 and toll-like receptor 4 (TLR4) prior to nuclear translocation of NF-kappa B. J. Immunol. *165*, 3541-3544.

Jiang,Z., Zamanian-Daryoush,M., Nie,H., Silva,A.M., Williams,B.R., and Li,X. (2003). Poly(I-C)-induced Toll-like receptor 3 (TLR3)-mediated activation of NFkappa B and MAP kinase is through an interleukin-1 receptor-associated kinase (IRAK)-independent pathway employing the signaling components TLR3-TRAF6-TAK1-TAB2-PKR. J. Biol. Chem. *278*, 16713-16719.

Jude,B.A., Pobezinskaya,Y., Bishop,J., Parke,S., Medzhitov,R.M., Chervonsky,A.V., and Golovkina,T.V. (2003). Subversion of the innate immune system by a retrovirus. Nat. Immunol. *4*, 573-578.

Juedes,A.E. and Ruddle,N.H. (2001). Resident and infiltrating central nervous system APCs regulate the emergence and resolution of experimental autoimmune encephalomyelitis. J. Immunol. *166*, 5168-5175.

Juurlink,B.H. and Hertz,L. (1985). Plasticity of astrocytes in primary cultures: an experimental tool and a reason for methodological caution. Dev. Neurosci. *7*, 263-277.

Kadowaki,N., Ho,S., Antonenko,S., Malefyt,R.W., Kastelein,R.A., Bazan,F., and Liu,Y.J. (2001c). Subsets of human dendritic cell precursors express different toll-like receptors and respond to different microbial antigens. J. Exp. Med. *194*, 863-869.

Kadowaki,N., Ho,S., Antonenko,S., Malefyt,R.W., Kastelein,R.A., Bazan,F., and Liu,Y.J. (2001a). Subsets of human dendritic cell precursors express different toll-like receptors and respond to different microbial antigens. J. Exp. Med. *194*, 863-869.

Kadowaki,N., Ho,S., Antonenko,S., Malefyt,R.W., Kastelein,R.A., Bazan,F., and Liu,Y.J. (2001b). Subsets of human dendritic cell precursors express different toll-like receptors and respond to different microbial antigens. J. Exp. Med. *194*, 863-869.

Kaisho,T., Hoshino,K., Iwabe,T., Takeuchi,O., Yasui,T., and Akira,S. (2002). Endotoxin can induce MyD88-deficient dendritic cells to support T(h)2 cell differentiation. Int. Immunol. *14*, 695-700.

Kaisho,T., Takeuchi,O., Kawai,T., Hoshino,K., and Akira,S. (2001). Endotoxin-induced maturation of MyD88-deficient dendritic cells. J. Immunol. *166*, 5688-5694.

Kakinuma,Y., Hama,H., Sugiyama,F., Yagami,K., Goto,K., Murakami,K., and Fukamizu,A. (1998). Impaired blood-brain barrier function in angiotensinogen-deficient mice. Nat. Med. *4*, 1078-1080.

Kaluza,G., Lell,G., Reinacher,M., Stitz,L., and Willems,W.R. (1987). Neurogenic spread of Semliki Forest virus in mice. Arch. Virol. *93*, 97-110.

Kane,M.D., Jatkoe,T.A., Stumpf,C.R., Lu,J., Thomas,J.D., and Madore,S.J. (2000). Assessment of the sensitivity and specificity of oligonucleotide (50mer) microarrays. Nucleic Acids Res. *28*, 4552-4557.

Karin,M. and Ben Neriah,Y. (2000). Phosphorylation meets ubiquitination: the control of NF-[kappa]B activity. Annu. Rev. Immunol. *18*, 621-663.

Kaser,A., Enrich,B., Ludwiczek,O., Vogel,W., and Tilg,H. (1999). Interferon-alpha (IFN-alpha) enhances cytotoxicity in healthy volunteers and chronic hepatitis C infection mainly by the perforin pathway. Clin. Exp. Immunol. *118*, 71-77.

Kawai,T., Adachi,O., Ogawa,T., Takeda,K., and Akira,S. (1999). Unresponsiveness of MyD88-deficient mice to endotoxin. Immunity. *11*, 115-122.

Kawai,T., Takeuchi,O., Fujita,T., Inoue,J., Muhlradt,P.F., Sato,S., Hoshino,K., and Akira,S. (2001). Lipopolysaccharide stimulates the MyD88-independent pathway and results in activation of IFN-regulatory factor 3 and the expression of a subset of lipopolysaccharide-inducible genes. J. Immunol. *167*, 5887-5894.

Kelly,W.R., Blakemore,W.F., Jagelman,S., and Webb,H.E. (1982). Demyelination induced in mice by avirulent Semliki Forest virus. II. An ultrastructural study of focal demyelination in the brain. Neuropathol. Appl. Neurobiol. *8*, 43-53.

Kerr,I.M. and Brown,R.E. (1978). pppA2'p5'A2'p5'A: an inhibitor of protein synthesis synthesized with an enzyme fraction from interferon-treated cells. Proc. Natl. Acad. Sci. U. S. A *75*, 256-260.

Khush,R.S., Leulier,F., and Lemaitre,B. (2001). Drosophila immunity: two paths to NF-kappaB. Trends Immunol. *22*, 260-264.

Kielian,M. and Helenius,A. (1985). pH induced alterations in the fusogenic spike protein of Semliki Forest virus. J. Cell Biol. *101*, 2284-2291.

Kielian,T. (2004). Microglia and chemokines in infectious diseases of the nervous system: views and reviews. Front Biosci. *9*, 732-750.

Kielian,T., Mayes,P., and Kielian,M. (2002). Characterization of microglial responses to Staphylococcus aureus: effects on cytokine, costimulatory molecule, and Toll-like receptor expression. J. Neuroimmunol. *130*, 86-99.

Kirschning,C.J. and Schumann,R.R. (2002). TLR2: cellular sensor for microbial and endogenous molecular patterns. Curr. Top. Microbiol. Immunol. *270*, 121-144.

Kobayashi,K., Hernandez,L.D., Galan,J.E., Janeway,C.A., Jr., Medzhitov,R., and Flavell,R.A. (2002). IRAK-M is a negative regulator of Toll-like receptor signaling. Cell *110*, 191-202.

Kretzschmar,H.A., Prusiner,S.B., Stowring,L.E., and DeArmond,S.J. (1986). Scrapie prion proteins are synthesized in neurons. Am. J. Pathol. *122*, 1-5.

Krieger,M. (1999). Charting the fate of the "good cholesterol": identification and characterization of the high-density lipoprotein receptor SR-BI. Annu. Rev. Biochem. *68*, 523-558.

Krieger,M. and Stern,D.M. (2001). Series introduction: multiligand receptors and human disease. J. Clin. Invest *108*, 645-647.

Krug,A., Luker,G.D., Barchet,W., Leib,D.A., Akira,S., and Colonna,M. (2004). Herpes simplex virus type 1 activates murine natural interferon-producing cells through toll-like receptor 9. Blood *103*, 1433-1437.

Krug,A., Rothenfusser,S., Selinger,S., Bock,C., Kerkmann,M., Battiany,J., Sarris,A., Giese,T., Speiser,D., Endres,S., and Hartmann,G. (2003). CpG-A oligonucleotides induce a monocyte-derived dendritic cell-like phenotype that preferentially activates CD8 T cells. J. Immunol. *170*, 3468-3477.

Krug,A., Towarowski,A., Britsch,S., Rothenfusser,S., Hornung,V., Bals,R., Giese,T., Engelmann,H., Endres,S., Krieg,A.M., and Hartmann,G. (2001). Toll-like receptor expression reveals CpG DNA as a unique microbial stimulus for plasmacytoid dendritic cells which synergizes with CD40 ligand to induce high amounts of IL-12. Eur. J. Immunol. *31*, 3026-3037.

Krum,J.M. and Rosenstein,J.M. (1998). VEGF mRNA and its receptor flt-1 are expressed in reactive astrocytes following neural grafting and tumor cell implantation in the adult CNS. Exp. Neurol. *154*, 57-65.

Kulka,M., Alexopoulou,L., Flavell,R.A., and Metcalfe,D.D. (2004). Activation of mast cells by double-stranded RNA: evidence for activation through Toll-like receptor 3. J. Allergy Clin. Immunol. *114*, 174-182.

Kurt-Jones,E.A., Chan,M., Zhou,S., Wang,J., Reed,G., Bronson,R., Arnold,M.M., Knipe,D.M., and Finberg,R.W. (2004a). Herpes simplex virus 1 interaction with Toll-like receptor 2 contributes to lethal encephalitis. Proc. Natl. Acad. Sci. U. S. A *101*, 1315-1320.

Kurt-Jones,E.A., Chan,M., Zhou,S., Wang,J., Reed,G., Bronson,R., Arnold,M.M., Knipe,D.M., and Finberg,R.W. (2004b). Herpes simplex virus 1 interaction with Toll-like receptor 2 contributes to lethal encephalitis. Proc. Natl. Acad. Sci. U. S. A *101*, 1315-1320.

Kurt-Jones,E.A., Popova,L., Kwinn,L., Haynes,L.M., Jones,L.P., Tripp,R.A., Walsh,E.E., Freeman,M.W., Golenbock,D.T., Anderson,L.J., and Finberg,R.W. (2000). Pattern recognition receptors TLR4 and CD14 mediate response to respiratory syncytial virus. Nat. Immunol. *1*, 398-401.

Lacroix,S., Feinstein,D., and Rivest,S. (1998). The bacterial endotoxin lipopolysaccharide has the ability to target the brain in upregulating its membrane CD14 receptor within specific cellular populations. Brain Pathol. *8*, 625-640.

Laflamme,N., Echchannaoui,H., Landmann,R., and Rivest,S. (2003). Cooperation between toll-like receptor 2 and 4 in the brain of mice challenged with cell wall components derived from gram-negative and gram-positive bacteria. Eur. J. Immunol. *33*, 1127-1138.

Laflamme,N. and Rivest,S. (2001). Toll-like receptor 4: the missing link of the cerebral innate immune response triggered by circulating gram-negative bacterial cell wall components. FASEB J. *15*, 155-163.

Laflamme,N., Soucy,G., and Rivest,S. (2001). Circulating cell wall components derived from gram-negative, not gram-positive, bacteria cause a profound induction of the gene-encoding Toll-like receptor 2 in the CNS. J. Neurochem. *79*, 648-657.

Langland,J.O., Pettiford,S., Jiang,B., and Jacobs,B.L. (1994). Products of the porcine group C rotavirus NSP3 gene bind specifically to double stranded RNA and inhibit activation of the interferon induced protein kinase PKR. J. Virol. *68*, 3821-3829.

Latz,E., Schoenemeyer,A., Visintin,A., Fitzgerald,K.A., Monks,B.G., Knetter,C.F., Lien,E., Nilsen,N.J., Espevik,T., and Golenbock,D.T. (2004). TLR9 signals after translocating from the ER to CpG DNA in the lysosome. Nat. Immunol. *5*, 190-198.

Le,Y., Oppenheim,J.J., and Wang,J.M. (2001). Pleiotropic roles of formyl peptide receptors. Cytokine Growth Factor Rev. *12*, 91-105.

Lee,S., Hong,J., Choi,S.Y., Oh,S.B., Park,K., Kim,J.S., Karin,M., and Lee,S.J. (2004). CpG oligodeoxynucleotides induce expression of proinflammatory cytokines and chemokines in astrocytes: the role of c-Jun N-terminal kinase in CpG ODN-mediated NF-kappaB activation. J. Neuroimmunol. *153*, 50-63.

Lee,S.J. and Lee,S. (2002). Toll-like receptors and inflammation in the CNS. Curr. Drug Targets. Inflamm. Allergy *1*, 181-191.

Lehnardt,S., Lachance,C., Patrizi,S., Lefebvre,S., Follett,P.L., Jensen,F.E., Rosenberg,P.A., Volpe,J.J., and Vartanian,T. (2002). The toll-like receptor TLR4 is necessary for lipopolysaccharide-induced oligodendrocyte injury in the CNS. J. Neurosci. *22*, 2478-2486.

Lehnardt,S., Massillon,L., Follett,P., Jensen,F.E., Ratan,R., Rosenberg,P.A., Volpe,J.J., and Vartanian,T. (2003). Activation of innate immunity in the CNS triggers neurodegeneration through a Toll-like receptor 4-dependent pathway. Proc. Natl. Acad. Sci. U. S. A *100*, 8514-8519.

Lehner,M.D., Morath,S., Michelsen,K.S., Schumann,R.R., and Hartung,T. (2001). Induction of cross-tolerance by lipopolysaccharide and highly purified lipoteichoic acid via different Toll-like receptors independent of paracrine mediators. J. Immunol. *166*, 5161-5167.

Lehrer,R.I. and Ganz,T. (2002). Defensins of vertebrate animals. Curr. Opin. Immunol. *14*, 96-102.

Leifer,C.A., Kennedy,M.N., Mazzoni,A., Lee,C., Kruhlak,M.J., and Segal,D.M. (2004). TLR9 is localized in the endoplasmic reticulum prior to stimulation. J. Immunol. *173*, 1179-1183.

Lemaitre,B., Meister,M., Govind,S., Georgel,P., Steward,R., Reichhart,J.M., and Hoffmann,J.A. (1995). Functional analysis and regulation of nuclear import of dorsal during the immune response in Drosophila. EMBO J. *14*, 536-545.

Lemaitre,B., Nicolas,E., Michaut,L., Reichhart,J.M., and Hoffmann,J.A. (1996). The dorsoventral regulatory gene cassette spatzle/Toll/cactus controls the potent antifungal response in Drosophila adults. Cell *86*, 973-983.

Lemm,J.A., Rumenapf,T., Strauss,E.G., Strauss,J.H., and Rice,C.M. (1994). Polypepti de requirements for assembly of functional Sindbis virus replication complexes: a model for the temporal regulation of minus- and plus-strand RNA synthesis. EMBO J. *13*, 2925-2934.

Letournel-Boulland,M.L., Fages,C., Rolland,B., and Tardy,M. (1994). Lipopoly saccharides (LPS), up-regulate the IL-1-mRNA and down-regulate the glial fibrillary acidic protein (GFAP) and glutamine synthetase (GS)-mRNAs in astroglial primary cultures. Eur. Cytokine Netw. *5*, 51-56.

Levashina,E.A., Langley,E., Green,C., Gubb,D., Ashburner,M., Hoffmann,J.A., and Reichhart,J.M. (1999). Constitutive activation of toll-mediated antifungal defense in serpin-deficient Drosophila. Science *285*, 1917-1919.

Levine,B., Hardwick,J.M., Trapp,B.D., Crawford,T.O., Bollinger,R.C., and Griffin,D.E. (19 91). Antibody-mediated clearance of alphavirus infection from neurons. Science *254*, 856-860.

Levy,D.E. (2002). Whence interferon? Variety in the production of interferon in response to viral infection. J. Exp. Med. *195*, F15-F18.

Liberto,C.M., Albrecht,P.J., Herx,L.M., Yong,V.W., and Levison,S.W. (2004). Pro-regenerative properties of cytokine-activated astrocytes. J. Neurochem. *89*, 1092-1100.

Lieberman,A.P., Pitha,P.M., Shin,H.S., and Shin,M.L. (1989). Production of tumor necrosis factor and other cytokines by astrocytes stimulated with lipopolysaccharide or a neurotropic virus. Proc. Natl. Acad. Sci. U. S. A *86*, 6348-6352.

Lien,E., Means,T.K., Heine,H., Yoshimura,A., Kusumoto,S., Fukase,K., Fenton,M.J., Oikawa,M., Qureshi,N., Monks,B., Finberg,R.W., Ingalls,R.R., and Golenbock,D.T. (2000). Toll-like receptor 4 imparts ligand-specific recognition of bacterial lipopolysaccharide. J. Clin. Invest *105*, 497-504.

Lien,E., Sellati,T.J., Yoshimura,A., Flo,T.H., Rawadi,G., Finberg,R.W., Carroll,J.D., Espevik,T., Ingalls,R.R., Radolf,J.D., and Golenbock,D.T. (1999). Toll-like receptor 2 functions as a pattern recognition receptor for diverse bacterial products. J. Biol. Chem. *274*, 33419-33425.

Liu,S., Salyapongse,A.N., Geller,D.A., Vodovotz,Y., and Billiar,T.R. (2000). Hepatocyte toll-like receptor 2 expression in vivo and in vitro: role of cytokines in induction of rat TLR2 gene expression by lipopolysaccharide. Shock *14*, 361-365.

Liu,Y.J. (2001). Dendritic cell subsets and lineages, and their functions in innate and adaptive immunity. Cell *106*, 259-262.

Liu,Y.J., Kanzler,H., Soumelis,V., and Gilliet,M. (2001). Dendritic cell lineage, plasticity and cross-regulation. Nat. Immunol. *2*, 585-589.

Lloyd,R.M. and Shatkin,A.J. (1992). Translational stimulation by reovirus poly peptide sigma 3: substitution for VAI RNA and inhibition of phosphorylation of the alpha subunit of eukaryotic initiation factor 2. J. Virol. *66*, 6878-6884.

Lockhart,D.J., Dong,H., Byrne,M.C., Follettie,M.T., Gallo,M.V., Chee,M.S., Mittmann,M., Wang,C., Kobayashi,M., Horton,H., and Brown,E.L. (1996). Expression monitoring by hybridization to high-density oligonucleotide arrays. Nat. Biotechnol. *14*, 1675-1680.

Lord,K.A., Hoffman-Liebermann,B., and Liebermann,D.A. (1990). Nucleotide sequence and expression of a cDNA encoding MyD88, a novel myeloid differentiation primary response gene induced by IL6. Oncogene *5*, 1095-1097.

Lu,Y., Wambach,M., Katze,M.G., and Krug,R.M. (1995). Binding of the influenza virus NS1 protein to double-stranded RNA inhibits the activation of the protein kinase that phosphorylates the eIF-2 translation initiation factor. Virology *214*, 222-228.

Lund,J., Sato,A., Akira,S., Medzhitov,R., and Iwasaki,A. (2003). Toll-like receptor 9-mediated recognition of Herpes simplex virus-2 by plasmacytoid dendritic cells. J. Exp. Med. *198*, 513-520.

Lustig,S., Danenberg,H.D., Kafri,Y., Kobiler,D., and Ben Nathan,D. (1992). Viral neuroinvasion and encephalitis induced by lipopolysaccharide and its mediators. J. Exp. Med. *176*, 707-712.

Mabbott,N.A. and Bruce,M.E. (2001). The immunobiology of TSE diseases. J. Gen. Virol. *82*, 2307-2318.

Mack,C.L., Vanderlugt-Castaneda,C.L., Neville,K.L., and Miller,S.D. (2003). Microglia are activated to become competent antigen presenting and effector cells in the inflammatory environment of the Theiler's virus model of multiple sclerosis. J. Neuroimmunol. *144*, 68-79.

Magnus,T., Chan,A., Savill,J., Toyka,K.V., and Gold,R. (2002). Phagocytotic removal of apoptotic, inflammatory lymphocytes in the central nervous system by microglia and its functional implications. J Neuroimmunol. *130*, 1-9.

Major,E.O., Rausch,D., Marra,C., and Clifford,D. (2000). HIV-associated dementia. Science *288*, 440-442.

Marie,I., Durbin,J.E., and Levy,D.E. (1998). Differential viral induction of distinct interferon-alpha genes by positive feedback through interferon regulatory factor-7. EMBO J. *17*, 6660-6669.

Marrack,P., Kappler,J., and Mitchell,T. (1999). Type I interferons keep activated T cells alive. J Exp. Med. *189*, 521-530.

Marsh,M., Kielian,M.C., and Helenius,A. (1984). Semliki forest virus entry and the endocytic pathway. Biochem. Soc. Trans. *12*, 981-983.

Martinez-Costas,J., Gonzalez-Lopez,C., Vakharia,V.N., and Benavente,J. (2000). Possible involvement of the double-stranded RNA-binding core protein sigmaA in the resistance of avian reovirus to interferon. J. Virol. *74*, 1124-1131.

Massari,P., Henneke,P., Ho,Y., Latz,E., Golenbock,D.T., and Wetzler,L.M. (2002). Cutting edge: Immune stimulation by neisserial porins is toll-like receptor 2 and MyD88 dependent. J. Immunol. *168*, 1533-1537.

Masters,C.L. and Richardson,E.P., Jr. (1978). Subacute spongiform encephalopathy (Creutzfeldt-Jakob disease). The nature and progression of spongiform change. Brain *101*, 333-344.

Mathiot,C.C., Grimaud,G., Garry,P., Bouquety,J.C., Mada,A., Daguisy,A.M., and Georges,A.J. (1990). An outbreak of human Semliki Forest virus infections in Central African Republic. Am. J. Trop. Med. Hyg. *42*, 386-393.

Matsuguchi,T., Musikacharoen,T., Ogawa,T., and Yoshikai,Y. (2000). Gene expressio ns of Toll-like receptor 2, but not Toll-like receptor 4, is induced by LPS and inflammatory cytokines in mouse macrophages. J. Immunol. *165*, 5767-5772.

Matsumoto,M., Funami,K., Tanabe,M., Oshiumi,H., Shingai,M., Seto,Y., Yamamoto,A., and Seya,T. (2003). Subcellular localization of Toll-like receptor 3 in human dendritic cells. J. Immunol. *171*, 3154-3162.

Matsumoto,M., Tanaka,T., Kaisho,T., Sanjo,H., Copeland,N.G., Gilbert,D.J., Jenkins,N.A., and Akira,S. (1999). A novel LPS-inducible C-type lectin is a transcriptional target of NF-IL6 in macrophages. J. Immunol. *163*, 5039-5048.

McCurdy,J.D., Lin,T.J., and Marshall,J.S. (2001). Toll-like receptor 4-mediated activation of murine mast cells. J. Leukoc. Biol. *70*, 977-984.

Means,T.K., Wang,S., Lien,E., Yoshimura,A., Golenbock,D.T., and Fenton,M.J. (1999). Human toll-like receptors mediate cellular activation by Mycobacterium tuberculosis. J. Immunol. *163*, 3920-3927.

Meda,L., Cassatella,M.A., Szendrei,G.I., Otvos,L., Jr., Baron,P., Villalba,M., Ferrari,D., and Ros si,F. (1995). Activation of microglial cells by beta-amyloid protein and interferon-gamma. Nature *374*, 647-650.

Medzhitov,R. (2001). Toll-like receptors and innate immunity. Nat. Rev. Immunol. *1*, 135-145.

Medzhitov,R. and Janeway,C., Jr. (2000). The Toll r eceptor family and microbial recognition. Trends Microbiol. *8*, 452-456.

Medzhitov,R., Preston-Hurlburt,P., and Janeway,C.A., Jr. (1997). A human homologue of the Drosophila Toll protein signals activation of adaptive immunity. Nature *388*, 394-397.

Meng,X., Khanuja,B.S., and Ip,Y.T. (1999). Toll receptor-mediated Drosophila immune response requires Dif, an NF-kappaB factor. Genes Dev. *13*, 792-797.

Meurs,E., Chong,K., Galabru,J., Thomas,N.S., Kerr,I.M., Williams,B.R., and Hovanessian,A.G. (1990). Molecular cloning and characterization of the human double-stranded RNA-activated protein kinase induced by interferon. Cell *62*, 379-390.

Meurs,E.F., Watanabe,Y., Kadereit,S., Barber,G.N., Katze,M.G., Chong,K., Williams,B.R., and Hovanessian,A.G. (1992). Constitutive expression of human double-stranded RNA-activated p68 kinase in murine cells mediates phosphorylation of eukaryotic initiation factor 2 and partial resistance to encephalomyocarditis virus growth. J. Virol. *66*, 5805-5814.

Meylan,E., Burns,K., Hofmann,K., Blancheteau,V., Martinon,F., Kelliher,M., and Tschopp,J. (2004). RIP1 is an essential mediator of Toll-like receptor 3-induced NF-kappa B activation. Nat. Immunol. *5*, 503-507.

Michel,T., Reichhart,J.M., Hoffmann,J.A., and Royet,J. (2001). Drosophila Toll is activated by Gram-positive bacteria through a circulating peptidoglycan recognition protein. Nature *414*, 756-759.

Michelsen,K.S., Wong,M.H., Shah,P.K., Zhang,W., Yano,J., Doherty,T.M., Akira,S., Rajavashisth,T.B., and Arditi,M. (2004). Lack of Toll-like receptor 4 or myeloid differentiation factor 88 reduces atherosclerosis and alters plaque phenotype in mice deficient in apolipoprotein E. Proc. Natl. Acad. Sci. U. S. A *101*, 10679-10684.

Miettinen,M., Sareneva,T., Julkunen,I., and Matikainen,S. (2001). IFNs activate toll-like receptor gene expression in viral infections. Genes Immun. *2*, 349-355.

Milhavet,O., McMahon,H.E., Rachidi,W., Nishida,N., Katamine,S., Mange,A., Arlotto,M., Casanova,D., Riondel,J., Favier,A., and Lehmann,S. (2000). Prion infection impairs the cellular response to oxidative stress. Proc. Natl. Acad. Sci. U. S. A *97*, 13937-13942.

Miller,D.M., Rahill,B.M., Boss,J.M., Lairmore,M.D., Durbin,J.E., Waldman,J.W., and Sedmak,D.D. (1998). Human cytomegalovirus inhibits major histocompatibility complex class II expression by disruption of the Jak/Stat pathway. J. Exp. Med. *187*, 675-683.

Minagar,A., Shapshak,P., Fujimura,R., Ownby,R., Heyes,M., and Eisdorfer,C. (2002). The role of macrophage/microglia and astrocytes in the pathogenesis of three neurologic disorders: HIV-associated dementia, Alzheimer disease, and multiple sclerosis. J. Neurol. Sci. *202*, 13-23.

Mogensen,K.E., Lewerenz,M., Reboul,J., Lutfalla,G., and Uze,G. (1999). The type I interferon receptor: structure, function, and evolution of a family business. J. Interferon Cytokine Res. *19*, 1069-1098.

Mohty,M., Vialle-Castellano,A., Nunes,J.A., Isnardon,D., Olive,D., and Gaugler,B. (2003). IFN-alpha skews monocyte differentiation into Toll-like receptor 7-expressing dendritic cells with potent functional activities. J. Immunol. *171*, 3385-3393.

Mokuno,Y., Matsuguchi,T., Takano,M., Nishimura,H., Washizu,J., Ogawa,T., Takeuchi,O., Akira,S., Nimura,Y., and Yoshikai,Y. (2000). Expression of toll-like receptor 2 on gamma delta T cells bearing invariant V gamma 6/V delta 1 induced by Escherichia coli infection in mice. J. Immunol. *165*, 931-940.

Moller,T., Nolte,C., Burger,R., Verkhratsky,A., and Kettenmann,H. (1997). Mechanisms of C5a and C3a complement fragment-induced [Ca2+]i signaling in mouse microglia. J. Neurosci. *17*, 615-624.

Morris,M.M., Dyson,H., Baker,D., Harbige,L.S., Fazakerley,J.K., and Amor,S. (1997). Characterization of the cellular and cytokine response in the central nervous system following Semliki Forest virus infection. J Neuroimmunol. *74*, 185-197.

Morris-Downes,M.M., Sheahan,B.J., Fleeton,M.N., Liljestrom,P., Reid,H.W., and Atkins,G.J. (2001). A recombinant Semliki Forest virus particle vaccine encoding the prME and NS1 proteins of louping ill virus is effective in a sheep challenge model. Vaccine *19*, 3877-3884.

Mrkic,B., Pavlovic,J., Rulicke,T., Volpe,P., Buchholz,C.J., Hourcade,D., Atkinson,J.P., Aguzzi,A., and Cattaneo,R. (1998). Measles virus spread and pathogenesis in genetically modified mice. J. Virol. *72*, 7420-7427.

Muhleisen,H., Gehrmann,J., and Meyermann,R. (1995). Reactive microglia in Creutzfeldt-Jakob disease. Neuropathol. Appl. Neurobiol. *21*, 505-517.

Muller,U., Steinhoff,U., Reis,L.F., Hemmi,S., Pavlovic,J., Zinkernagel,R.M., and Aguet,M. (1994). Functional role of type I and type II interferons in antiviral defense. Science *264*, 1918-1921.

Murphy,G.M., Jr., Jia,X.C., Yu,A.C., Lee,Y.L., Tinklenberg,J.R., and Eng,L.F. (1993). Reverse transcription and polymerase chain reaction technique for quantification of mRNA in primary astrocyte cultures. J. Neurosci. Res. *35*, 643-651.

Muzio,M., Bosisio,D., Polentarutti,N., D'amico,G., Stoppacciaro,A., Mancinelli,R., van't Veer,C., Penton-Rol,G., Ruco,L.P., Allavena,P., and Mantovani,A. (2000). Differential expression and regulation of toll-like receptors (TLR) in human leukocytes: selective expression of TLR3 in dendritic cells. J. Immunol. *164*, 5998-6004.

Nadeau,S. and Rivest,S. (2000). Role of microglial-derived tumor necrosis factor in mediating CD14 transcription and nuclear factor kappa B activity in the brain during endotoxemia. J. Neurosci. *20*, 3456-3468.

Nagai,Y., Akashi,S., Nagafuku,M., Ogata,M., Iwakura,Y., Akira,S., Kitamura,T., Kosugi,A., Kimoto,M., and Miyake,K. (2002). Essential role of MD-2 in LPS responsiveness and TLR4 distribution. Nat. Immunol. *3*, 667-672.

Nakagawa,R., Naka,T., Tsutsui,H., Fujimoto,M., Kimura,A., Abe,T., Seki,E., Sato,S., Takeuchi,O., Takeda,K., Akira,S., Yamanishi,K., Kawase,I., Nakanishi,K., and Kishimoto,T. (2002). SOCS-1 participates in negative regulation of LPS responses. Immunity. *17*, 677-687.

Nakamura,K., Funakoshi,H., Miyamoto,K., Tokunaga,F., and Nakamura,T. (2001). Molecular cloning and functional characterization of a human scavenger receptor with C-type lectin (SRCL), a novel member of a scavenger receptor family. Biochem. Biophys. Res. Commun. *280*, 1028-1035.

Neumann,H., Schmidt,H., Wilharm,E., Behrens,L., and Wekerle,H. (1997). Interferon gamma gene expression in sensory neurons: evidence for autocrine gene regulation. J. Exp. Med. *186*, 2023-2031.

Nguyen,M.D., D'Aigle,T., Gowing,G., Julien,J.P., and Rivest,S. (2004). Exacerbation of motor neuron disease by chronic stimulation of innate immunity in a mouse model of amyotrophic lateral sclerosis. J. Neurosci. *24*, 1340-1349.

Nilsen,N.J., Nonstad,U., Khan,N., Knetter,C.F., Akira,S., Sundan,A., Espevik,T., and Lien,E. (2004). Lipopolysaccharide and double-stranded RNA upregulate toll-like receptor 2 independently of myeloid differentiation factor 88. J. Biol. Chem.

Nilsen,T.W. and Baglioni,C. (1979). Mechanism for discrimination between viral and host mRNA in interferon-treated cells. Proc. Natl. Acad. Sci. U. S. A *76*, 2600-2604.

Nitsch, R. M. and Hock, C. Vaccination against beta-amyloid in Alzheimer's disease. J Neuroimmunol. 154[Special Issue 1], 7. 2004.

Ref Type: Abstract

Nomura,F., Akashi,S., Sakao,Y., Sato,S., Kawai,T., Matsumoto,M., Nakanishi,K., Kimoto,M., Miyake,K., Takeda,K., and Akira,S. (2000). Cutting edge: endotoxin tolerance in mouse peritoneal macrophages correlates with down-regulation of surface toll-like receptor 4 expression. J. Immunol. *164*, 3476-3479.

O'Neill,L.A. (2004). Immunology. After the toll rush. Science *303*, 1481-1482.

Ohashi,K., Burkart,V., Flohe,S., and Kolb,H. (2000). Cutting edge: heat shock protein 60 is a puta tive endogenous ligand of the toll-like receptor-4 complex. J. Immunol. *164*, 558-561.

Okuno,T., Nakatsuji,Y., Kumanogoh,A., Koguchi,K., Moriya,M., Fujimura,H., Kikutani,H., and Sakoda,S. (2004). Induction of cyclooxygenase-2 in reactive glial cells by the CD40 pathway: relevance to amyotrophic lateral sclerosis. J. Neurochem. *91*, 404-412.

Oliver,K.R. and Fazakerley,J.K. (1998). Transneuronal spread of Semliki Forest virus in the developing mouse olfactory system is determined by neuronal maturity. Neuroscie nce *82*, 867-877.

Oliver,K.R., Scallan,M.F., Dyson,H., and Fazakerley,J.K. (1997). Susceptibility to a neurotropic virus and its changing distribution in the developing brain is a function of CNS maturity. J. Neurovirol. *3*, 38-48.

Olmsted,J.B., Carlson,K., Klebe,R., Ruddle,F., and Rosenbaum,J. (1970). Isolation of microtubule protein from cultured mouse neuroblastoma cells. Proc. Natl. Acad. Sci. U. S. A *65*, 129-136.

Olson,J.K., Girvin,A.M., and Miller,S.D. (2001). Direct activation of innate and antigen-presenting functions of microglia following infection with Theiler's virus. J. Virol. *75*, 9780-9789.

Olson,J.K. and Miller,S.D. (2004). Microglia Initiate Central Nervous System Innate and Adaptive Immune Responses through Multiple TLRs. J. Immunol. *173*, 3916-3924.

Omar,A. and Koblet,H. (1988). Semliki Forest virus particles containing only the E1 envelope glycoprotein are infectious and can induce cell-cell fusion. Virology *166*, 17-23.

Oshiumi,H., Matsumoto,M., Funami,K., Akazawa,T., and Seya,T. (2003). TICAM-1, an adaptor molecule that participates in Toll-like receptor 3-mediated interferon-beta induction. Nat. Immunol. *4*, 161-167.

Ozinsky,A., Underhill,D.M., Fontenot,J.D., Hajjar,A.M., Smith,K.D., Wilson,C.B., Schroeder,L., and Aderem,A. (2000). The repertoire for pattern recognition of pathogens by the innate immune system is defined by cooperation between toll-like receptors. Proc. Natl. Acad. Sci. U. S. A *97*, 13766-13771.

Pachter,J.S., de Vries,H.E., and Fabry,Z. (2003). The blood-brain barrier and its role in immune privilege in the central nervous system. J. Neuropathol. Exp. Neurol. *62*, 593-604.

Paglinawan,R., Malipiero,U., Schlapbach,R., Frei,K., Reith,W., and Fontana,A. (2003). TGFbeta directs gene expression of activated microglia to an anti-inflammatory phenotype strongly focusing on chemokine genes and cell migratory genes. Glia *44*, 219-231.

Palecanda,A., Paulauskis,J., Al Mutairi,E., Imrich,A., Qin,G., Suzuki,H., Kodama,T., Tryggvason,K., Koziel,H., and Kobzik,L. (1999). Role of the scavenger receptor MARCO in alveolar macrophage binding of unopsonized environmental particles. J. Exp. Med. *189*, 1497-1506.

Parsons,L.M. and Webb,H.E. (1982). Blood brain barrier disturbance and immunoglobulin G levels in the cerebrospinal fluid of the mouse following peripheral infection with the demyelinating strain of Semliki Forest virus. J. Neurol. Sci. *57*, 307-318.

Pathak,S. and Webb,H.E. (1978). An electron-microscopic study of avirulent and virulent Semliki forest virus in the brains of different ages of mice. J. Neurol. Sci. *39*, 199-211.

Paul,R., Koedel,U., Winkler,F., Kieseier,B.C., Fontana,A., Kopf,M., Hartung,H.P., and Pfister,H.W. (2003). Lack of IL-6 augments inflammatory response but decreases vascular permeability in bacterial meningitis. Brain *126*, 1873-1882.

Pearson,A.M. (1996). Scavenger receptors in innate immunity. Curr. Opin. Immunol. *8*, 20-28.

Pennell,N.A. and Streit,W.J. (1998). Tracing of fluoro-gold prelabeled microglia injected into the adult rat brain. Glia *23*, 84-88.

Peress,N.S., Fleit,H.B., Perillo,E., Kuljis,R., and Pezzullo,C. (1993). Identification of Fc gamma RI, II and III on normal human brain ramified microglia and on microglia in senile plaques in Alzheimer's disease. J. Neuroimmunol. *48*, 71-79.

Perry,S. and Marotta,R.F. (1987). AIDS dementia: a review of the literature. Alzheimer Dis. Assoc. Disord. *1*, 221-235.

Perry,V.H. (2004). The influence of systemic inflammation on inflammation in the brain: implications for chronic neurodegenerative disease. Brain Behav. Immun. *18*, 407-413.

Perry,V.H., Newman,T.A., and Cunningham,C. (2003). The impact of systemic infection on the progression of neurodegenerative disease. Nat. Rev. Neurosci. *4*, 103-112.

Picard,C., Puel,A., Bonnet,M., Ku,C.L., Bustamante,J., Yang,K., Soudais,C., Dupuis,S., Feinberg, J., Fieschi,C., Elbim,C., Hitchcock,R., Lammas,D., Davies,G., Al Ghonaium,A., Al Rayes,H., Al Jumaah,S., Al Hajjar,S., Al Mohsen,I.Z., Frayha,H.H., Rucker,R., Hawn,T.R., Aderem,A., Tufenkeji,H., Haraguchi,S., Day,N.K., Good,R.A., Gougerot-Pocidalo,M.A., Ozinsky,A., and Casanova,J.L. (2003). Pyogenic bacterial infections in humans with IRAK-4 deficiency. Science *299*, 2076-2079.

Piccio,L., Rossi,B., Scarpini,E., Laudanna,C., Giagulli,C., Issekutz,A.C., Vestweber,D., Butcher,E.C., and Constantin,G. (2002). Molecular mechanisms involved in lymphocyte recruitment in inflamed brain microvessels: critical roles for P-selectin glycoprotein ligand-1 and heterotrimeric G(i)-linked receptors. J. Immunol. *168*, 1940-1949.

Poltorak,A., He,X., Smirnova,I., Liu,M.Y., Van Huffel,C., Du,X., Birdwell,D., Alejos,E., Silva,M., Galanos,C., Freudenberg,M., Ricciardi-Castagnoli,P., Layton,B., and Beutler,B. (1998). Defective LPS signaling in C3H/HeJ and C57BL/10ScCr mice: mutations in Tlr4 gene. Science *282*, 2085-2088.

Poltorak,A., Ricciardi-Castagnoli,P., Citterio,S., and Beutler,B. (2000). Physical contact between lipopolysaccharide and toll-like receptor 4 revealed by genetic complementation. Proc. Natl. Acad. Sci. U. S. A *97*, 2163-2167.

Powell,P.P., Dixon,L.K., and Parkhouse,R.M. (1996). An IkappaB homolog encoded by African swine fever virus provides a novel mechanism for downregulation of proinflammatory cytokine responses in host macrophages. J. Virol. *70*, 8527-8533.

Prinz,M., Heikenwalder,M., Schwarz,P., Takeda,K., Akira,S., and Aguzzi,A. (2003). Prion pathogenesis in the absence of Toll-like receptor signalling. EMBO Rep. *4*, 195-199.

Prusiner,S.B. (1998). Prions. Proc. Natl. Acad. Sci. U. S. A *95*, 13363-13383.

Pusztai,R., Gould,E.A., and Smith,H. (1971). Infection patterns in mice of an avirulent and virulent strain of Semliki Forest virus. Br. J. Exp. Pathol. *52*, 669-677.

Qi,H., Denning,T.L., and Soong,L. (2003). Differential induction of interleukin-10 and interleukin-12 in dendritic cells by microbial toll-like receptor activators and skewing of T-cell cytokine profiles. Infect. Immun. *71*, 3337-3342.

Qureshi,S.T., Lariviere,L., Leveque,G., Clermont,S., Moore,K.J., Gros,P., and Malo,D. (1999). Endotoxin-tolerant mice have mutations in Toll-like receptor 4 (Tlr4). J. Exp. Med. *189*, 615-625.

Raff,M.C., Miller,R.H., and Noble,M. (1983). A glial progenitor cell that develops in vitro into an astrocyte or an oligodendrocyte depending on culture medium. Nature *303*, 390-396.

Raivich,G., Bohatschek,M., Kloss,C.U., Werner,A., Jones,L.L., and Kreutzberg,G.W. (1999). Neuroglial activation repertoire in the injured brain: graded response, molecular mechanisms and cues to physiological function. Brain Res. Brain Res. Rev. *30*, 77-105.

Rappert,A., Biber,K., Nolte,C., Lipp,M., Schubel,A., Lu,B., Gerard,N.P., Gerard,C., Boddeke,H.W., and Kettenmann,H. (2002). Secondary lymphoid tissue chemokine (CCL21) activates CXCR3 to trigger a Cl- current and chemotaxis in murine microglia. J. Immunol. *168*, 3221-3226.

Rassa,J.C., Meyers,J.L., Zhang,Y., Kudaravalli,R., and Ross,S.R. (2002). Murine retroviruses activate B cells via interaction with toll-like receptor 4. Proc. Natl. Acad. Sci. U. S. A *99*, 2281-2286.

Re,F. and Strominger,J.L. (2001). Toll-like receptor 2 (TLR2) and TLR4 differentially activate hum an dendritic cells. J. Biol. Chem. *276*, 37692-37699.

Reis e Sousa (2001). Dendritic cells as sensors of infection. Immunity. *14*, 495-498.

Reis e Sousa (2004). Toll-like receptors and dendritic cells: for whom the bug tolls. Semin. Immunol. *16*, 27-34.

Rezaie,P. and Lantos,P.L. (2001). Microglia and the pathogenesis of spongiform encephalopathies. Brain Res. Brain Res. Rev. *35*, 55-72.

Riek,R., Hornemann,S., Wider,G., Billeter,M., Glockshuber,R., and Wuthrich,K. (1996). NMR structure of the mouse prion protein domain PrP(121-321). Nature *382*, 180-182.

Righi,M., Mori,L., De Libero,G., Sironi,M., Biondi,A., Mantovani,A., Donini,S.D., and Ricciardi-Castagnoli,P. (1989). Monokine production by microglial cell clones. Eur. J. Immunol. *19*, 1443-1448.

Rikkonen,M. (1996). Functional significance of the nuclear-targeting and NTP-binding motifs of Semliki Forest virus nonstructural protein nsP2. Virology *218*, 352-361.

Rissoan,M.C., Soumelis,V., Kadowaki,N., Grouard,G., Briere,F., de Waal,M.R., and Liu,Y.J. (1999). Reciprocal control of T helper cell and dendritic cell differentiation. Science *283*, 1183-1186.

Rivas,F., Diaz,L.A., Cardenas,V.M., Daza,E., Bruzon,L., Alcala,A., De la,H.O., Caceres,F.M., Aristizabal,G., Martinez,J.W., Revelo,D., De la,H.F., Boshell,J., Camacho,T., Calderon,L., Olano,V.A., Villarreal,L.I., Roselli,D., Alvarez,G., Ludwig,G., and Tsai,T. (1997). Epidemic Venezuelan equine encephalitis in La Guajira, Colombia, 1995. J. Infect. Dis. *175*, 828-832.

Rock,F.L., Hardiman,G., Timans,J.C., Kastelein,R.A., and Bazan,J.F. (1998). A family of human receptors structurally related to Drosophila Toll. Proc. Natl. Acad. Sci. U. S. A *95*, 588-593.

Roger,T., David,J., Glauser,M.P., and Calandra,T. (2001). MIF regulates innate immune responses through modulation of Toll-like receptor 4. Nature *414*, 920-924.

Roger,T., Froidevaux,C., Martin,C., and Calandra,T. (2003). Macrophage migration inhibitory factor (MIF) regulates host responses to endotoxin through modulation of Toll-like receptor 4 (TLR4). J. Endotoxin. Res. *9*, 119-123.

Ronco,L.V., Karpova,A.Y., Vidal,M., and Howley,P.M. (1998). Human papillomavirus 16 E6 oncoprotein binds to interferon regulatory factor-3 and inhibits its transcriptional activity. Genes Dev. *12*, 2061-2072.

Rousseau,V., Cremer,I., Lauret,E., Riviere,I., Aguet,M., and De Maeyer,E. (1995). Antiviral activity of autocrine interferon-beta requires the presence of a functional interferon type I receptor. J. Interferon Cytokine Res. *15*, 785-789.

Rutschmann,S., Jung,A.C., Hetru,C., Reichhart,J.M., Hoffmann,J.A., and Ferrandon,D. (2000). The Rel protein DIF mediates the antifungal but not the antibacterial host defense in Drosophila. Immunity. *12*, 569-580.

Rutschmann,S., Kilinc,A., and Ferrandon,D. (2002). Cutting edge: the toll pathway is required for resistance to gram-positive bacterial infections in Drosophila. J. Immunol. *168*, 1542-1546.

Sangfelt,O., Erickson,S., Castro,J., Heiden,T., Gustafsson,A., Einhorn,S., and Grander,D. (1999). Molecular mechanisms underlying interferon-alpha-induced G0/G1 arrest: CKI-mediated regulation of G1 Cdk-complexes and activation of pocket proteins. Oncogene *18*, 2798-2810.

Santagati,M.G., Maatta,J.A., Itaranta,P.V., Salmi,A.A., and Hinkkanen,A.E. (1995). The Semliki Forest virus E2 gene as a virulence determinant. J. Gen. Virol. *76 (Pt 1)*, 47-52.

Sato,M., Hata,N., Asagiri,M., Nakaya,T., Taniguchi,T., and Tanaka,N. (1998). Positive feedback regulation of type I IFN genes by the IFN-inducible transcription factor IRF-7. FEBS Lett. *441*, 106-110.

Sato,S., Sugiyama,M., Yamamoto,M., Watanabe,Y., Kawai,T., Takeda,K., and Akira,S. (2003). Toll/IL-1 receptor domain-containing adaptor inducing IFN-beta (TRIF) associates with TNF receptor-associated factor 6 and TANK-binding kinase 1, and activates two distinct transcription factors, NF-kappa B and IFN-regulatory factor-3, in the Toll-like receptor signaling. J. Immunol. *171*, 4304-4310.

Savill,J., Dransfield,I., Gregory,C., and Haslett,C. (2002). A blast from the past: clearance of apoptotic cells regulates immune responses. Nat. Rev. Immunol. *2*, 965-975.

Schluesener,H.J., Seid,K., Deininger,M., and Schwab,J. (2001). Transient in vivo activation of rat brain macrophages/microglial cells and astrocytes by immunostimulatory multiple CpG oligonucleotides. J. Neuroimmunol. *113*, 89-94.

Schmid,C.D., Sautkulis,L.N., Danielson,P.E., Cooper,J., Hasel,K.W., Hilbush,B.S., Sutcliffe,J.G., and Carson,M.J. (2002). Heterogeneous expression of the triggering receptor expressed on myeloid cells -2 on adult murine microglia. J. Neurochem. *83*, 1309-1320.

Schnare,M., Barton,G.M., Holt,A.C., Takeda,K., Akira,S., and Medzhitov,R. (2001). Toll-like receptors control activation of adaptive immune responses. Nat. Immunol. *2*, 947-950.

Schwandner,R., Dziarski,R., Wesche,H., Rothe,M., and Kirschning,C.J. (1999). Peptidoglycan- and lipoteichoic acid-induced cell activation is mediated by toll-like receptor 2. J. Biol. Chem. *274*, 17406-17409.

Seibl,R., Birchler,T., Loeliger,S., Hossle,J.P., Gay,R.E., Saurenmann,T., Michel,B.A., Seger,R.A., Gay,S., and Lauener,R.P. (2003). Expression and regulation of Toll-like receptor 2 in rheumatoid arthritis synovium. Am. J. Pathol. *162*, 1221-1227.

Selkoe,D.J. (1999). Translating cell biology into therapeutic advances in Alzheimer's disease. Nature *399*, A23-A31.

Servant,M.J., Grandvaux,N., tenOever,B.R., Duguay,D., Lin,R., and Hiscott,J. (2003). Identification of the minimal phosphoacceptor site required for in vivo activation of interferon regulatory factor 3 in response to virus and double-stranded RNA. J. Biol. Chem. *278*, 9441-9447.

Sethi,S., Lipford,G., Wagner,H., and Kretzschmar,H. (2002). Postexposure prophylaxis against prion disease with a stimulator of innate immunity. Lancet *360*, 229-230.

Shankar,V., Dietzschold,B., and Koprowski,H. (1991). Direct entry of rabies virus into the central nervous system without prior local replication. J. Virol. *65*, 2736-2738.

Sharma,S., tenOever,B.R., Grandvaux,N., Zhou,G.P., Lin,R., and Hiscott,J. (2003). Triggering the interferon antiviral response through an IKK-related pathway. Science *300*, 1148-1151.

Shea,T.B. and Beermann,M.L. (1994). Respective roles of neurofilaments, microtubules, MAP1B, and tau in neurite outgrowth and stabilization. Mol. Biol. Cell *5*, 863-875.

Shimazu,R., Akashi,S., Ogata,H., Nagai,Y., Fukudome,K., Miyake,K., and Kimoto,M. (1999). MD-2, a molecule that confers lipopolysaccharide responsiveness on Toll-like receptor 4. J. Exp. Med. *189*, 1777-1782.

Shrestha,B., Gottlieb,D., and Diamond,M.S. (2003). Infection and injury of neurons by West Nile encephalitis virus. J. Virol. *77*, 13203-13213.

Shuai,K., Horvath,C.M., Huang,L.H., Qureshi,S.A., Cowburn,D., and Darnell,J.E., Jr. (1994). Interferon activation of the transcription factor Stat91 involves dimerization through SH2-phosphotyrosyl peptide interactions. Cell *76*, 821-828.

Siegal,F.P., Kadowaki,N., Shodell,M., Fitzgerald-Bocarsly,P.A., Shah,K., Ho,S., Antonenko,S., and Liu,Y.J. (1999). The nature of the principal type 1 interferon -producing cells in human blood. Science *284*, 1835-1837.

Sippy,B.D., Hofman,F.M., Wallach,D., and Hinton,D.R. (1995). Increased expression of tumor necrosis factor-alpha receptors in the brains of patients with AIDS. J. Acquir. Immune. Defic. Syndr. Hum. Retrovirol. *10*, 511-521.

Slack,J.L., Schooley,K., Bonnert,T.P., Mitcham,J.L., Qwarnstrom,E.E., Sims,J.E., and Dower,S.K. (2000). Identification of two major sites in the type I interleukin-1 receptor cytoplasmic region responsible for coupling to pro-inflammatory signaling pathways. J. Biol. Chem. *275*, 4670-4678.

Smiley,S.T., King,J.A., and Hancock,W.W. (2001). Fibrinogen stimulates macrophage chemokine secretion through toll-like receptor 4. J. Immunol. *167*, 2887-2894.

Smithburn and Haddow (1944). J. Immunol. *49*, 141-145.

Smyth,J.M., Sheahan,B.J., and Atkins,G.J. (1990). Multiplication of virulent and demyelinating Semliki Forest virus in the mouse central nervous system: consequences in BALB/c and SJL mice. J. Gen. Virol. *71 (Pt 11)*, 2575-2583.

Soilu-Hanninen,M., Eralinna,J.P., Hukkanen,V., Roytta,M., Salmi,A.A., and Salonen,R. (1994). Semliki Forest virus infects mouse brain endothelial cells and causes blood-brain barrier damage. J. Virol. *68*, 6291-6298.

Soilu-Hanninen,M., Roytta,M., Salmi,A.A., and Salonen,R. (1997). Semliki Forest virus infection leads to increased expression of adhesion molecules on splenic T-cells and on brain vascular endothelium. J. Neurovirol. *3*, 350-360.

Solomon,T. (2004). Flavivirus encephalitis. N. Engl. J. Med. *351*, 370-378.

Sorensen,J.C., Dalmau,I., Zimmer,J., and Finsen,B. (1996). Microglial reactions to retrograde degeneration of tracer-identified thalamic neurons after frontal sensorimotor cortex lesions in adult rats. Exp. Brain Res. *112*, 203-212.

Stranden,A.M., Staeheli,P., and Pavlovic,J. (1993). Function of the mouse Mx1 protein is inhibited by overexpression of the PB2 protein of influenza virus. Virology *197*, 642-651.

Strauss,J.H. and Strauss,E.G. (1994). The alphaviruses: gene expression, replication, and evolution. Microbiol. Rev. *58*, 491-562.

Streit,W.J. (2002). Microglia as neuroprotective, immunocompetent cells of the CNS. Glia *40*, 133-139.

Streit,W.J., Walter,S.A., and Pennell,N.A. (1999). Reactive microgliosis. Prog. Neurobiol. *57*, 563-581.

Subak-Sharpe,I., Dyson,H., and Fazakerley,J. (1993). In vivo depletion of CD8+ T cells prevents lesions of demyelination in Semliki Forest virus infection. J Virol *67*, 7629-7633.

Subramaniam,P.S., Cruz,P.E., Hobeika,A.C., and Johnson,H.M. (1998). Type I interferon induction of the Cdk inhibitor p21WAF1 is accompanied by ordered G1 arrest, differentiation and apoptosis of the Daudi B-cell line. Oncogene *16*, 1885-1890.

Suckling,A.J., Jagelman,S., and Webb,H.E. (1982). Immunoglobulin synthesis in nude (nu/nu), nu/+ and reconstituted nu/nu mice infected with a demyelinating strain of Semliki Forest virus. Clin. Exp. Immunol. *47*, 283-288.

Suckling,A.J., Pathak,S., Jagelman,S., and Webb,H.E. (1978). Virus-associated demyelination. A model using avirulent Semliki Forest virus infection of mice. J. Neurol. Sci. *39*, 147-154.

Sun,S., Zhang,X., Tough,D.F., and Sprent,J. (1998). Type I interferon-mediated stimulation of T cells by CpG DNA. J Exp. Med. *188*, 2335-2342.

Supajatura,V., Ushio,H., Nakao,A., Okumura,K., Ra,C., and Ogawa,H. (2001). Protective roles of mast cells against enterobacterial infection are mediated by Toll-like receptor 4. J. Immunol. *167*, 2250-2256.

Suzuki,T., Higgins,P.J., and Crawford,D.R. (2000). Control selection for RNA quantitation. Biotechniques *29*, 332-337.

Swantek,J.L., Tsen,M.F., Cobb,M.H., and Thomas,J.A. (2000). IL-1 receptor-associated kinase modulates host responsiveness to endotoxin. J. Immunol. *164*, 4301-4306.

Sweet,M.J., Campbell,C.C., Sester,D.P., Xu,D., McDonald,R.C., Stacey,K.J., Hume,D.A., and Liew,F.Y. (2002). Colony-stimulating factor-1 suppresses responses to CpG DNA and expression of toll-like receptor 9 but enhances responses to lipopolysaccharide in murine macrophages. J. Immunol. *168*, 392-399.

Symons,J.A., Alcami,A., and Smith,G.L. (1995). Vaccinia virus encodes a soluble type I interferon receptor of novel structure and broad species specificity. Cell *81*, 551-560.

Tabeta,K., Georgel,P., Janssen,E., Du,X., Hoebe,K., Crozat,K., Mudd,S., Shamel,L., Sovath,S., Goode,J., Alexopoulou,L., Flavell,R.A., and Beutler,B. (2004). Toll-like receptors 9 and 3 as essential components of innate immune defense against mouse cytomegalovirus infection. Proc. Natl. Acad. Sci. U. S. A *101*, 3516-3521.

Takaesu,G., Kishida,S., Hiyama,A., Yamaguchi,K., Shibuya,H., Irie,K., Ninomiya-Tsuji,J., and Matsumoto,K. (2000). TAB2, a novel adaptor protein, mediates activation of TAK1 MAPKKK by linking TAK1 to TRAF6 in the IL-1 signal transduction pathway. Mol. Cell *5*, 649-658.

Takaesu,G., Surabhi,R.M., Park,K.J., Ninomiya-Tsuji,J., Matsumoto,K., and Gaynor,R.B. (2003). TAK1 is critical for IkappaB kinase-mediated activation of the NF-kappaB pathway. J. Mol. Biol. *326*, 105-115.

Takeda,K., Kaisho,T., and Akira,S. (2003). Toll-like receptors. Annu. Rev. Immunol. *21*, 335-376.

Takeuchi,O., Hoshino,K., and Akira,S. (2000). Cutting edge: TLR2-deficient and MyD88-deficient mice are highly susceptible to Staphylococcus aureus infection. J. Immunol. *165*, 5392-5396.

Takeuchi,O., Hoshino,K., Kawai,T., Sanjo,H., Takada,H., Ogawa,T., Takeda,K., and Akira,S. (1999a). Differential roles of TLR2 and TLR4 in recognition of gram-negative and gram-positive bacterial cell wall components. Immunity. *11*, 443-451.

Takeuchi,O., Kawai,T., Muhlradt,P.F., Morr,M., Radolf,J.D., Zychlinsky,A., Takeda,K., and Akira,S. (2001). Discrimination of bacterial lipoproteins by Toll-like receptor 6. Int. Immunol. *13*, 933-940.

Takeuchi,O., Kawai,T., Sanjo,H., Copeland,N.G., Gilbert,D.J., Jenkins,N.A., Takeda,K., and Akira,S. (1999b). TLR6: A novel member of an expanding toll-like receptor family. Gene *231*, 59-65.

Takeuchi,O., Sato,S., Horiuchi,T., Hoshino,K., Takeda,K., Dong,Z., Modlin,R.L., and Akira,S. (2002). Cutting edge: role of Toll-like receptor 1 in mediating immune response to microbial lipoproteins. J. Immunol. *169*, 10-14.

Tan,J., Town,T., Crawford,F., Mori,T., DelleDonne,A., Crescentini,R., Obregon,D., Flavell,R.A., and Mullan,M.J. (2002). Role of CD40 ligand in amyloidosis in transgenic Alzheimer's mice. Nat. Neurosci. *5*, 1288-1293.

Tanaka,N., Sato,M., Lamphier,M.S., Nozawa,H., Oda,E., Noguchi,S., Schreiber,R.D., Tsujimoto,Y., and Taniguchi,T. (1998). Type I interferons are essential mediators of apoptotic death in virally infected cells. Genes Cells *3*, 29-37.

Taniguchi,T. and Takaoka,A. (2002). The interferon-alpha/beta system in antiviral responses: a multimodal machinery of gene regulation by the IRF family of transcription factors. Curr. Opin. Immunol. *14*, 111-116.

Thanos,S., Kacza,J., Seeger,J., and Mey,J. (1994). Old dyes for new scopes: the phagocytosis-dependent long-term fluorescence labelling of microglial cells in vivo. Trends Neurosci. *17*, 177-182.

Theerasurakarn,S. and Ubol,S. (1998). Apoptosis induction in brain during the fixed strain of rabies virus infection correlates with onset and severity of illness. J Neurovirol. *4*, 407-414.

Thibeault,I., Laflamme,N., and Rivest,S. (2001). Regulation of the gene encoding the monocyte chemoattractant protein 1 (MCP-1) in the mouse and rat brain in response to circulating LPS and proinflammatory cytokines. J. Comp Neurol. *434*, 461-477.

Thoma-Uszynski,S., Stenger,S., Takeuchi,O., Ochoa,M.T., Engele,M., Sieling,P.A., Barnes,P.F., Rollinghoff,M., Bolcskei,P.L., Wagner,M., Akira,S., Norgard,M.V., Belisle,J.T., Godowski,P.J., Bloom,B.R., and Modlin,R.L. (2001). Induction of direct antimicrobial activity through mammalian toll-like receptors. Science *291*, 1544-1547.

Toshchakov,V., Jones,B.W., Perera,P.Y., Thomas,K., Cody,M.J., Zhang,S., Williams,B.R., Major,J., Hamilton,T.A., Fenton,M.J., and Vogel,S.N. (2002). TLR4, but not TLR2, mediates IFN-beta-induced STAT1alpha/beta-dependent gene expression in macrophages. Nat. Immunol. *3*, 392-398.

Tsai,E. (2002). Alphaviruses. In Clinical Virology, D.D.Rickmann, R.J.Whitley, and F.G.Hayden, eds. (Washington, D.C.: ASM press).

Tsuji,S., Matsumoto,M., Takeuchi,O., Akira,S., Azuma,I., Hayashi,A., Toyoshima,K., and Seya,T. (2000). Maturation of human dendritic cells by cell wall skeleton of Mycobacterium bovis bacillus Calmette-Guerin: involvement of toll-like receptors. Infect. Immun. *68*, 6883-6890.

Tsunawaki,S., Kagara,S., Yoshikawa,K., Yoshida,L.S., Kuratsuji,T., and Namiki,H. (1996). Involvement of p40phox in activation of phagocyte NADPH oxidase through association of its carboxyl-terminal, but not its amino-terminal, with p67phox. J. Exp. Med. *184*, 893-902.

Tuittila,M. and Hinkkanen,A.E. (2003). Amino acid mutations in the replicase protein nsP3 of Semliki Forest virus cumulatively affect neurovirulence. J. Gen. Virol. *84*, 1525-1533.

Tuittila,M.T., Santagati,M.G., Roytta,M., Maatta,J.A., and Hinkkanen,A.E. (2000). Replicase complex genes of Semliki Forest virus confer lethal neurovirulence. J. Virol. *74*, 4579-4589.

Tunaru,S., Kero,J., Schaub,A., Wufka,C., Blaukat,A., Pfeffer,K., and Offermanns,S. (2003). PUMA-G and HM74 are receptors for nicotinic acid and mediate its anti-lipolytic effect. Nat. Med. *9*, 352-355.

Tzou,P., Reichhart,J.M., and Lemaitre,B. (2002). Constitutive expression of a single antimicrobial peptide can restore wild-type resistance to infection in immunodeficient Drosophila mutants. Proc. Natl. Acad. Sci. U. S. A *99*, 2152-2157.

Underhill,D.M., Ozinsky,A., Hajjar,A.M., Stevens,A., Wilson,C.B., Bassetti,M., and Aderem,A. (1999a). The Toll-like receptor 2 is recruited to macrophage phagosomes and discriminates between pathogens. Nature *401*, 811-815.

Underhill,D.M., Ozinsky,A., Smith,K.D., and Aderem,A. (1999b). Toll-like receptor-2 mediates mycobacteria-induced proinflammatory signaling in macrophages. Proc. Natl. Acad. Sci. U. S. A *96*, 14459-14463.

Vabulas,R.M., Braedel,S., Hilf,N., Singh-Jasuja,H., Herter,S., Ahmad-Nejad,P., Kirschning,C.J., Da Costa,C., Rammensee,H.G., Wagner,H., and Schild,H. (2002). The endoplasmic reticulum-resident heat shock protein Gp96 activates dendritic cells via the Toll-like receptor 2/4 pathway. J. Biol. Chem. *277*, 20847-20853.

van den Broek,M.F., Muller,U., Huang,S., Aguet,M., and Zinkernagel,R.M. (1995). Antiviral defense in mice lacking both alpha/beta and gamma interferon receptors. J. Virol. *69*, 4792-4796.

van der Laan,L.J., Dopp,E.A., Haworth,R., Pikkarainen,T., Kangas,M., Elomaa,O., Dijkstra,C.D., Gordon,S., Tryggvason,K., and Kraal,G. (1999). Regulation and functional involvement of macrophage scavenger receptor MARCO in clearance of bacteria in vivo. J. Immunol. *162*, 939-947.

Vandesompele,J., De Preter,K., Pattyn,F., Poppe,B., Van Roy,N., De Paepe,A., and Speleman,F. (2002). Accurate normalization of real-time quantitative RT-PCR data by geometric averaging of multiple internal control genes. Genome Biol. *3*, RESEARCH0034.

Veals,S.A., Schindler,C., Leonard,D., Fu,X.Y., Aebersold,R., Darnell,J.E., Jr., and Levy,D.E. (1992). Subunit of an alpha-interferon-responsive transcription factor is related to interferon regulatory factor and Myb families of DNA-binding proteins. Mol. Cell Biol. *12*, 3315-3324.

Viriyakosol,S., Tobias,P.S., Kitchens,R.L., and Kirkland,T.N. (2001). MD-2 binds to bacterial lipopolysaccharide. J. Biol. Chem. *276*, 38044-38051.

Visintin,A., Mazzoni,A., Spitzer,J.H., Wyllie,D.H., Dower,S.K., and Segal,D.M. (2001). Regulation of Toll-like receptors in human monocytes and dendritic cells. J. Immunol. *166*, 249-255.

Wagner,H. (2001). Toll meets bacterial CpG-DNA. Immunity. *14*, 499-502.

Wahlberg,J.M. and Garoff,H. (1992). Membrane fusion process of Semliki Forest virus. I: Low pH-induced rearrangement in spike protein quaternary structure precedes virus penetration into cells. J. Cell Biol. *116*, 339-348.

Wald,D., Qin,J., Zhao,Z., Qian,Y., Naramura,M., Tian,L., Towne,J., Sims,J.E., Stark,G.R., and Li,X. (2003). SIGIRR, a negative regulator of Toll-like receptor-interleukin 1 receptor signaling. Nat. Immunol. *4*, 920-927.

Wang,T., Lafuse,W.P., Takeda,K., Akira,S., and Zwilling,B.S. (2002). Rapid chromatin remodeling of Toll-like receptor 2 promoter during infection of macrophages with Mycobacterium avium. J. Immunol. *169*, 795-801.

Wang,T., Lafuse,W.P., and Zwilling,B.S. (2000). Regulation of toll-like receptor 2 expression by macrophages following Mycobacterium avium infection. J. Immunol. *165*, 6308-6313.

Wang,T., Lafuse,W.P., and Zwilling,B.S. (2001). NFkappaB and Sp1 elements are necessary for maximal transcription of toll-like receptor 2 induced by Mycobacterium avium. J. Immunol. *167*, 6924-6932.

Wang,T., Town,T., Alexopoulou,L., Anderson,J.F., Fikrig,E., and Flavell,R.A. (2004). Toll-like receptor 3 mediates West Nile virus entry into the brain causing lethal encephalitis. Nat. Med. *10*, 1366-1373.

Wang,Y., Lobigs,M., Lee,E., and Mullbacher,A. (2003). CD8+ T cells mediate recovery and immunopathology in West Nile virus encephalitis. J. Virol. *77*, 13323-13334.

Warrington,J.A., Nair,A., Mahadevappa,M., and Tsyganskaya,M. (2000). Comparison of human adult and fetal expression and identification of 535 housekeeping/maintenance genes. Physiol Genomics *2*, 143-147.

Weiss,D.S., Raupach,B., Takeda,K., Akira,S., and Zychlinsky,A. (2004). Toll-like receptors are temporally involved in host defense. J. Immunol. *172*, 4463-4469.

Weissmann,C. (1999). Molecular genetics of transmissible spongiform encephalopathies. J. Biol. Chem. *274*, 3-6.

Werner,T., Liu,G., Kang,D., Ekengren,S., Steiner,H., and Hultmark,D. (2000). A family of peptidoglycan recognition proteins in the fruit fly Drosophila melanogaster. Proc. Natl. Acad. Sci. U. S. A *97*, 13772-13777.

Werts,C., Tapping,R.I., Mathison,J.C., Chuang,T.H., Kravchenko,V., Saint,G., I, Haake,D.A., Godowski,P.J., Hayashi,F., Ozinsky,A., Underhill,D.M., Kirschning,C.J., Wagner,H., Aderem,A., Tobias,P.S., and Ulevitch,R.J. (2001). Leptospiral lipopolysaccharide activates cells through a TLR2-dependent mechanism. Nat. Immunol. *2*, 346-352.

Wille,H., Michelitsch,M.D., Guenebaut,V., Supattapone,S., Serban,A., Cohen,F.E., Agard,D.A., and Prusiner,S.B. (2002). Structural studies of the scrapie prion protein by electron crystallography. Proc. Natl. Acad. Sci. U. S. A *99*, 3563-3568.

Williams,A., Lucassen,P.J., Ritchie,D., and Bruce,M. (1997a). PrP deposition, microglial activation, and neuronal apoptosis in murine scrapie. Exp. Neurol. *144*, 433-438.

Williams,A.E., Lawson,L.J., Perry,V.H., and Fraser,H. (1994). Characterization of the microglial response in murine scrapie. Neuropathol. Appl. Neurobiol. *20*, 47-55.

Williams,M.J., Rodriguez,A., Kimbrell,D.A., and Eldon,E.D. (1997b). The 18-wheeler mutation reveals complex antibacterial gene regulation in Drosophila host defense. EMBO J. *16*, 6120-6130.

Wolfs,T.G., Buurman,W.A., van Schadewijk,A., de Vries,B., Daemen,M.A., Hiemstra,P. S., and van,'., V (2002). In vivo expression of Toll-like receptor 2 and 4 by renal epithelial cells: IFN-gamma and TNF-alpha mediated up-regulation during inflammation. J. Immunol. *168*, 1286-1293.

Wong,A.H., Tam,N.W., Yang,Y.L., Cuddihy,A.R., Li,S., Kirchhoff,S., Hauser,H., Decker,T., and Koromilas,A.E. (1997). Physical association between STAT1 and the interferon-inducible protein kinase PKR and implications for interferon and double-stranded RNA signaling pathways. EMBO J. *16*, 1291-1304.

Wright,S.D., Ramos,R.A., Tobias,P.S., Ulevitch,R.J., and Mathison,J.C. (1990). CD14, a receptor for complexes of lipopolysaccharide (LPS) and LPS binding protein. Science *249*, 1431-1433.

Wyllie,D.H., Kiss-Toth,E., Visintin,A., Smith,S.C., Boussouf,S., Segal,D.M., Duff,G.W., and Dower,S.K. (2000). Evidence for an accessory protein function for Toll-like receptor 1 in anti-bacterial responses. J. Immunol. *165*, 7125-7132.

Xiao,S.Y., Guzman,H., Zhang,H., Travassos Da Rosa,A.P., and Tesh,R.B. (2001). West Nile virus infection in the golden hamster (Mesocricetus auratus): a model for West Nile encephalitis. Emerg. Infect. Dis. *7*, 714-721.

Yamaguchi,K., Shirakabe,K., Shibuya,H., Irie,K., Oishi,I., Ueno,N., Taniguchi,T., Nishida,E., and Matsumoto,K. (1995). Identification of a member of the MAPKKK family as a potential mediator of TGF-beta signal transduction. Science *270*, 2008-2011.

Yamamoto,M., Sato,S., Hemmi,H., Sanjo,H., Uematsu,S., Kaisho,T., Hoshino,K., Takeuchi,O., Kobayashi,M., Fujita,T., Takeda,K., and Akira,S. (2002a). Essential role for TIRAP in activation of the signalling cascade shared by TLR2 and TLR4. Nature *420*, 324-329.

Yamamoto,M., Sato,S., Hemmi,H., Uematsu,S., Hoshino,K., Kaisho,T., Takeuchi,O., Takeda,K., and Akira,S. (2003). TRAM is specifically involved in the Toll-like receptor 4-mediated MyD88-independent signaling pathway. Nat. Immunol. *4*, 1144-1150.

Yamamoto,M., Sato,S., Mori,K., Hoshino,K., Takeuchi,O., Takeda,K., and Akira,S. (2002b). Cutting edge: a novel Toll/IL-1 receptor domain-containing adapter that preferentially activates the IFN-beta promoter in the Toll-like receptor signaling. J. Immunol. *169*, 6668-6672.

Yang,Y.L., Reis,L.F., Pavlovic,J., Aguzzi,A., Schafer,R., Kumar,A., Williams,B.R., Aguet,M., and Weissmann,C. (1995). Deficient signaling in mice devoid of double-stranded RNA-dependent protein kinase. EMBO J. *14*, 6095-6106.

Yoneyama,M., Suhara,W., Fukuhara,Y., Fukuda,M., Nishida,E., and Fujita,T. (1998). Direct triggering of the type I interferon system by virus infection: activation of a transcription factor complex containing IRF-3 and CBP/p300. EMBO J. *17*, 1087-1095.

Yoshimura,A., Lien,E., Ingalls,R.R., Tuomanen,E., Dziarski,R., and Golenbock,D. (1999). Cutting edge: recognition of Gram-positive bacterial cell wall components by the innate immune system occurs via Toll-like receptor 2. J. Immunol. *163*, 1-5.

Zarember,K.A. and Godowski,P.J. (2002). Tissue expression of human Toll-like receptors and differential regulation of Toll-like receptor mRNAs in leukocytes in response to microbes, their products, and cytokines. J. Immunol. *168*, 554-561.

Zasloff,M. (2002). Antimicrobial peptides of multicellular organisms. Nature *415*, 389-395.

Zekki,H., Feinstein,D.L., and Rivest,S. (2002). The clinical course of experimental autoimmune encephalomyelitis is associated with a profound and sustained transcriptional activation of the genes encoding toll-like receptor 2 and CD14 in the mouse CNS. Brain Pathol. *12*, 308-319.

Zelko,I.N., Mariani,T.J., and Folz,R.J. (2002). Superoxide dismutase multigene family: a comparison of the CuZn-SOD (SOD1), Mn-SOD (SOD2), and EC-SOD (SOD3) gene structures, evolution, and expression. Free Radic. Biol. Med. *33*, 337-349.

Zhang,D., Zhang,G., Hayden,M.S., Greenblatt,M.B., Bussey,C., Flavell,R.A., and Ghosh,S. (2004). A toll-like receptor that prevents infection by uropathogenic bacteria. Science *303*, 1522-1526.

Zhao,M.L., Kim,M.O., Morgello,S., and Lee,S.C. (2001). Expression of inducible nitric oxide synthase, interleukin-1 and caspase-1 in HIV-1 encephalitis. J. Neuroimmunol. *115*, 182-191.

Zhou,A., Paranjape,J.M., Der,S.D., Williams,B.R., and Silverman,R.H. (1999). Interferon action in triply deficient mice reveals the existence of alternative antiviral pathways. Virology *258*, 435-440.

Zimmermann,S., Egeter,O., Hausmann,S., Lipford,G.B., Rocken,M., Wagner,H., and Heeg,K. (1998). CpG oligodeoxynucleotides trigger protective and curative Th1 responses in lethal murine leishmaniasis. J. Immunol. *160*, 3627-3630.

Zou,W.Q., Zheng,J., Gray,D.M., Gambetti,P., and Chen,S.G. (2004). Antibody to DNA detects scrapie but not normal prion protein. Proc. Natl. Acad. Sci. U. S. A *101*, 1380-1385.

Zychlinsky,A., Prevost,M.C., and Sansonetti,P.J. (1992). Shigella flexneri induces apoptosis in infected macrophages. Nature *358*, 167-169.

Appendix 1 – solutions

2.1.1 Fixatives and solutions for cell culture and immunocytochemistry

- PBS = Phosphate Buffered Saline
  - 137 mM NaCl
  - 2.7 mM KCl
  - 4.3 mM Na_2HPO_3
  - 1.7 mM NaH_2PO_3
- PLP = Phosphate Lysine Periodate
  - 75 ml Phosphate buffer containing 80 mM Na_2HPO_4 and 21 M NaH_2PO_4 pH 7.4
  - 75 ml 0.2M Lysine pH7.4
  - 0.9 g Sodium Periodate to give final concentration 21 mM
  - 50 ml paraformaldehyde solution
    - 4% paraformaldehyde solution made up using 2 g paraformaldehyde, 100µl 10M NaOH and gentle heating to dissolve paraformaldehyde, followed by addition of concentrated HCl drop-wise until pH=7.4
  - final solution of 200 ml was pH 7.4
  - PLP was made up fresh and used within 24 hours
- Sucrose solutions
  - 12%, 16% and 18% (wt:vol) sucrose solutions were made by the addition of 24, 32 a nd 36g of sucrose respectively to 200 ml PBS.

2.1.2 Microarray solutions

- 10% SDS= sodium dodecyl sulphate
  - 10 g SDS dissolved in 100ml nuclease free water
- 20XSSC = sodium chloride / sodium citrate
  - NaCl: 175.3g
  - Na_3 $citrate_2$ H_2O: 88.2g
  - 800ml of milliQ water added
  - pH7 with HCl.
  - volume made up to 1litre with milliQ water
- Sodium Borate
  - 30.9g Boric Acid + 450ml milliQ water
  - pH8 with NaOH , adjusted volume to 500ml
- Succinic anhydride/N-methyl-2-pyrrolidinone solution
  - 210 ml N-methyl-2-pyrrolidinone solution
  - 3.6 g Succinic anhydride (sigma – stored in desiccator) added and stirred very vigorously for 5 minutes until dissolved
  - 7.5 ml sodium borate buffer (see above) cleaned by passing through 0.45 µm filter and added to solution
  - Solution used immediately for blocking of microarray slides

Appendix 2 – function of genes assayed by microarray

Gene		Function
Toll-like Receptors		
TLR1	NM_030682	Confers specific recognition to lipoproteins with TLR2
TLR2	NM_011905	Responds to LTA, lipoproteins, peptidoglycan
TLR3	AF355152	Recognises dsRNA
TLR4	NM_021297	Signals in response to LPS
TLR5	NM_016928	Recognises bacterial flagellin
TLR6	NM_011604	Enhances TLR2-mediated recognition of lipoproteins
TLR7	AY035889	Recognises virus ssRNA in mice
TLR8	AY035890	Recognises virus ssRNA in humans
TLR9	NM_031178	Recognises CpG DNA
Rp105	NM_010739	Mediates LPS recognition in B cells
Screted PRRs		
CRP	NM_007768	Opsonisation
LBP	NM_008489	LPS Binding protein
MBL1	NM_010775	Bind carbohydrates
MBL2	NM_010776	Fix complement
SAP	NM_011318	Opsonisation
Lectins		
Mannose Receptor (MRC1)	NM_008625	Endocytosis of glygosylated particulates
Mannose Receptor (MRC2)	NM_008626	Endocytosis of glygosylated particulates
Dectin-1 (type-C lectin/Clecsf12)	AF262985	Binds β-glucans
Dectin-2	AF240357	Unknown
Clecsf10/CD209	NM_020001	Dendritic cell associated
Clecsf9 (Mincle)	NM_019948	Induced by LPS
Clecsf5(MDL-1)	NM_021364	Associates with DAP-12 to activate cell
CR3 (CD11b)	NM_008401	Adhesion, phagocytic receptor, oxidative burst
Sialoadhesin	NM_011426	sialic acid-dependent interactions
CD14	NM_009841	LPS/apoptotic cell "tethering"
Scavenger Receptors		
SRA-I	NM_031195	Can bind LTA,LPS and recognize
SRA-II	NM_030707	and in uptake of apoptotic cells, bacteria
MARCO	U18424	Binds: gram +ve/-ve bacteria, modified LDL
SRCL-I	BC009162	Bind E.coli, S.aureus
CD36 (SR-B)	NM_007643	Binds apoptotic cells, modified LDL
SR-BI (CD36L1)	NM_016741	Binds apoptotic cells, modified LDL
CD36L2	NM_007644	Role unsure, scavenger receptor
CD68 (SR-D)	NM_009853	Macrophage/Microglia cell marker
LOX1/OLR1 (SR-E)	AF303744	Expressed on endothelial cells, binds oxLDL
M130 (CD163)	AF274883	Scavenger for Hemoglobin
Crp-ductin (Crpd/DMBT1)	NM_007769	Protective role in inflammation

PGRP family		
Pgrp	AF076482	Binds peptidoglycan
N-formyl PR		
FPR1	NM_013521	migration/activation to N-formyl oligopeptides...
FPRL1 (FRP2)=Fpr-rs1	NM_008042	Binds N-formyls, PrP^{Sc} and . -amyloid
FPR-rs2	AF071180	Unknown
FPR-rs3	AF071181	Unknown
FPR-rs4	AF071182	Unknown
Other PRRs		
HM74 (Puma-g)	NM_030701	Similar to FPR, function unknown/chemotaxis
NOD1	NM_021406	Binds LPS, role not characterized
NOD2	NM_021410	Binds LPS, role not characterized
TREM-1	NM_021407	Binds LPS, activates monocytes
TREM-2	XM_132577	Binds LPS, activates monocytes
Apoptotic cell recognition		
PS Receptor	NM_033398	Recognizes exposed Phosphotidyl serine
C1q Receptor/Ly68	NM_010740	Binds complement component C1q
C1q (alpha chain)	NM_007572	Complement component
alpha V integrin	NM_008402	Integrin that binds apoptotic cells
beta 3 integrin	NM_016780	Integrin that binds apoptotic cells
beta 5 integrin	NM_010580	Integrin that binds apoptotic cells
ABC1	NM_013454	Mediates apoptotic cell engulfment
Prion protein receptors		
CR1 (mCRY)	NM_013499	Binds complement (C3b) that can coat PrPSc
CR2	M29281	Binds complement (C3b) that can coat PrPSc
Doppel	NM_023043	Homologous to Prion Protein
Prnp (Prion protein)	NM_011170	Central for prion disease, SOD-like activity
Protocadherin 2 (PCDHGC3)	AY013811	Putative PrP receptor
Laminin Receptor1 (LAMR1)	NM_011029	Putative PrP receptor
Caveolin-1	NM_007616	Signaling to PrP, NO
RAGE	NM_007425	Binds AD fibrils, up-regulated in AD brain
Stress genes		
arachidonate 12-lipoxygenase (ALOX12)	S80446	Biochemical pathway for eicosanoid production
CD40 (TNFRSF5)	NM_011611	Present on microglia - implicated in AD
CD40 Ligand (TNFSF5)	NM_011616	Immune control
Crystallin alpha B	NM_009964	Heat shock protein
Crystallin beta B2	NM_007773	Unknown-role in CNS neurodegeneration
CXCR3	NM_009910	Promotes microglial survival
Hsp25/27	L11609	Heat shock protein
GFAP	K01347	Expressed on activated astrocytes
Fractalkine (Scyd1)	NM_009142	Expressed by neurons to activate microglia
Heme oxygenase(decycling)1	X13356	Anti-oxidant, implicated in scrapie
Nos1	NM_008712	Neuronal NOS
Nos2 (iNOS/Nos2a)	NM_010927	Inducible form of NO synthase, due to infection
SOD1	M35725	Converts free radicals to O and peroxide

SOD2	NM_013671	Mitochondrial free radical scavenger
Phopholipase A2 (PLA2G4A)	NM_008869	biochemical pathway for eicosanoid production
Ptgs1 (Cox-1)	NM_008969	Prostaglandin biosynthesis
Ptgs2 (Cox-2)	NM_011198	Mitogen inducible form of Ptgs1
Catalase (CAT)	NM_009804	Peroxidase, up-regulated in AD Hippocampus
GPX1	NM_008160	Protection against oxidative stress
GSS	NM_008180	Makes GSH, protects against O
GSR	NM_010344	Reductase of GSH
GST-Pi (GST3)	BC002048	Conjugates Glutathione to toxins
Cathepsin D	NM_009983	Lysosomal protein, mutant has neurodegeneration
Osi (Sqstm1)	NM_011018	Induced by oxidative stress in Mphapes
SLC(SCYA21)	NM_011335	Chemokine
SLC1A1	NM_009199	Glutamate Transporter
SLC1A2	NM_011393	Decrease = increased Extracellular glutatmate in ALS
SLC1A3	D63816	Neuroprotective in ischemia of retina
TNFSF6 (Fas-Ligand)	NM_010177	Induces apoptosis
PAF Receptor	D50872	Activates microglia to produce H2O2
NCF1	AB002663	Part of the phagocyte NADPH-oxidase system
NCF2	NM_010877	As above: generates free radicals to fight infection
Cytokines and growth factors		
TNF-α	NM_013693	Pro-inflammatory, neurotoxic
INF-α 4	NM_010504	Anti-viral
INF-beta 1	NM_010510	Anti-viral
INF-γ	K00083	Anti-viral
IL-1 α	X01450	Induces apoptosis, pro-inflammatory
IL-1β	M15131	Mediates acute phase response
IL-6	NM_031168	Induced by IL-1 and TNF
IL-12	NM_008352	Pro-inflammatory, Th1 from Macrophages
Scya3 (MIP-α)	NM_011337	Chemokine
Scya4 (MIP-β)	NM_013652	Chemokine
SCYB9 (MIG)	M34815	Chemokine
Scyb10 (IP-10)	M33266	Chemokine
CD200 (MOX2 or OX2)	AF004023	Suppresses microglial activation
CD200R	NM_021325	Present on microglia. Promotes quiescence
IDO	NM_008324	Limits T cell activation
TGFβ	NM_011577	Anti-inflammatory, can promote AB clearance
IL-10	NM_010548	Anti-inflammatory, inhibits antigen presenting
Glia Maturation Factor β	NM_022023	Inhibits the mitogens ERK1/2, activates NF-KB
GDNF	NM_010275	Growth factor
BDNF	NM_007540	Growth factor
NGF-beta	NM_013609	GF (Subunit responsible for activity)
NT3	NM_008742	Promotes survival of neurites
CTNF	U05342	Neuroprotective
IGF2	NM_010514	Mitogen, on Alan's array
FGF2	NM_008006	Protects neurones from oxidative damage

Appendix 3 – probe names

Probe Name	Target gene	Accession number
12-lopxy:2024	arachidonate 12-lipoxygenase	S80446
12-lopxy:2259	arachidonate 12-lipoxygenase	S80446
ABC1:6829	ABC1	NM_013454
ABC1:7627	ABC1	NM_013454
Ald5H:1123	aldehyde 5-hydroxylase	AF139532
Ald5H:117	aldehyde 5-hydroxylase	AF139532
B-actin:1197	Beta-actin	X03672
B-actin:1702	Beta-actin	X03672
BDNF:597	BDNF	NM_007540
BDNF:782	BDNF	NM_007540
C1qAlpha:500	C1q alpha	NM_007572
C1qAlpha:513	C1q alpha	NM_007572
C1qR:1910	C1qR	NM_010740
C1qR:2939	C1qR	NM_010740
Catalase:1779	Catalase	NM_009804
Catalse:1787	Catalase	NM_009804
cathepsinD:1011	CathepsinD	NM_009983
CathepsinD:1481	CathepsinD	NM_009983
Caveolin:439	Caveolin	NM_007616
Caveolin:454	Caveolin	NM_007616
CCR1:636	CCR1 (Arabidopsis)	AF320624
CCR1:843	CCR1 (Arabidopsis)	AF320624
CD14:1200	CD14	NM_009841
CD14:260	CD14	NM_009841
CD200:1413	CD200	AF004023
CD200:1691	CD200	AF004023
CD200R:368	CD200R	NM_021325
CD200R:635	CD200R	NM_021325
CD36:1298	CD36	NM_007643
CD36:2164	CD36	NM_007643
CD36L2:1001	CD36L2	NM_007644
CD36L2:1356	CD36L2	NM_007644
CD40:1196	CD40	NM_011611
CD40:1467	CD40	NM_011611
CD40L:1028	CD40L	NM_011616
CD40L:505	CD40L	NM_011616
CD68:614	CD68	NM_009853 (X68273)
CD68long:1116	CD68	NM_009853 (X68273)
CelA:83	cellodextrinase (Ruminococcus flavefaciens)	X51944
Cellodex.:1215	cellodextrinase (Ruminococcus flavefaciens)	X51944
Cellodex.:923	cellodextrinase (Ruminococcus flavefaciens)	X51944
Chlorophyll:355	CHLOROPHYLL A-B BINDING PROTEIN 7 (EST)	BF069666
Chlorophyll:85	CHLOROPHYLL A-B BINDING PROTEIN 7 (EST)	BF069666
Cleccsf9:2201	Clecsf9	NM_019948
Clecsf9:2135	Clecsf9	NM_019948
Clecsf10:1140	Clecsf10 (Dectin-2)	NM_020001
Clecsf10:674	Clecsf10 (Dectin-2)	NM_020001
Clecsf12:2133	Clecsf12 (Dectin-1)	AF262985
Clecsf12:2192	Clecsf12 (Dectin-1)	AF262985

Probe Name	Target gene	Accession number
Clecsf5:682	Clecsf5	NM_021364
Clecsf5:694	Clecsf5	NM_021364
CNTFfull:1151	CNTF	U05342
CNTFfull:1391	CNTF	U05342
Cofilin:459	Cofilin	D00472
Cofilin:964	Cofilin	D00472
CR1:1694	CR1	NM_013499
CR1:933	CR1	NM_013499
CR2:2017	CR2	M29281
CR2:2052	CR2	M29281
CR3:3335	CR3	NM_008401
CR3:4094	CR3	NM_008401
CRP:1431	CRP	NM_007768
CRP:213	CRP	NM_007768
CRP-Ductin:5915	CRP-Ductin	NM_007769
CRP-Ductin:6420	CRP-Ductin	NM_007769
Cryst.A2:1098	Crystallin Alpha2	NM_009964
Cryst.A2:403	Crystallin Alpha2	NM_009964
CrystB2:327	Crystallin BetaB2	NM_007773
CrystB2:367	Crystallin BetaB2	NM_007773
Cxcr3:1368	CXCR3	NM_009910
Cxcr3:1522	CXCR3	NM_009910
c-yes:4338	c-yes	X67677
c-yes:4384	c-yes	X67677
Doppell:2212	Doppell	NM_023043
Doppell:2940	Doppell	NM_023043
EF-1a:1143	EF-1a	X13661
EF-1a:1469	EF-1a	X13661
Endo:1808	delta-endotoxin	Y09663
Endo:3357	delta-endotoxin	Y09663
FasL:1264	Fas-L	NM_010177
FasL:1445	Fas-L	NM_010177
Ferritin:252	Ferritin heavy chain	NM_010177
Ferritin:468	Ferritin heavy chain	NM_010177
Fgf2:244	FGF2	NM_008006
Fgf2:301	FGF2	NM_008006
Fpr:787	FPR	NM_013521
Fpr:825	FPR	NM_013521
FPRL1:1041	Fpr-rs1	NM_008042
Fpr-rs1:515	Fpr-rs1	NM_008042
Fpr-rs2long:1014	Fpr-rs2	AF071180
Fpr-rs2long:873	Fpr-rs2	AF071180
Fpr-rs3:603	Fpr-rs3	AF071181
Fpr-rs3:615	Fpr-rs3	AF071181
Fpr-rs4long:468	Fpr-rs4	AF071182
Fpr-rs4long:875	Fpr-rs4	AF071182
Frac. 1939	Fractalkine (Scyd1)	NM_009142
Frac.:2918	Fractalkine (Scyd1)	NM_009142
Gdnf:2952	GDNF	NM_010275

Probe Name	Target gene	Accession number
Gdnf:2992	GDNF	NM_010275
Gfap:1371	GFAP	K01347
Gfap:1921	GFAP	K01347
GMFb:3760	GMFb	NM_022023
GMFb:4067	GMFb	NM_022023
GNAS:1936	GNAS	NM_010310
GNAS:2241	GNAS	NM_010310
GPX1:348	GPX1	NM_008160
GPX1:863	GPX1	NM_008160
GSK3b:1205	GSk3b	NM_019827
GSK3b:808	GSk3b	NM_019827
GSR:1231	GSR	NM_010344
GSR:1244	GSR	NM_010344
GSS:1299	GSS	NM_008180
GSS:624	GSS	NM_008180
GST-Pi:702	GST-Pi(B)	BC002048
GST-Pi:707	GST-Pi(B)	BC002048
HemeOx.:1314	HemeOxygenase	X13356
HemeOx.:1429	HemeOxygenase	X13356
HM74:1212	HM74 (puma-g)	NM_030701
HM74:1863	HM74 (puma-g)	NM_030701
Hsp25:736	Hsp25/27	L11609
Hsp25:745	Hsp25/27	L11609
IDO:1107	IDO	NM_008324
IDO:1312	IDO	NM_008324
IFNa4:232	IFNalpha4	NM_010504
IFNa4:29	IFNalpha4	NM_010504
IFNb:457	IFNbeta	NM_010510
IFNb:507	IFNbeta	NM_010510
IFNg:773	IFNgamma	K00083
IFNg:862	IFNgamma	K00083
IGF2:3007	IGF2	NM_010514
IGF2:4032	IGF2	NM_010514
IL-10:692	IL-10	NM_010548
IL-10:889	IL-10	NM_010548
IL-12b:1446	IL-12b	NM_008352
IL-12b:1562	IL-12b	NM_008352
IL-1aii:1027	IL-1a	X01450
IL-1aii:1836	IL-1a	X01450
IL-1b:1125	IL-1b	M15131
IL-1b:612	IL-1b	M15131
IL-6:149	IL-6	NM_031168
IL-6:514	IL-6	NM_031168
Integ.aV:3061	Integrin alpha V	NM_008402
Integ.aV:3226	Integrin alpha V	NM_008402
Integ.b3:2367	Integrin beta 3	NM_016780
Integ.b3:2506	Integrin beta 3 (CD61)	NM_016780
Integ.b5:1204	Integrin beta 5B	NM_010580
Integ.b5:2246	Integrin beta 5B	NM_010580

Probe Name	Target gene	Accession number
Lac.dehy:1491	Lactate dehydrogenase	NM_010699
Lac.dehy:1602	Lactate dehydrogenase	NM_010699
LamR:664	Laminin Receptor	NM_011029
LamR:676	Laminin Receptor	NM_011029
LBP:1111	LBP	NM_008489
LBP:1401	LBP	NM_008489
Lox-1:2872	Lox-1	AF303744
Lox-1:3423	Lox-1	AF303744
Lpo:1188	lignin peroxidase	L08963
M130:2853	M130	AF274883
M130:3823	M130	AF274883
MARCO:137	MARCO	U18424
MARCO:1446	MARCO	U18424
Mbl1:400	Mbl1	NM_010775
Mbl1:51	Mbl1	NM_010775
Mbl2:939	Mbl2	NM_010776
Mbl2:955	Mbl2	NM_010776
Mrc1:4659	Mrc1	NM_008625
Mrc1:4829	Mrc1	NM_008625
Mrc2:2784	Mrc2	NM_008626
Mrc2:4501	Mrc2	NM_008626
NCF1:145	NCF1	AB002663
NCF1long:1179	NCF1	AB002663
NCF2:1664	NCF2	NM_010877
NCF2:343	NCF2	NM_010877
NGFb:287	NGFbeta	NM_013609
NGFb:772	NGFbeta	NM_013609
Nod1:1451	Nod1	XM_132577
Nod1:964	Nod1	XM_132577
Nos1:3936	Nos1	NM_008712
Nos1:4287	Nos1	NM_008712
Nos2:3519	Nos2	NM_010927
Nos2:3932	Nos2	NM_010927
NT3:3	NT3	NM_008742
NT3:563	NT3	NM_008742
Osi:1747	Osi	NM_011018
Osi:1835	Osi	NM_011018
P2AG4A:1715	P2AG4A	NM_008869
P2AGA4A:2201	P2AG4A	NM_008869
PafR:1091	PAF Receptor	D50872
PafR:132	PAF Receptor	D50872
Pbp:661	Pbp	NM_018858
Pbp:786	Pbp	NM_018858
Pgrp:529	PGRP	AF076482
Pgrp533	PGRP	AF076482
Pgrp-L:1697	PGRP-L	AF149837
Pgrp-L:1734	PGRP-L	AF149837
PP1cg:2017	PP1cgamma	U53456
PP1cg:2050	PP1cgamma	U53456
Prnp:1473	Prnp	NM_011170
Prnp:1824	Prnp	NM_011170

Probe Name	Target gene	Accession number
ProtoCadg:4180	Protocadherin 2 (PCDHGC3)	AY013811
ProtoCadg:4240	Protocadherin 2 (PCDHGC3)	AY013811
PSR:1081	PSR	NM_033398
PSR:629	PSR	NM_033398
Ptgs-1:1259	Ptgs-1 (Cox1)	NM_008969
Ptgs-1:2595	Ptgs-1 (Cox1)	NM_008969
Ptgs-2:3181	Ptgs-2 (Cox2)	NM_011198
Ptgs-2:3843	Ptgs-2 (Cox2)	NM_011198
RAGE:1296	RAGE	NM_007425
RAGE:486	RAGE	NM_007425
Rheb:473	Rheb (Ras homolg)	AB039919
Rheb:763	Rheb (Ras homolg)	AB039919
Rp105:2124	Rp105	NM_010739
Rp105:2828	Rp105	NM_010739
SAP:764	SAP	NM_011318
SAP:923	SAP	NM_011318
Scya3:472	Scya3 (MIP1-alpha)	NM_011337
Scya3:636	Scya3 (MIP1-alpha)	NM_011337
Scya4:431	Scya4 (MIP1-beta)	NM_013652
Scya4:451	Scya4 (MIP1-beta)	NM_013652
Scyb10:267	Scyb10 (IP-10)	M33266
Scyb10:786	Scyb10 (IP-10)	M33266
Scyb9:1098	Scyb9 (MIG)	M34815
Scyb9:956	Scyb9 (MIG)	M34815
SDO-1:375	SOD-1	M35725
Sialoadhesin:6487	Sialoadhesin	NM_011426
Sialoadhesin:6600	Sialoadhesin	NM_011426
SLC:158	SLC (SCYA21)	NM_011335
SLC:658	SLC (SCYA21)	NM_011335
SLC1A1	SLC1A1	NM_009199
SLC1A1	SLC1A1	NM_009199
SLC1A2:1591	SLC1A2	NM_011393
SLC1A2:1953	SLC1A2	NM_011393
SLC1A3:146	SLC1A3	D63816
SLC1A3:172	SLC1A3	D63816
SOD-1:153	SOD-1	M35725
SOD-2:407	SOD-2	NM_013671
SOD-2:605	SOD-2	NM_013671
SRA-I:1024	SRA-I	NM_031195
SRA-I:1505	SRA-I	NM_031195
SRA-II:1983	SRA-II	NM_030707
SRA-II:2139	SRA-II	NM_030707
SRB-I:2222	SRB-I (CD36L1)	NM_016741
SRB-I:908	SRB-I (CD36L1)	NM_016741
SRCL:2277	SRCL	BC009162
SRCL:2536	SRCL	BC009162
TGFb:1371	TGFbeta	NM_011577
TGFb:714	TGFbeta	NM_011577
TLR1full:2416	TLR1	NM_030682
TLR1full:2431	TLR1	NM_030682
TLR2:2621	TLR2	NM_011905
TLR2:2626	TLR2	NM_011905

Probe Name	Target gene	Accession number
TLR3:2727	TLR3	AF355152
TLR3:2740	TLR3	AF355152
TLR4:3412	TLR4	NM_021297
TLR4:3513	TLR4	NM_021297
TLR5:4038	TLR5	NM_016928
TLR5:4048	TLR5	NM_016928
TLR5:4226	TLR5	NM_016928
TLR6:2400	TLR6	NM_011604
TLR6:2490	TLR6	NM_011604
TLR7:2942	TLR7	AY035889
TLR7:3157	TLR7	AY035889
TLR8:2630	TLR8	AY035890
TLR8:2706	TLR8	AY035890
TLR9:2081	TLR9	NM_031178
TLR9:3386	TLR9	NM_031178
TNFa:1326	TNFalpha	NM_013693
TNFa:1495	TNFalpha	NM_013693
TNFa:1508	TNFalpha	NM_013693
TREM-1:482	TREM-1	NM_021406
TREM-1:713	TREM-1	NM_021406
TREM-2:741	TREM-2	NM_021410
TREM-2:754	TREM-2	NM_021410
TREM-3:633	TREM-3	NM_021407
TREM-3:707	TREM-3	NM_021407
Tuba1:1509	Tuba1	NM_011653
Tuba1:1522	Tuba1	NM_011653
Vimentim:1569	Vimentim	NM_011701
Vimentim:1588	Vimentim	NM_011701
y-box:1164	y-box	M60419
Y-box:792	y-box	M60419
Zeta-p:184	zeta proteasome	AF019661
Zeta-p:607	zeta proteasome	AF019661

Appendix 4 – microarray probe sequences

Part A, genes of interest

Identity	Probe
12-lopxy:2259	GGCCACCCACTTTCTACCACAATTACTTAGCTTTCTCACTATACCACTAG
12-lopxy:2024	CTTATGAATACCTCAAGCCCAGCCGCATAGAGAACAGTATCACCATCTGA
ABC1:7627	ACTTTTTCAAATACATTAGATCCTCCTAAGCAGCAAAGATTAGCAGCCAA
ABC1:6829	CCTTTTTGCAGGATGAGAAAGTGAAAGAAAGTTATGTATGAAGAATCCCG
BDNF:597	GTATCCAAAGGCCAACTGAAGCAGTATTTCTACGAGACCAAGTGTAATCC
BDNF:782	AGACACTTCCTGTGTATGTACACTGACCATTAAAAGGGGAAGATAGTGGA
C1qAlpha:513	AACTTCCAAGTGATCTCCAAGTGGGACCTTTGTCTGTTTATCAAGTCTTC
C1qAlpha:500	CTTCTATTACTTCAACTTCCAAGTGATCTCCAAGTGGGACCTTTGTCTGT
C1qR:2939	CAGGTTACTCTCCTCCTTAGAGCTACAACATAACATTCTGAGGGGAGTCA
C1qR:1910	TTTATCATAAACGCAGAGCCAAGAAGGAGGAGATAAAAGAGAAGAAGCCT
Catalase:1779	TGATGACTTTAAAACGATAATCCGGGCTTCTAGAGTGAATGATAACCATG
Catalse:1787	TTAAAACGATAATCCGGGCTTCTAGAGTGAATGATAACCATGCTTTTGAT
cathepsinD:1011	GGTCTACCTGAAGCTAGGAGGCAAAAACTATGAACTACACCCAGACAAGT
CathepsinD:1481	CTTCAAAGGCCCCTACTGGTTTAATAGCTGCTGAGATGGATTGTCTTGTC
Caveolin:439	GTCTACTCCATCTACGTCCATACCTTCTGCGATCCACTCTTTGAAGCTAT
Caveolin:454	GTCCATACCTTCTGCGATCCACTCTTTGAAGCTATTGGCAAGATATTCAG
CD14:260	GCAGTTCACTGATATTATCAAGTCTCTGTCCTTAAAGCGGCTTACGGTGC
CD14:1200	AAATCTTAATCCACGATGTAAGGAAAGAAAGGCAGTCAAGATGGTTCAGT
CD36:2164	GCAACTGTCAGCACATGGCATAAGTATAACATCTTGAAAGACTTAAGAAT
CD36:1298	GTATATTTCGCTTCCACATTTCCTACATGCAAGTCCAGATGTTTCAGAAC
CD36L2:1356	AGATCAACACTTACGTTAGGAAACTGGATGACTTTGTTGAAACGGGAGAC
CD36L2:1001	CTGTACCTCTTCCCGTCAGACTTGTGCAGGTCAGTACATATCACTTTCAG
CD40:1467	CCTAAAATGGATGTGGTGGTGTATTGTAGAAATTATTTAATCCGCCCTGG
CD40:1196	ATTATTTATACAATGGCATCTCAGAAACTCTAGCAGGTGGGGCAGAAAAC
CD40L:1028	AACCCCACTGATTCAGACAACCAGAAAAGACAAAGCCATAATACACAGAT
CD40L:505	GAAGGACTCTATTATGTCTACACTCAAGTCACCTTCTGCTCTAATCGGGA
CD68:614	GATTCAAACAGGACCTACATCAGAGCCCGAGTACAGTCTACCTGGACTAC
CD68long:1116	ATCTCTTCACCATGCCACTGACTCAACAGTTACCTTCCTTCTCTGTCTTT
CD200:1413	CGCCAGTGTGTTTCCCTGTTGTTTGAGTATCTAGTTGACTACCTGTTACT
CD200:1691	CAATAACACTTTCTTTGAGGCCATTCTGAATCCTGTCTCGTGTAATGATA
CD200R:635	CCTGCATTGTCTCTCATTTGACTGGTAACCAATCTCTGTCCATAGAACTG
CD200R:368	ATGAGGGGACTTACACATGTGAGACAGTAACACCTGAAGGGAATTTTGAA
Clecsf12:2192	CCACTGAATTGTTCTCTTGAAAATGATTGGGTTTATGTCACTTTCATCTC
Clecsf12:2133	GGGGATCTGTTTATAGCTTTCTCAGACTAATCAATATGTGGGCAGAAATT
Clecsf10:1140	GGTCTTGCCCTGGTTTCTTTCTATGAACTGCTGTTACTTGAAAGTATAAG
Clecsf10:674	GTTTCAATAGTTTACTGGAATCCTTCGAAATGGGGCTGGAATGATGTTTT
Cleccsf9:2201	TTCTGTCCTTGGGTTTATTTGCATGGTTCATTACACTCCTTGACTTGTAT
Clecsf9:2135	GCTTCATATTAAAAGATTCTGAATTCCATCAAAGGGCACACAAAGAAATC
Clecsf5:694	ATTAGTTGTGACTGAAACCAGCCCAGGAAATATAGAGCATCAAAGACTGT
Clecsf5:682	CTAGCAAAGGAGATTAGTTGTGACTGAAACCAGCCCAGGAAATATAGAGC
CR1:1694	TAAATTATAAAGAAGACAGCTGTGTCCGCCTTCAGTCTCTGCTCACAAGT
CR1:933	TTGATTGGGATACTGAGGACCTATTTGTGAGTGGATTCCTTGTGAGATAC
CR2:2052	GGGCTCAGCACTTATCATTTTGATGAGTGTCGGCTTCTGTATGATATTAA
CR2:2017	CGGTCAACTATTCCTCTTATTTGTGGTATTTCTGTGGGCTCAGCACTTAT
CR3:3335	CTGTGAAGTACGCCATCTACATGATTGTCACCAGTGATGAGAGTTCTATC
CR3:4094	CAACACCGAAGCTAGTGACACATATGTTGTTGCTGTGATGTCTTATACAA
CRP:213	GTCAAAGAAGCCACTGAACACCTTTACTGTGTGTCTCCATTTCTACACTG
CRP:1431	CAGCCACTGATTACCTCTAGCTCTTCATATAGGGTTCTGTCTTTGTGAAA
CRP-Ductin:6420	GCCAAGTTTTCCCAGGATCTATCAGACTGAAGGCTAGGAAGAATGTCATA
CRP-Ductin:5915	CCCCTCAGTGTACCTGCAGTGTAAACTGGTAGTATGTCGAGCGTATGATA
Cryst.A2:1098	TGATTGAAAATCTGTGACTAGTGCTGAAGCTTATTAATGCTAAGGGCTGG
Cryst.A2:403	TAAAACCCCTGACCTCACCATTCCAGAAGCTTCAGAAGACTGCATATATA

Identity	Probe
CrystB2:327	GGACAGCCAAGAGCACAAGATCATCTTATATGAGAACCCCAACTTTACTG
CrystB2:367	AACTTTACTGGCAAGAAGATGGAGATTGTAGACGACGATGTGCCCAGCTT
CNTFfull:1391	CAATACATACTCTTACGCTCCAAGTTTCTGCCTTCGCCTACCAGCTAGAG
CNTFfull:1151	GTTCAGACCTGACTGCTCTTATGGAATCTTATGTAAAACATCAAGGCCTG
Cxcr3:1522	TGAATGTGCCCATCTCAGTATCTCAATATTTGCCCAATTTTATTTCTAGA
Cxcr3:1368	ATTACTGTGCCTTAGCTGCCATGCCCTATCTTGCTGTTTTAGAACTAGCT
Doppell:2940	CAACGATCACTTGTATAATATTTGTTTCTCTGCGGTTTGTATTCCTGATT
Doppell:2212	ACAGTTTACCCCTTGCACGCCATTTTAAATATCAGACAATAAAGAAGGAA
FasL:1264	GCCAAGAGAATTTTAACCATTGAAGAAGACACCTTTACACTCACTTCCAG
FasL:1445	CCATCTTTACTGTTACCTAATGTTTTCTGAGCCGACCTTTGATCCTAACG
Fgf2:301	TTCTTCTTTGAACGACTGGAATCTAATAACTACAATACTTACCGGTCACG
Fgf2:244	CTTGCTATGAAGGAAGATGGACGGCTGCTGGCTTCTAAGTGTGTTACAGA
Fpr:825	ATTGCCAGTTATCATTCGTTTGACCACAGTCCCTAATAGTAGACTTGGAC
Fpr:787	GTAATCATCGTACCCTGGATTTGTGCATTTCTTCTTACATTGCCAGTTAT
FPRL1:1041	GACTCTGGTCATATCAGTGATACAAGAACCAATTTGGCTTCACTTCCTGA
Fpr-rs1:515	GTAGATTGAGCTTTGTATCCTGGGGCAACTCTGTTGAGGAAAGGTTGAAC
Fpr-rs2long:873	CCTTTTGGGCACAGTCTGGTTTAAAGAGACATTGCTTAGTGGTAGTTATA
Fpr-rs2long:1014	CTTTCGTGAGAGATTTATTCATTCCCTGCCTTATAGTCTTGAGAGAGCCC
Fpr-rs3:603	GAATCATCAGTTTTATTAATTGCTTCAGCCTACCCATGTCCTTCATTGCC
Fpr-rs3:615	TTTTATTAATTGCTTCAGCCTACCCATGTCCTTCATTGCCGTCTGCTATG
Fpr-rs4long:875	AGATGCAAGAGGGGATGTGTACTGTATATCTAAATTTGAATCCTGGGTTG
Fpr-rs4long:468	CTCTTTATAACCTTTGTCCTCGGTGTTCTAGGTAATGGGCTTGTGATTTG
Frac.:2918	AGAATGTGGGCCGTAACAATCTGAGGAGGACTTTAAAAGTTGTTGATCCT
Frac. 1939	ATAACCTATGGCCCTGACATCATCACTTTCTCTGAGATCCTTGTCTCCAC
Gdnf:2992	AAGAGGTAAAAGTTACTAGGTATCCTTTCCCCTTCCGTGGCCCTAAAGAC
Gdnf:2952	GGCCTCTCTCGAATAGTCATGTCAAATTTTCAAAGTAACCAAGAGGTAAA
Gfap:1921	CACTGGTAGAGATCATTTGGACACTCGGAGTTGAAAGTTACAGGCAATCT
Gfap:1371	GCTTCATAGATGGCATAGATGGCATATACCCTTCACCTTCAACTAACAGG
GMFb:3760	GGTTCTGAGCTGAATATTTCTTGGTAGGCCATGTGACACTTCAGATCAGT
GMFb:4067	TTTCTGCTAGTTCATACCGCATGTTTATTTTGGAGTCTTTTGGTAAGCAT
GPX1:863	CTGTGTCATTGTCACCTTTTGGATAGCCTCATAGTCAGGGATAAGGAACT
GPX1:348	AGCCCAATTTTACATTGTTTGAGAAGTGCGAAGTGAATGGTGAGAAGGCT
GSR:1244	AAGACAATGTGAAAATCTACTCGACTGCCTTTACCCCGATGTATCACGCT
GSR:1231	CATAAGTATGGGAAAGACAATGTGAAAATCTACTCGACTGCCTTTACCCC
GSS:1299	GTATTTTTGGAGTCTATGTCAGACAGGGAACAACACTGGTGATGAACAAG
GSS:624	CTAATGCGGTGGTGCTACTGATTGCTCAAGAGAAGGAAAGGAACATATTT
GST-Pi:707	CTTCTTGTCCCCGTTTTCCCAGCACTAATAAAGTTTGTAAGACAGAAAAA
GST-Pi:702	AAGAGCTTCTTGTCCCCGTTTTCCCAGCACTAATAAAGTTTGTAAGACAG
HemeOx.:1429	GGGGTGGGTGGGAAAGAATTATTTAATAGTTGTAACCTTGGTCTCTAACT
HemeOx.:1314	TTCTGTCTCGTATTTCTGTCTTGTTTTTTATTATTTCCCCAGTTCTACCA
HM74:1863	GGGCGGTTCATTACTTGGGTTTCTGTACTTTAACATCTACCATTTCAATA
HM74:1212	GAACAGGGTAACATCTTCAGATTTGGCTTACGCTTTCTTGGAACTTCTAG
Hsp25:745	CAATCTGTGCGCTCTTTTGATACATACATTTACCTGCTGTTTTTCTCAAA
Hsp25:736	CCTCTCTGTCAATCTGTGCGCTCTTTTGATACATACATTTACCTGCTGTT
IFNa4:232	ATCCTTGTGCTAAGAGATCTTACCCAGCAGATTTTGAACCTCTTCACATC
IFNa4:29	TCCTAGTAATGATGAGCTACTACTGGTCAGCCTGTTCTCTAGGATGTGAC
IFNb:457	AAAGGTACCTTAAACTCATGAAGTACAACAGCTACGCCTGGATGGTGGTC
IFNb:507	CGAGCAGAGATCTTCAGGAACTTTCTCATCATTCGAAGACTTACCAGAAA
IFNg:773	ATTATTCTTTCTGACTAATTAGCCAAGACTGTGATTGCGGGGTTGTATCT
IFNg:862	TGTAGCTTGTACCTTTACTTCACTGACCAATAAGAAACATTCAGAGCTGC
IGF2:3007	ATTAGGACCCCAAATTTATGCCAATGATCTATTCCCCTCTTTTTATTTCT
IGF2:4032	TCAAAGAGTAAATTGTTATAATTGGAGACTATGAATTGGCCTGGTATCCA
IL-10:692	TAACGGAAACAACTCCTTGGAAAACCTCGTTTGTACCTCTCTCCGAAATA

Identity	Probe
IL-10:889	GTATTTAAAGGGAGATTATATTATATGATGGGAGGGGTTCTTCCTTGGGA
IL-12b:1446	TTCACATTTGTATACCAAGATGTATTGAATATTTCATGTGCTTGTGGCCT
IL-12b:1562	TCAGGGCTTCGTAGGTACATTAGCTTTTGTGACAACCAATAAGAACATAA
IL-1aii:1027	GCAAACCCTAGTGGAGCCACCCCGACATATGATACTATCTGTTATTTTAA
IL-1aii:1836	TGAAGTTTCTTTTCTAGAATGTAATCAGTGTTTCCCCTGGATTCCAATTT
IL-1b:1125	TTAAGTTGATTCAAGGGGACATTAGGCAGCACTCTCTAGAACAGAACCTA
IL-1b:612	CTCAAAGGAAAGAATCTATACCTGTCCTGTGTAATGAAAGACGGCACACC
IL-6:514	TAAAATAGTCCTTCCTACCCCAATTTCCAATGCTCTCCTAACAGATAAGC
IL-6:149	ACTCCCAACAGACCTGTCTATACCACTTCACAAGTCGGAGGCTTAATTAC
Integ.aV:3226	GCTACTGGCTGTGTTGGTATTTGTAATGTACAGGATGGGCTTTTTCAAAC
Integ.aV:3061	GTCATCTGCTTCCTTTAATATCATAGAATTCCCTTACAAGAACCTGCCAA
Integ.b3:2506	GGGCTGGAAGAATGTCAGTATGTGGGAATGTATCTCTCTGTGTGTACTTA
Integ.b3:2367	CTTCACCAATATCACCTACCGGGGGACTTAATGAGACCACTTCAGATGAC
Integ.b5:2246	GCTTCTACAAAACTGCTAAGGACTGCGTTATGATGTTCAGCTACACAGAA
Integ.b5:1204	TTTGCTGTGACGAAGAACCACTATATGCTCTACAAGAATTTTACAGCCCT
IDO:1312	CTATCAGGGCACAGAAAACACCTTCATCCTGTCATAGCTCATTAAATCAG
IDO:1107	TGAGAAAGTTCCACCTCGCAATAGTAGATACTTACATTATGAAACCTTCG
LamR:676	ATCTTTACTTCTACAGAGACCCAGAGGAGATTGAGAAGGAGGAGCAGGCT
LamR:664	AGGTCATGCCTGATCTTTACTTCTACAGAGACCCAGAGGAGATTGAGAAG
Lox-1:3423	TGGAATTACAGACGTTTTTGAACAATCCTATAGACTCTGGGAACTGAACC
Lox-1:2872	TGGATCTATAGTGTCATTTGTTATCTGTGTATTTGTTGATGCCATTTGGG
LBP:1401	AGGCATTCCTTAACTACTACCTTCTCAACAGCCTCTACCCTGATGTCAAT
LBP:1111	ATACAAAAAGTATCCCGACATGAAATTGGAGCTCCTTAGAACAGTGGTCT
M130:2853	GATCATCTGTGACAACAAAATAAGACTCCAGGAAGGGCATACAGACTGTT
M130:3823	TAAATTTCTGGTTGGTTTTTCTGACGTTTTTAGGGTTTCGTGAATATAAA
MARCO:1446	CAACAGAGGCCGAGCTGAAGTTTACTATAACAATGAGTGGGGGACAATTT
MARCO:137	TTGGCCACCTATAAAGCTTAGCAATGGGAAGTAAAGAACTCCTCAAAGAG
Mbl1:400	GAGAAGCTGGCAAATATGGAGGCAGAGATAAGGATCCTGAAATCAAAACT
Mbl1:51	CAGAAGCTGGACTCGAGACATAGTTTCTCTTCCACTGCTCCTTTACTCTA
Mbl2:955	TGACGTCCGCAGTTTGTTCTGAAAAATAAAATATGGGAAAATATAAACAA
Mbl2:939	CTTGATTCTTTAGGGTACTCCTGACGTCCGCAGTTTGTTCTGAAAAATAA
Mrc1:4829	TTCAGGACCTCCCAGAGATATGTTATACACCGAATTGTAATTCAACATTT
Mrc1:4659	AAAACAGAAGAGGGATAATAATGTTGATTGTTGATTGCCACTTTTGAAGA
Mrc2:2784	GAGAGTGACGGACGCTTCAGGTGGACAGATGGTTCTATTATAAACTTCAT
Mrc2:4501	ACATTCTGGTGTCTGACATGGAAATGAACGAACAGCAAGAATAGAGCCAA
NCF1long:1179	CCCTAGACGGCTCCTATCCCTATCTCTGTATATACTTGTGTATAGCCTCA
NCF1:145	GGAGAAGGTGGTCTACAGAAAATTCACCGAGATCTACGAGTTCCATAAAA
NCF2:1664	GAGAAGTCTAGGATCTACAAAGCTGAAGCAAAGTGTTGTTTTTCCCCTTG
NCF2:343	AGAATGGAGAAGTACGACCTTGCTATCAAAGACCTTAAAGAGGCCTTGAC
NGFb:772	AGTGCTGGCCGAGGTGAACATTAACAACAGTGTATTCAGACAGTACTTTT
NGFb:287	GTGCATAGCGTAATGTCCATGTTGTTCTACACTCTGATCACTGCGTTTTT
Nod1:1451	GACAGTTGGAATGTTGCAGATAACGTGTTCTTTTGCCAGTTCATTTGTTA
Nod1:964	CATGGTTATTCTGAGTCCTCCTTCCTCTGCTTAGTCCCTCTCACTGTACA
Nos1:4287	GTCACCCTCAGAACATATGAAGTGACCAACCGCCTTAGATCTGAGTCCAT
Nos1:3936	GTCTTCGGGTGTCGACAATCCAAGATAGATCATATCTACAGAGAGGAGAC
Nos2:3932	CACCATGCCGCCGCTCTAATACTTAGCTGCACTATGTACAGATATTTATA
Nos2:3519	AGAGCCAGAAACGTTATCATGAAGATATCTTCGGTGCAGTCTTTTCCTAT
NT3:563	AACAATATTTTTATGAAACGAGATGTAAAGAAGCCAGGCCGGTCAAAAAC
NT3:3	GTCCATCTTGTTTTATGTGATATTTCTTGCTTATCTCCGTGGCATCCAAG
Osi:1835	ATGTGAAGCCGAATGAAGGATCTTATCTTATACTGTCCCCCTTTCTAATG
Osi:1747	AATAAAGCCATTATGTTAAGAGGGGACTGTCCATAGTGAGTGAAAGGTGG
P2AGA4A:2201	TCAACACACTGAACAACATTGATGTGATAAAGGATGCCATTGTTGAGAGC
P2AG4A:1715	CACTGGATGTCAAAAGTAAGAAGATTCATGTGGTAGATAGTGGGCTCACA
PafR:1091	AGCCAACCAGACTCCTATTGTGTCGCTGAAAAATTAATCTCTGCTTATTA

Identity	Probe
PafR:132	TCTGAGTTTCGATACACGCTCTTTCCGATTGTTTACAGTGTCATCTTTAT
Pgrp:529	AAAGCTGGGAACACTACCGAGAGTGAGAGACCTTGAGACCTAGTGAGAAT
Pgrp533	CTGGGAACACTACCGAGAGTGAGAGACCTTGAGACCTAGTGAGAATCCCC
Pgrp-L:1734	GAGGTATTATCCCTGATGATCCTTTGAGCAACCACAGACCTCCAATAAAG
Pgrp-L:1697	AACTAAGAACTCCTTTGAGAGACCCTTGAAGATCCAGGAGGTATTATCCC
Prnp:1824	AGACATAAACTGCGATAGCTTCAGCTTGCACTGTGGATTTTCTGTATAGA
Prnp:1473	AGGGCACTAGAATGATCTTTAGCCTTGCTTGGATTGAACTAGGAGATCTT
ProtoCadg:4240	GTAGAATAGCCAATAGTATAGTGTGGTGTGCTTTTACGTGATGGCGAGTG
ProtiCadg:4180	ATAGAACTTCCTCTGCCCTAGCCCTTACAGTAGTGTAGAAGATCCCCCTC
PSR:1081	TGGCACAAGACGGTAAGAGGGAGACCAAAGTTATCAAGGAAGTGGTATAG
PSR:629	TGGAAGACTACAAGGTGCCCAAGTTTTTCACAGATGATCTTTTCCAATAC
Ptgs-1:2595	GTCAAGGCAGTAAGGTGTTCTTGGGAGCCACACTTAGACTCTTTCCAAAG
Ptgs-1:1259	AGTTTTTATTTAACACTTCTATGCTGGTGGACTATGGGGTTGAGGCACTG
Ptgs-2:3181	CGCTGATTGGGTTTTCGTAGCTGTGTTACCAGGTTTTTAGTATCAGAACT
Ptgs-2:3843	TGCATAGGATCCAATATTGACTGACCCAAGCATGTTATAAAGACTGACAT
RAGE:1296	CCTTCTCCAACCAGAGCCCACATGATCCATGCTGAGTAAACATTTGATAC
RAGE:486	AAACTTCTGATTCCCGATGGCAAAGAAACACTCGTGAAGGAAGAGACCAG
Rp105:2828	TACATCCATCATCTGTCTTTTTAAATGTAATTGTGCCCTCGTGTCTGTCT
Rp105:2124	AAGAGTTGATTTTCTCCAGTTAGTACAGAATGCTATGGCAATTGGTGTGG
SAP:923	TGTGAACATCTTGTATACATATCTGCCAAATAAAAATCCTCTCCAATTCC
SAP:764	TGAATTGGCAGGCTCTTAACTATGAAATAAATGGCTACGTAGTCATCAGG
Scya3:636	CTCCCAGTTGTTCACACTGTTTGGTGACAGCTATTCTAGGTAGACATGAT
Scya3:472	GCTGCCAAGTAGCCACATCGAGGGACTCTTCACTTGAAATTTTATTTAAT
Scya4:451	GATTTCCTGCCCCTCTTCTTAATTTAAATCTCTGTGTAGACTTTGTTTTG
Scya4:431	GTCCTTGCTCCTCACGTTCAGATTTCCTGCCCCTCTTCTTAATTTAAATC
Scyb9:1098	TTTGCCTCTTCAATAAAACTCTCCTAGAAGGTTGTGGCTGTAGCTTAGTG
Scyb9:956	ATTGTGTCTCAGAGATGGTGCTAATGGTTTTGGGGTTCTACAGTGGAGAC
Scyb10:786	TCCCAAGGGGTTATCAAGATACTCAGAGGAACCTGAAAATGTATGTGTAA
Scyb10:267	ATCCGGAATCTAAGACCATCAAGAATTTAATGAAAGCGTTTAGCCAAAAA
Sialoadhesin:6600	AAAATTTGGCGTTTCCCTAGGTGTCTTACTTACTGTTCTTTTGCTGTGAG
Sialoadhesin:6487	ATGTTGAAGAGAGTGGCATTATTAGGCTAGGGTCTGAATTAGTGTTCCGA
SLC:658	GGGGTAGACCTAGAGAGTCAGAAGAAAGAGTGTCTCCCAGGGAATGAGGA
SLC:158	AGAAAATTCCCTACAGTATTGTCCGAGGCTATAGGAAGCAAGAACCAAGT
SLC1A1	TTCCCGAAGATGGCTTATAAAAGTCTACACTTCTGTCCTCATCCTGTAAA
SLC1A1	CTGCCTGTCTTTCTCCTGCTAATTCCCGAAGATGGCTTATAAAAGTCTAC
SLC1A2:1591	TTTACGACGACAAGAACCACAGGGAAAGCAACTCTAATCAGTGTGTCTAT
SLC1A2:1953	CAAGAATTGGTGGTTGTCAGAACTTTAATGGCCTTCAGATATTCTCTTCC
SLC1A3:172	ATATAAGTGAACTAACAAGGCGTGAACGTGGTCTACGGAGCAAAACAAAG
SLC1A3:146	TCTCAGGTCCTGATTTTGCGTTTCTAATATAAGTGAACTAACAAGGCGTG
SOD-1:375	AAGATGACTTGGGCAAAGGTGGAAATGAAGAAAGTACAAAGACTGGAAAT
SOD-1:153	AGTATGGGGACAATACACAAGGCTGTACCAGTGCAGGACCTCATTTTAAT
SOD-2:605	TGGGAGCACGCTTACTACCTTCAGTATAAAAACGTCAGACCTGACTATCT
SOD-2:407	GAGGCTATCAAGCGTGACTTTGGGTCTTTTGAGAAGTTTAAGGAGAAGCT
SRA-I:1505	TTTCCTCAAATACAAATAGAGATTGAAATAGGGGTCTGTCCATCCATTCA
SRA-I:1024	GACAAAAGGGAGAGAAGGGGAGTGTAGGCGGATCAAGATCAGTATAACTC
SRA-II:2139	GCCAAAGTCACACAGTCAGAAGTAACTGATACTAACCAAAGGATCATGAA
SRA-II:1983	TCTAACAAAGCACATACAACAAAAGAAACTCTCAGTGCGTGTTCATTTCT
SRB-I:2222	GCGCTTTTTCTATCGTCTCTGCTATGTCACTGAATTAACCACTGTACGTG
SRB-I:908	GACTCAGCAAGATCGATTATTGGCATTCAGAGCAGTGTAACATGATCAAT
SRCL:2536	GGACTGAATCGCATAGATTTTCTCAGCCATTAACCATAGAATTTATGCAA
SRCL:2277	TTCATTTGTGAGAAGGAAAGGGAGGCAGTACCATCATCCATATTATAGCA
TGFb:1371	GGAACTCTACCAGAAATATAGCAACAATTCCTGGCGTTACCTTGGTAACC
TGFb:714	GCTGCTTTCTCCCTCAACCTCAAATTATTCAGGACTATCACCTACCTTTC
TNFa:1495	ATTTATCTAACCCAATTGTCTTAATAACGCTGATTTGGTGACCAGGCTGT
TNFa:1508	AATTGTCTTAATAACGCTGATTTGGTGACCAGGCTGTCGCTACATCACTG

Identity	Probe
TNFa:1326	ATTTATTTGCTTATGAATGTATTTATTTGGAAGGCCGGGGTGTCCTGGAG
TLR1full:2431	GCTGCTCTGGGGAGTTCTAATAATAGTACCATTCATATCAGCAAGAACCT
TLR1full:2416	CACCTCAATGATGTTGCTGCTCTGGGGAGTTCTAATAATAGTACCATTCA
TLR2:2626	GCAGGAAGTGTTTTGGGTAAATCTGAGAACTGCAATAAAGTCCTAGGTTC
TLR2:2621	GGCCAGCAGGAAGTGTTTTGGGTAAATCTGAGAACTGCAATAAAGTCCTA
TLR3:2740	ATCTCGGAATTCAGCACATTAAACTCATTTGAAGATTTGGAGTCGGTAAA
TLR3:2727	AAGTAGCACTTGGATCTCGGAATTCAGCACATTAAACTCATTTGAAGATT
TLR4:3513	TAACATCCTTTTCCTTCATCATTCTCATTTCTGGACATGCCTTGTGAGAT
TLR4:3412	TCACATAGCTGAATGACAAGACTACATATGCTGCAACTGATGTTCCTTCT
TLR5:4226	CCTTCTTTCTTCCCCACAACTATACAAGAGCTGTTGCAACCACTGAAAAA
TLR5:4048	CACAAGTGATAAGAAGTTGGACAGATAGACAGATAGCAGCAGTCCCATTG
TLR5:4038	CACCTAAGTGCACAAGTGATAAGAAGTTGGACAGATAGACAGATAGCAGC
TLR6:2400	ATGAAGTTAGCCTTAGTCAATGAGGATGATGTGAAAACTTGAAACTTGGG
TLR6:2490	ACTGTGGTTTTCAGTTCCTACCTGGAGGTACTTCTGTTGTGGTGTCTTAG
TLR7:2942	CTGAGAGTTTTAAGATGGCATTTTATTTGTCTCATCAGAGGCTCCTGGAT
TLR7:3157	GACAATCATGTGGCTTATAGTCAAATGTTCAAGGAAACAGTCTAGCTCTC
TLR8:2706	CTGTTACTGACTGGGTAATCAATGAACTGCGCTACCACCTTGAAGAGAGT
TLR8:2630	TTAAAAGGCTACAGGACTTCATCCACATCCCAAACTTTCTATGATGCTTA
TLR9:2081	CTGAGCCTCCGAGACAACTACCTATCTTTCTTTAACTGGACCAGTCTGTC
TLR9:3386	GAGAGTGAAGATAGACACCAGACCCACACAGAACAGGACTGGAGTTCATT
TREM-1:713	GAAGCTATACAATAGTGACCTTCAGCGGTGTCTATTTCACAGGAGGAGCT
TREM-1:482	TATTACCACAAAATACTCACCCAGTGACACAACTACAACCCGATCCCTAC
TREM-2:754	AATTCTGAGTGGGAGGAGAACTACAGCTTAAGTCCAGCCAGGAGTCAATC
TREM-2:741	AGGTACGTGAGAGAATTCTGAGTGGGAGGAGAACTACAGCTTAAGTCCAG
TREM-3:707	CTTCCTACATTCTCCTTGTGAACTCTAGTTAGCACATGATACTCCCAGAG
TREM-3:633	CTACAAGCTGTGAGCACACCTTCCCTTATCTATTAACAACATACCAGATG

Appendix 4, probe sequences
Part B, Control probes

Identity	Probe
EF-1a:1469	GGAAGAACGGTCTCAGAACTGTTTGTCTCAATTGGCCATTTAAGTTTAAT
EF-1a:1143	ATGCAAGTTTGCTGAGCTTAAAGAAAAGATCGATCGTCGTTCTGGTAAGA
c-yes:4384	CACCAGAAACGAAAGTTGTTAAAAGCAGCCTTCTAGCACAAACACTTTTT
c-yes:4338	TTTTCAACAGCTTTCATCTGTATTGTCTTAACGTGGAACTTTAACACACC
Zeta-p:607	TTGCAAGAAGTTTACCATAAGTCTATGACTCTGAAGGAGGCCATCAAGTC
Zeta-p:184	ATCCAGACCTCAGAGGGTGTATGTCTAGCTGTGGAGAAGAGAATTACCTC
PP1cg:2050	AACAACACTGTCCTATACGAGTGACCGATAATGCTTTCTTTGGCTACATT
PP1cg:2017	AACCCGTCCATTCAGAAAGCTTCAAATTATAGAAACAACACTGTCCTATA
Tuba1:1522	TTATGAATGATTGATTTTGACAGAGACCCCAAGCTGCCCATTTCACTTAT
Tuba1:1509	TACAGTTACTGACTTATGAATGATTGATTTTGACAGAGACCCCAAGCTGC
Vimentim:1588	GGAGCGCAAGATAGATTTGGAATAGAAAGAAGCTCAGCACTTAACAACTG
Vimentim:1569	CCTTTACTGCAGTTTTTCAGGAGCGCAAGATAGATTTGGAATAGAAAGAA
GNAS:2241	TGAAAAACCCCTCTTCCCTTCAGCTTGCTTAGATTTCCAAATTTAGTAAG
GNAS:1936	AGTACTTCATTCGGGATGAGTTTCTGAGAATCAGCACTGCTAGTGGAGAT
Cofilin:964	TTGTCTGTTTAGTTCTGTGTGTAAATGAAATGTGGAAATGACCCTCCCTG
Cofilin:459	ATGCCATCAAGAAGAAGCTGACAGGAATCAAGCATGAATTACAAGCTAAC
y-box:1164	TAAGAAATGAACAAAGATTGGAGCTGAAGACCTTAAGTGCTTGCTTTTTG
Y-box:792	AGGAGAGCAAGGTAGACCAGTGAGACAGAATATGTATCGGGGTTACAGAC
Lac.dehy:1602	ATTATGTGAGATGTAAGATCTGCATATGGATGATGGAACCAACCACCCAA
Lac.dehy:1491	GTTAAGTCGTATAACCTGGCTCCAGTGTGTACGTCCATGATGCATATCTT
Pbp:786	GGGGAGGGGTCTAATGTTCTGATGGAGTCATTCTGTTGTTGATATAAAAA
Pbp:661	CTCTCATTGGGAGTTCTTAGCTGTGCTAGGATAGAGGTTTAGGGTGTCTT
B-actin:1702	GCCTTAATACTTCATTTTTGTTTTTAATTTCTGAATGGCCCAGGTCTGAG
B-actin:1197	AAGTGCTTCTAGGCGGACTGTTACTGAGCTGCGTTTTACACCCTTTCTTT
Rheb:763	TATATTCCACCTGAGGAGCAAACTGCCCGTCATCCTTGAGATAAAACTAT
Rheb:473	CATGGCAAGTTGTTGGATATGGTGGGGAAAGTGCAGATACCTATTATGTT
Ferritin:468	CTACTGACAAGAATGATCCCCACTTATGTGACTTCATTGAGACGCATTAC
Ferritin:252	AGAACTTTGCCAAATACTTTCTCCATCAATCTCATGAAGAGAGGGAGCAT
GSK3b:1205	AATGTCAAACTACCAAATGGGCGAGACACACCTGCACTCTTCAACTTTAC
GSK3b:808	TTCATATATCTGTTCTCGGTACTACAGGGCACCAGAGTTGATCTTTGGAG

Identity	Probe
CCR1:843	GAACCCTAGAGCCAAGCCATACAAATTCACTAACCAGAAGATTAAGGACT
CCR1:636	CGGCTCGGCTAAGACTTATGCTAATTTGACTCAAGCTTATGTGGATGTTC
Chlorophyll:355	TGGCATTTTCATTCCAGAATTCCTAACAAAGATTGGTGTCTTGAACACTC
Chlorophyll:85	AGGAGGTTGTTTTCTTAGTGGAAGGAAATTGAGGGTGAAAAAGGAGAGAG
Cellodex.:1215	TCTCCCTCAAACTCCCTTCCTAAAACTTTCAGTATTAATTTTTGCCCATT
Cellodex.:923	AGAAGTACGGCACTACTCTTTACTGCGGTGAATACGGTGTGATCGATGTC
CelA:83	CGCTGTTCTTCATTATACCTTTGCTACTCTTATTGGGCCTAGTATCTCGG
Lpo:1188	TTCGTCACGGAATATCGGTCTCTGTACTAGAAGTGTTCCTCTCGTGTATC
Endotoxin:3357	AGAGAATCCTTGTGAATTTAACAGAGGGTATAGGGATTACACGCCACTAC
Endotoxin:1808	TTGTTCCGGCAGAAGTAACCTTTGAGGCAGAATATGATTTAGAAAGAGCA
Ald5H:117	CGCTGTTCTTCATTATACCTTTGCTACTCTTATTGGGCCTAGTATCTCGG
Ald5H:1123	AGAGAAAGACTTCGAGAAGCTCACCTACTTGAAATGCGTACTGAAGGAAG

Appendix 7: SpotReport Validation System

Arabidopsis thaliana mRNA spikes (*in vitro* transcribed, polyadenylated RNA)

mRNA spike	Length (bp)	Accession number
Photosystem I chlorophyll a/b binding protein(Cab)	500	X56062
RUBISCO activase (RCA)	513	X14212
Ribulose-1,5-bisphosphate carboxylase large sub unit (rbcL)	521	U91966
Lipid transfer protein 4 (LTP4)	527	AF159801
Lipid transfer protein 6 (LTP6)	477	AF159803
Papain-type cysteine endopeptidase (XCP2)	507	AF191028
Root cap 1 (RCP1)	533	AF168390
NAC1 (NAC1)	457	AF198054
Triosphosphate isomerase (TIM)	498	AF247559
PRKase gene for ribulose-5-phosphate kianse (PRKase)	497	X58149

Arabidopsis thaliana 70-mer oligonucleotides that hybridise to the above targets were supplied by Stratagene (probe sequences are not in the puiblic domain).